Fluorescent Molecular Sensors: Design, Synthesis and Ion Recognition Study

A Thesis
Submitted to the Bhavnagar University,
For the Degree of

Doctor of Philosophy
in
Chemistry

By

Subrata Patra

Under the Guidance of

Dr. Parimal Paul

Analytical Science Discipline
Central Salt and Marine Chemicals Research Institute (CSMCRI)
Bhavnagar: 364002, Gujarat, India

April, 2010

Dedicated
To
My
Parents…

CANDIDATE'S STATEMENT

I hereby declare that the work incorporated in the present thesis is original and has not been submitted to any University / Institution for the award of a Diploma or a Degree. Further, I hereby declare that the results presented in this thesis and the considerations made therein, contribute in general to the advancement of knowledge in Chemistry and on particular topic, entitled ***"Fluorescent Molecular Sensors: Design, Synthesis and Ion Recognition Study"***

(Subrata Patra)

Signature of the candidate

CSMCRI

केन्द्रीय नमक व समुद्री रसायन अनुसंधान संस्थान
गीजुभाई बधेका मार्ग, भावनगर-३६४ ००२.
CENTRAL SALT & MARINE CHEMICALS RESEARCH INSTITUTE
Gijubhai Badheka Marg, Bhavnagar 364 002, Gujarat, India.

Dr. Parimal Paul
Deputy Director
Head, Analytical Science Division
Email: ppaul@csmcri.org

Date: 9.4.2010

CERTIFICATE BY THE Ph. D. SUPERVISOR

This is to certify that the contents of this thesis entitled "***Fluorescent Molecular Sensors: Design, Synthesis and Ion Recognition Study***" is the original research work of **Mr. Subrata Patra**, carried out under my supervision in Analytical Science Division at Central Salt and Marine Chemicals Research Institute, Bhavnagar 364 002 (Gujarat), India.

Further, I hereby certify that the work has not been submitted either partly or fully to any other University or Institution for the award of any degree.

(Dr. Parimal Paul)

Signature of Ph.D. Supervisor

Acknowledgement

I would like to express my gratitude and profound respect, to my Ph. D. supervisor **Dr. Parimal Paul** for his splendid and valuable guidance, constant encouragement and support that he shared with me during my research period. His profound knowledge, enormous enthusiasm and keen insight in the field of chemistry are great source of inspiration to me. He has always been wonderfully supportive and encouraging of new ideas and independence of thought, which helped me to become a good research scholar. I feel privileged and indeed fortunate for being his student.

I wish to record my respectful regards to **Dr. P. K. Ghosh**, Director, CSMCRI, for giving me the opportunity and providing me the infrastructure facility to carry out my Ph. D. work at CSMCRI.

I would like to express my extreme indebtedness and thanks to **Dr. E. Suresh** and **Dr. B. Ganguly** for their contribution in X-ray crystallography and computational studies, respectively, and also for their guidance and constant encouragement, which has helped me enormously to shape up this thesis in a wholesome way.

I also extend my sincere gratitude to **Dr. A. Das, Dr. Dr. P. S. Subramanian, Dr. Pradyut Ghosh, Dr. A. Hussain, Dr. P. Dastidar, Dr. D. N. Srivastava, Dr. R. S. Thakur, Dr. S. Das, Dr. A. Panda, Dr. I. Mukhopadhay, Dr. A. Bhattachariya, Dr. N. H. Khan, Dr. R. I. Kureshy, Dr. S. H. R. Abdi, Dr. B. Rebary, Mr. R. Patidar** and **Mr. H**. **Gupta** for devoting their precious time and many valuable suggestion which indeed helped me during this research work.

I would like to express my sincere thanks to **Vinod Boricha, Arun Das, Harshad Brahmbhatt, Vinod Agarwal, C. K. Chandrakanth, Dr. (Mrs.) P. Bhatt, Dr. (Mrs.) A. Bhatt, Hitesh, Daksha, Sheetal, Mridul, Viral, Jayesh, Sattyabir** who have been kind enough to analyze my sample during this Ph. D. work, without which I could not have completed to the target of my research work.

I wish to express my cordial appreciation to my senior **Dr. (Mrs.) Pragati Agnihotri,** for her valuable guidance, suggestions and help through out this course.

I would like to express my special thanks to my labmates **Debdeep, Ashish, Ravi G, Kamal, Sandip, Yogen, Pankaj, Saju, Srinidhi, Neha, Giriraj, sanjay, Subin** and **Yowan** for their unconditional help offered during my research work.

I wish to thank my friends, **Mosae, Amal, Ravi, Arunachalam, Gignesh and Nisar**, for being true friends, an extraordinary source of suggestion and for helping me to visualize the importance of cordial sound working environment in doing research.

I acknowledge **Dr. Laxminarayanan** wholeheartedly for his support and encouragement during his tenure in CSMCRI. The time whatever I spent with him is always memorable to me. To me, he will be always remembered as a fantastic labmate.

I would like to express my special thanks to **Prasenjit Kar** for his valuable suggestions and instructions regarding thin layer chromatography and column chromatography of my initial day in CSMCRI. He also helped me lot in my thesis writing. I also express my sincere thanks to **M. Suresh** for his help towards my learning the different spectroscopic techniques and solving the spectroscopic problems.

My sincere thanks to all my friends and well wishers **Amar, Darshak, Krishna Kumar, Amilan, Amrita, Adarsh, Pathik, Subhobrata, Amal, Mahato, Priyadip, Sukdeb, Tanmay, Ramkrishna, Jyoti, Shibin, Shampa, Ajeet, Manoj, Anik, Rabindra, Safi, Girdhar, Rajendra, Manoj Agarwal** and **Kaushik.** I am also thankful to **Churchil, Subhankar** and **Kannan** for their moral support in my research carrier.

I am specially thankful to **Mr. Chiman bhai** for his kind help. Thanks to **Pramod Makwana, Miss Avani Shah** and all other members of IT CELL for their support for any computer related problems. I would like to express gratitude to **Baraiya Bhai, Tushar, Mr. zalabhai, Mr. Kapure** and canteen/ stores/administration/security staffs. I will be failing in my duty, if I don't acknowledge the spontaneous help extended to me by **Mr. Atul M. Saha, Mr. Mehul. Bhatt, Mr. Sanat Bhai, Jitubhai** and **Dhirubhai.**

I am thankful to my friends and colleagues for the great time I had in CSMCRI. I enjoyed the atmosphere, their friendship, and their support, viz., **Surendra, Irshad, Kavita, Vishal, Pratap, Manish, Balchand, Arpan, Nirali, Arghya, Tamal, Nabin, Prasanta, Anjan, Saravanan, Siva, Koil, Thillai, Munuswami, Selvamani, Gangadharan, Michel, Prakash, Tina, Abhishek, Apurba, Narottom, Sandip, Jinka Krisha Mohan, Sudhir, Subba Reddy, Phani, Yogesh, Teji, Sumitra, Gopal, Gaurav**

Mehta, Sanjay Balia, Kunal, B. P. T., Mahendra Shukla, Sanjeev Mishra, Anupama, G. P. Dangi, Govind Sethia, Manoj Lazar, Jinesh, Prasanth, Manu, Praveen, M. V. Patil, Barun, Biplab, Ganesh, and **Chota Saravanan**.

I want to express my deepest thank to **Santosh Agarwal** for his wonderful friendship, support and encouragement. He always extended his helping hands towards me when I was in trouble.

I wish to express my warm and sincere gratitude to my M. Sc. Project guide **Dr. Bibhutosh Adhikary**, who inspired me to involve in research. I also gratefully acknowledge **Dr. S. P. Goswami** and **Dr. S. K. Chattopadhya** for their advice and encouragement.

I am also thankful to all my Institute's staff members whose names although not mentioned individually here, but have always been ready to understand my problem and helped me in all possible manners.

I gratefully acknowledge the funding sources, **Department of Science and Technology (DST)** for Project JRF and **Council of Scientific & Industrial Research (CSIR)-New Delhi** for awarding SRF that made my Ph.D. work possible.

With core of my heart, I am thankful to my beloved Parents, brothers, sister, brother in-law and all my well wishers whose continuous encouragement and support have been a source of inspiration in completion of this tough task.

Last but not the least; I am thankful to the Almighty, who has provided me sound health and strength to complete this work. What I am and what I would be I owe to the Almighty for leading me the path of Light and Success.

CONTENTS

List of Abbreviations

THF	Tetra Hydro Furan
DMF	N,N'-dimethyl Formamide
DCM	Dichloromethane
FTIR	Fourier Transform Infrared
FT-NMR	Fourier Transformed Nuclear Magnetic Resonance
UV-Vis	Ultraviolet-Visible
LC-MS	Liquid Chromatography Mass Spectroscopy
MHz	Mega Hertz
Hz	Hertz
HOMO	Highest Occupied Molecular Orbital
LUMO	Lowest Unoccupied Molecular Orbital
PET	Photoelectron Transfer
FRET	Fluorescence Resonance Energy Transfer
PCT	Photoinduced Charge Transfer
MLCT	Metal to Ligand Charge Transfer
DPV	Differential Pulse Voltametry
SCE	Saturated Calomel Electrode
bpy	2,2'-bipyridine
Ar	Aromatic

Chapter-I

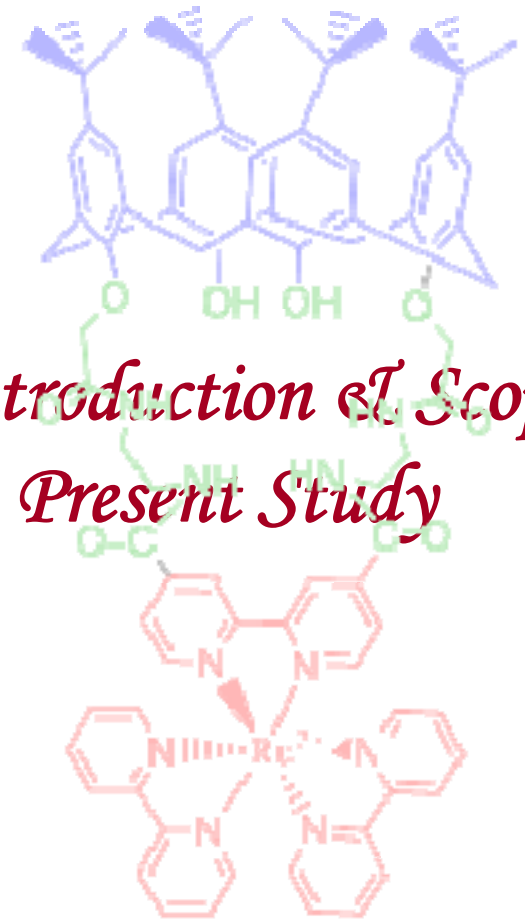

General Introduction & Scope of the Present Study

1. Introduction

1.1. General Overview

Cations and anions play an important role in wide range of chemical, biological and environmental processes.[1-3] Selective recognition of cations and anions is an emerging area of current research because of their diverse application in many fields.[3-6] Heavy metals are extensively used in industrial, agricultural and military purposes for several decades of time.[6-9] As a result, these are now widely dispersed in a range of different forms, and there are environmental problems arising from their mining, extraction and purification. Not only cations, the anions, specially halides and oxo anions play a fundamental role for resolving various chemical, biological and environmental issues.[9-11] These are highly health hazardous and toxic in nature. In recent years, significant effort has been made for the development of highly sensitive techniques for selective detection of various hazardous cations and anions and also methods for monitoring the recognition event in solution.[12-15]

Among the various analytical methods that are available for the detection of cations and anions, flame photometry, atomic absorption spectrometry, ion sensitive electrodes, electron microprobe analysis, neutron activation analysis, etc., are expensive, often require large amount of sample and do not allow continuous monitoring. In contrast, the method based on fluorescence offers distinct advantages in terms of sensitivity, selectivity, time and sample required for analysis and moreover it is a nondestructive method of analysis. Many researchers including chemists, biologists and environmentalists are intensively involved in the development of fluorescence sensors suitable for selective detection of various ions.[16-20] Such type of fluorescent sensors can be developed by the combination of a ion recognition unit with a luminescent fragement whose photophysical properties perturbed during the recognition process.

1.2.1. Important Cations and Anions for Detection

Alkali and alkaline earth metal ions are of great importance because of their involvement in numerous biological/clinical and environmental processes.[21-23] For example, the recent elucidation of the structure of the streptomyces lividans potassium channel has stimulated further research into elucidating the essential structural and mechanistic features of ion channels through the construction of abiotic systems.[24-28] Sodium and potassium ions have significant role in Na^+/K^+ pump of our blood circulatory system to maintain the blood pressure.[29,30] The Rb^+ ion is widely used in radiopharmaceutical treatments.[31-32] Large quantity of radioactive Cs^+ is present in the nuclear fuel industrial wastes,[33-35] its detection and possible isolation is highly demanding. Selective detection and extraction of K^+ ion is extremely important because of its use as fertilizer (potash) and our country imports entire amount of its requirement. Therefore selective recognition and possible isolation of these metal ions are of great interest to many scientists.

Transition metals are important in biomedical and environmental point of view.[36] Among various transition metal ions, Cu^{2+}, Zn^{2+}, Mn^{2+} and Fe^{2+} are known to be involved in the structural, catalytic, and regulatory aspects of the biological systems.[36,37] For example, Cu^{2+}, Zn^{2+} and Fe^{2+} have been found to be involved in aggregating β-amyloid peptides during the onset of Alzheimer's disease.[38] The Cu^{2+} ion is an essential element in the human body and also plays important role in various biological processes. However, it is toxic at higher concentrations and, for example, the accumulation of Cu^{2+} in the liver and kidney may cause gastrointestinal problems, Wilson disease, hypoglycemia, dyslexia, and infant liver damage.[39-40]

The toxic elements such as Hg^{2+}, Pb^{2+} and Cd^{2+} , which are highly health hazardous, is also a serious concern and require their detection in the environment. For example, Pb^{2+} ion can affect almost every organ and system in the human body, causing various symptoms such as anemia, kidney damage, memory loss, muscle paralysis, mental retardation etc.[41] Mercury is a dangerous and wide spread global pollutant, it remains a danger to human health and the environment. Atmospheric oxidation of mercury vapor to water-soluble inorganic Hg^{2+} ions and its subsequent metabolism by

aquatic microbes produces methylmercury, a potent neurotoxin linked to many cognitiveand motion disorders.[42-44]

Anions, which are highly toxic, and those which play important role in biological systems (F^-, PO_4^{3-}, $H_2PO_4^-$, SO_4^{2-}, NO_3^- etc.) also require detection in various systems. For example, fluoride ion (F^-) is of particular interest because of its role in preventing from dental caries and in treatment of osteoporosis.[45-46] However, an excess of fluoride ion can lead to fluorosis, which corresponds to a fluoride 'disease'. Therefore, development of reliable and sensitive methods for detection of all of these ions are extremely important in view of human health care and environment.

1.2.2. Ligands for Recognition of Ions

For ion recognition, different kinds of approach have been applied to encapsulate metal ion selectively into the cavity of ionophore. One of such approach involves the use of molecular replication to generate molecules that can selectively recognize metal ions. In this regard, non-covalent intermolecular interactions have received intense attention owing to their implications in designing artificial receptors capable of binding substrate molecules strongly and selectively.[47-49] The correct manipulation of the energetic and stereochemical features of these intermolecular forces can form supramolecular architectures with inner cavities/cages of desired size, which can encapsulate molecules or ions selectively by complementing each other both in size and shape.[50-52]

The most common approach is the use of macrocyclic ligands, which are noted for their remarkable selectivity towards cations and have also been widely used as extractants for various ions.[53-55] Macrocyclic ligands have some advantages such as macrocyclic effect that give such complexes a higher stability over their open chain analogs. The other advantage is that the selectivity of metal ion binding can be achieved by matching the size of the cavity of macrocycles with that of the metal ion.[56,57] Among macrocyclic ligands, crown ethers, which have only oxygen atoms as donor, have been intensively used for complexation with alkali and alkaline earth metal ions.[58-60] They have been used in analytical separations, recovery or removal of specific species, ion selective electrodes, biological mimics and reaction catalysts.[61,62] Another important class

of macrocyclic compound is calixarenes, which are cyclic condensation products derived from a phenol and formaldehyde, and are recently being widely used as ionophores/extractants for alkali metal ions.[63-66] These are conformationally mobile oligomers that can be chemically modified to function as preorganized chelate type complexants. An advantage of calixarenes is that in the addition to having a cavity for occultation of molecules, they can also be designed to offer an array of functional groups that can coordinate with metal ions. The current state of the art in extractant design is the incorporation of a macrocycles into the calixarene framework. This has allowed for the development of new ionophores that have extremely high selectivity for metal ions.[67-69]

In the present work, modified calixarenes have been used as ionophores, therefore literature survey is restricted to fluoroionophores containing calixarene based ionophore.

1.3. Calixarene

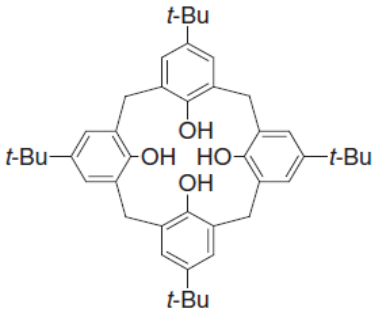

[1]

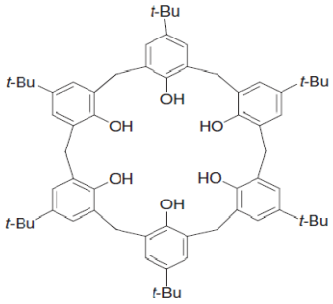

[2]

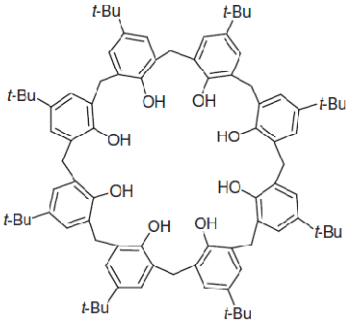

[3]

Calixarenes are phenolic metacyclophanes, which posses a cavity and distinct hydrophilic (lower rim) and hydrophobic (upper rim) regions in their molecular architecture. The term *calixarene* was introduced by David Gutsche in 1978 to describe homologous series of macrocyclic phenol-formaldehyde condensates whose constitution and structure had been the subject of much interest. Adlof Von Baeyer actually pioneered the chemistry of calixarenes in 1872 although he was unable to determine its structure. Synthesis of calixarene is really difficult because it is easy to end up with complex mixture of linears and cyclic oligomers with different number of repeating units. The most convenient way

for the synthesis of calix[4]arenes **(1),** calix[6]arenes **(2)** and calix[8]arenes **(3)** was first reported by David Gutsche.[70]

1.3.1. Conformation of calixarene

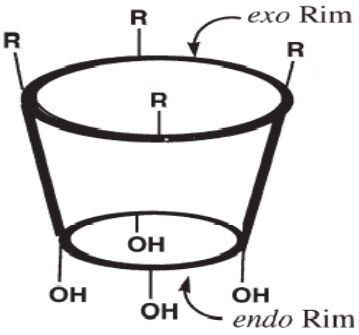

[a]

[b]

Figure 1. Calixarenes **[a]** representation and designation of the rim, **[b]** space filling molecular model of cyclic tetramer.

Calixarenes are characterised by a three-dimensional basket, cup or bucket shape with a wide upper rim and a narrow lower rim and a central annulus (Figure-1). Calixarenes exist in different chemical conformations because of the rotation around the methylene bridge and thus calix[4]arene exsists in *cone***,** (point group C_{2v},C_{4v}), *partial cone* (C_s), *1,3 alternate* (D_{2d}) and *1,2 alternate* (C_{2h}) conformations as shown below **(4-7)** respectively. In cone conformation, the four hydroxyl groups interact by hydrogen bonding and it is the most stable conformation without derivatization.

This conformation is in dynamic equilibrium with the other conformations, however it can be locked in place with proper substituents replacing the hydroxyl groups which increase the rotational barrier. Alternatively placing a bulky substituent on the upper rim also locks the conformation **(8-10).**

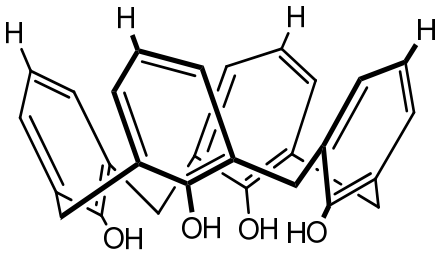

[4]

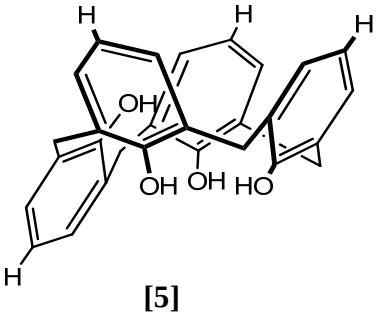

[5]

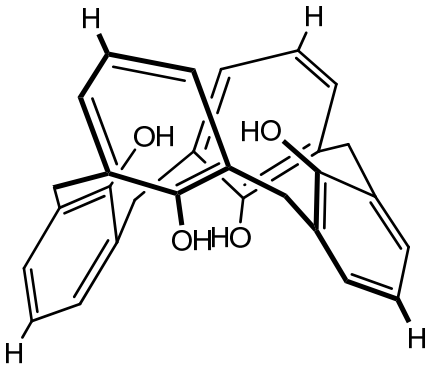

[6]

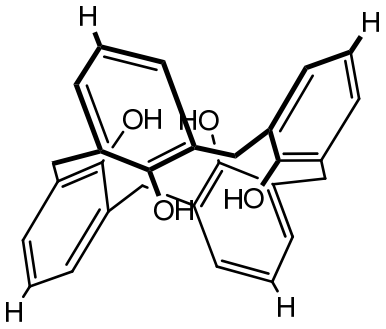

[7]

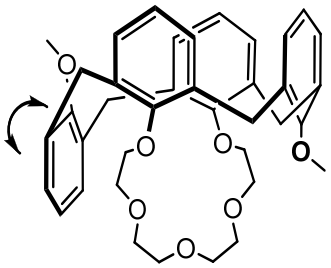

[8]

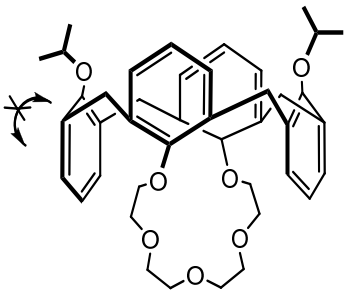

[9]

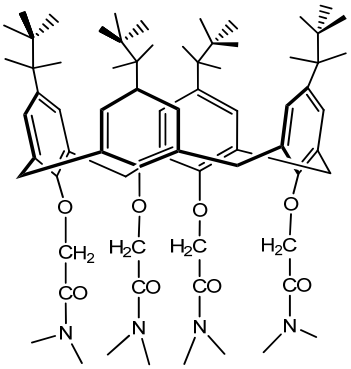

[10]

1.3.2. Calixarene as Ionophore

Calixarene derivatives having additional binding sites at the lower rim and also in upper rim enhance its ability as ionophore.[71] Synthesis of such polytopic receptors employs the organizing ability of calixarene platform to bring together various binding subunits in a single molecule.[72] In this area, a large numbers of calixarenes incorporating ketone, amine, ester, amide, carboxylic acid or other functional groups to perform specific functions such as recognition, separation, discrimination, catalysis etc. have been reported.[73,74,75] Incorporating crown ethers into calix[4]arene a new class of hybrid molecule has been developed, which attracted intense interest as receptors, specially for alkali and alkaline earth metal ions.[76]

1.3.3. Calix[4]arene-crown ethers as sensors

Among calixarene derivatives, calix[4]arene-crown ethers are widely used for the extraction of alkali and alkaline earth metal ions. The ion selectivity of this class of compounds is mainly controlled by the conformation of the calixarene platform, the size of the crown ether ring, the substituents at the upper rim of the calixarene and appended functional groups at the two sides of the crown rings. The calix[4]arene crown ethers also exist in cone, partial cone and 1,3-alternate conformation. A. Ikeda et al have reported 1,3-alternate calix[4]arene bearing a nitrogen-containing crown cap at one side and poly ethoxy group at other side[77] and its complexation with Ag^+ ion **(11).**

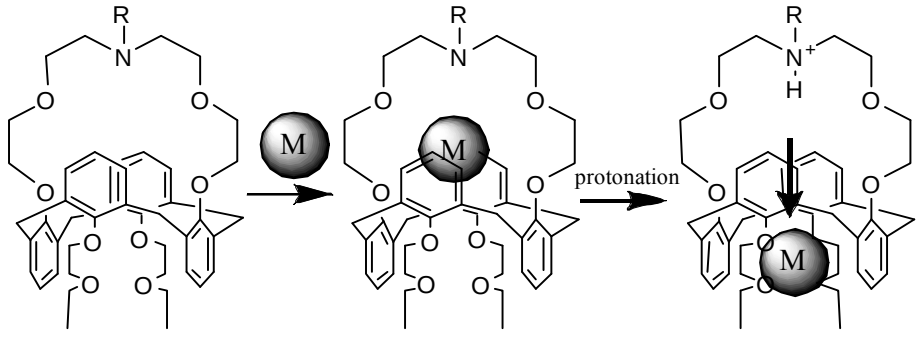

[11] **[11.Ag^+]** **[11.Ag^+.H^+]**

R. A. Bartsch et al has reported a series of *p*-tert-butylcalix[4]arene-crown-6 compounds **(12), (13)** and **(14)** in cone, partial cone and 1,3 alternate conformation and studied their complexation with different alkali and alkaline earth metal ions.[78] Among them, 1,3-alternate conformers have been studied more extensively due to their high Cs^+/Na^+ selectivity. Calix[4]arene-crowns with other conformations have also been prepared, however study on complexation behavior for partial cone conformation is rare except for one that reports a partial cone isomer with a K^+/Na^+ selectivity of 1.18×10^4, the highest observed to date for a synthetic ionophore **(15, 16).**[79]

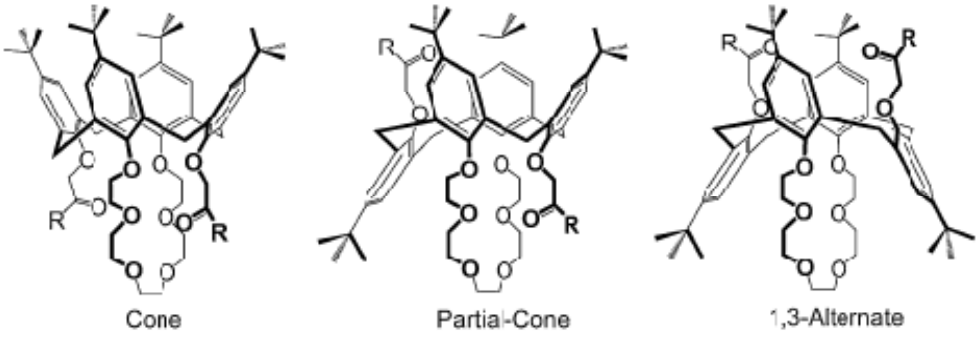

[12] **[13]** **[14]**

[15] **[16]**

H. Zhou et al have reported a series of proton di-ionizable calix[4]arene-crown-6 ligands in cone, partial-cone and 1,3-alternate conformations **(17-20).**[80] They also studied the effect of *para*-substituents on alkaline earth metal ion extraction on the calix[4]arene scaffold of the ligands. They observed that the partial-cone *p-tert*-butylcalix[4]arene-crown-5 conformer **(17)** exhibits higher K^+ association constants in chloroform than the cone or 1,3-alternate analogues. On the other hand, for calix[4]arene-crown-5 ligands with *p*-H substituents, the 1,3-alternate conformer **(20)** is a better K^+ complexing agent than the cone or partial-cone conformer.

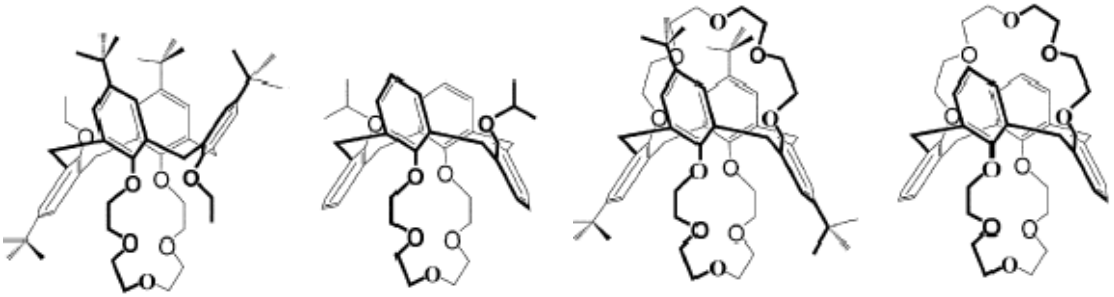

[17] **[18]** **[19]** **[20]**

P. Agnihotri et al have reported the synthesis, crystal structures, cation-binding properties and the influence of intramolecular C–H···O interactions on the complexation behaviour of a family of cone *p-tert*-butylcalix[4]arene-crown-5 compounds **(21-25)** towards Na^+, K^+, Mg^{2+} and Ca^{2+} ions.[81] The selectivity study with a mixture of cations showed the highest selectivity towards K^+; the association constants also follow the same order. But surprisingly the compound **(23)** didn't show any interaction towards metal ions. From the crystal structure it has been shown that the strong C–H···O interactions between the pendant $COCH_3$ substituent and the crown moiety prevents the entry of the metal ion in the cavity **(23).**

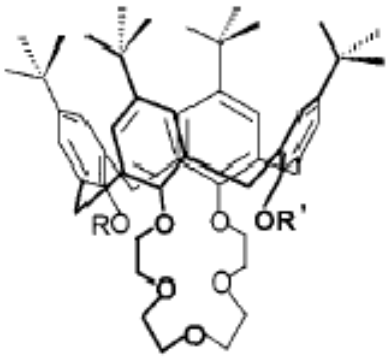

R = R' = H **[21]**

R = H, R' = $COCH_3$ **[22]**

R = R' = $COCH_3$ **[23]**

R = R' = CH_2CO_2Et **[24]**

R = R' = CH_2CO_2H **[25]**

Figure 2. Capped stick model of compound **[23]**, showing C–H···O interactions(dotted line) involving methyl hydrogen atoms of $COCH_3$ groups and oxygen atoms (O6 and O8) of the crown moiety.

L. Prodi et al have reported a calix-crown hybrid ionophore in 1,3-alternate conformation **(26)**, which shows the highest selectivity towards Na^+ ion among all alkali metal ions. This is explained on the basis of the cation-π interaction in 1,3-alternate conformation and size of the crown ether ring.[82] Calix[4]arene crown-5/6 have been reported by A. Jaiyu et al, interestingly ionophore containing the crown-5 unit **(27)**[83] showed significantly greater K^+/Cs^+ selectivity whereas the ionophore with crown-6 **(28)**[83] displayed impressively high Cs^+/K^+ selectivity.

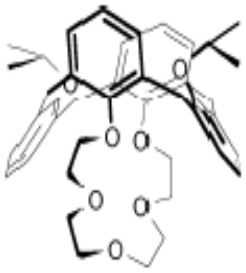

[26]

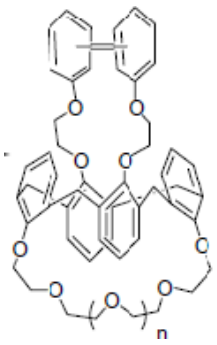

n = 1 **[27]**

n = 2 **[28]**

An interesting system of a calix[4]arene based heteroditopic receptor molecule **(29)** has been reported by Evans et al.[84] It forms 1:1 sandwich type complex with K^+ **(29a)** favouring simultaneous anion complexation due to structural reorganization, however in presence of Na^+, it accommodated two metal ions in the two crown rings **(29b)** and is unable to cooperatively bind an anion.

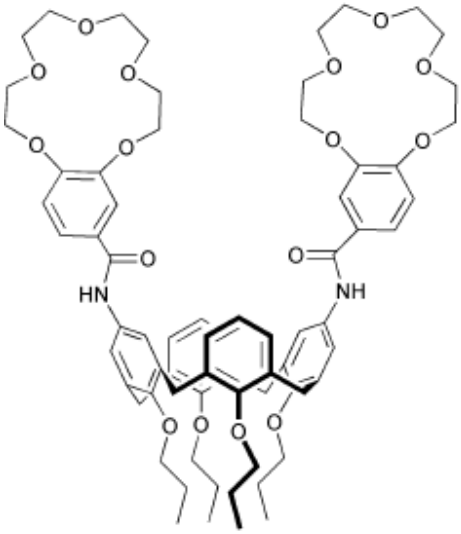

[29]

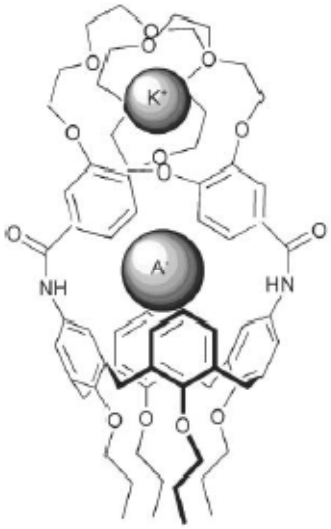

[29a]

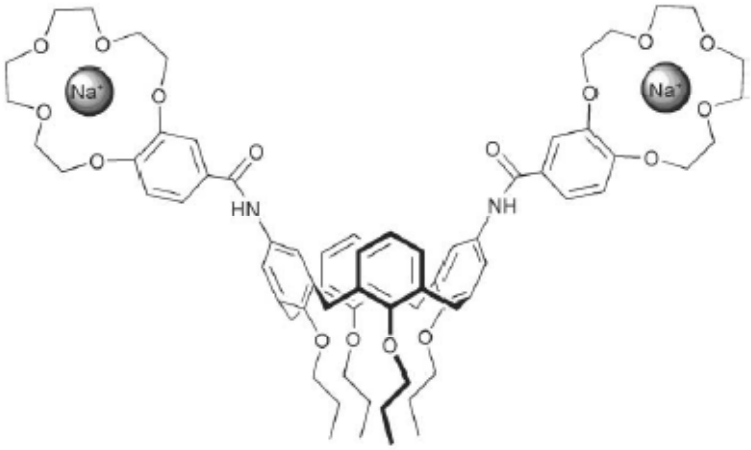

[29b]

Calix[4]arene based heteroditopic receptor with 1,3-alternate conformation is also reported by A. Casanti et al.[85] The polyether loop on one side of it is for cation binding and two pentafluoro benzamide groups on the other side are anion binding units **(30).** It shows strong interaction with CH_3COO^- and Br^-. Interestingly, the acetate anion binding experiences a four-fold increase if the crown ether loop is first complexed with K^+ , which indicates a cooperative effect between the two binding sites.

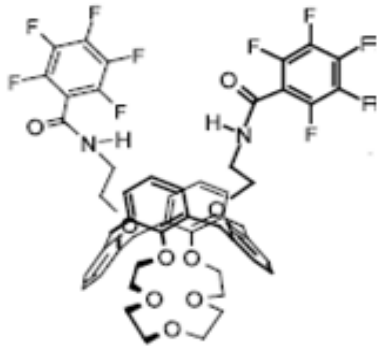

[30]

Calix[4]arene-based neutral semicarbazone and thiosemicarbazone receptor **(31),** which selectively recognize HSO_4^- in preference of Cl^-, Br^-, I^-, PF_6^- and $H_2PO_4^-$, has been reported by H. M. Chawla et al.[86] The possible binding mode with HSO_4^- is shown below **(31a).**

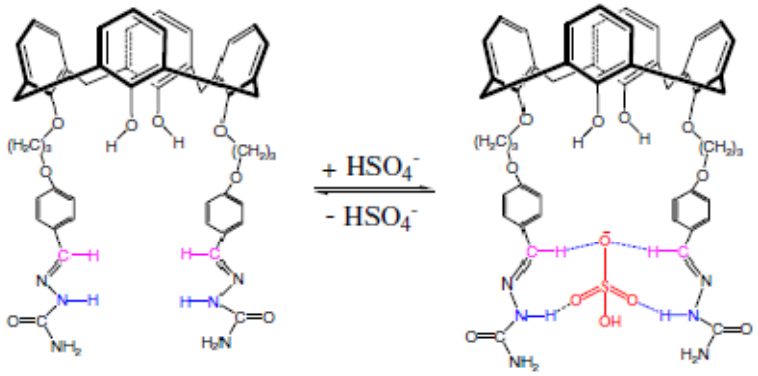

[31] **[31a]**

1.3.4. Calixarene Tubes

Calixarene tubes are another class of ionophores, which are cryptand like molecules that are three-dimensional hybrids of calixarenes and crown ethers. Beer and co-workers, who were the first to report a calixtube system **(32)**[87] selective for K^+ over other alkali and alkaline earth metals, developed much of this area.[88,94a,b] Another interesting system, calix[4]crown-5 trimer **(33),**[89] has also been reported by Beer et al and from proton NMR study it has been demonstrated that the two K^+ were entrapped in both the end-crown loops, but not in the internal polyether chains. Extensions of this work have led to calixtubes that "shuttle" ions rather than binding them. Lee et al. reported the syntheses of several calixtube shuttles that are based on thiacalix[4]crowns[90]. The presence of sulfur diminished the binding to hard cations, resulting in rapid ion exchange through the tube. On the basis of early work utilizing calixcrowns, Williams et al. demonstrated that the rate of K^+ complexation by the calixtube can be tuned by structural modifications at the calixarene "upper rim". They also propose that the preferred route of entry for K^+ into

the calixtube is the axial route (through the calixarenes) rather than through the ethyleneoxy chains.[95,90]

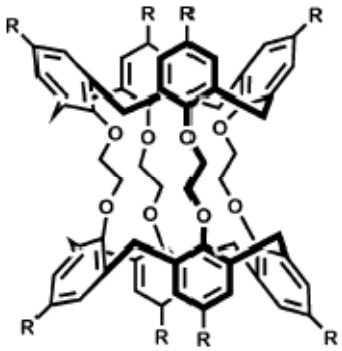

[32]

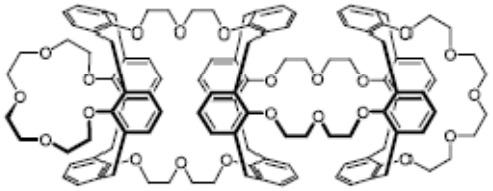

[33]

Kim et al have reported a series of calixthia tube **(34),**[91] **(35)** and **(36).**[92] The Ag^{+} ion forms 1:1 complex with these calixtubes and the ^{1}H NMR study revealed that the silver ion oscillates through the central thiacalix spacer.

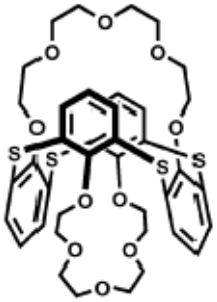

[34]

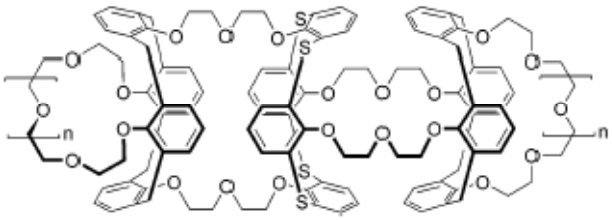

n = 1 **[35]**

n = 2 **[36]**

Rudkevich et al recently discovered that simple calix[4]arenes based synthetic nano tube **(37),**[93] reversibly interact with NO_2/N_2O_4 and entrap highly reactive nitrosonium (NO^+) cation within their π-electron-rich interiors. NO^+ is generated from N_2O_4, which is known to disproportionate to NO^+/NO_3^-. Stable nitrosonium complexes **(37a)** and **(37b)** were quantitatively isolated upon addition of a lewis acid $SnCl_4$.

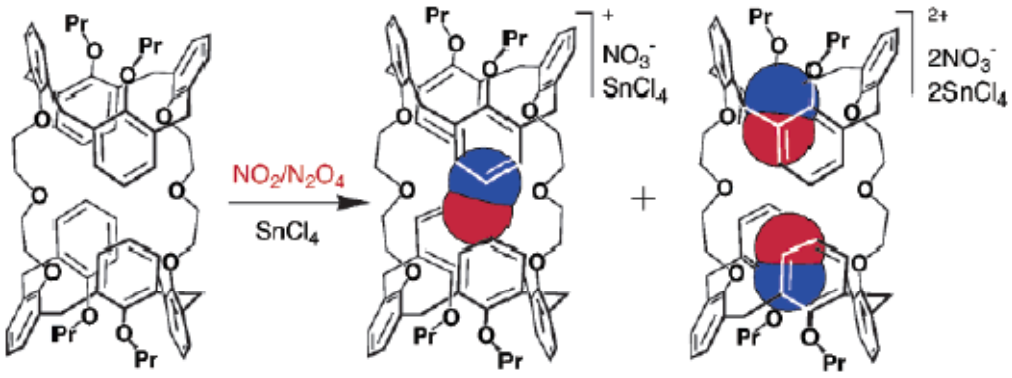

[37] **[37a]** **[37b]**

1.4. Calixarene Based Fluorescence Sensors

Fluorescence molecular sensors can be constructed by the combination of an ionophore, designed for the binding of specific incoming ion, and a luminescent fragment whose photophysical properties perturbed during the recognition processes to produce a measurable output signal. Suitably modified calixarene unit can be used as an ionophore and covalenty linked photoactive organic molecules or polypyridyl based metal complexes can act as fluorophore. Upon binding of metal ion by ionophore the electronic communication between the chromophores may take place in several ways, such as photoinduced electron transfer (PET), photoinduced charge transfer (PCT), fluorescence resonance energy transfer (FRET) etc. A brief description of each category with the examples available in the literature is given below.

1.4.1. Calix[4]arene based PET Systems:

This process, expressed in terms of molecular orbital energy diagram, is shown in Figure-3. The energy of the HOMO of the free receptor lies between those of the HOMO and LUMO of the excited fluorophore and then electron transfer from the HOMO of the receptor to the hole in the HOMO of the fluorophore takes place. This process does not occur in presence of analyte bound to the receptor causing enhancement of emission intensity. The PET also provides a mechanism for nonradiative deactivation of the excited state, leading to a decrease in emission intensity or "quenching" of the fluorescence.

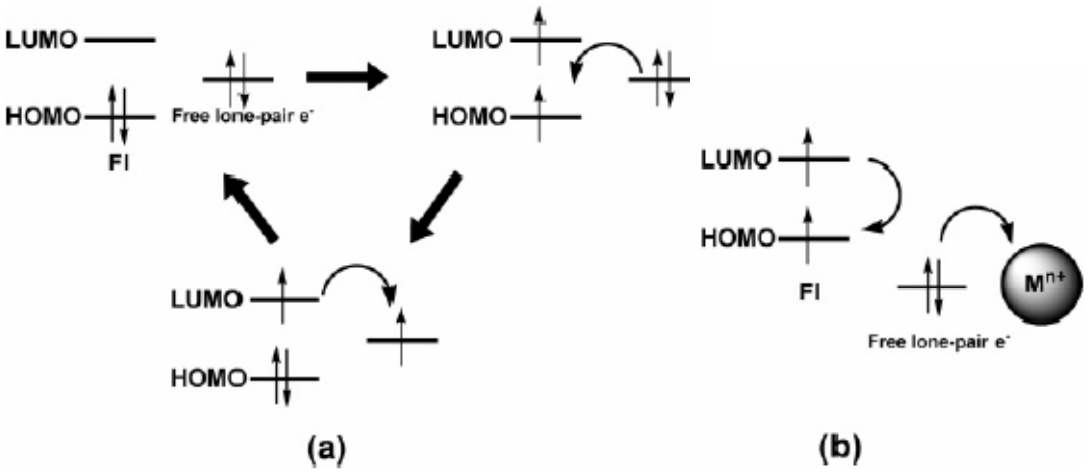

Figure 3. Principle of cation recognition by fluorescent PET sensors, (a) in absence of metal ion and (b) in presence of metal ion.

In an effort to develop a technique for sensing of Cs^+ ion, Reza Dabestani et al have developed calix-crown based fluoroionophore incorporating organic photoactive molecule as fluorophore **(38).**[94] In absence of metal ion, this compound shows very weak emission due to PET process. However, in presence of Cs^+ [60a] in CH_2Cl_2/CH_3OH (1:1), the intensity of the fluorescence is enhanced nearly 12 times.

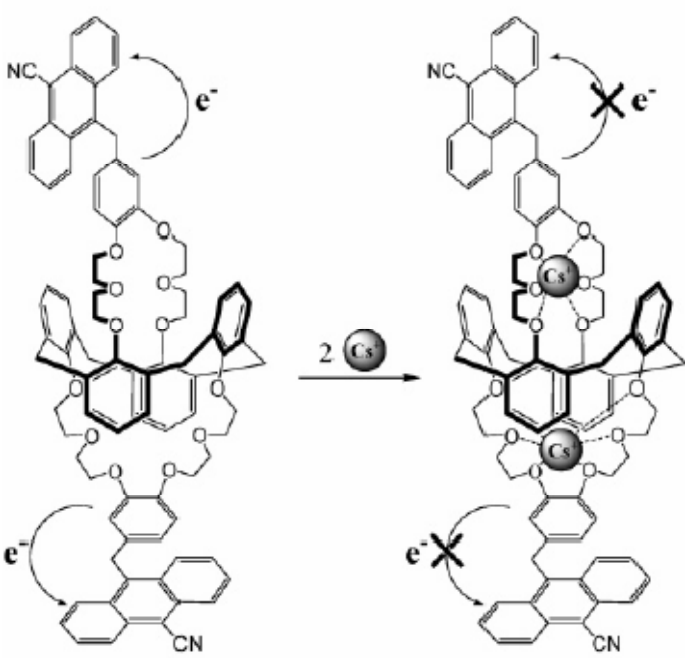

[38] **[38a]**

The emission intensity of another system **(39),** reported by Kim et al,[95] was almost completely quenched because of the PET process. However, upon addition of Ag^+ **(39a)** the emission intensity enhanced significantly due to the inhibition of the PET mechanism. When K^+ ion was added into the solution containing Ag^+ (10 equiv) ion, fluorescence quenching effect was further observed. As the K^+ ion binds strongly with the crown ether site induced the decomplexation of Ag^+ from the azacrown site **(39b)**. In the present study, this "molecular taekwondo: coming-in and kicking-out" process was easily monitored via fluorescence change.

The fluorescence intensity of the calix-biscrown hybrid molecule **(40)**[96] is reported to be almost quenched by PET. However, binding of Ag^+ produces enhanced emission intensity due to CHEF effect because of its coordination with the N atom **(40a)**. Like (39a) it also exhibited "molecular taekwondo" effect in presence of K^+. Interestingly, upon addition of CF_3COOH into the Ag^+ bound compound, a process related to the action of a "molecular syringe" and presumably involving cation tunneling through the π-basic calixtube enhancing fluorescence intensity is observed **(40b)**.

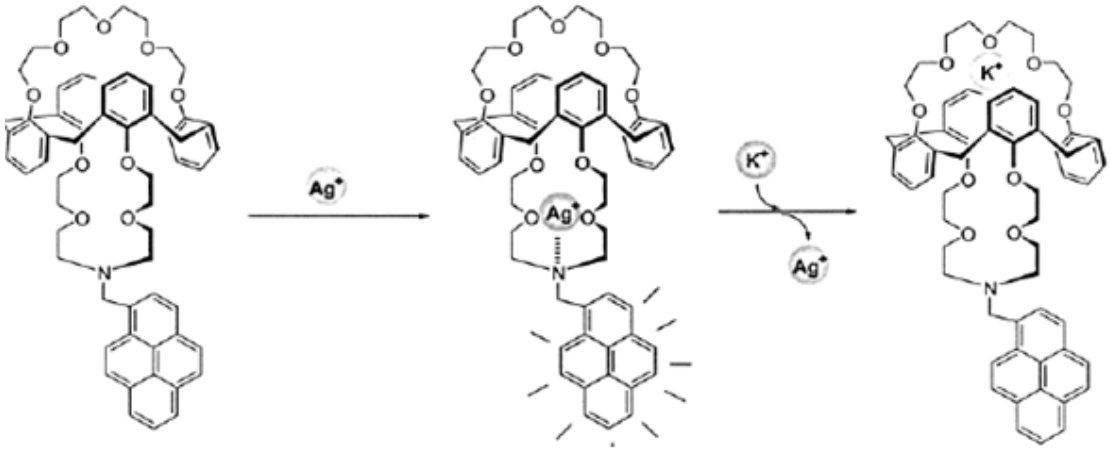

Nonfluorescent Fluorescent Less fluorescent

[39] **[39a]** **[39b]**

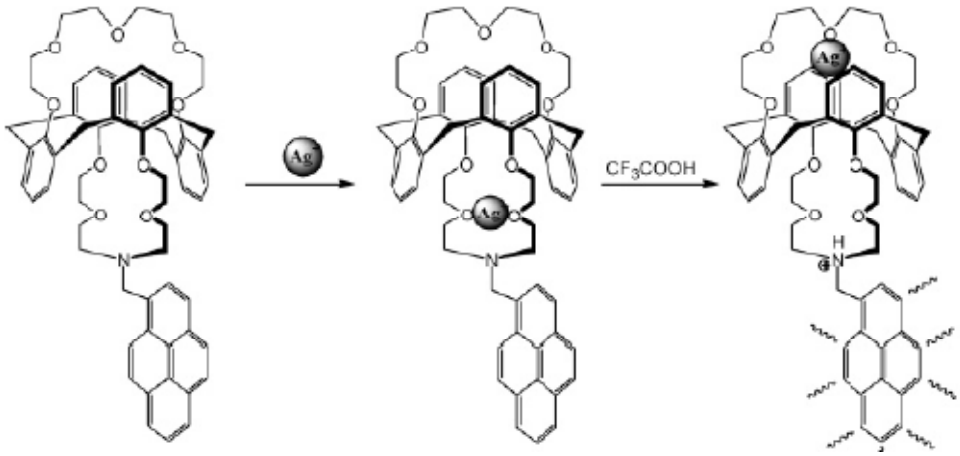

Non-fluorescent Fluorescent Strongly Fluorescent

[40] **[40a]** **[40b]**

Ji et al. has reported an interesting dual sensor **(41)**[97] for detection of both Cs^+ and K^+. In basic medium, it shows a weak emission due to the quenching of anthracene fluorescence by PET process, however selective binding of K^+ to the azacrown unit leads to the 6.4-fold enhancement of emission intensity. Interestingly, in acidic medium it is highly sensitive to Cs^+ over the other alkali-metal ions **(41a)**.

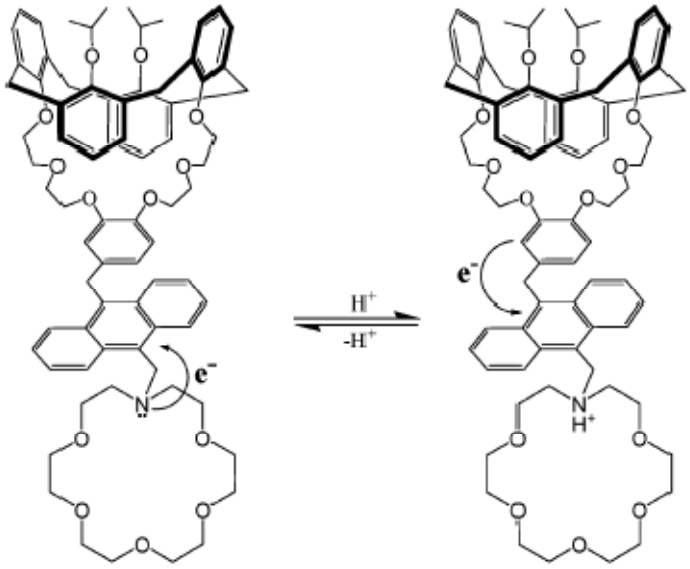

[41] **[41a]**

Calixarene derivative bearing four carbonyl functions, two of them being linked to pyrene and nitrobenzene at opposite sites on the lower rim **(42),**[98] shows weak fluorescence due to PET process, however upon binding with Na^+ **(42a)**, it exhibits significant enhancement in fluorescence intensity. Binding of Na^+ appears to cause a conformational change where the nitrobenzyl and pyrenyl substituents become more distant, leading to reduced PET.

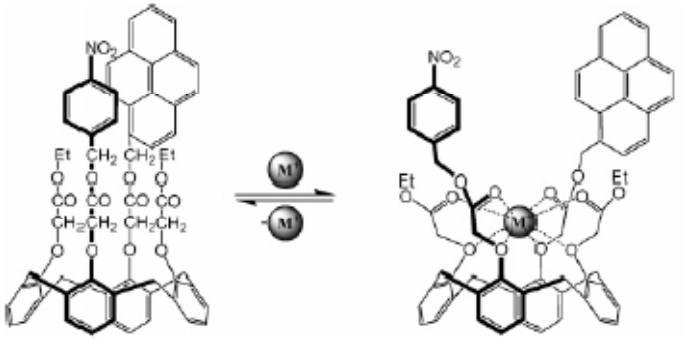

Weakly Fluorescent Strongly fluorescent

[42] **[42a]**

A new type of calixarene based fluorogenic sensor bearing two pyrene amide groups **(43)**[99] has been reported by Lee et al. It functions as both cation and anion selective chemosensor. It forms complexes with Pb^{2+} **(43a)** and Co^{2+} and also with F^- **(43b)** through H-bonding in the crown cavity. Both the cases quenching in flurescence intensity is observed due to conformation changes and PET effect.

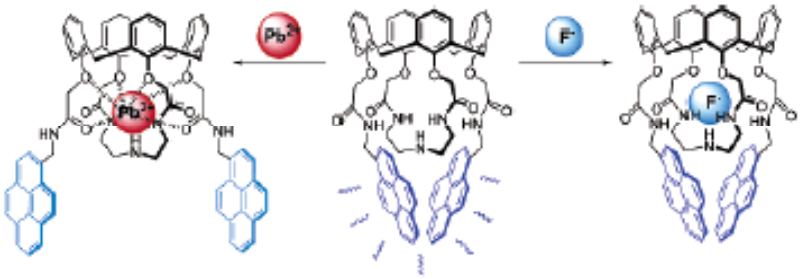

[43a] **[43]** **[43b]**

Kim et al have reported calix[4]triazacrowns **(44), (45)** and **(46)** as fluorescence sensor for both cations and anions.[100] The pendent amine group ($-CH_2CH_2NH_2$) in the compounds **(44)** and **(45)** resulted in quenching of monomer emission due to PET process, an electron from the lone-pair of electron of the nitrogen atom transferred to two

pyrene units. When Pb^{2+} is added to a CH_3CN solution of **[44]**, the monomer emission increases with an excimer emission quenched due to conformational changes. In contrast, the addition of Li^+ to the compound **[44]** causes both monomer and excimer emission to increase, which is mainly attributed to the CHEF effect without conformational changes of the carbonyl groups. When F^- ions are bound to **[44]** and **[45]** via hydrogen bonding between the amide N*H* of the triazacrown ring and F^-, both their monomer and excimer emissions are weakened due to PET from the bound F^- to the pyrene units.

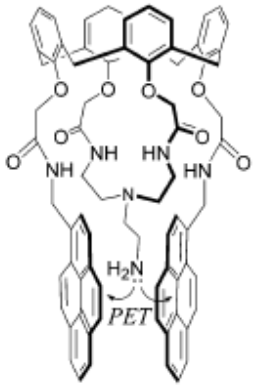

[44]

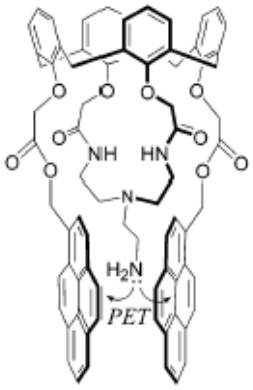

[45]

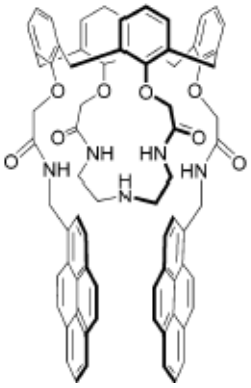

[46]

Like metal ions, H^+ also may bind to an electron-donor site such as N, and thus, the emission from **(47)**[101] is much stronger in acidic solution than in neutral or basic solutions due to the inhibition of PET. However, complexation of K^+ in acidified solution leads to a diminished basicity at N atom and hence to a reduced degree of protonation and a weaker luminescence.

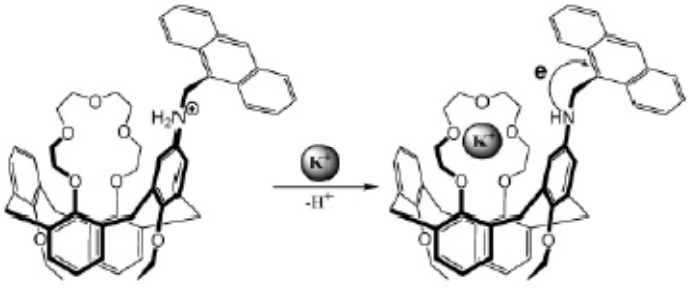

[47] **[47a]**

Fluorescence quenching by PET processes was also reported for calixarene derivative containing amide incorporated macrocyclic unit **(48)**.[102] Addition of Hg^{2+} into the solution **(48a)** causes quenching of fluorescence due to electron transfer from the excited dansyl moiety to Hg^{2+}. The presence of alkali, alkaline earth, and transition metal ions does not affect the quenching induced by Hg^{2+}.

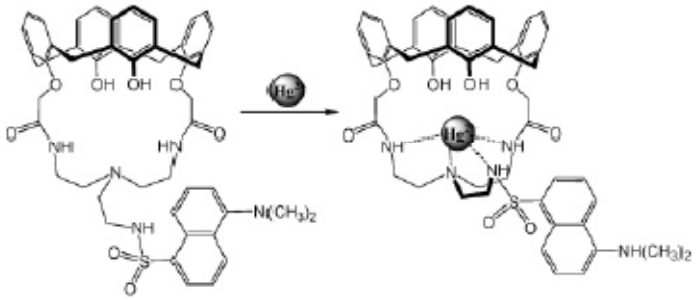

[48] **[48a]**

Calix[4]arene based fluoroionophore **(49)** is also reported by Samanta et al.[103] This system showed significantly high selectivity towards Cu^{2+} and the fluorescence intensity is substantially enhanced upon addition of Cu^{2+}.

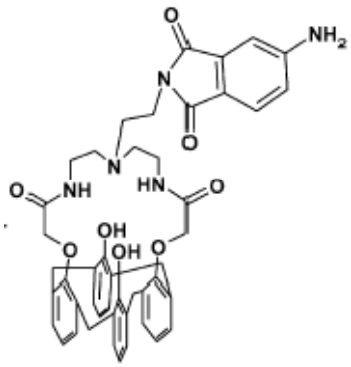

[49]

1.4.2. Calix[4]arene based PCT Systems

Electronic excitation necessarily involves some degree of charge transfer, but in fluorophores containing electron withdrawing and electron-donating substituents, this charge transfer may occur over long distances and be associated with major dipole moment changes, making the process particularly sensitive to the microenvironment of the fluorophore. Thus, it can be expected that cations or anions in close interaction with the donor or the acceptor moiety will change the photophysical properties of the fluorophore. Complexation of cation with an electron donor group within the fluorophore reduces the electron-donating ability of it causing a blue shift of the absorption spectrum with a decrease of the molar absorptivity. On the other hand, binding of metal ion with the acceptor group enhances its electron-withdrawing character, and the absorption spectrum is thus red-shifted with an increase in molar absorptivity. This phenomenon is illustrated in the Figure-4. A number of examples of this class of fluoroionophore from literature are described below.

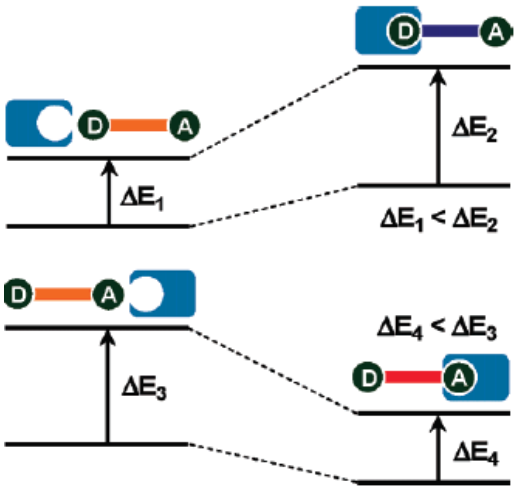

Figure 4. Principle of ion recognition by fluorescent PCT sensors

Kim et al have reported a novel calix[4]arene-based PCT chemosensor **(50)** with a specific optical response to F^- and delineation of the complexation mode by comparison of the static excimer with the dynamic excimer.[104] In this compound, the pyrene signaling

subunit conjugated to an amide group as the recognition site can act as a PCT chemosensor. Among a large number of anions, only F^- interacts with it causing substantial red shift in its absorption band. The interaction of the amide hydrogen atoms with F^- promotes the delocalization of π electrons from the anionic nitrogen atoms to the pyrene moieties and a change of the π-π* transition from colourless to yellow is reported.

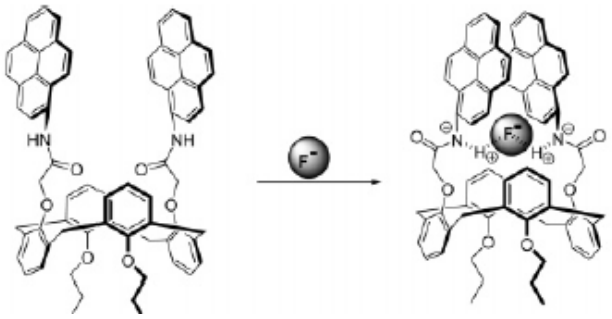

[50] **[50a]**

Calixarene derivatives bearing two coumarin signaling units and two amido groups as the binding sites **(51,52)** have been reported as PCT-based chemosensor.[105] Out of a large number of anions only F^- and $CH_3CO_2^-$ showed interaction with these ionophores. Both of them exhibited significant changes in absorption as well as fluorescence spectra.

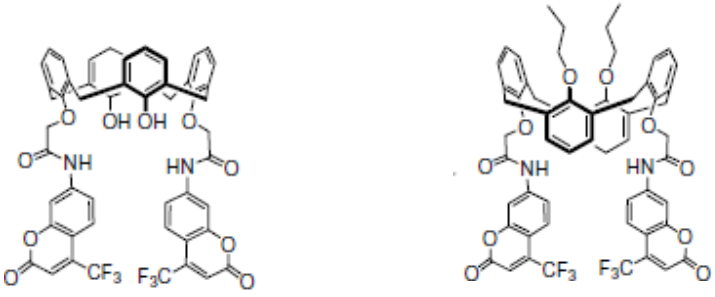

[51] **[52]**

A number of calixarene-based fluorescent PCT sensors have also been reported by Valeur et al. These compounds bear 6-acyl-2-methoxynaphthalene fluorophores **(53** and **54)**, which contain the methoxy moiety as a donor unit and the carbonyl group as an acceptor in the PCT process.[106] It was reported that the addition of metal ions to these two compounds in CH_3CN induces a red shift of the absorption and emission spectra associated with a major increase in fluorescence quantum yield. The ratio of stability constant for Na^+/K^+ selectivity is reported to be 500 for **(53)** and 407 for **(54)** in a C_2H_5OH/H_2O.

.

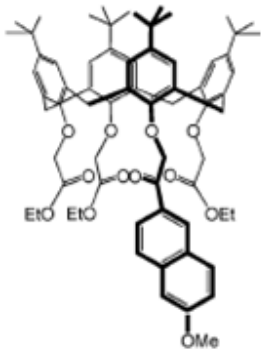

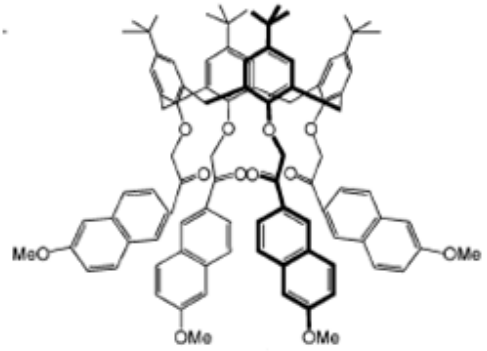

[53] **[54]**

Examples of coumarin containing PCT sensors **(55,56)** have also been reported by Z. Asfari et al.[107] In ethanol, the fluorescence emission band is blue-shifted and the fluorescence quantum yield is decreased upon addition of alkali-metal ions. They formed both 1:1 and 2:1 (metal:ligand) complexes, in which the latter showed a larger cation-induced blue shift than that of the former, suggesting a stronger interaction between the cation and excited coumarin fluorophore in the 2:1 complex than that in the 1:1 complex.

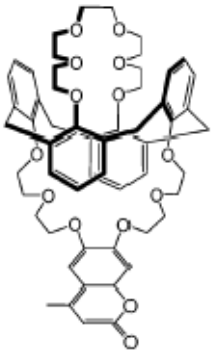

[55]

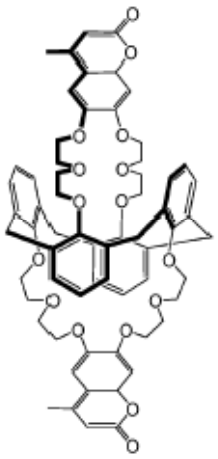

[56]

1.4.3. Calix[4]arene based other Fluoroionophores

Where aromatic rings are involved in weak interactions (such as π-stacking) which bring them within Van der Waals contact distances, electronic excitation of one ring can cause an enhanced interaction with its neighbor, leading to what is termed an excited-state dimer or "excimer". Excimer emission typically provides a broad fluorescence band without vibrational structure, shifted to lower energies compared to that of the uncomplexed ("monomer") fluorophore emission.

There are some examples of fluoroionophore which are capable of showing excimer property. In this category, the first example reported is the calix[4]arene derivative with pyrene moieties as shown in **(57)** and **(58).**[108] The two pyrene units were introduced in the lower rim as fluorophores and they were able to form an intramolecular excimer. The fluorescence spectrum of **(57)** shows a dual emission with the excimer at ca. 480 nm and the monomer at ca. 390 nm. In the absence of Na^+, the excimer emission is dominant compared with the monomer emission. When this compound **(57)** formed complex with Na^+, the intensity ratio of excimer and monomer are altered compared to that of the uncomplexed fluorophore emission. The separation and relative orientation of multiple fluorophore units attached to ligands can be controlled by metal ion

coordination, therefore, recognition of a cation can be monitored by the monomer:excimer fluorescence intensity ratio.

.

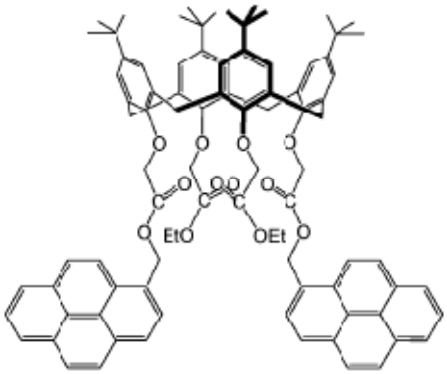

[57]

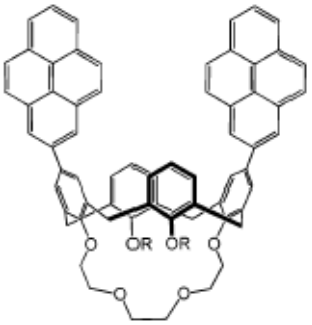

[58]

Matsumoto and Shinkai reported that the calixarene derivative, which bears an ionophoric cavity on the lower rim and two pyrene units on the upper rim **(58)**, are used for sensing of some alkali-metal ions in CH_3CN/THF. The encapsulation of Na^+ into the ionophoric cavity induces a change in distance between the two pyrene moieties, which is reflected by a remarkable change in the ratio of intensity of excimer and monomer.

Pyrene incorporated fluoroionophore has also been reported by Kim et al., in which two facing amide groups bridged to pyrene units **(59,60).**[109] These have distinctly different emission characteristics, the first one **(59)** showed only monomer emission at 398 nm, while the latter one **(60)** showed a strong excimer emission, indicating that in the latter the two pyrene units are in close proximity, presumably as a result of π-π stacking, while in the former they must be remote. Upon addition of In^{3+} to a solution of **(60),** the excimer emission is quenched because the conformational change caused by two outward-facing amide carbonyl groups turned inward to bind to the metal ion whereas addition of metal ion to the other one **(59)** enhances the excimer emission with quenching of monomer emission.

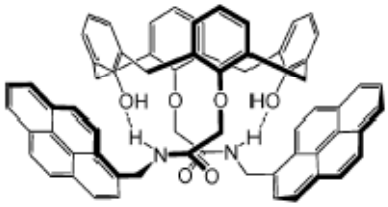

[59]

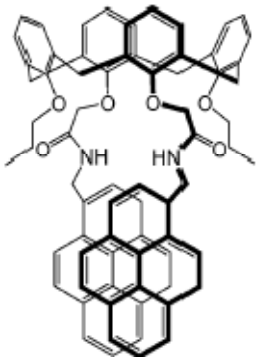

[60]

Another class of fluoroionophores, where intramolecular interaction between a pair of dissimilar fluorophores in which one acts as a donor of excited-state energy to the other (acceptor), has also been reported. As a result that the donor returns to its electronic ground state and emission may then occur from the acceptor center. This process is known as fluorescence resonance energy transfer (FRET) and a few examples of this category are also reported in the literature.

A fluoroionophore containing anthroyloxy as an acceptor and pyrene as a donor **(61)** is reported by Jin. et al.[110] The overlap between the emission band of the donor pyrene and absorption band of acceptor anthroxy moiety promotes the FRET from pyrene to anthroyloxy The complexation of Na^+ or K^+ in CH_3OH/THF induces major changes in the emission intensity, with the effects being greater for Na^+ than K^+.

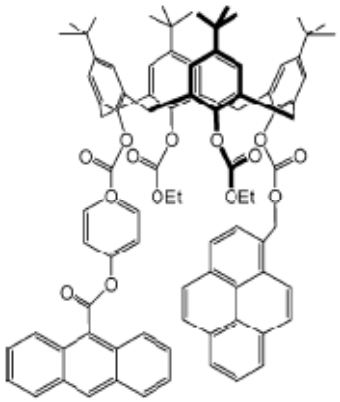

[61]

Kim et al. has recently reported a fluoroionophore bearing pyrene as a donor and (*p*-nitrophenyl)azo as an acceptor **(62),** which shows FRET effect.[111] Complexation of it with Pb^{2+} **(62a)** in CH_3CN induces an increase in the pyrene emission, which is believed to be due to diminished overlap of the donor and acceptor bands caused by a hypsochromic shift of the azo unit's absorption (diminished FRET effect).

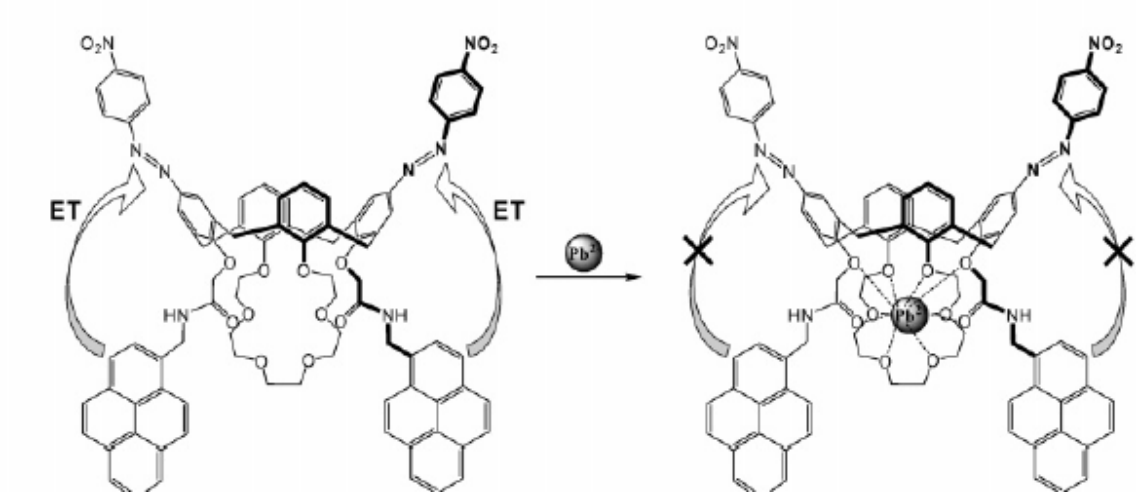

[62] **[62a]**

The FRET based sensor molecule has also been reported by M. H. et al.[112] It contains two amide groups **(63)** capable of binding anions and one crown-6 loop as a binding site for metal cations **(63a).** It shows two strong absorption bands at 242 and 344 nm arising from the naphthalene and the coumarin moieties, respectively, and a weak naphthalene emission bands ranging from 326 to 340 nm along with a broad coumarin emission band at 422 nm. The spectral overlap between naphthalene emission and coumarin absorption is optimized to provide the FRET On. F^- ion binding promotes a red-shift of the coumarin absorption band by 91 nm with a visual color change from colorless to pale yellow. Interestingly, the coumarin emission of **(63)** is markedly enhanced when the Cs^+ ion is added into the solution **(64)**. This is because of the CHEF effect, complexation with Cs^+ leads to the repression of the PET from oxygen atoms to the naphthalene group, making the spectral overlap (FRET) between donor emission (naphthalene) and acceptor absorption (coumarin) more effectively.

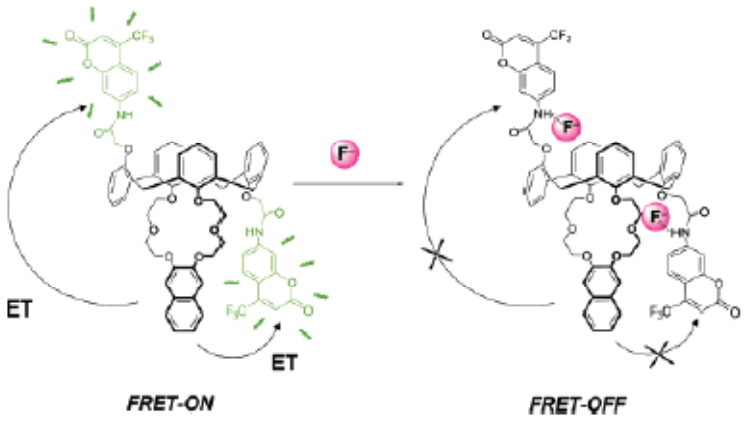
ET
ET
F⁻
FRET-ON
FRET-OFF

[63] **[63a]**

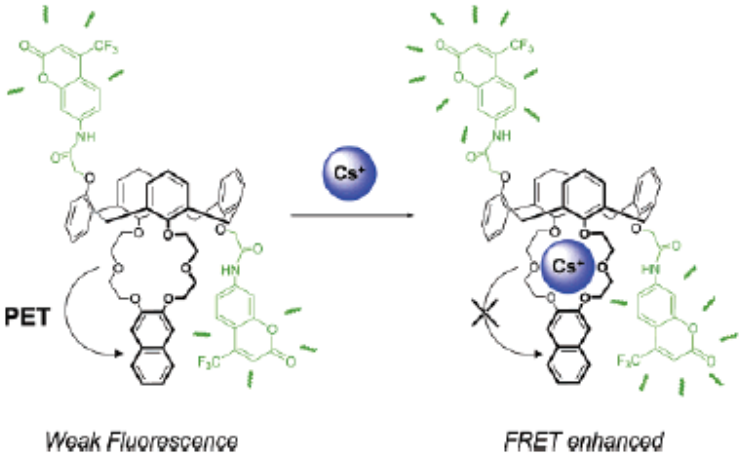
PET
Cs⁺
Cs⁺
Weak Fluorescence
FRET enhanced

[63] **[64]**

1.5. Calixarene based Fluoroionophores containing Metal complex as fluorophore

It has been mentioned earlier that photoactive organic molecules or polypyridyl based metal complexes can be used as fluorophore for the construction of fluoroionophores. Photoactive metal complexes such as ruthenium(II)/rhenium(I)-polypyridine complexes, whose photophysical properties are known and exhibits photophysical changes during the ion recognition process are used as fluorophore. It has some advantages over organic molecules, besides changes in luminescence like organic molecules, they also exhibit measurable changes in electrogenerated chemiluminesence and redox property in the event of ion recognition process. This class of sensors with crown ethers as ionophore has been extensively studied but examples with calixarene is limited to a few compounds.

In this category, Beer et al have reported a series of compounds incorporating amide unit as shown in **(65-68)** for the recognition of anions.[113] Among these receptors, **(65)** exhibits strong interaction with $H_2PO_4^-$ whereas **(66-68)** show strong interactions with acetate and chloride and weaker complexes with $H_2PO_4^-$. These complexes were formed by hydrogen-bonding interactions between the amide subunits and the corresponding anion.

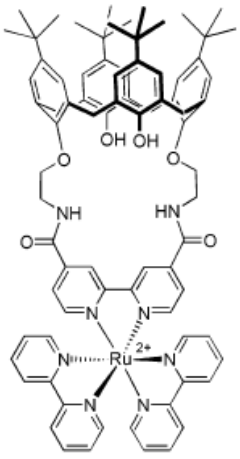

[65]

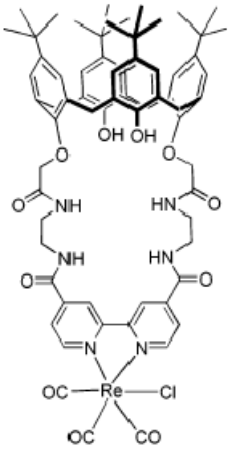

[66]

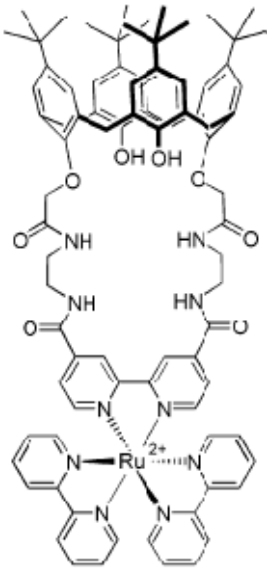

[67]

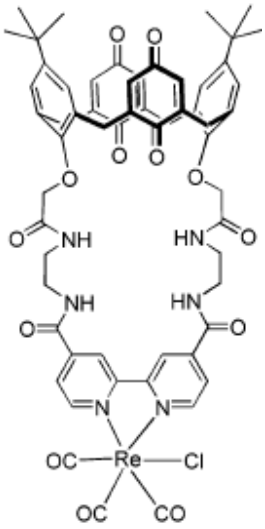

[68]

Cooper et al reported the new heteroditopic bis(calix[4]arene) rhenium(I) bipyridyl receptor molecule **(69)**[114] which has been used to bind a variety of anions at the upper rim and alkali metal cations at the lower rim of the calix[4]arene moiety. Due to special design, this complex molecule is able to bind simultaneously cations and anions. It is observed that the presence of co-bound alkali metal cations would enhance the strength of anion binding via favourable electrostatic interactions and preorganisation effects.

The same group also reported a series of new heteroditopic rhenium(I) and ruthenium(II)bipyridyl calix[4]arene receptors **(70)**[115] that simultaneously complex alkali metal cation–anion ion pairs at the calixarene lower rim. NMR titration with halide anion in the absence and in presence of lithium and sodium cations revealed that the lower rim ester co-bound alkali metal cation significantly enhances the strength of bromide and iodide binding, with the largest positive co-operative anion binding effect of sixtyfold being displayed by bromide and lithium complex.

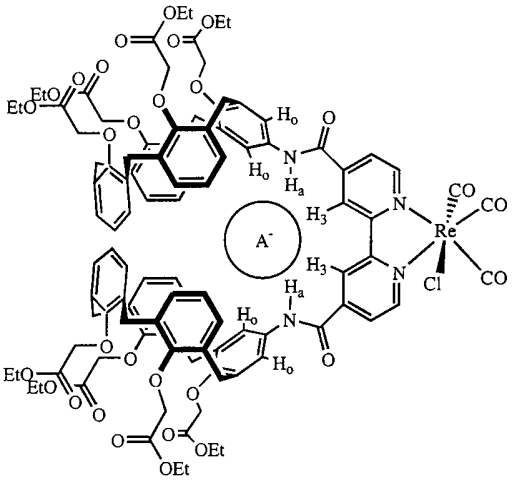

[69]

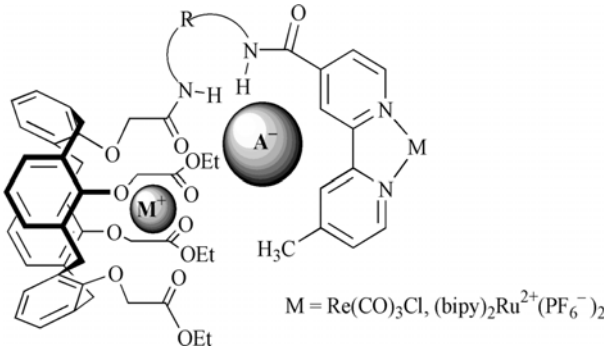

[70]

Norbert et al reported the first calixarene-based pH (PET) sensor **(71).**[116] Here the trisbipyridylruthenium(II) moiety was chosen as luminophore with the free phenolic units of a calix[4]arene acting as the acid-base site. In basic pH, the formation of the phenolate anion(s) causes photoinduced intramolecular electron transfer to take place from the phenoxide ion to trisbipyridineruthenium(II) moiety and as a result quenching the luminescence of the complex. Once the phenolate ions are protonated no such electron transfer takes place and hence luminescence is restored.

[71]

1.6. Aim and Outline of the Thesis

The objective of the present work is to develop calixarene-based fluorescent molecular sensors which can selectively interact with specific cations and anions. With this aim, series of fluoroionophores have been synthesized, characterized and their ion-recognition property with a large number of cations and anions has been studied. Fluoroionophores are synthesized by covalent linking of photoactive Ru(II)-polypyridine moiety with calix[4]arene-crown hybrid molecules, which can act as ionophore for binding of ions. In some cases, photoactive organic molecules such as coumarine and aminoquinoline are also used as fluorophore. All of these compounds are characterized on the basis of elemental and spectroscopic analysis, molecular structures of some of the complexes are established by single crystal X-ray study. Interactions of these ionophores with various cations and anions have been investigated and the ion recognition process monitored by luminescence, ^{1}H NMR, UV-Vis spectral changes and also by electrochemical study. Binding constants were calculated and the data have been analyzed to evaluate their binding ability with various ions and it ascertains the energy/electron transfer process involved in the recognition event.

The present thesis comprised of seven chapters.

Chapter 1, as seen above, deals with the brief literature survey on various type of calix[4]arene based fluorescent and non-fluorescent molecular sensors. This section also described the designing aspects of various calix[4]arene based fluoroionophores comprising of various fluorophores including Ru(II)/Re(I)-polypyridyl units.

Chapter 2 describes synthesis and characterization of a series of fluoroionophores where photoactive Ru(II)-polypyridyl unit is covalently linked to a designed functionalized calix[4]arene azacrown moiety. The cation binding property of the newly synthesized fluoroionophores has been investigated with a large number of cations monitored by ^{1}H NMR, luminescence and oxidation potential of the Ru centre.

Chapter 3 reports design, synthesis and characterization of various fluoroionophores comprising of Ru(II)/Re(I)-polypyridine based unit as fluorophore and modified calix[4]arene unit containing amide-crown as ionophore. The ion recognition property of these fluoroionophores has been tested with a series of environmentally and biologically important cations and anions. The recognition event of these luminescent molecules is monitored by ^{1}H NMR, luminescence and Uv/Vis spectroscopic methods. Among large number of cations and anions, a few exhibit strong complexation as indicated by emission and NMR spectral changes. Binding constant of strongly interacting ions has been calculated.

Chapter 4 deals with a series of calix[4]arene-based fluoroionophores. In this series of compounds, calix[4]arenes attached to coumarin through ethylene glycol units are described. This series of compounds exhibits high selectivity toward Fe^{3+} and Cu^{2+} and Ca^{2+} in few cases. The ion recognition event of these fluoroionophores is monitored by emission spectroscopic methods. Binding constant of strongly interacting ions has been calculated.

Chapter 5 reports the design, synthesis, characterization and crystal structures of a series of fluoroionophores containing 3-aminoquinoline based unit as fluorophore and amide functionlised calix[4]arene unit as ionophore. The ion recognition property of these fluoroionophores has been tested with a series of environmentally and biologically important cations and anions. The recognition event of these luminescent molecules is monitored by ^{1}H NMR, luminescence and Uv/Vis spectroscopic methods. They exhibit high selectivity toward biologically and environmentally important cations such as Hg^{2+}, Pb^{2+} and Cd^{2+} and anions like F^{-} and HSO_4^{-}.

Chapter 6 describes the synthesis, characterization and the effect of steric crowding of a number of calix[4]arene-azacrown with variation in ring size and substituents at the upper and lower rim. The structural elucidation of these ionophores have been carried out by ^{1}H NMR and mass spectrometry in solution and single crystal X-ray analysis in solid state. The interaction of these ionophores with a series of metal ions has been investigated. The

binding constants with strongly interacting cations have been calculated using NMR titration data.

Chapter 7 deals with the synthesis and characterization of new series of calix[4]arene based ionophores. Here all the ionophores are trisubstituted calix[4]arene containing different substituents and they exist in partial cone conformation. The ion recognition property of all these ionophores have been examined and one of them exhibits high selectivity towards K^+ ions.

1.7. References

1. Valeur, B.; Leray, I. *Coord. Chem. Re*V. **2000**, *205*, 3.
2. Bianchi, A., Bowman-James, K., Garcı´a-Espan˜a, E., Eds. *Supramolecular Chemistry of Anions*; Wiley-VCH: New York, **1997.**
3. Va`zquez, M.; Fabrizzi, L.; Taglietti, A.; Pedrido, R. M.; Gonza`lez-Noya, A. M.; Bermejo, M. R. *Angew. Chem., Int. Ed*. **2004**, *43*, 1962.
4. Schmidtchen, F. P.; Berger, M. *Chem. Re*V. **1997**, *97*, 1609.
5. Schere, M.; Sessler, J. L.; Gebauer, A.; Lynch V. *Chem. Commun*. **1998**, 85.
6. Anzenbacher, P., Jr.; Jursı´kova´, K.; Lynch, V. M.; Gale, P. A.; Sessler, J. L. *J. Am. Chem. Soc*. **1999**, *121*, 11020.
7. Manahan, S. *Toxicoligical chemistry.* Lewis Publishers inc. **1992.**
8. Lindoy, L. F. *The Chemistry of Macrocyclic ligand Complexes,* Cambridge University Press. **1989**.
9. *Heavy Metals Release in Soils.* Edited by H. Magdi, Selim and Donald L. Sparks. **2001.**
10. Krik, K. L. *Biochemistry of Halogens and Inorganic Halides;* Plenum Press: New York, **1991**, p 591.
11. Beer, P. D.; Hopkins, P. K.; McKinney, J. D. *Chem. Commun*. **1999**, 1253–1254.
12. (a) Matsumoto, H.; Shinkai, S. *Chem Letters*. **1994**, 2431; (b) Beer, P. D.; Gale, P. A. *Angew. Chem., Int. Ed*. **2001**, 40, 486.
13. (a) de Silva, A. P.; Gunaratne, H. Q. N.; Gunnlaugsson, T.; Huxley, A. J. M; McCoy, C. P.; Rademacher, J. T.; Rice, T. E. *Chem. Re*V.**1997**, *97*, 1515; (b) Kim, S. H.; Kim, H. J.; Yoon, J.; Kim, J. S. *Calixarenes in the Nanoworld*; Vicens, J.; Harrowfield, J., Eds.; Springer: Dordrecht, The Netherlands, **2007.** Chapter 15; (c) Desvergne, J.-P., Czarnik, A. W., Eds. *Chemosensors of Ion and Molecule*

Recognition; NATO ASI Series; Kluwer Academic: Dordrecht, The Netherlands, **1997**.

14. Valeur, B.; Bardez, E. *Chem. Br*. **1995**, *31*, 216.

15. Buhlmann, P.; Pretsch, E.; Bakker, E. *Chem. Rev*. **1998**, *98*, 1593.

16. Bianchi, E., Bowman-James, K., Garcı´a-Espan˜a, E., Eds. *Supramolecular Chemistry of Anions*; Wiley-VCH: New York, **1997**.

17. Zolotov, A. Yu. *Macro cyclic Compounds in Analytical Chemistry* Wiley: New York, **1997**.

18. Ludwig, R.; Dzung, T. k. *Sensors*. **2002**, *2*, 397.

19. Fabbrizzi, L.; Poggi, A. *Chem. Soc. Re*V**. 1995**, 197.

20. Valeur, B.; Bourson, J.; Pouget, J.; Czarnik, A. W. *Fluorescent Chemosensors for Ion and Molecule Recognition*; ACS Symposium Series 538; American Chemical Society: Washington, DC, **1993**; p 25.

21. Roundhill, D. M. *Extraction of Metals from Soils and water*. **2001**.

22. Sidgwick, N. V. *The Chemical Elements and Their Compounds.* Oxford University Press, London, **1950**, *Vol 1*.

23. Philips, C. S. G.; Williams, R. J. P. *Inorganic Chemistry*. Clarendon Press, Oxford, **1966**, *Vol 2.*

24. Doyle, D. A.; Cabral, J. M.; Pfuetzner, R. A.; Kuo, A.; Gulbis, J. M.; Cohen, S. L.; Chait, B. T.; MacKinnon, R. *Science.* **1998.** *280*, 69.

25. Gokel, G. W. *Chem. Commun***. 2000**, 1

26. Mendoza, J. De.; Cuevas, F.; Prados, P.; Meadows, E. S.; Gokel, G. W. *Angew. Chem*. **1998,** *110*, 1650.

27. Tanake, Y.; Kobuke, Y.; Sokabe, M. *Angew. Chem Int. Ed. Engl.* **1995**, *34*, 693.

28. Iwamoto, K.; Shinkai, S. *J. Org. Chem*. **1992**, *116*, 3102.

29. Dijkstra, P. J.; Brunink, J. A. J.; Bugge, K.-E.; Reinhoudt, D. N.; Harkema, S.; Ungaro, R.; Ugozzoli, F.; Ghidini, E. *J. Am. Chem. Soc.* **1989**, *111*, 7567.

30. Beer, P. D.; Gale, P. A.; Chen, Z.; Drew, M. G. B.; Heath, J. A.; Ogden, M. I.; Powell, H. R. *Inorg. Chem*. **1997**, *36*, 5880.

31. Brewer, K. *J. Am. Chem. Soc.* **1938**, *60*, 691.

32. Anderson, C. J.; Welch, M. J. *Chem. Rev.* **1999**, *99*, 2219.

33. *Radioactive Waste Management and Disposal.* Cecille, L., Ed.; Elsevier: New York, **1991.**

34. Hill, C.; Dozol, J.-F.; Lamare, V.; Rouquette, H.; Eymard, S.; Tournois, B.; Vincens, J.; Asfari, Z.; Bressot, C. *J. Inclusion Phenom. Mol. Recognit. Chem*. **1994,** *19*, 399.

35. McDowell, W. J.; Case, G. N.; McDonough, J. A.; Bartsch, R. A. *Anal. Chem*. **1992**, *64*, 3013.

36. Eiichi, K.; Koike, T. *Chem. Soc. Rev.* **1998,** *27*, 179–184.

37. Ngwendson, J. N.; Amiot, C. L.; Srivastava, D. K.; Banerjee, A. *Tetrahedron Lett.* **2006**, *47*, 2327.

38. Bush, A. L. *Trends Nurosci*. **2003**, *26*, 207.

39. Linder, M. C.; Hazegh-Azam, M. *Am. J. Clin. Nutr*. **1996**, *63*, 797S.

40. Uauy, R.; Olivares, M.; Gonzalez, M. *Am. J. Clin. Nutr.* **199**8, *67*, 952S.

41. Rifai, N.; Cohen, G.; Wolf, M.; Cohen, L.; Faser, C.; Savory, J.; DePalma, L. *Ther. Drug Monit*. **1993**, *15*, 71.

42. Mottet, N. K.; Vahter, M. E.; Charleston, J. S.; Friberg, L. T. *Met. Ions Biol. Syst*. **1997**, *34*, 371.

43. Davidson, P. W.; Myers, G. J.; Cox, C.; Axtell, C.; Shamlaye, C.; Sloane-Reeves, J.; Cernichiari, E.; Needham, L.; Choi, A.; Wang, Y.; Berlin, M.; Clarkson, T. W. *J. Am. Med. Assoc.* **1998**, *280*, 701.

44. Hennrich, G.; Sonnenschein, H.; Resch-Genger, U. *J. Am.Chem. Soc*. **1999**, *121*, 5073.

45. Kirk, K. L. *Biochemistry of Halogens and Inorganic Halide*s. Plenum Press: New York, **1991**

46. Martinez-Manez, R.; Sancenon, F. *Chem. Rev*. **2003**, *103*, 4419.

47. Lehn, J. –M. *Science,* **1985**, *227,* 4689.

48. Desiraju, G. R. *Angew. Chem., Int. Ed*. **1995**, *34*, 2311.

49. Lehn, J. –M. *Science,* **2000,** *295***,** 2403**.**

50. Conn, M. M.; Rebek, J. *Chem. Rev*. **1997,** *97***,** 1647.

51. Cui, Y.; Ngo, H. L.; lin, W. *Inorg. Chem.* **2002**, *41*, 5940.

52. Li, Y.; Hao, N.; Wang, E.; Yuan, M.; Hu, C.; Hu, N.; Jia, H. *Inorg. Chem.* **2003**, *42*, 2729.

53. Lehn, J. M. *Science,* **1985,** *227***,** 849.

54. Bajaj, A. V.; Poonia, N. S. *Coord. Chem. Rev*. **1988***, 87*, 55.

55. Izatt, R. M.; Pawlak, K.; Bradshaw, J. S. *Chem. Rev*. **1991**, *91*, 1721.

56. *Comprehensive Co-ordination Chemistry, The Synthesis, Reactions, Properties & Applications of Coordination Compounds,* edited in chief Sir Geoffrey Wilkinson. Frs. *Vol. 2.* 931.

57. Izatt, R. M.; Bradshaw, J. S.; Nielsen, S. A.; lamb, J. D.; Christensen, J. J. *Chem. Rev*. **1985,** *85*, 271.

58. Kaneda, T.; Sugihara, K.; Kamiya, H.; Misumi, S. *Terahedront. Lett.* **1981,** *22,* 4407.

59. Zhang, X. X.; Izatt, R. M.; bradshaw, J. S.; Krakowiak, K. E. *Coord. Chem. Rev*. **1998**, *174*, 179.

60. Buhlmann, P.; Pretsch, E.; Bakker, E. *Chem. Rev*. **1998**, *98*, 1593.

61. Gokel, G. W.; Mukhopadhyay, A. *Chem. Soc. Rev.* **2001**, *30*, 274.

62. Lehn, J. M. *Angew. Chem., Int. Ed. Engl.* **1988**, *27*, 89.

63. Gutsche, C. D. *Calixarenes, Monograph in supramolecular Chemistry, Stoddort, J. F. Ed. The Royal Society of Chemistry*. Cambridge, U. K. **1989.**

64. Ikeda, A.; shinkai, S. *Chem. Rev*. **1997**, *97*, 1713.

65. Bohmer, V. *Angew. Chem., Int. Ed. Engl.* **1995**, *34,*713.

66. Namor, A. F. D. de.; Cleverly R. M.; Ormachea, M. L. *Z. Chem. Rev*. **1998**, *98*, 2495.

67. Diamond, D.; Mckervey, M. A. *Chem. Soc. Rev.* **1996,** 15.

68. Kim, S. K.; Lee, J. K.; Lee, S. H.; Lim, Mi. S.; Lee, S. W.; Sim, W.; Kim, J. S. *J. Org Chem.* **2004**, *69*, 2877.

69. Guillon, J.; Leger, J-M.; Sonnet, P.; Jarry, C.; Robba, M. *J. Org. Chem.***2000,** *65,* 8283.

70. Gutsche, C. D.; Iqbal, M. *Organic Syntheses*, **1990**, *68*, 234.

71. Shinkai, S. *Tetrahedron.* **1993**, *49*, 8933.

72. Rudkevich, D. M. *Chem. Euro. J*. **2000**, *6*, 2679.

73. Zheng, Y.-S.; Zhang,C.; Tian, Z.-F.; Jang, A. *Synth. Commun*. **2004**, *34*, 679.

74. *Calixarenes Revisited;* Gutsche, C. D., Ed.; The Royal Society of Chemistry: Cambridge, **1998.**

75. Gaeta, C.; De Rosa, M.; Fruilo, M.; Soriente, A.; Neri, P.*Tetrahedron: Asymmetry.* 2005, *16*, 2333.

76. (a) Ghidini, E.; Ugozzoli, F.; Ungaro, R.; Harkema, S.; El-Fadl, A. A.; Reinhoudt, D. N. *J. Am. Chem. Soc.*, **1990**, *112,* 6979; (b) Casnati, A.; Pochini, A.; Ungaro, R.; Ugozzoli, F.; Arnaud, F.; Fanni, S.; Schwing, M-J.; Egberink, R. J. M.; Jong, F. de.; Reinhoudt, D. N. *J. Am. Chem. Soc.*, **1995**, *117,* 2767; (c) Ikeda, A.; Tsudera, T.; Shinkai, S. *J. Org. Chem.***1997**, *62*, 3568; (d) Takahashi, K.; Gunji, A.; Guillaumont, D.; Pichierri , F.; Nakamura, S. *Angew. Chem.*, **2000**, *39*, 2925; (e) Luo, J.; Zheng, Q.-Y.; Chen, C.-F.; Huang, .; Z.-T. *Chem.–Eur. J.*, **2005**, *11*, 5917.

77. Ikeda, A.; Shinkai, S. *J. Org. Chem.* **1997,** *62,* 3568.

78. Zhou, H.; Surowiec, K.; Purkiss, D. W.; Bartsch, R. A. *Org. Biomol. Chem.* **2005**,*3,*1676.

79. Ghidini, E.; Ugozzoli, F.; Ungaro, R.; Harkema, S.; EI-Fadi, A. A.; Reinhoudt, D. N. *J. Am. Chem. Soc*. **1990**, *112*, 6979.

80. Zhou, H.; Liu, D.; Gega, J.; Surowiec, K.; Purkiss, D. W.; Bartsch, R. A. *Org. Biomol. Chem.* **2007***, 5,* 324.

81. Agnihotri, P.; suresh, E.; Paul, P.; Ghosh, P. K. *Eur. J. Inorg. Chem.* **2006**, 3369.

82. Prodi, L.; Bolletta, F.; Montalti, M.; Zaccheroni, N.; Casnati, A.; Sansone, F.; Ungaro, R. *New J. Chem.* 2000, *24*, 155.

83. Jaiyu, A.; Rojanathanes, R.; Sukwattanasinitt, M. *Terahedront. Lett***.** **2007**, *48*, 1817.

84. Evans, A. J.; Beer, P. D. *Dalton Trans*. **2 0 0 3**, 4 4 5 1.

85. Casnati, A.; Massera, C.; Pelizzi, N.; Stibor, I.; Pinkassik, E.; Ugozzoli, F.; Ungaro, R. *Tetrahedron. Lett***. 2002**, *43*, 7311.

86. Chawla, H. M.; Sahu, S.N. Shrivastava, R. *Tetrahedron. Lett***. 2007**, *48*, 6054.

87. Matthews, S. E.; Felix, V.; Drew, M. G. B.; Beer, P. D. *Org. Biomol. Chem.* **2003**,*1,* 1232.

88. (a) Matthews, S. E.; Schmitt, P.; Felix, V.; Drew, M. G. B.; Beer, P. D. *J. Am. Chem. Soc*. **2002**, *12*4, 1341; (b) Webber, P. R. A.; Cowley, A.; Drew, M. G. B.; Beer, P. D. *Chem. Eur. J*. **2003,** *9,* 2439.

89. Kim, S. K.; Vicens, J.; Park, K-Min.; Lee, S. S.; Kim, J.S. *Tetrahedron. Lett***. 2003**, *44*, 993.

90. Lee, J. K.; Kim, S. K.; Bartsch, R. A.; Vicens, J.; Miyano, S.; Kim, J. S. *J. Org. Chem.* **2003**, *68*, 6720.

91. Lee, J. K.; Kim, S. K.; Lee, S. H.; Thuery, P.; vicens, J.; kim, J. S. *Bull. Korean Chem. Soc*. **2003**, *24,* 524.

92. Kim, S. K.; Lee, J. K.; Lee, S. H.; Lim, Mi. S.; Lee, S. W.; Sim, W.; Kim, J. S. *J. Org. Chem.* **2004**, *69*, 2877.

93. Zyryanov, G. V.; Rudkevich, D. M. *J. Am. Chem. Soc*. **2004**, *126*, 4264.

94. Ji, H.-F.; Brown, G. M.; Dabestani, R. *Chem. Commun.* **1999**, 609.

95. Kim, J. S.; Shon, O. J.; Rim, J. A.; Kim, S. K.; Yoon, J. *J. Org. Chem.* **2002**, *67*, 2348.

96. Kim, J. S.; Noh, K. H.; Lee, S. H.; Kim, S. K.; Kim, S. K.; Yoon. J. *J. Org. Chem.* **2003**, *68*, 597.

97. Ji, H.F.; Dabestani, R.; Brown, G. M. *J. Am. Chem. Soc.* **2000**, *122*, 9306.

98. Aoki, I.; Sakaki, T.; Shinkai, S. *J. Chem. Soc., Chem. Commun.* **1992**, 730.

99. Lee, J. Y.; Kim, S. K.; Jung, J. H.; Kim, J. S. *J. Org. Chem.* **2005**, *70*, 1463.

100. Lee, S. H.; Kim, S. H.; Kim, S. K.; Jung, J. H.; Kim, J. S. *J. Org.Chem.* **2005**, *70*, 9288.

101. Bu, J.H.; Zheng, Q.-Y.; Chen, C.-F.; Huang, Z.-T. *Org. Lett.* **2004**, *6*, 3301.

102. Chen, Q.Y.; Chen, C.-F. *Tetrahedron Lett.* **2005**, *46*, 165.

103. Banthia, S.; samanta, A. *Org. Biomol. Chem.* **2 0 0 5**, ***3*** , 1 4 2 8.

104. Kim, S. K.; Bok, J. H.; Bartsch, R. A.; Lee, J. Y.; Kim, J. S. *Org. Lett.* 2005, 7, 4839.

105. Lee, S. H.; Kim, H. J.; Lee, Y. O.; Vicens, J.; Kim, J. S. *Tetrahedron Lett.* **2006**, *47*, 4373.

106. Leray, I.; Lefevre, J.-P.; Delouis, J.-F.; Delaire, J.; Valeur, B. *Chem.Eur. J.* **2001**, *7*, 4590.

107. Leray, I.; Asfari, Z.; Vicens, J.; Valeur, B. *J. Chem. Soc., Perkin Trans. 2.* **2002**, 1429.

108. Matsumoto, H.; Shinkai, S. *Tetrahedron Lett.* **1996**, *37*, 77.

109. Kim, S. K.; Kim, S. H.; Kim, H. J.; Lee, S. H.; Lee, S. W.; Ko, J.; Bartsch, R. A.; Kim, J. S. *Inorg. Chem.* **2005**, *44*, 7866.

110. Jin, T. *Chem. Commun.* **1999**, 2491.

111. Lee, S. H.; Kim, S. K.; Bok, J. H.; Lee, S. H.; Yoon, J.; Lee, K.; Kim, J. S. *Tetrahedron Lett.* **2005**, *46*, 8163.

112. Lee, M. H.; Quang, D. T.; Jung, H. S.; Yoon, J.; Lee, C-H.; Kim, J. S. *J. Org. Chem.* **2007**, *72*, 4242.

113. Beer, P. D.; Timoshenko, V.; Maestri, M.; Passaniti, P.; Balzani, V. *Chem. Commun.* **1999**, 1755.

114. Cooper, J. B.; Drew, M. G. B.; Beer, P. D. *J. Chem. Soc*., *Dalton Trans*., **2000**, 2721.

115. Cooper, J. B.; Drew, M. G. B.; Beer, P. D. *J. Chem. Soc*., *Dalton Trans*., **2001,** 392.

116. Grigg, R.; Holmes, J. M.; Jones, S. K.; Norbert, W. D. J. A. *J. Chem. Soc*., *Chem. Commun.* **1994,** 185.

Chapter-II

Synthesis, characterization, electrochemistry and ion-binding studies of ruthenium(II) bipyridine receptor molecules containing calix[4]arene-azacrown as ionophore

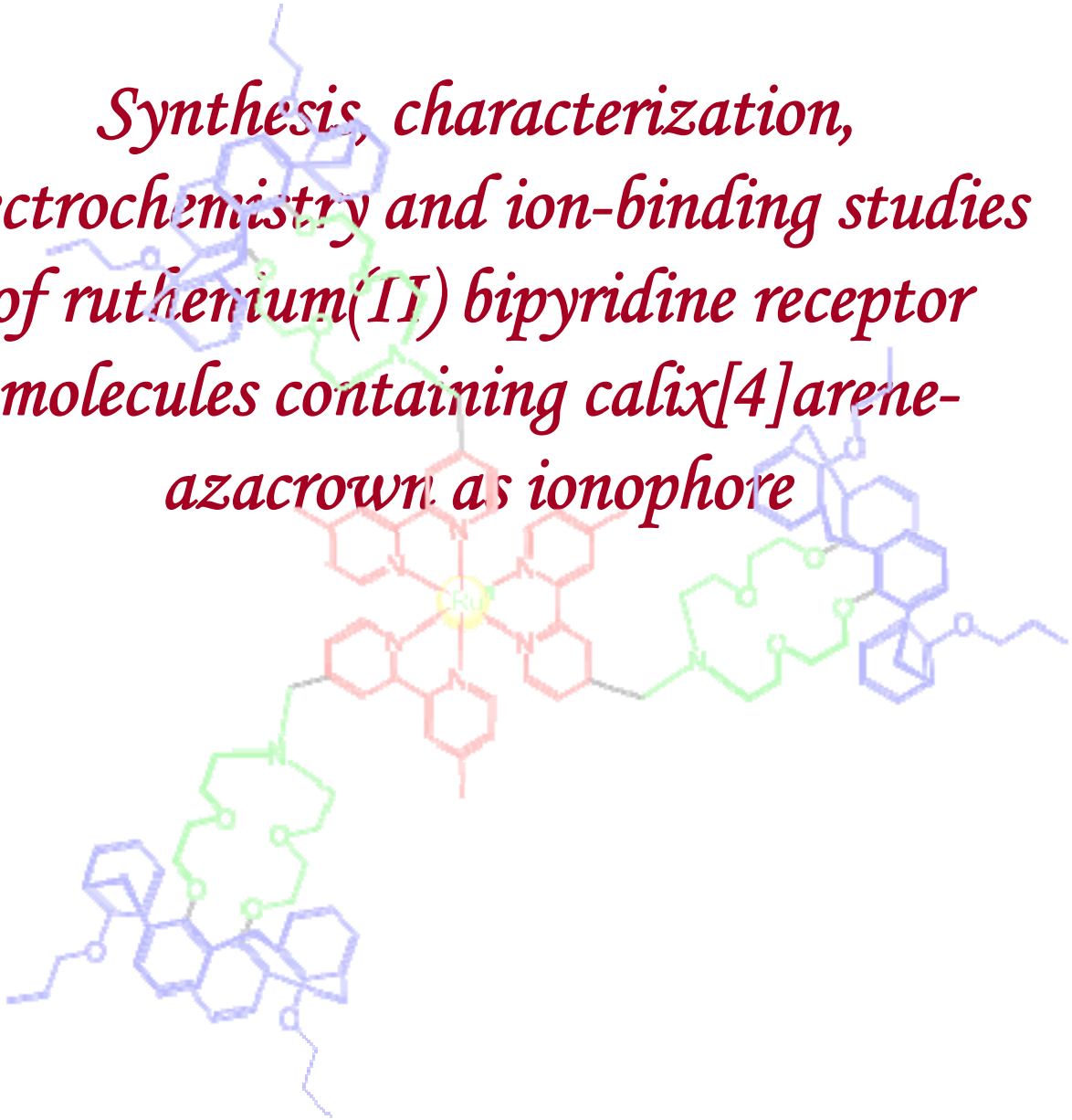

2.1. Introduction

In *Chapter – I*, the growing importance of calixarenes as ionophore have been described and literature survey on some of the specific aspects has been done. It has also been pointed out that this chemistry has become more versatile because of the ease with which calix[4]arene can be modified with various functional groups and these modified calixarenes provide a highly preorganized architecture for the assembling of converging binding sites.[1] Incorporating crown ethers into calix[4]arene a new class of hybrid molecule has been developed, which attracted intense interest as receptors, specially for alkali and alkaline earth metal ions.[2]

For designing fluoroionophores, Ru(II)-bipyridine moiety, which exhibits strong absorption band in the near UV-Vis region and an intense emission band in the visible region, has also been used as luminescent fragment for many receptors. Though Ru(II)-bipyridine moiety has been widely used for the fluorophore containing crown ethers, however, it has rarely been used in calixarene containing ionophores.[3] A few examples are available where the Ru(II)-bipyridine unit is connected to the lower rim of the calixarene moiety through some spacer, but to the best of our knowledge no fluoroionophore so far has been reported in which the Ru(II)-bipyridine unit is covalently attached to the nitrogen atom of the azacrown ring of the calix[4]azacrown ionophore.[4] Ru(II)-bipyridine as fluorophore possess some advantages over the organic luminescent molecules in the event of ion recognition process, beside change in fluorescence, the former may also exhibit electrogenerated chemiluminesence (ECL) and change in the oxidation potential of metal ion.[3c,3f,3g,3i] It is often observed that selectivity is reported on the basis of a particular method of detection, e.g. change in the emission intensity for a fluoroionophore.[5] However, recent reports indicate that response of complex formation also depends on methods of detection, the same receptor shows selectivity towards Cu^{2+} in UV-vis, Pb^{2+} and Cu^{2+} in fluorescence, Hg^{2+} in electrogenerated chemiluminesence (ECL) and Pb^{2+} in electrochemical study.[3f-3h] NMR is also a powerful technique to determine selectivity.[3h]

In this chapter, synthesis, characterization, electrochemical behavior and ion binding property of a number of fluoroionophores comprising Ru(II)-bipyridine unit as fluorophore and calix[4]arene-azacrown hybrid molecule as ionophore is reported. The cavity size of the ionophore is varied by incorporating azacrown-5, azacrown-6 and also biscrown moiety. Cation-binding property of these receptors with a large number of metal ions studied with different methods of detection is reported. The binding constants of metal ions and stoichiometries of the complexes determined by fluorescence and NMR titration data are also reported, along with a detail discussion on the ion-recognition behavior of the receptors and sensitivity of the methods of detection towards recognition of various ions.

2.2. Experimental

2.2.1. Materials and measurements

The compounds 2,2'-bipyridine, 4,4'dimethyl 2,2'-bipyridine, *p*-toluene sulfonamide, ammonium hexafluorophosphate, tetrabutylammonium tetrafluoroborate and all the perchlorate salts used in this study were purchased from Alfa Aesar (Johnson Matthey Company). Hydrated ruthenium trichloride was purchased from Arora Matthey. Neutral alumina and silica gel were obtained from the National Chemical Co. All other reagents used in this study were purchased from S.D. Fine Chemicals. All organic solvents were analytical grade and were used as received for synthetic purpose. Solvents for spectral and electrochemical studies were freshly purified by standard procedures before use.[6] The reagents 2-(2-chloroethoxy)ethyl 4-methylbenzenesulfonate, 2-(2-(2-chloriethoxy)ethoxy)ethyl 4-methylbenzenesulfonate and tetraethylene glycol ditosylate were prepared following the literature procedures.[7] The starting compounds *p-tert*-butylcalix[4]arene,[8] calix[4]arene,[9] 25,27-dipropyloxy calix[4]arene,[2b] calix[4]arene monocrown-5,[10] *cis*-$[Ru(bpy)_2Cl_2].2H_2O$[11] and 4-(bromomethyl)-4'-methyl-2,2'-bipyridine[12] were synthesized following the literature procedures.

Elemental analyses (C, H, and N) were performed on a model 2400 Perkin-Elmer elemental analyzer. Mass spectra were recorded on a Q-TOF Micro^{TM} LC-MS instrument. Infrared spectra were recorded on a Perkin-Elmer spectrum GX FT-system as

KBr pellets. NMR spectra were recorded on models DPX 200 and Avance II 500 Brucker FT-NMR instruments. The UV/vis spectra were recorded on a UV-3101PC (Shimadzu) spectrophotometer. Luminescence spectra were recorded on a model Fluorolog Horiba Jobin Yvon spectrofluorimeter at room temperature. Luminescence quantum yields were measured in optically diluted solution, using $[Ru(bpy)_3]^{2+}$ in oxygen-free acetonitrile (ϕ= 0.062) as reference emitter.[13,14] Electrochemical measurements were carried out using CHI 660A electrochemical workstation equipment. Cyclic and differential pulse voltammetry (DPV) studies were carried out in a three-electrode cell consisting of a platinum working electrode, a platinum-wire auxiliary electrode, and an SCE reference electrode. Solutions of the complexes in purified acetonitrile containing 0.1M tetrabutylammonium tetrafluoroborate as supporting electrolyte were deaerated by bubbling nitrogen for 10 min prior to each experiment.

Caution: Perchlorate salts of metal ions are potentially explosive. So they should be handled with great care.

2.2.2. Synthesis of ligands

The intermediate compounds **B** – **G** were synthesized by modification of literature procedures.[2f] Description for the synthesis of **B** and the modifications made for synthesis of other compounds along with mass data are given below. Micro analytical (C, H and N) and ^{1}H NMR data of these compounds are similar to the reported values.[2f]

25,27-Bis(1-propyloxy)-26,28-bis(5-chloro-3-oxapentyloxy) calix[4]arene, 1,3-Alternate (B)

A solution of 1,3-dipropyl calix[4]arene (**A**) (1.53 g, 3 mmol), 2-(2-chloroethoxy)-ethanol *p*-toluenesulfonate (1.67 g, 6 mmol), and Cs_2CO_3 (3.91 g, 12 mmol) in 100 mL of freshly distilled acetonitrile was heated at reflux for 32 h under nitrogen. The reaction mixture was allowed to cool to room temperature and evaporated to dryness by rotary evaporation. To the residue dilute HCl (10%, 150 mL) and CH_2Cl_2 (100 mL) were added and the organic phase was separated and washed with water (100 mL, 3 times). The

organic layer was dried over anhydrous sodium sulfate and evaporated to afford brownish oil. Column chromatography on silica gel (100-200 mesh) with ethyl acetate/hexane (1:8) as an eluent provided **B** as white solid. Yield: (1.54 g, 71%). MS (*m/z*): calcd for [**B** + K^+], 759.26; found, 759.81(32%); calcd for [**B** + Na^+], 743.29; found, 743.83 (100%).

25,27-Bis(8-chloro-3,6-dioxaoctyloxy)-26,28-bis(1-propyloxy) calix [4]arene, 1, 3-Alternate (C)

This compound was prepared following the same procedure as described above for **B**. Yield: (80%). MS (*m/z*): calcd for [**C** + K^+], 847.31; found, 847.69 (75%); calcd for [**C** + Na^+], 831.34; found, 831.70 (100%).

***N*-Tosyl 25,27-Bis(1-propyloxy)calix[4]arene azacrown-5 (D)**

This compound was prepared following the similar procedure as described in the literature, except purification of the compound in the final step.[2f] It was done by recrystallization from diethyl ether by slow evaporation at low temperature, which gave crystalline compound. Yield: (70%). MS (*m/z*): calcd for [**D** + K^+], 858.34; found, 858.59 (70%); calcd for [**D** + Na^+], 842.37; found, 842.61 (100%).

***N*-Tosyl 25,27-Bis(1-propyloxy)calix[4]arene azacrown-7, 1,3-Alternate (E)**

This compound was prepared following the same procedure as described above for **D**. Yield: (75%). MS (*m/z*): calcd for [**E** + K^+], 946.40; found, 946.87 (22%); calcd for [**E** + Na^+], 930.42; found, 930.88 (100%).

25,27-Bis(1-propyloxy)calix[4]arene azacrown-5, 1,3-Alternate (F)

This compound was prepared following the literature procedure except the reaction mixture was refluxed for 40 h during which 0.5 mL of methanol was added in each 6 h interval and the compound was purified by column chromatography using silica gel (100-200 mesh) as column material and ethyl acetate/hexane (1:1) as eluent. Yield: (58%). MS (*m/z*): calcd for [**F** + K^+], 704.34; found 704.38 (50%); calcd for [**F** + H^+], 666.38; found, 666.41 (100%).

25,27-Bis(1-propyloxy)calix[4]arene azacrown-7, 1,3-Alternate (G)

This compound was prepared following the same procedure as described above for **F**. Yield: (50%). MS (*m/z*): calcd for [**G** + K^+], 792.39; found 791.92 (82%); calcd for [**G** + Na^+], 776.41; found, 775.89 (78%); calcd for [**G** + H^+], 754.43; found, 754.06 (100%).

25,27-Bis(1-propyloxy)calix[4]arene azacrown-5 bipyridine, 1,3-Alternate (L^1)

To a stirring mixture of 0.33 g (0.5 mmol) of **F** and 0.22 mL (3 mmol) of triethylamine in dry THF (60 mL) was added dropwise 0.263 g (1 mmol) of 4-(bromomethyl)-4'-methyl-2,2'-bipyridine dissolved in dry THF (30 mL) over a period of 1 h at 0˚C under nitrogen atmosphere. After complete addition, the temperature of the reaction mixture was maintained at 0˚C for additional 2 h with stirring, after which it was heated to reflux for 36 h. The reaction mixture was then allowed to cool to room temperature and the solvent was removed by rotary evaporation. To the solid mass thus obtained was added 70 mL of water and the mixture was extracted three times with CH_2Cl_2 (50 mL each time). The combined extracts were dried over anhydrous Na_2SO_4, filtered and evaporated to dryness. The residue was dissolved in minimum volume of chloroform (2 mL), the residue was loaded onto a silica gel column (100-200 mesh, deactivated with hexane with 10% Et_3N and washed with hexane before use) and was eluted with ethyl acetate. After evaporation of the solvent the semisolid mass (**L^1**) was dried in vacuo. Yield: (0.25 g, 60%). Elemental analysis: calcd for $C_{54}H_{61}N_3O_6$: C, 76.47; H, 7.25; N, 4.95; found: C, 75.81; H, 7.38; N, 4.74. ^{1}H NMR ($CDCl_3$) δ = 0.71 (t, *J = 7.4*, 6H), 1.23 (m, 4H), 2.45 (s, 3H), 2.67 (t, *J = 5.0*, 4H), 3.36-3.43 (m, 12H), 3.53 (t, *J = 4.4*, 4H), 3.75 (s, 2H), 3.80 (s, 8H), 6.76-6.89 (m, 4H), 7.03 (d, *J = 7.4*, 4H), 7.10 (d, *J = 7.4*, 4H), 7.14 (overlapped d, 1H), 7.42 (d, *J = 4.0*, 1H), 8.25 (s, 1H), 8.38 (s, 1H), 8.56 (d, *J = 4.8*, 1H), 8.66 (d, *J = 4.8*, 1H). MS (*m/z*): calcd for [**L^1** + K^+], 886.41; found, 886.83 (100%); calcd for [**L^1** + Na^+], 870.44; found, 870.85 (90%); calcd for [**L^1** + H^+], 848.46; found 848.86 (35%).

25,27-Bis(1-propyloxy)calix[4]arene azacrown-7 bipyridine, 1,3-alternate (L^2)

This compound was prepared following the same procedure as described above for **L^1** using compound **G** as starting material instead of **F**. Yield: (52%). Elemental analysis: calcd for $C_{58}H_{69}N_3O_8$: C, 74.41; H, 7.43; N, 4.48; found: C, 73.82; H, 7.50; N, 4.31. ^{1}H

NMR [$CDCl_3$] δ = 0.79 (t, *J = 7.4*, 6H), 1.32-1.47 (m, 4H), 2.44 (s, 3H), 2.89 (t, *J = 5.4*, 4H), 3.42-3.68 (m, 24H), 3.72 (s, 8H), 3.84 (s, 2H), 6.72-6.83 (m, 4H), 7.01 (d, *J = 7.4*, 4H), 7.10 (overlapped d, 1H), 7.12 (d, *J = 7.4*, 4H), 7.46 (d, *J = 4.4*, 1H), 8.23 (s, 1H), 8.34 (s, 1H), 8.55 (d, *J = 4.8*, 1H), 8.63 (d, *J = 4.8*, 1H). MS (*m/z*): calcd for [$\mathbf{L^2}$ + Na^+], 958.49; found, 958.89 (100%); calcd for [$\mathbf{L^1}$ + H^+], 936.51; found, 936.89 (32%).

26,28-bis(5-chloro-3-oxapentyloxy)-calix[4]arene-monocrown-5 (I), N-Tosyl-azacrown-5-calix[4]arene-crown-5 (J), and azacrown-5-calix[4]arene-crown-5 (K) These three compounds were synthesized following the published procedures.[10,5d] Elemental analysis (C, H and N) and ^{1}H NMR data of **I-K** are similar to those reported in the literature. MS (*m/z*): for **I**, calcd for [**I** + K^+], 833.26; found, 833.44 (100%); calcd for [**I** + Na^+], 817.29; found, 817.47 (60%); for **J**, MS (*m/z*): calcd for [**J** + K^+], 932.34; found, 932.60 (100%); and for **K**, MS (*m/z*): calcd for [**K** + K^+], 778.33; found, 778.36 (85%); calcd for [**K** + Na^+], 762.36; found, 762.50 (75%); calcd for [**K** + H^+], 740.38; found, 740.45 (100%).

Calix[4]arene-crown-5-azacrown-5-bipyridine (L^3)

This compound was synthesized following the same procedure as described for $\mathbf{L^1}$ starting from **K** instead of **F**. Yield: (53%). Elemental analysis: calcd for $C_{56}H_{63}N_3O_9$: C, 72.94; H, 6.88; N, 4.56; found: C, 72.06; H, 6.78; N, 4.35. ^{1}H NMR [$CDCl_3$] δ = 2.45 (s, 3H), 2.66 (br, 4H), 3.12 (m, 4H), 3.28 (m, 8H), 3.45-3.62 (m, 16H), 3.76 (s, 2H), 3.86 (s, 8H), 6.85-6.93 (m, 4H), 7.09 (d, *J = 7.4*, 4H), 7.12 (d, *J = 7.4*, 4H), 7.15 (overlapped d, 1H), 7.43 (br, 1H), 8.24 (s, 1H), 8.36 (s, 1H), 8.56 (d, *J = 4.8*, 1H), 8.65 (d, *J = 4.8*, 1H). MS (*m/z*): calcd for [$\mathbf{L^3}$ + K^+], 960.43; found, 960.48 (100%); calcd for [$\mathbf{L^3}$ + H^+], 922.46; found, 922.53 (20%).

2.2.3. Synthesis of complexes

$[Ru(bpy)_2(L^1)](PF_6)_2$ (1); $[Ru(bpy)_2(L^2)](PF_6)_2$ (2) and $[Ru(bpy)_2(L^3)](PF_6)_2$ (3)

A mixture of *cis*-$[Ru(bpy)_2Cl_2].2H_2O$ (0.13 g, 0.25 mmol) and respective ligand ($\mathbf{L^1/L^2/L^3}$, 0.25 mmol) in ethanol-water (2:1, 60 mL) was refluxed for 10 h. The reaction mixture was then allowed to cool to room temperature; volume was reduced to *ca*. 20 mL

by rotary evaporation, filtered and to the filtrate was added solid NH_4PF_6 (0.815 g, 5 mmol). The precipitate thus separated was collected by filtration washed with water and diethyl ether. The complex was purified by column chromatography using a column packed with deactivated (2% water) alumina and acetonitrile-toluene (1:1) as eluent. The small first fraction was discarded; the large orange-red colored second fraction gave the desired complex. After removing solvent, the residue was again dissolved in acetonitrile and was precipitated by vapor diffusion method using diethyl ether. Yield: 60-70%.

For **1.** Elemental analysis: calcd for $C_{74}H_{77}RuN_7O_6P_2F_{12}$: C, 57.29; H, 5.00; N, 6.32; found: C, 56.88; H, 5.08; N, 6.45. ^{1}H NMR [CD_3CN] δ = 0.78 (t, *J* = *7.4*, 6H), 1.27 (m, 4H), 2.54 (s, 3H), 2.63 (t, *J* = 5.6, 4H), 3.35-3.50 (m, 14H), 3.70-3.83 (m, 12H), 6.50 (m, 2H), 6.77 (m, 2H), 6.96 (m, 4H), 7.05 (d, *J* = 7.4, 4H), 7.20 (m, 2H), 7.38 (m, 4H), 7.50 (m, 2H), 7.67-7.78 (m, 4H), 7.91-8.08 (m, 4H), 8.36-8.53 (m, 6H). MS (*m/z*): calcd for [**1** - PF_6^-]$^+$, 1406.46; found, 1406.77 (100%); calcd for [**1**- $2PF_6^-$ + H^+]$^+$, 1262.50; found, 1262.94 (10%). UV-Vis: λ_{max}(CH_3CN)/nm (ε/dm^3 mol^{-1} cm^{-1}): 456 (14 900), 287 (82 300).

For **2**. Elemental analysis: calcd for $C_{78}H_{85}RuN_7O_8P_2F_{12}$: C, 57.13; H, 5.22; N, 5.98; found: C, 56.72; H, 5.08; N, 5.92. ^{1}H NMR [CD_3CN] δ = 0.86 (t, *J* = *7.4*, 6H), 1.51-1.62 (m, 4H), 2.54 (s, 3H), 2.86 (t, *J* = 5.3, 4H), 3.46-3.66 (m, 30H), 3.96 (s, 2H), 6.67-6.76 (m, 4H), 7.01-7.09 (m, 7H), 7.24 (d, *J* = 5.6, 2H), 7.38 (t, *J* = 6.5, 4H), 7.54 (d, *J* = 5.8, 2H), 7.64 (d, *J* = 5.8, 1H), 7.73 (m, 4H), 8.04 (t, *J* = 7.7, 4H), 8.42 (s, 1H), 8.49 (d, *J* = 8.0, 4H), 8.60 (s, 1H). MS (*m/z*): calcd for [**2** - PF_6^-]$^+$, 1494.51; found, 1495.09 (100%); calcd for [**2**- $2PF_6^-$ + H^+]$^+$, 1350.56; found, 1349.99 (15%). UV-Vis: λ_{max}(CH_3CN)/nm (ε/dm^3 mol^{-1} cm^{-1}): 456 (14 700), 288 (78 100).

For **3**. Elemental analysis: calcd for $C_{76}H_{79}RuN_7O_9P_2F_{12}$: C, 56.15; H, 4.90; N, 6.03, found: C, 56.38; H, 5.08; N, 6.05. ^{1}H NMR [CD_3CN] δ = 2.53-2.58 (m, 7H), 3.24-3.50 (m, 6H), 3.61-3.78 (m, 30H), 3.99 (s, 2H), 6.86-7.12 (m, 6H), 7.26-7.36 (m, 9H), 7.54-7.78 (m, 9H), 8.04 (m, 4H), 8.39-8.48 (m, 6H). MS (*m/z*): calcd for [**3** - PF_6^-]$^+$, 1480.46; found, 1481.71 (100%). UV-Vis: λ_{max}(CH_3CN)/nm (ε/dm^3 mol^{-1} cm^{-1}): 454 (12 600), 287 (70 100).

$[Ru(L^1)_3](PF_6)_2$ (4)

A mixture of $RuCl_3.3H_2O$ (0.058 g, 0.25 mmol) and $\mathbf{L^1}$ (0.636 g**,** 0.75 mmol) in ethanol-water (2:1, 45 mL) was refluxed under nitrogen for 12 h. The complex was then isolated and purified following the similar procedure as described for **1-3**. Yield: (0.3 g, 40%). Elemental analysis: calcd for $C_{162}H_{183}RuN_9O_{18}P_2F_{12}$: C, 66.28; H, 6.28; N, 4.29; found: C, 65.56; H, 6.08; N, 4.35. ^{1}H NMR [CD_3CN] δ = 0.76 (t, *J* = 7.4, 18H), 1.34 (m, 12H), 2.33-2.61 (m, 21H), 3.55-3.83 (m, 34H), 6.48 (m, 4H), 6.81 (t, *J* = 7.4, 8H), 6.94 (m, 8H), 7.05 (d, *J* = 7.4, 16H), 7.28-7.13 (m, 4H), 7.54-7.78 (m, 8H), 8.22-8.50 (m, 6H). MS (*m/z*): calcd for [**4** - PF_6^-]$^+$, 2789.24; found, 2789.10 (100%); calcd for [**4** - $2PF_6^-$ + H^+]$^+$, 2644.27; found, 2643.30 (80%). UV-Vis: λ_{max}(CH_3CN)/nm (ε/dm^3 mol^{-1} cm^{-1}): 463 (14 100), 288 (75 600).

2.2.4. Ion-binding study

2.2.4.1. Luminescence study

Stock solutions of the complexes **1-4** (2 x 10^{-5} M) and that of perchlorate salts (2 x 10^{-3} M) of various metal ions (Na^+, K^+, Mg^{2+}, Ca^{2+}, Cs^+, Zn^{2+}, Cd^{2+}, Hg^{2+} and Pb^{2+}) were prepared in freshly purified acetonitrile. Then 2 mL stock solution of the complex and 2 mL stock solution of each metal salts were taken in a 5 mL volumetric flask, so that the effective concentration of the complex is 1 x 10^{-5} M and that of the metal ions are 1 x 10^{-3} M (100 fold). The luminescence spectra of the resulting solutions and that of the original complex (1 x 10^{-5} M) were recorded with excitation at the absorption maxima (λ_{max}) of the MLCT band, which is 456, 456, 454, 463 nm for **1-4,** respectively. The spectra of the cation added solutions were compared with that of the original solution to ascertain the interactions of the metal ions with the ionophore.

For emission titration study, the same stock solutions of the complexes were used and the metal perchlorate solutions of desired concentration (0.4 x 10^{-5} – 2 x 10^{-3} M) were prepared by proper dilution of the stock solution. Then 2 mL of each solution were mixed in a 5 mL volumetric flask to prepare reaction mixture with 0.2 to 100 molar equivalent of the concentration of metal ion with respect to the concentration of complexes and the luminescence spectra of the resulting solutions were recorded. Binding constants and

stoichiometry of complex formation were calculated following the literature procedure as described in the Results and Discussion section.[15] The UV-Vis spectra in absence and in presence of guest metal ions (100 equiv) were also recorded.

2.2.4.2. NMR study

^{1}H NMR spectra of the complexes were recorded with 2 mg of the sample dissolved in 0.5 mL of CD_3CN. Solid perchlorate salt of various metal ions (20 equiv) was added into this solution and the spectra of the resulting reaction mixture were recorded. The spectra of the cation added solutions were compared to that of the original complexes to ascertain the interaction of the metal ion with the ionophore. On the basis of the observation of this study (details is given in the results and discussion section), three metal ions were chosen to carry out NMR titration.

Stock solutions with desired concentration of metal (Na^+, K^+ and Cs^+) perchlorate salts were prepared in acetonitrile. ^{1}H NMR of the solution containing 2 mg of the complex in 0.5 mL CD_3CN was recorded and into this solution required amount of stock solution was added by micro syringe to make the concentration of guest metal ion 0.3 to 10 equivalent of the original complex and the spectra of the resulting solutions were recorded. From the change in chemical shift of some selected signal binding constants were calculated using the literature procedure.[16,17] The stoichiometry of the complexes formed were determined by Job's plot using the NMR titration data.[3h]

2.2.4.3. Electrochemical study

To investigate the effect of guest cation on the oxidation potential of Ru(II) of the ionophores **1-4**, differential pulse voltammetry (DPV) of all these four complexes in the region +1.0 to +1.8 V were recorded in presence of 50 equivalent of Na^+, Hg^{2+} and Pb^{2+} in acetonitrile. The other experimental conditions were same as described above for recording CV and DPV for the complexes.

2.3. Results and Discussion

2.3.1. Synthesis of the ligands (L^1-L^3)

The routes followed for the synthesis of **L^1- L^3** are shown in Schemes 1 and 2, respectively. The intermediate compounds **A**-**G** (Scheme 1) and **H**-**K** (Scheme 2) were synthesized following the modified published procedures.[2f,5d,10] The ligands (**L^1-L^3**) were obtained by the reaction of 4-(bromomethyl)-4'-methyl-2,2'-bipyridine with the NH group of the aza-crown moiety of **F**, **G** and **K**, respectively. Elemental analysis (C, H and N), and ^{1}H NMR data of all these compounds are similar to those of reported values, mass spectrometric data are given in the Experimental Section and they exhibit excellent agreement with the calculated values. It may be noted that *e/m* values of all these compounds correspond to the $Na^+/K^+/H^+$ adduct, which is a well known phenomenon when LC-MS is used for the measurement of mass.[18] In the ^{1}H NMR spectra of **L^1-L^3**, the *meta*- and *para*-protons (with respect to OH substituent) of the calixarene moiety appear as doublets and triplets, respectively. In fact, two sets of signals appear for these protons, the two doublets appear in the range δ 7.01 – 7.12 and the two triplets appear in the region δ 6.72 – 6.93. The bipyridine moiety exhibits four doublets for 6, 6' (δ 8.55 – 8.66) and 5, 5' (δ 7.08 – 7.46) protons (usual numbering of bpy is used) and two singlets for 3, 3' (δ 7.08 – 7.46) protons, each one of which corresponds to one proton, as expected from unsymmetrically substituted bipyridine unit. The CH_2, which connect the bipyridine unit with aza-crown moiety, and the CH_3 attached to bipyridine unit appear as singlet in the range δ 3.75 – 3.84 and at δ 2.45, respectively. In the aza-crown moiety, the protons due to –N(CH_2)$_2$ group appear as triplet in the range δ 2.66 – 2.89, whereas other CH_2 protons of the crown ring appear as multiplets (overlapped) in the region δ 3.12 – 3.68. The Ar-CH_2-Ar protons of the calix moiety appear as a singlet in the region δ 3.72 – 3.86, the appearance of singlet for these protons suggest 1,3-alternate conformation of the calixarene moiety as shown in schemes 1 (**L^1** and **L^2**) and 2 (**L^3**).[2a,2f,5c,5e,5g] The CH_3 protons of the propyl group of **L^1** and **L^2** appear as triplet at δ 0.71 (**L^1**) and δ 0.79 (**L^2**); and the adjacent CH_2 appear as multiplet at δ 1.23 (**L^1**) and δ 1.41 (**L^2**). The OCH_2 protons of the same propyl group for **L^1** appear as triplet at δ 3.53, whereas for **L^2** the

same signal is overlapped with the signals from crown moiety. The proposed structures of $\mathbf{L^1}$ – $\mathbf{L^3}$ are shown in Schemes 1 and 2.

Scheme 1

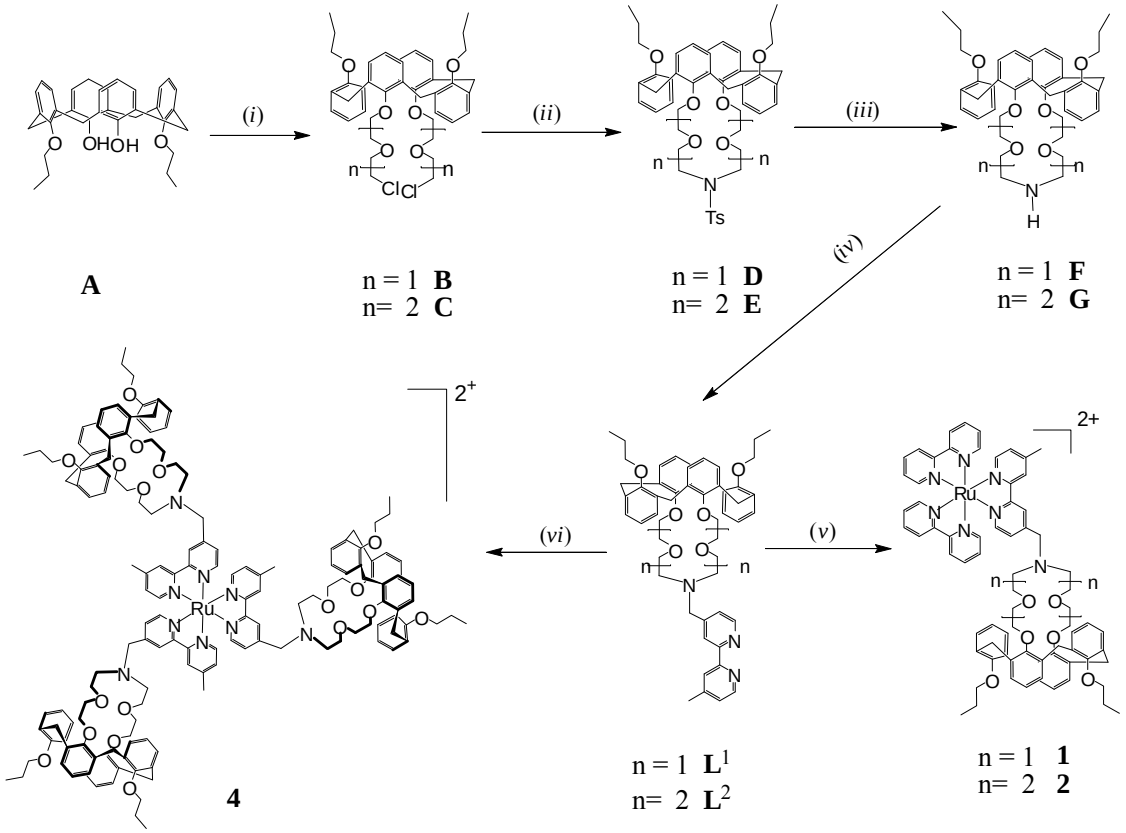

Reagents and conditions: (i) $ClCH_2(CH_2OCH_2)_nCH_2OTs$ (n = 1,2), Cs_2CO_3/ACN, reflux (ii) $TsNH_2$, K_2CO_3/DMF, reflux (iii) Na(Hg), Na_2HPO_4/dioxane and MeOH, 80^0C (iv) 4-bromomethyl-4'methyl-2,2'-bipyridine, Et_3N/THF, reflux (v) $Ru(bpy)_2Cl_2.2H_2O$, EtOH and H_2O, reflux (vi) $RuCl_3.XH_2O$, EtOH and H_2O, reflux.

Scheme 2

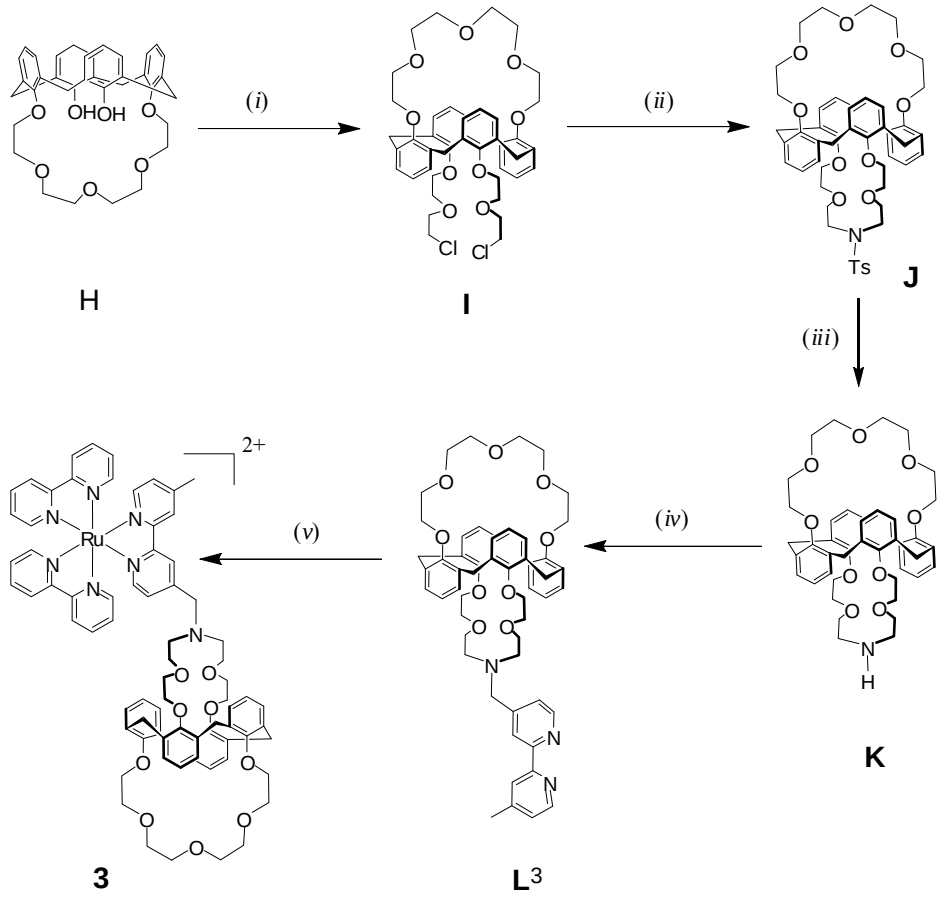

Reagents and conditions: (i) $ClCH_2CH_2OCH_2CH_2OTs$, Cs_2CO_3/ACN, reflux (ii) $TsNH_2$, K_2CO_3/DMF, reflux (iii) Na(Hg), Na_2HPO_4/dioxane and MeOH, 80^0C (iv) 4-bromomethyl-4'methyl-2,2'-bipyridyl, Et_3N/THF, reflux (v) $Ru(bpy)_2Cl_2.2H_2O$, EtOH and H_2O, reflux.

2.3.2. Synthesis of complexes (1-4)

The Ru(II) complexes were synthesized by the reaction of *cis*-$[Ru(bpy)_2Cl_2].2H_2O$ and $\mathbf{L^1/L^2/L^3}$ in refluxing ethanol-water, isolated with PF_6^- counter ion and purified by column chromatography as described in the experimental section. All of these complexes gave satisfactory C, H and N analysis. Mass spectrometry data are in excellent agreement with the calculated values. Partial view of the mass spectra of **4** is shown in Figure. 2.1.

The ^{1}H NMR spectra of complexes **1-4** were recorded in CD_3CN and all data are given in the experimental section. For complexes **1-3**, the signals due to protons of the two bipyridine units attached to Ru(II) appeared in the aromatic region along with the signals due to bpy attached to the ligands (**L^1-L^3**). In the case of complex **1**, the triplets due to the *para*-hydrogen atoms of the calix moiety are not overlapped as observed for **L^1,** they appear in well separated places at δ 6.50 and δ 6.77. One set of the *meta*-hydrogen atoms (four atoms) appear as doublet (δ 7.05) like **L^1** but the other set of four atoms are not equivalent, they appear as closely spaced doublets centering at δ 6.96. The signals due to other protons of the ligand also appear in the spectrum of the complex with slight change in chemical shifts. The Ar-CH_2-Ar protons are partially overlapped with that of crown moiety but it appears like a singlet indicating that the calixarene moiety retains it's 1,3-alternate conformation in the complex. For complex **2**, the two triplets due to *para*-protons of the calix moiety are overlapped like **L^2,** two doublets due to meta protons are also overlapped. Signals due to all other protons are similar to that of ligands with slight change in chemical shifts, indicating that there is no significant change in conformation of the calixarene moiety compared to that of the ligand. For **3**, the triplet due to the N(CH_2)$_2$ group of the azacrown moiety partially covered with the singlet due to CH_3 of the bipyridine moiety. All other signals due to two crown moieties appear as multiplets, as observed in **L^3**. In the case of **4**, the signals due to calixarene and crown moieties are similar to that of **1**, however the signals due to bpy and also CH_3 attached to bpy are fragmented and appear as multiplets, which is attributed to stereoisomerism of the complex. Octahedral metal centers with bidentate ligands generally show stereoisomerism,[13,19] in this case three unsymmetrically substituted bpy ligands coordinated to metal ion resulted in the formation of a number of stereoisomers. Since calixarene units are far away from metal centers, therefore there is a remote chance to affect the chemical shifts of these protons due to stereoisomerism at metal center, but the protons and methyl groups directly attached to the coordinated bpy is affected and the signals due to different stereoisomers are not superimposed. Because of this stereoisomerism, each signal has fragmented and appears closely, look like a multiplet. The proposed structures of **1** – **4** are shown in schemes 1 and 2.

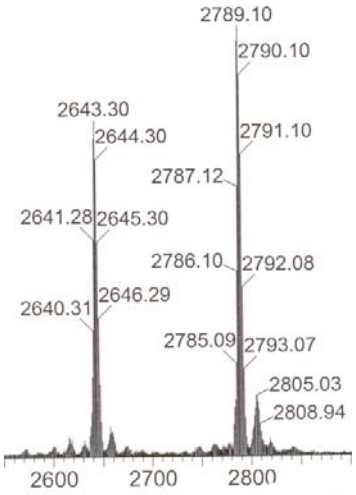

Figure. 2.1. Mass spectra of $[Ru(L^1)_3](PF_6)_2$ **(4)**.

2.3.3. Absorption and luminescence spectra

Absorption spectra of **1-4** were recorded in acetonitrile and the data are given in the experimental section. The luminescence spectra were also recorded in acetonitrile with excitation at the absorption maxima (λ_{max}) of the MLCT band, which is 456, 456, 454, 463 nm for **1-4**, respectively. Luminescence quantum yields were also measured in acetonitrile, the data for emission maxima ($\lambda_{max.em}$) and quantum yields are given in Table 2.1. In the absorption spectra, the low energy band in the region 456-463 nm is due to metal-to-ligand (bpy) charge-transfer (MLCT) transitions ($d\pi \rightarrow \pi^*$).[3h,13,20] The high-energy band around 288 nm is ligand-centered charge transfer (CT) due to $\pi \rightarrow \pi^*$ transitions.[13,20] The strong luminescence band observed in the range 613 – 618 nm (Table 1) is due to ^{3}MLCT emission.[3h,18b,13,20] The luminescence quantum yields for **1-3** are ranging from 0.0557 to 0.0564, which is close to the value for $[Ru(bpy)^3]^{2+}$ ($\phi = 0.062$) in acetonitrile, whereas for **4**, the quantum yield is considerably low (0.0478).

Table 2.1. Emission maxima, quantum yield, binding constant (K_s) with metal ions and stoichiometry of complex formation for the Ru(II) receptors.

Complex	λ_{em}	Quantum yield (ϕ)	In presence of guest metal ions			
			Metal ion	λ_{em}[1]	Binding constant (K_s) M^{-1}	Value of n[2]
1	616	0.0557	Zn^{2+}	627	$1.46 \pm 0.44 \times 10^5$	1.04 ± 0.04
			Cd^{2+}	627	$2.36 \pm 0.41 \times 10^4$	0.89 ± 0.02
			Hg^{2+}	628	$3.44 \pm 0.33 \times 10^4$	1.18 ± 0.04
2	616	0.0564	Zn^{2+}	629	$2.81 \pm 0.52 \times 10^4$	0.98 ± 0.03
			Cd^{2+}	629	$6.27 \pm 0.42 \times 10^3$	0.91 ± 0.02
			Hg^{2+}	627	$2.53 \pm 0.36 \times 10^5$	1.28 ± 0.03
			Pb^{2+}	618	$2.00 \pm 0.33 \times 10^4$	1.15 ± 0.03
3	613	0.0558	Zn^{2+}	625	$6.93 \pm 0.54 \times 10^4$	0.95 ± 0.02
			Cd^{2+}	625	$9.65 \pm 0.48 \times 10^3$	1.05 ± 0.03
			Hg^{2+}	627	$1.34 \pm 0.38 \times 10^5$	1.20 ± 0.03
			Pb^{2+}	625	$1.61 \pm 0.47 \times 10^4$	0.98 ± 0.03
4	618	0.0478	Zn^{2+}	627		
			Cd^{2+}	629		
			Hg^{2+}	627		

[1] Emission maxima (λ_{em}) of the spectra recorded in presence of maximum concentration of metal ion. [2] Stoichiometry of the complexes formed with guest metal ion.

2.3.4. Electrochemistry

Cyclic voltammograms (CV) and differential pulse voltammetry (DPV) of all complexes were recorded in acetonitrile, and the data are summarized in Table 2.2. The cyclic voltammograms of **1-3** are illustrated in Figure. 2.2. All of these complexes exhibit a

metal-based oxidation in the potential range 1.28 to 1.31 V, which are attributed to Ru(II) → Ru(III) oxidation. [3h,13,20] The oxidation potential of the metal ion in **1** and **2** is slightly higher (1.31 V) compared to that generally observed in $[Ru(bpy)_3]^{2+}$ (1.27 V).[13,19b,20] The methyl group, which has electron donating ability, is attached to one of the bpy coordinated to Ru(II), therefore it is expected to shift the oxidation potential cathodically compared to $[Ru(bpy)_3]^{2+}$. However, for **1** and **2**, it has shifted slightly anodically, which may be due the influence of some intra-/intermolecular interactions.[18b] All of these complexes also exhibit three ligand-based redox couples in the potential range -1.23 to -1.78 V (Table 2), which are assigned to sequential one-electron reduction of the three bipyridine ligands (bpy → $bpy^{\cdot -}$) coordinated to the metal ion.[3d,3f,3h,18b]

Table 2.2. Electrochemical data for complexes **1**-**4** in acetonitrile solution[a]

Complex	$E_{1/2}^{ox}$/V (ΔEp/mV)[b]	$E_{1/2}^{red}$/V (ΔEp/mV)		
1	+1.31 (113)	-1.23 (69)	-1.44 (80)	-1.70 (103)
2	+1.31 (147)	-1.23 (80)	-1.46 (106)	-1.72 (93)
3	+1.29 (119)	-1.24 (79)	-1.46 (105)	-1.72 (93)
4	+1.28 (93)	-1.32 (40)	-1.52 (124)	-1.78 (101)

[a] V *vs* SCE. [b] $E_{1/2}$ = (*E*pa + *E*pc)/2; ΔEp = *E*pa - *E*pc.

2.3.5. Cation-binding study

Cation-binding ability of the ionophores **1**-**4** have been studied using a number of metal ions Na^+, K^+, Mg^{2+}, Ca^{2+}, Cs^+, Zn^{2+}, Cd^{2+}, Hg^{2+} and Pb^{2+}. The interaction of the host with these metal ions monitored by ^1H NMR, luminescence and UV-Vis spectral changes and also by electrochemical study on oxidation potential of metal ion.

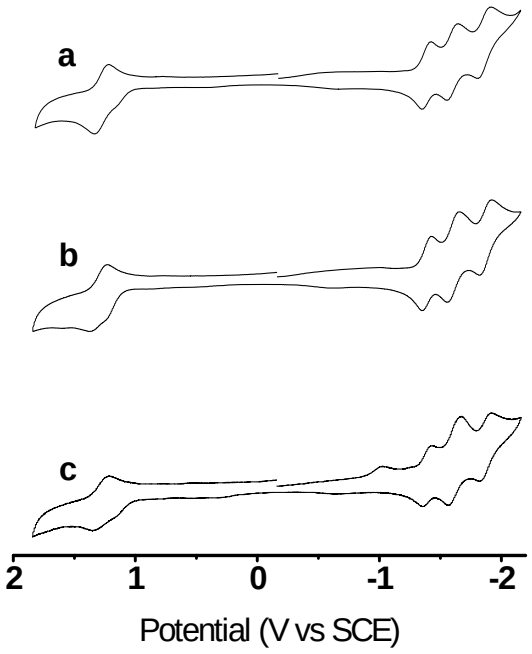

Figure. 2.2. Cyclic voltammograms of **1** (a), **2** (b) and **3** (c) recorded in acetonitrile solution.

2.3.5.1. Luminescent/UV-Vis binding studies

Luminescence spectra of all these ionophores were recorded in acetonitrile in presence of the above-mentioned metal ions. The characteristic luminescence from ^{3}MLCT state was found to increase in intensity in presence of Zn^{2+}, Cd^{2+} and Hg^{2+} (with 100 equiv) with a red shift (9-14 nm) of emission maxima for all four ionophores. Similar observation was also noted for **2** and **3** in presence of Pb^{2+}. The other metal ions studied did not induce any significant change in the emission spectra for all the four ionophores. The changes observed with the addition of increasing concentrations of Zn^{2+} for **1**, Cd^{2+} for **2**, Pb^{2+} for **3** and Hg^{2+} for **4,** respectively are shown in Figures. 2.3-2.6. The enhancement in emission intensity is attributed to the fact that complexation of metal ion with the aza-crown moiety resulted in decrease of the intramolecular reductive electron transfer quenching of the excited ruthenium state by the lone pair of the aza-N atom as it is involved in coordination with guest metal ion. The crown moiety is connected to bipyridine through a CH_2 spacer, which makes calix-crown moiety flexible with respect

to rigid $[Ru(bpy)_3]^{2+}$ unit. Because of this flexible nature and also due to lack of conjugation between donor and acceptor chromophores, the lone pair of the nitrogen atom acts as a poor reductive quencher for the ^{3}MLCT excited state. It is evident from the quantum yields of the ionophores (Table 2.2), the values of ϕ are close to that of $[Ru(bpy)_3]^{2+}$ (except **4)**, suggesting that intramolecular reductive quenching in these complexes is weak. This is consistent to the observation of low enhancement of emission intensity upon addition of metal ions. Charge of the guest cations also play significant role in changing the emission intensity. Cations with unit positive charge like Na^+ and K^+ also make interaction with the ionophore, as evident from NMR study (discussed below), but do not exhibit any significant change in emission intensity, whereas divalent cations (Cd^{2+}, Zn^{2+}, Hg^{2+} and Pb^{2+}) exhibit enhancement. This is due to the fact that the divalent cations interact strongly with the lone pair of electron of the nitrogen atom, making it a poor donor to quench the emissive ^{3}MLCT state. Interestingly for **4,** upon addition of guest cations initially (up to 0.5 equiv) the emission intensity slightly decreased with red shift of emission maxima (λ_{em}) from 620 to 636 nm, then emission intensity increased significantly (45 %) showing hypsochromic shift with λ_{em} at 628 nm in the final spectrum (Figure. 2.6). The value of λ_{em} of the final spectrum is similar to that of complex **1** with same metal ion. The irregular behavior of **4** at low concentration of guest metal ion is attributed to the formation of sandwich type complex formation with 1:2 metal-crown ratio. Similar irregular behavior is also noted when < 0.5 equivalent of Ba^{2+} ion was added into Ru(II) trisphenanthroline fluoroionophore containing six aza-crown moieties, attached to three phenantroline units. This unusual observation is attributed to the formation of sandwich complex involving two crown moieties.[3f] In the case of **4,** there are three possibilities: (i) the flexible calix-crown moiety can orient and adjust in space to make sandwich type of coordination involving two crown moieties, (ii) from NMR it is evident that **4** exists in stereoisomeric forms, therefore, in some isomers two ionophores may come close enough to make sandwich complex, as shown in Figure. 2.7, and (iii) intermolecular interaction can also form this type of complex. Increasing concentration of metal ion leads to breakdown of the sandwich complex and formation of usual 1:1 complex, the process is probably going through an equilibrium showing hypsochromic

shift of λ_{em} from 636 nm to 628 nm, this final value is similar to that found in complex **1** with same metal ion. For the formation of sandwich complex, the geometrical constrains may not allow the nitrogen atom to make interaction with the metal ion, as shown in Figure. 2.7, which makes the nitrogen lone pair available for reductive quenching of the emissive ^{3}MLCT state at the low concentration of metal ion.

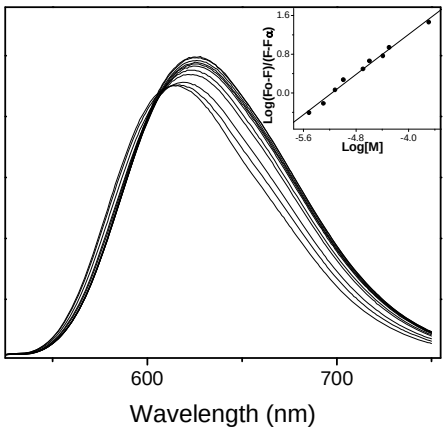

Figure. 2.3. Emission spectral changes of **1** (1 x 10^{-5} M) upon addition of increasing concentration of $Zn(ClO_4)_2$. Excitation wavelength: 456 nm. Inset: linear regression fit (double-logarithmic plot) of the titration data as a function of concentration of metal ion.

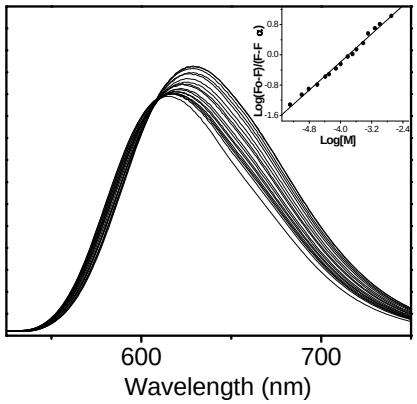

Figure. 2.4. Emission spectral changes for **2** (1 x 10^{-5} M) upon addition of increasing concentration of $Cd(ClO_4)_2$. Excitation wavelength: 456 nm. Inset: linear regression fit (double-logarithmic plot) of the titration data as a function of concentration of metal.

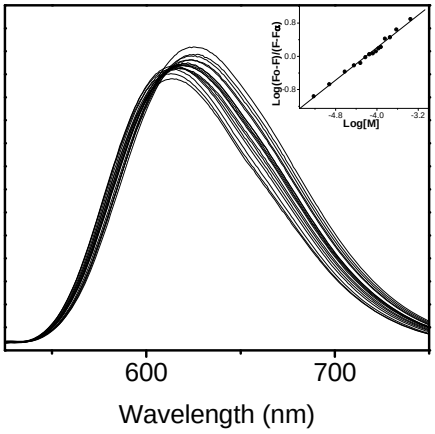

Figure. 2.5. Emission spectral changes of **3** (1 x 10^{-5} M) upon addition of increasing concentration of $Pb(ClO_4)_2$. Excitation wavelength: 454 nm. Inset: linear regression fit (double-logarithmic plot) of the titration data as a function of concentration of metal ion.

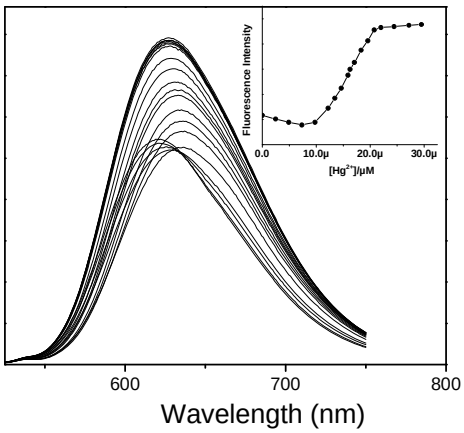

Figure. 2.6. Emission spectral changes for **4** (1 x 10^{-5} M) upon addition of increasing concentration of $Hg(ClO_4)_2$. Excitation wavelength: 463 nm. Inset: emission intensity as a function of concentration of metal ion.

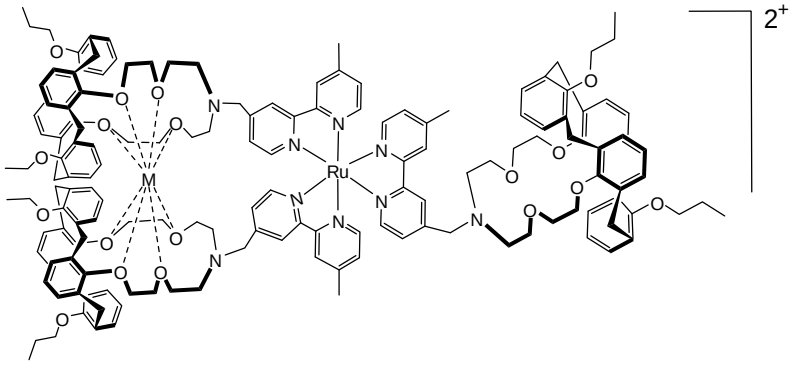

Figure. 2.7. Structural drawing of the sandwich complex for one of the isomeric form of **4**.

Binding constants for **1-3** with the metal ions, which changed emission intensity significantly**,** were calculated using emission titration data following literature procedure.[15] According to this procedure, the fluorescence intensity (F) scales with the metal ion concentration ([M]) according to the formula $(F_0 - F)/(F - F_\infty) = ([M]/K_{diss})^n$. The binding constant ($K_s$) is obtained by plotting $\log[(F_0 - F)/(F - F_\infty)]$ vs. log[M], where F_0 and F_∞ are the relative fluorescence intensities of the complex without addition of guest metal ion and with maximum concentration of metal ion (when no further change in emission intensity takes place), respectively. The slope of the plot obtained from experimental data gives the value of n, number of metal ion bound to each complex, whereas the value of log[M] at $\log[(F_0 - F)/(F - F_\infty)] = 0$ gives the value of $\log(K_{diss})$, the reciprocal of which is the binding constant (K_s). The plots $\log[(F_0 - F)/(F - F_\infty)]$ vs. log[M] are shown as insets in Figures. 2.3 – 2.6. The titration data showed very good linear fit ($R = 0.99$) with the above equation. The binding constants and values of n of all complexes are summarized in Table 2.1. The values of n for **1-3** with all metal ions studied are in the range 0.89 – 1.28, which suggests 1:1 complex formation. For complex **4,** at low concentration of metal ion an equilibrium between 1:2 and 1:1 complexes exists, and with increasing the concentration of metal ion the formation of 1:1 complex increases and finally all the three ionophres form 1:1 complex, as evident from NMR study (discussed below). It is, therefore, a complex phenomenon and no attempt has been made to calculate association constant for this system. However, the changes in emission

spectra with the addition of increasing concentration of metal ion has shown in Figure. 2.6 with the plot of emission intensity as a function of concentration of metal ion as inset.

Analysis of the data (Table 2.1) showed that for **1,** the binding constants (K_s) determined by fluorescence titration, follow the order $Zn^{2+} > Hg^{2+} > Cd^{2+}$; whereas for **2** and **3**, the decreasing order is $Hg^{2+} > Zn^{2+} > Cd^{2+}$. Binding constants for Zn^{2+} and Cd^{2+} of all the three ionophores follow the order **1** > **3** > **2**; but for Hg^{2+} the order is **2** > **3** > **1**. The ionic diameters of Hg^{2+} (1.86 Å) and Cd^{2+} (1.84 Å) are close but the same for Zn^{2+} (1.38 Å) is considerably small, the cavity size of the ionophore of **1** and **3** are expected to be similar but for **2** it should be higher. The Hg^{2+} ion, largest in size among three, exhibits highest binding constant with **2**, which expected to have largest cavity size. On the other hand Zn^{2+}, which is smallest in size, shows lowest binding constant with the ionophore having largest cavity size (**2)** but exhibits highest value with **1**, which expected to have lowest cavity size. The ionic size of Cd^{2+} is close to Hg^{2+} but shows lowest binding constants among the three cations for all three receptors. It may be noted that the aza-crown moiety in these complexes may not be in planar conformation because two bulky units, calix[4]arene and $[Ru(bpy)_3]^{2+}$, are attached with it and also there is strong possibility of intra- and intermolecular interactions. In this situation, complexation of the crown moiety with guest metal ion depends on effective size of the cavity available for incoming ions. Therefore, in this situation it is difficult to generalize size-matching selectivity though an approximate trend is noted. The other important factor, which influences the binding constant, is the affinity of the metal ion towards different donor atoms. The Zn^{2+} ion has class-a characteristic and form complex readily with O-donor atoms, on the other hand Hg^{2+} is the class-b metal ion and prefers to bind N-donor atoms, whereas Cd^{2+} is regarded as class-a/b borderline. This coordination property of the metal ions along with enthalpy of hydration/solvation of the cations also play significant role in the determination of binding constant.[21]

The UV/Vis spectra of **1**-**4** have been recorded in acetonitrile with 100 fold excess of various metal ions and in certain cases slight change in absorption of MLCT band was noted. However, changes are too small to calculate association constant with accuracy and therefore, no attempt has been made to do such calculation.

2.3.5.2. NMR binding study

The ^{1}H NMR spectra of all of the four complexes were recorded in presence of selected metal ions. Many of the metal perchlorate salts used in this study contain water as solvent of crystallization (e.g. $Zn(ClO_4)_2.6H_2O$, $Cd(ClO_4)_2.6H_2O$, $Hg(ClO_4)_2.3H_2O$, $Pb(ClO_4)_2.3H_2O$ etc.), which interferes ^{1}H NMR signals in the crucial region where changes in chemical shift is expected. For this reason, the ^{1}H NMR study is restricted to Na^+, K^+ and Cs^+ ions, dehydrated perchlorate salts of which are available commercially. In the ^{1}H NMR spectra, significant changes were noted upon addition of metal ions, the changes observed with Na^+ and K^+ for **1** and **4**, with K^+ and Cs^+ for **2**, and with only K^+ for **3**, indicating complexation of these metal ions with the respective fluoroionophores.

For the determination of binding constants, NMR titrations were carried out with the above-mentioned metal ions. Interestingly, in the case of K^+ for **1**, **3** and **4,** upon addition of increasing concentration of metal ions new peaks grew in with gradual disappearing of the original signals as shown in Figures. 2.8 and 2.9. In all other cases, gradual shift of certain signals were noted with the addition of metal ions. Major changes observed in the aliphatic region for the signals due to crown moiety because of its involvement in coordination with metal ion. However, changes in chemical shifts of some other signals were also noted due to conformational change induced by metal coordination. Upon addition of metal ion growing of new signals with disappearing of original one indicates formation of stable complex, i.e. the rate of decomplexation is too slow in NMR time scale. This is due to the fact that 1,3-alternate calix[4]arenes are conformationally rigid and the distance between two π-electron clouds in distal phenyl units is almost identical to K^+ diameter, which leads to strong binding of metal ion.[16] However, size of other metal ions (Na^+ for **1** and **4**; K^+ and Cs^+ for **2**) are not large enough compared to the cavity size to enjoy cation-π interaction with the π-electron clouds, which resulted in weak complexation compared to K^+. In this case, the rate of decomplxation is fast enough in NMR time scale to make average of chemical shifts due to complexed and uncomplxed species and a shift of NMR signal is observed. The extent of shift with respect to the limiting value corresponds to the concentration of the complex formed. Due to overlap of signals of the crown moiety, it is difficult to select signals of

that region to show metal induced changes clearly. In the Figure. 2.9, the changes are due to $-CH_2CH_3$ protons of the propyl groups of **1.** For **2** and **3,** the changes due to $-CH_3$ group attached to bpy and $-CH_2$ groups attached to the nitrogen atom of the aza-crown are clearly visible and were used for the calculation of binding constant.

Binding constants for the systems, where chemical shifts gradually changed upon addition of increasing concentration of metal ion (Na^+ for **1**, and K^+ and Cs^+ for **2**), were calculated using the program developed by Hirose[17] and the data are given in Table 2.3. The non-linear least square fit and Job's plot for **1** with Na^+ and for **2** with K^+ and Cs^+ are shown in Figures. 2.10 – 2.12. Complex **4** forms 1:3 complex with Na^+, the program used here for calculation of binding constants is not suitable for calculation of 1:3 complex, hence binding constant for this system was not calculated, however Job's plot using

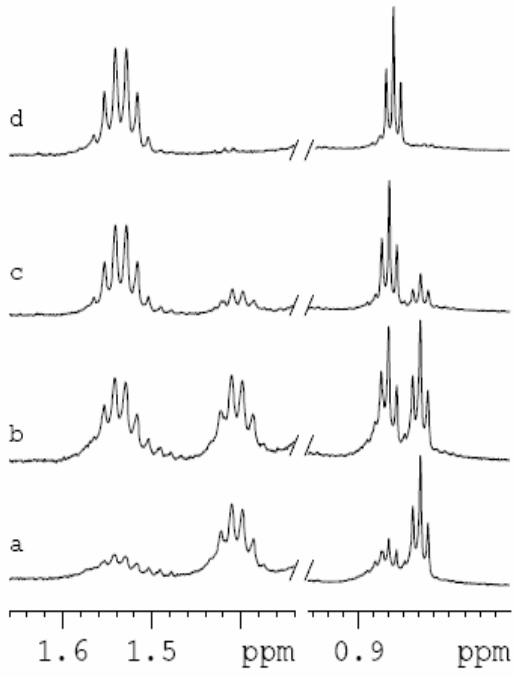

Figure. 2.8. Selected portion of the ^1H NMR spectral change for **1** upon addition of the increasing concentration of $KClO_4$, new peaks are growing in with disappearance of the peaks of original complex.

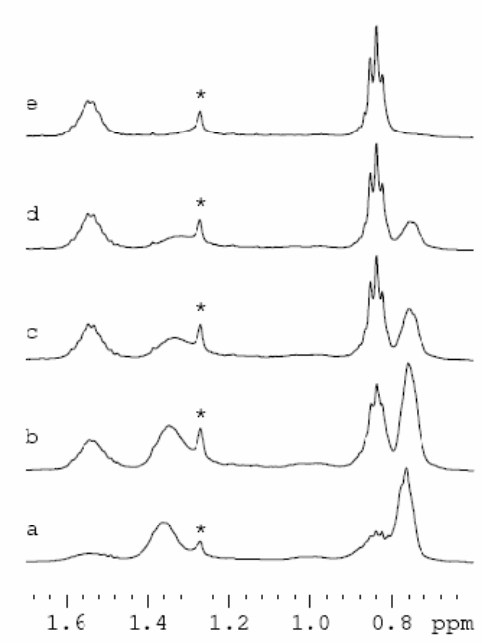

Figure. 2.9. Selected portion of the ^{1}H NMR spectral change for **4** upon addition of the increasing concentration of $KClO_4$, new peaks are growing with disappearance of the peaks of original complex.

Table 2.3. Binding constant (K_s) and stoichiometry of complex formed with cations for the Ru(II) receptors determined by ^{1}H NMR spectroscopy.

Complex	Metal ion	Binding constant (K_s)/ M^{-1}	Stoichiometry[2]
1	Na^+	$5.43 \pm 0.18 \times 10^2$	1:1
	K^{+} [1]	$6.81 \pm 0.44 \times 10^3$	1:1
2	K^+	$1.45 \pm 0.42 \times 10^3$	1:1
	Cs^+	$1.64 \pm 0.32 \times 10^3$	1:1
4	Na^+	-	1:3

[1]Calculated by direct method. [2]Obtained from Job's plot

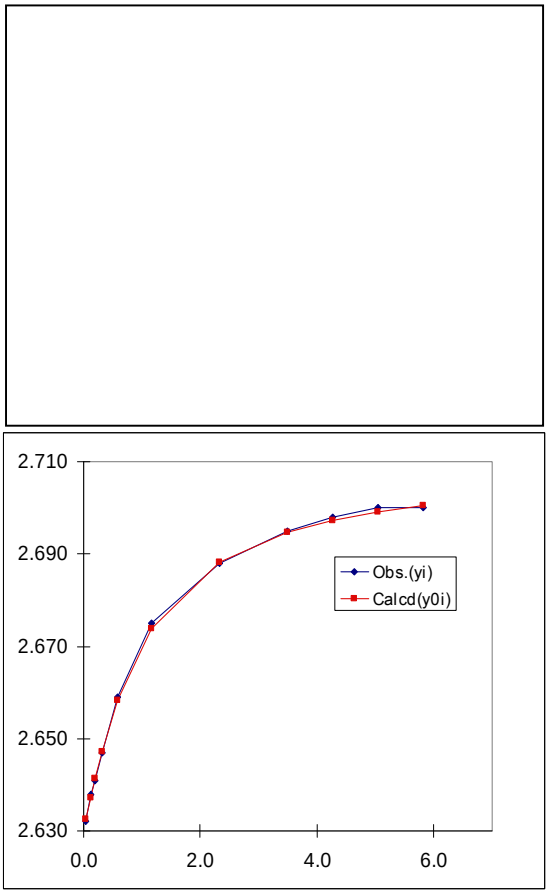

Figure.2.10. The non-linear least square fit (a) and Job's plot (b) from ^{1}H NMR titration data for the binding of **1** with $NaClO_4$ in CD_3CN.

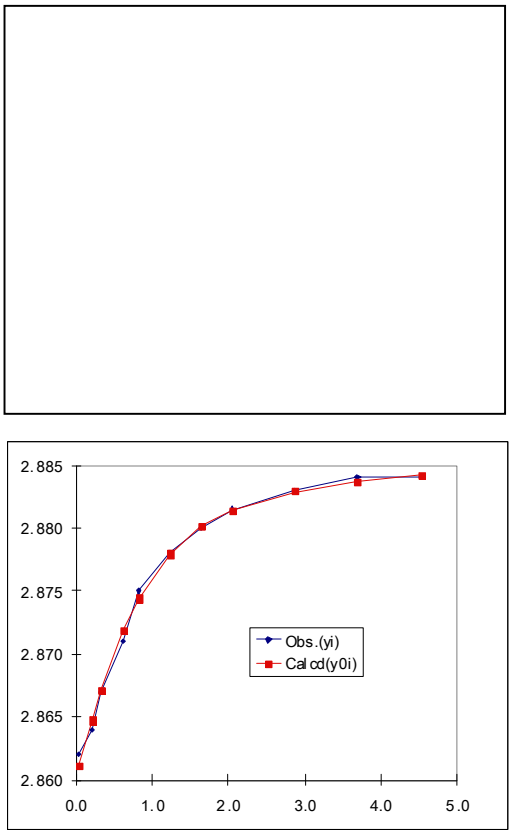

Figure. 2.11. The non-linear least square fit (a) and Job's plot (b) from ^{1}H NMR titration data for the binding of **2** with $KClO_4$ in CD_3CN.

NMR data showing 1:3 complex formation is displayed in Figure. 2.13. For the systems, where new peaks have grown, the binding constants were determined by direct method using peak intensity ratio.[16c,22] Summation of the intensities of both the peaks corresponds to the initial (total) concentration of the complex, the intensity ratio of the growing peak corresponds to the concentration of the cation-bound complex and the intensity ratio of the disappearing peak corresponds to the concentration of the remaining complex (without cation-binding). Binding constant (K_s) was then calculated using the equation $K_s = [C]/([H_t] - [C])([G_t] - [C])$, where [C] is the concentration of the guest metal-bound complex, $[H_t]$ is the total concentration of the host complex and $[G_t]$ is the total concentration of the guest metal ion.[17] Measurements were carried out with four different concentrations of complex and also K_s values with 20% to 80% complexation

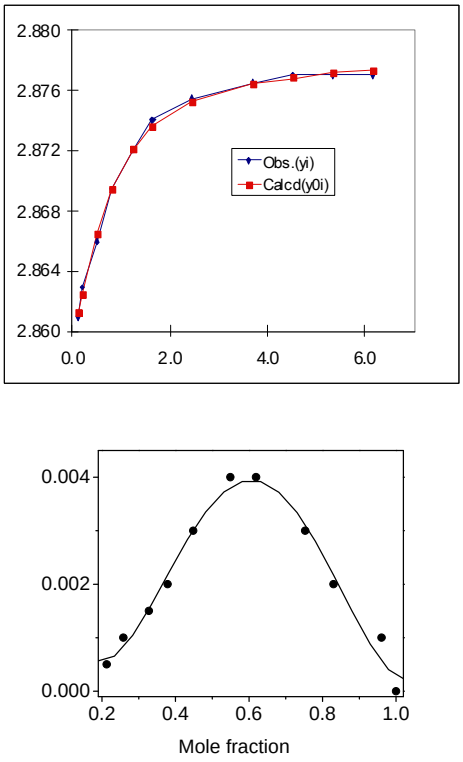

Figure. 2.12. The non-linear least square fit (a) and Job's plot (b) from ^{1}H NMR titration data for the binding of **2** with $CsClO_4$ in CD_3CN.

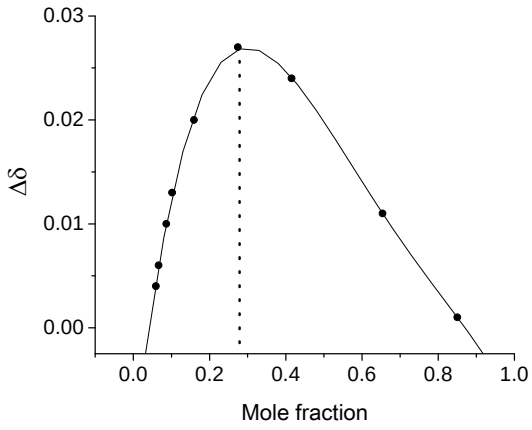

Figure. 2.13. Job's plot from the ^{1}H NMR titration data for the binding of **4** with $NaClO_4$ in CD_3CN showing 1:3 stoichiometry.

ratio is considered for calculation to minimize error in measurement.[17] The K_s values from NMR measurement are summarized in Table 2.3. For **3,** binding constant with K^+ was not calculated because of partial overlap of peaks, which resulted in significant error in the integration of peak area. The results thus obtained show that the binding constants for K^+ is higher than that of Na^+, indicating strong complex formation with the former. Complex **2** shows moderate values of binding constants with K^+ and Cs^+.

2.3.5.3. Electrochemical binding study

The oxidation potential of Ru(II) for **1-4** in presence of Na^+, Hg^{2+} and Pb^{2+} were also investigated. Upon addition of these ions (50 equiv), significant change in the Ru(II)→Ru(III) oxidation potential (>100 mV) were noted for **1** and **2,** however **3** and **4** exhibit little changes. The changes in the oxidation potential (DPV) of Ru(II) for **1-3** is shown in Figure. 2.14, and the data ($\Delta E_{1/2}$) for all of the four complexes are summarized in Table 2.4. It may be noted that the potential shift for **1** is maximum with the highest value for Pb^{2+} (263 mV), whereas for **3** and **4** the changes are insignificant. It is expected that after complexation with guest metal ion, the oxidation potential of the Ru(II) may shift anodically because of the electron withdrawing effect of the positively charged metal-complexed crown moiety. If the spacer does not make effective electronic communication between the Ru(II) chromophore and metal-bound crown moiety, then the oxidation potential of the former may not change significantly. This type of study with Ru(II)-bipyridyl moiety as fluorophore and aza-crown as ionophore have been reported[3d,3f,3g,18b,23] but to the best of our knowledge no such study with calix-crown hybrid molecule as ionophore has been reported so far. Some of the crown systems, where the aza-crown ring is directly attached with the Ru(II)-bound bipyridine moiety exhibit anodic shifts in presence of certain metal ions,[3f,3g] however some of the cases where a spacer is used to connect crown moiety with the Ru(II)-based fluorophore, the oxidation potential of the metal ion didn't show any change upon addition of guest metal ions.[23] In the present study, for **3,** slight anodic shift (11-30 mV) is observed in presence

of all the three metal ions (Table 2.4); for **4** little anodic shifts with Na^+ and Hg^{2+} is noted but with Pb^{2+} slight cathodic shift (-38 mV) was observed. Interestingly, for **1** and **2**, considerably high cathodic shifts (-100 to -263 mV) in presence of all the three metal

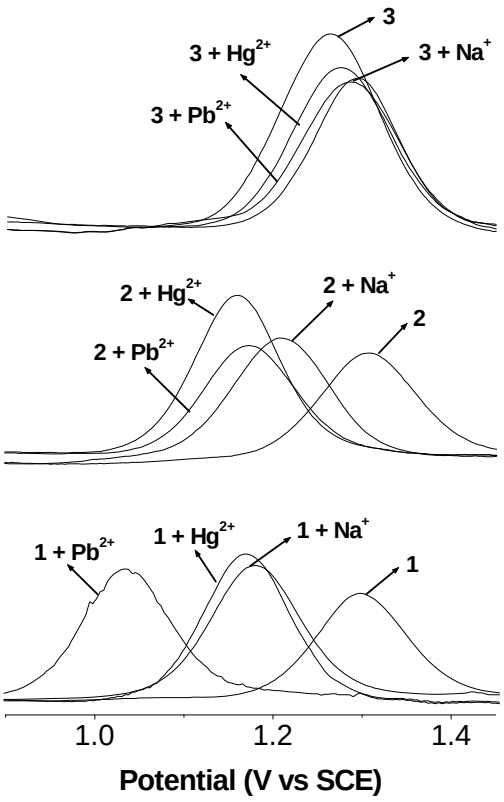

Figure. 2.14. Oxidation potential (DPV) of Ru(II) for **1** (a), **2** (b) and **3** (c), and the same in presence of Na^+, Hg^{2+} and Pb^{2+} (50 equiv) in acetonitrile.

ions are observed. Slightly cathodic shifts (~ 30 mV) of Ru(II) oxidation potential in presence of Li^+ and Na^+ was also reported for a system, where diarylaza crown moiety is connected to metal-bound bipyridine through -CH_2 bridge.[3d] For **3** and **4**, though the changes are in the expected direction (except for **4** with Pb^{2+}) but these are too small to be considered for discussion. However, changes observed in **1** and **2**, needs attention. Apparently there is no through bond electronic communication between Ru(II) chromophore and metal-bound crown moiety. If it would have exists, then upon addition of guest metal ion, the shift in oxidation potential of Ru(II) observed in **1** should have

been also noted for **4** more effectively (three times more) as all the three ionophores formed complex with the guest metal ions. Secondly, oxidation potential of Ru(II) should have been shifted anodically because of the reason mentioned above. These observations indicate that the cathodic shifts observed in **1** and **2** are not due to metal induced electronic communication through the spacer. Apparently it was an unusual observation and because of this reason, the experiments were repeated several times and consistent results were obtained. This cathodic shift is also increased with increasing the concentration of guest metal ion. Therefore, the observed shift is definitely the effect of the added metal salt. We believe that this cathodic change is either related to the ClO_4^- anion, which is used as counter ion of the guest metal ion, or it may be related to intra-/intermolecular H-bonding interactions involving Ru(II) chromophore. Generally, interaction with anions pushes electron density towards metal ion causing cathodic shift of the oxidation potential of metal ion.[3f,3g] If the presence of large excess of ClO_4^- anion makes any interaction with the hydrogen atoms surrounding Ru(II) center due to electrostatic interaction between cations and anions, then cathodic shift of the metal oxidation is likely. The other possibility is the intra-/intermolecular H-bonding interactions, which probably exists in **1** and **2** and is responsible for slightly higher oxidation potential of the Ru(II) ion compared to that of **3** and **4** with same chemical environment (Table 2.4)**. A**fter complexation with guest cation, due to metal induced conformational change and also because of electrostatic repulsion between two metal centers, the H-bonding interactions might have lost causing cathodic shift of the metal oxidation.[18b] Complex **3** contains a second crown ring at the opposite side of the aza-crown moiety and **4** is a bulky compound with three ionophores surrounding the metal center, which might have prevented ClO_4^- ion to come closer to Ru(II) center and to form any intra-/intermolecular H-bonding interactions involving metal chromophore. However, without crystal structure or any other direct evidence it is difficult to make this explanation conclusive for the observed experimental fact.

Table 2.4. Change in oxidation potential of Ru(II) upon addition of cations.

Complex	Change in oxidation potential (mV)[a]		
	Metal ions		
	Na^+	Hg^{2+}	Pb^{2+}
1	- 118 ± 12 [b]	- 129 ± 11	- 263 ± 14
2	- 100 ± 8	- 150 ± 12	- 139 ± 10
3	+ 23 ± 3 [c]	+ 11 ± 2	+ 30 ± 5
4	+ 7 ± 2	+ 16 ± 3	- 38 ± 4

[a]Average of three measurements with deviation [b] -ve sign indicates cathodic shift. [c] +ve sign indicates anodic shift

2.4. Conclusion

A number of fluoroionophores using ruthenium(II) bipyridine moiety as fluorophore and calix-crown hybrid molecule as ionophore have been reported. To the best of our knowledge, this is the first report where tris(bipyridine)Ru(II) unit as fluorophore is connected to the nitrogen atom of a calix-azacrown hybrid ionophore. Cation binding ability of these fluoroionophores has been investigated with a large number of cations. The fluorescence study shows strong complexing ability of all the four complexes with Zn^{2+}, Cd^{2+} and Hg^{2+}, and **2** and **4** also show complexation with Pb^{2+}. The ^1H NMR study shows complexing ability of **1** and **4** with Na^+ and K^+, **2** with K^+ and Cs^+, and **3** with K^+. Electrochemical study with selected cations exhibits interactions of **1** and **2** with Na^+, Hg^{2+} and Pb^{2+} whereas **3** and **4** do not show any significant electrochemical response with these metal ions. Binding constants for **1**-**3** and stoichiometries of the complexes formed for all fluoroionophores have been calculated using luminescence and ^1H NMR titrations data. The K_s values are ranging from 2.53 x 10^5 to 1.45 x 10^3 M^{-1}, the ionic size, conformation and effective cavity size of the ionophore, coordinating ability of cations

with O_4N donor set, and enthalpy of hydration/solvation of the cations are the primary factors to influence binding constants. The most important observation is that a single method of detection is not conclusive to determine the complexing ability of a particular receptor. A sensor molecule having single type of receptor site may act as a multi-ion analyzer by using an array of detection methods. For multi-ion sensing, the receptor should exhibit conformational preferences depending on the detection method and in this regard flexible ionophores with multi donor atoms are more suitable.

2.5 References

1. (a) Cobben, P. L. H. M.; Egberink, R. J. M.; Bomer, J. G.; Bergveld, P.; Verboom, W.; Reinhoudt, D. N. *J. Am. Chem. Soc.* **1992,** *114,* 10573; (b) Gansey, M. H. B. G., Verboom, nW.; Veggel, F. C. J. M. Van.; Vetrogon, V.; Arnaud-Neu, F.; Schwing-Weill, M.-J.; Reinhoudt, D. N. *J. Chem. Soc. Perkin Trans. 2.* **1998,** 2351; (c) Rebek Jr, J. *Chem. Commun*. **2000,** 637; (d) Diamond, D.; Nolan, K. *Anal. Chem*. **2001**, *23A;* (e) de Namor, A. F. D.; Kowalska, D.; Castellano, E. E.; Piro, O. E.; Velarde, F. J. S.; Salas, J. V. *Phys. Chem. Chem. Phys*. **2001**, *3*, 4010; (f) Matthews, S. E.; Schmitt, P.; Felix, V.; Drew, M. G. B.; Beer, P. D. *J. Am. Chem. Soc.* **2002**, *124,* 1341; (g) Webber, P. R. A.; Cowley, A.; Drew, M. G. B.; Beer, P. D. *Chem. Eur. J.* **2003,** *9,* 2439; (h) Li, G.-K.; Xu, Z.-X.; Chen, C.-F.; Huang, Z.-T. *Chem. Commun.* **2008,** 1774; (i) Dhir, A.; Bhalla, V.; Kumar, M. *Org. Lett.* **2008,** *10*, 4891.

2. (a) Ghidini, E.; Ugozzoli, F.; Ungaro, R.; Harkema, S.; El-Fadl, A. A.; Reinhoudt, D. N. *J. Am. Chem. Soc.* **1990**, *112,* 6979; (b) Casnati, A.; Pochini, A.; Ungaro, R.; Ugozzoli, F.; Arnaud, F.; Fanni, S.; Schwing, R. M.-J.; Egberink, J. M.; de Jong, F.; Reinhoudt, D. N. *J. Am. Chem. Soc.* **1995,** *117,* 2767; (c) Ikeda, A.; Tsudera, T.; Shinkai, S. *J. Org. Chem.* **1997,** *62*, 3568; (d) Guillon, J.; Leger, J-M.; Sonnet, P.; Jarry, C.; Robba, M. *J. Org. Chem*. **2000,** *65,* 8283; (e) Takahashi, K.; Gunji, A.; Guillaumont, D.; Pichierri, F.; Nakamura, S. *Angew. Chem. Int. Ed.* **2000,** *39,* 2925; (f) Kim, J. S.; Shon, O. J.; Ko, J. W.; Cho, M. H.; Yu, I. Y.; Vicens, J. *J. Org. Chem*. **2000,** *65*, 2386; (g) Zhou, H.; Surowiec, K.; Purkiss, D. W.; Bartsch, R. A. *Org. Biomol. Chem.* **2005**, *3*, 1676; (h) Luo, J.; Zheng, Q-Y.; Chen, C-F.; Huang, Z-T.; *Chem. Eur. J.* **2005,** *11*, 5917; (i) Oueslati, I.; Abidi, R.; Thuery, P.; Nierlich, M.; Asfari, Z.; Harrowfield, J.; Vicens, J. *Tetrahedron. Lett*. **2000**, *41,* 8263; (j) Prodi, L.; Bolletta, F.; Montalti, M.; Zaccheroni, N.; Casnati, A.; Sansone, F.; Ungaro, R. *New J. Chem*. **2000,** *24,* 155; (k) Casnati, A.; Ca Della, N.; Sansone, F.; Ugozzoli, F.; Ungaro, R. *Tetrahedron.* **2004,** *60,* 7869; (l) Lee, Y. J.; Kwon, J.; Park, C.S.; Lee, J-E.; Sim, W.; Kim, J. S.; Seo, J.; Yoon, II.; Jung, J. H.; Lee, S.

S.; *Org. Lett.* **2007,** *9*, 493; (m) Yuan, M.; Zhou, W.; Liu, X.; Zhu, M.; Li, J.; Yin, X.; Zheng, H.; Zuo, Z.; Ouyang, C.; Liu, H.; Li, Y.; Zhu, D. *J. Org. Chem.* **2008,** *73*, 5008.

3. (a) Chiba, M.; Ogawa, K.; Tsuge, K.; Abe, M.; Kim, H-B.; Sasaki, Y.; Kitamura, N.; *Chem. Lett.* **2001,** 692; (b) Chiba, M.; Kim, H-B.; Kitamura, N. *Anal. Sc.* **2002**, *18,* 461; (c) Muegge, B. D.; Richter, M. M. *Anal. Chem.* **2002,** *74,* 547; (d) Charbonnière, L. J.; Ziessel, R. J.; Sams, C. A.; Harriman, A.; *Inorg. Chem.* **2003,** *42,* 3466; (d) Lazarides, T.; Miller, T. A.; Jeffery, J. C.; Ronson, T. K.; Adams, H.; Ward, M. D. *Dalton Trans*. **2005,** 528; (f) Schmittel, M.; Lin, H-W.; Thiel, E.; Meixner, A. J.; Ammon, H. *Dalton Trans*. **2006,** 4020; (g) Schmittel, M.; Lin, H-w. *Angew. Chem*. *Int. Ed.* **2007,** *119,* 911; (h) Li, M-J.; Chu, B. W-K.; Zhu, N.; Yam, V. W-W. *Inorg. Chem.* **2007**, *46*, 720; (i) Li, M-J.; Chen, Z.; Zhu, N.; Yam, V. W-W. Zy, Y. *Inorg. Chem.* **2008**, *47,* 1218.

4. (a) Grigg, R.; Holmes, J. M.; Jones, S. K.; Norbet, W. D. J. A. *Chem. Commun.* **1994,** 185; (b) Hissler, M.; Harriman, A.; Jost, P.; Wipff, G.; Ziessel, R. *Angew. Chem. Int. Ed*. **1998**, *37,* 3249; (c) Beer, P. D.; Timoshenko, M.; Maestri, M.; Passaniti, P.; Balzani, V. *Chem. Commun*. **1999**, 1755; (d) Cooper, J. B.; Drew, M. J. B.; Beer, P. D.; *Dalton Trans*. **2001,** 392; (e) Dorta, R.; Shimon, L. J. W.; Rozenberg, H.; Ben-David, Y.; Milstein, D. *Inorg. Chem.* **2003**, *42*, 3160; (f) Beer, P. D.; Szemes, F.; Passaniti, P.; Maestri, M. *Inorg. Chem.* **2004,** ***43***, 3965.

5. (a) Ji, H-F.; Dabestani, R.; Brown, G. M. *J. Am. Chem. Soc.* **2000,** *122,* 9306; (b) Benco, J. S.; Nienaber, H. A.; Dennen, K.; Mcgimpsey, W. G. *J. Photochemistry and Photobiology A: Chemisty.* **2002,** *152,* 33; (c) Kim, J. S.; Shon, O. J.; Rim, J. A.; Kim, S. K.; Yoon, J. *J. Org. Chem.* **2002**, *67*, 2348; (d) Kim, J. S.; Noh, K. H.; Lee, S. H.; Kim, S. K.; Kim, S. K.; Yoon, J. *J. Org. Chem.* **2003**, *68*, 597; (e) Kim, S. K.; Lee, S. H.; Lee, J. Y.; Bartsch, R. A.; Kim, J. S. *J. Am. Chem. Soc.* **2004,** *126,* 16499; (g) Choi, J. K.; Kim, S. H.; Yoon, J. Lee, K.-H.; Bartsch, R. A.; Kim, J. S. *J. Org. Chem.* **2006,** *71,* 8011;

(g) Kim, J. S.; Quang, D. T. *Chem. Rev.* **2007,** *107,* 3780; (h) Choi, J. K.; Kim, S. H.; Yoon, J.; Lee, K.-H.; Barsch, R. A.; Kim, J. S. *J. Org. Chem.* **2006,** *71*, 8011; (i) Lee, M. H.; Quang, D. T.; Jung, H. S.; Yoon, J.; Lee, C-H.; Kim, J. S. *J. Org. Chem.* **2007,** *72,* 4242; (j) Xu, Z.; Kim, S.; Kim, H. N.; Han, S. J.; Lee, C.; Kim, J. S.; Qian, X.; Yoon, J. *Tetra. Lett*. **2007,** *48,* 9151; (k) Buie, N. M.; Talanov, V. S.; Butcher, R. J.; Talanova, G. G. *Inorg. Chem*. **2008,** *47*, 3549.

6. (a) Perrin, D. D.; Armarego, W. L. F.; Perrin, D. R. *Purification of Laboratory Chemicals,* 2nd Ed, Pergamon, Press, Oxford, **1980**.

7. (a) Ouchi, M.; Inoue, Y.; Kanzaki, T.; Hakushi, T.; *J. Org. Chem*. **1984,** *49,* 1408.

8. Gutsche, C. D.; Iqbal, M. *Organic Syntheses*. **1990**, *68*, 234.

9. Gutsche, C. D.; Levine, J. A.; Sujeeth, P. K. *J. Org. Chem*. **1985,** *50*, 5802.

10. Kim, J. S.; Lee, W. K.; Sim, W.; Ko, J. W.; Cho, M. H.; Ra, D. Y.; Kim, J. W. *J. Incl. Phenom.* **2000**, *37*, 359.

11. Sullivan, B. P.; Salmon, D. J.; Meyer, T. J. *Inorg. Chem*. **1978,** *17*, 3334.

12. Strouse, G. F.; Schoonover, J. R.; Duesing, R.; Boyde, S. *Inorg. Chem*. **1995,** *34,* 473.

13. Bilakhiya, A. K.; Tyagi, B.; Paul, P.; Natarajan, P. *Inorg. Chem*. **2002,** *41,* 3830.

14. Li, M.; Liu, J.; Zhao, C.; Sun, L. *J. Organometallic Chem*. **2006,** *691*, 4189.

15. (a) Tedesco, A. C.; Oliveria, D. M.; Lacava, Z. J. M.; Azevedo, R. B.; Lima, E. C. D.; Morais, P. C. *J. Magn. Magn. Mater.* **2004,** *272-276*, 2404; (b) Lehrer, S. S.; Fashman, G. D. *Biochem. Biophys. Res. Commun*. **1966,** *2,* 133; (c) Chipman, D. M.; Grisaro, V.; Shanon, N. *J. Biol. Chem.* **1967,** *242*, 4388.

16. (a) Grootenhuis, P. D. J.; Kollman, P. A.; Groenen, L. C.; Reinhoudt, D. N.; Hummel, G. J. M.; Ugozzoli, F.; Andreeti, G. D. *J. Am. Chem. Soc.* **1990**, *112,*

4165; (b) Harda, T.; Rudzinski, J. M.; Shinkai, S. *J. Chem. Soc. Perkin Trans. 2.,* **1992,** 2109; (c) Harda, T.; Ohseto, F.; Shinkai, S. *Tetrahedron*. **1994,** *50*, 13377; (d) Koh, K. N.; Araki, K.; Shinkai, S.; Asfari, Z.; Vicens, J. *Tetrahedron Lett*. **1995**, *36,* 6095.

17. Hirose, K. *J. Incl. Phenoena.* **2001,** *39,* 193.

18. (a) Agnihotri, P.; Suresh, E.; Paul, P.; Ghosh, P. K. *Eur. J. Inorg. Chem*. **2006,** 3369; (b) Boricha, V. P.; Patra, S.; Chouhan, Y. S.; Sanavada, P.; Suresh, E.; Paul, P. *Eur. J. Inorg. Chem*. **2009,** 1256.

19. (a) Keene, F. R. *Coord. Chem. Rev.* **1997,** *166,* 121; (b) Paul, P.; Tyagi, B.; Bilakhiya, A. K.; Dastidar, P.; Suresh, E. *Inorg. Chem*. **2000,** *39,* 14.

20. Juris, A.; Balzani, V.; Barigelletti, F.; Campagna, S.; Belser, P.; Von Zelewsky, A. *Coord. Chem.. Rev*. **1998**, *84*, 85.

21. (a) Suresh, E.; Agnihotri, P.; Ganguly, B.; Bhatt, P.; Subramanian, P. S.; Paul, P.; Ghosh, P. K. *Eur. J. Inorg. Chem.* **2005**, 2198; (b) Agnihotri, P.; Patra, S.; Suresh, E.; Paul, P.; Ghosh, P. K. *Eur. J. Inorg. Chem.* **2006**, 4938; (c) Nasarbadi, M. R.; Ahmadi, F.; Pourmortazavi, S. M.; Ganjali, M. R.; Alizadeh, K. *J. Mol. Liquid***. 2009,** *144*, 97.

22. Ikeda, A.; Shinkai, S. *J. Am. Chem. Soc.* **1994,** *116*, 3102.

23. Beer, P. D.; Dent, S. W.; Fletcher, N. C.; Wear, T. J. *Polyhedron.* **1996,** *15,* 2983.

Chapter-III

Synthesis, Characterization, Electrochemistry and Ion-Binding Property of Ruthenium(II) and Rhenium(I) Containing Receptors Having appended Modified Calix[4]arene as Ionophore

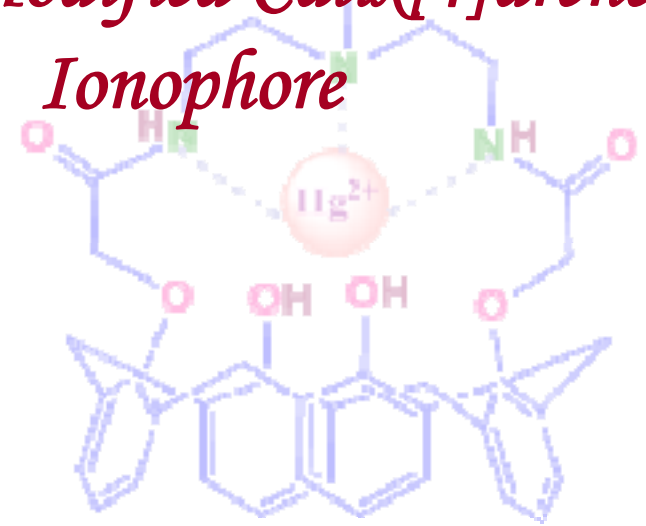

3.1. Introduction

For designing cation sensors, different strategies have been successfully applied using various luminescent ruthenium(II)-polypyridyl complexes, as mentioned in *Chapter-I*.[1-8] *Chapter-II* described synthesis and ion-binding property of luminophores containing Ru(II)-polypyridyl units as signaling unit and calix[4]arene-azacrown hybrid moiety as ionophore. In this chapter, some modifications in the receptor molecules have been made with certain objectives. Re(I)-polypyridyl unit is also photoactive,[9-11] therefore it is interesting to incorporate this unit as fluorophore to ascertain it's photophysical response upon interaction of ionophore with metal ions. This also gives opportunity to compare it's photophysical changes with that of other systems containing Ru(II) polypyridyl unit with similar ionophore. The other objective was to make changes in azacrown moiety, particularly in donor atoms to investigate their performance towards other metal ions, particularly with heavy and toxic metal ions. It was also kept in mind to design fluoroionophore, which can act for both cation and anions. For designing of anion receptors, incorporation of metal-complex based fluorophores offers some advantages over organic molecules. The positive charge on the metal ion makes electrostatic interaction with negatively charged species leading to strong host-guest interaction.

In this chapter, synthesis, characterization, electrochemical behavior and ion binding property of four fluoroionophores are presented. In this series of fluoroionophores, $(bpy)_3Ru(II)$ and $(bpy)Re(I)(CO)_3Cl$ units are used as fluorophore and calix[4]arene-azacrown, modified by introducing amide groups (-CONH-), are used as ionophores. The fluorophore is attached to the nitrogen atom of the azacrown moiety. *Tert*-butyl calix[4]arene is used in some of the ionophores to impose controlled steric crowding in ionophore. Hydrogen atoms of two of the OH groups are replaced by propyl groups to make 1,3-alternate conformation of the calixarien unit. All of these new complexes have been characterized on the basis of analytical and spectroscopic data. The ion binding property of all complexes has been tested with a large number of cations and anions. The ion recognition event is monitored by fluorescence spectral changes and the binding constants for strongly interacting ions (Hg^{2+}, Pb^{2+}, $H_2PO_4^-$ and F^-) were determined from fluorescence titration data. All these results are presented and discussed

in light of ion-binding ability of the new receptors and perturbation of luminescence property due to complexation.

3.2. Experimental Section

3.2.1. Materials and measurements

Reagents and starting materials used for this study are similar to those reported in *Chapter –II*. Some starting compound/complexes were synthesized following the literature procedures as described in the earlier *Chapter*. Physical measurements were also carried out using the instruments described in the *Chapter-II*.

Caution: Perchlorate salts of metal ions are potentially explosive. Therefore, they should be handled with great care.

3.2.2. Synthesis of ligands

Synthesis of the intermediate compounds

The intermediate compounds **C**, **D** (Scheme 3.1) and **H** (Scheme 3.2) were synthesized following the literature procedure.[12-13]

Synthesis of the intermediate compound E

A solution of (**C**) (0.79 g, 1.0 mmol) and diethylenetriamine (0.34 g, 2.2 mmol) in freshly distilled 1: 1 methanol–toluene (70 mL) were refluxed for 24 h under inert atmosphere. The solution was then allowed to cool to room temperature and evaporated to dryness by rotary evaporation. After removal of the solvents, the crude mixture was washed with methanol (50 mL) and filtered off the white solid. The desired white compound was dried in high vacuum. Yield: 0.62 g (75%). IR, ν_{max}(KBr pellet)/cm^{-1} 3395 ν(OH), 1701 ν(C=O); ^{1}H NMR (200 MHz, $CDCl_3$): δ 8.31 (br s, 2H, -CON-*H*), 7.12 (s, 4H, Ar-H_m), 6.71 (s, 4H, Ar-H_m), 6.35 (s, 2H, Ar-*OH*), 4.48 (s, 4H, -OCH_2CO), 4.16 (d, 4H, *J* = 13.4 Hz, ArCH_2Ar), 3.53 (br s, 4H, -CONH$CH_2$$CH_2$-NH-), 3.37 (d, 4H, *J* = 13.4 Hz, ArCH_2Ar), 2.95 (t, 4H, *J* = 4.8 Hz, -CONHCH$_2$$CH_2$-NH-), 1.33 (s, 18H, -C($CH_3$)$_3$), 0.88 (s, 18H, -C($CH_3$)$_3$). ESMS (*m/z*): found

871.03(100%) calcd for [**E** + K^+] 871.20. Anal calcd for $C_{52}H_{69}O_6N_3$: calcd C, 75.05; H, 8.35; N, 5.04. Found: C, 74.58; H, 8.57; N, 4.98.

Synthesis of ligand L^1

To a stirring mixture of 0.42 g (0.5 mmol) of **E** and 1.0 mL (14 mmol) of triethylamine in dry THF (90 mL) was added dropwise 0.26 g (1 mmol) of 4-(bromomethyl)-4'-methyl-2,2'-bipyridine dissolved in dry THF (50 mL) over a period of 2 h at 0˚C under nitrogen atmosphere. After complete addition, the temperature of the reaction mixture was maintained at 0˚C for additional 4 h with stirring, after which it was heated to reflux for 24 h. The reaction mixture was then allowed to cool to room temperature and the solvent was removed by rotary evaporation. The residue was then dissolved in $CHCl_3$ (100 mL), and the organic layer was washed three times with water (50 mL each time), dried over $MgSO_4$ and evaporated in vacuo. The crude product was purified by column chromatography on silica gel column (230-400 mesh, deactivated with hexane with 10% Et_3N and washed with hexane before use) and was eluted by using 2:49 (v/v) methanol/chloroform as eluent. Yield: 0.30 g, (59 %). IR, ν_{max}(KBr pellet)/cm^{-1} 3383 (OH), 3187 (NH), 1705 (C=O). ^{1}H NMR (500 MHz, $CDCl_3$): δ 8.52 (d, 1H, *J* = 4 Hz, bipy-*H*), 8.48 (br-t, 2H, -CON-*H*), 8.31 (s, 2H, bipy-*H*), 8.19 (s, 2H, bipy-*H*), 7.55 (br-s, 1H, bipy-*H*), 7.14 (s, 4H, Ar-H_m), 6.78 (s, 4H, Ar-H_m), 6.72 (s, 2H, Ar-*OH*), 4.52 (s, 4H, -OCH_2CO), 4.18 (d, 4H, *J* = 13 Hz, ArCH_2Ar), 3.78 (s, 2H, -N-CH_2-bipy), 3.55 (br-t, 4H, -CONH$CH_2$$CH_2$-NH-), 3.39 (d, 4H, *J* = 13.2 Hz, ArCH_2Ar), 2.85 (br-s, 4H, -CONHCH$_2$$CH_2$-NH-), 2.43 (s, 3H, -$CH_3$), 1.33 (s, 18H, -C($CH_3$)$_3$), 0.92 (s, 18H, -C($CH_3$)$_3$). ESMS (*m/z*): found 1014.51(100%) calcd for [$\mathbf{L^1}$+ H^+] 1014.31. Anal calcd for $C_{64}H_{79}N_5O_6$: calcd C, 75.78; H, 7.85; N, 6.90. Found: C, 75.37; H, 7.98; N, 6.73.

Synthesis of the intermediate compound F

The compound **F** was synthesized from the intermediate **D** following the modified literature procedure,[14] similar to that described for synthesis of **E.** Yield: (83 %). IR, ν_{max}(KBr pellet)/cm^{-1} 3376 (OH), 1667 (C=O). ^{1}H NMR (500 MHz, $CDCl_3$): δ 8.27 (br-s, 2H, -CON-*H*), 7.13 (d, 4H, , *J* = 7 Hz, Ar-H_m), 6.81-6.76 (m, 6H, 4H of Ar-H_m & 2H of Ar-H_p), 6.69 (t, 2H, *J* = 7.5 Hz, Ar-H_p), 4.5 (s, 4H, -OCH_2CO), 4.19 (d, 4H, *J* = 13.5 Hz, ArCH_2Ar), 3.55 (t, 4H, *J* = 5 Hz, -CONH$CH_2$$CH_2$-NH-), 3.45 (d, 4H, *J* = 13.5 Hz, ArCH_2Ar), 2.97 (t, 4H, *J* = 5

Hz, -CONHCH$_2$*CH$_2$*-NH-). ESMS (*m/z*): found 608.52 (100%) calcd for [**F** + H$^+$] 608.68. Anal calcd for $C_{36}H_{37}O_6N_3$: calcd C, 71.15; H, 6.13; N, 6.91. Found: C, 70.67; H, 6.20; N, 6.86.

Synthesis of ligand L^2

The ligand **L^2** was prepared from the intermediate **F** following the similar procedure as described for **L^1** except purification step. The crude product was purified by column chromatography on silica gel (100-200 mesh, deactivated with hexane with 10% Et_3N and washed with hexane before use) and was eluted by chloroform. After evaporation of the solvent a semisolid mass was obtained. The crude product was purified by reprecipitation; the solid mass was dissolved in 5 mL $CHCl_3$ and poured into the stirring solution of hexane (40 mL). The desired white precipitate (**L^2**) was separated and kept in high vacuum for overnight. Yield: (65 %). IR, ν_{max} (KBr pellet)/cm^{-1} 3364 (OH), 3065 (NH), 1678 (C=O). ^{1}H NMR (500 MHz, $CDCl_3$): δ 8.55 (br-s, 2H, bipy-*H*), 8.49 (br-s, 2H, -CON-*H*), 8.40 (s, 1H, bipy-*H*), 8.25 (s, 1H, bipy-*H*), 7.49 (br-s, 2H, bipy-*H*), 7.15 (d, 4H, *J* = 7.5 Hz, Ar-*H$_m$*), 6.91 (d, 4H, *J* = 7.5 Hz, Ar-*H$_m$*), 6.8 (t, 4H, *J* = 7.5 Hz, Ar-*H$_p$*), 4.57 (s, 4H, -O*CH$_2$*CO), 4.22 (d, 4H, *J* = 13.5 Hz, Ar*CH$_2$*Ar), 3.82 (s, 2H, -N-*CH$_2$*-bipy), 3.58 (br-t, 4H, -CONH*CH$_2$*CH$_2$-NH-), 3.5 (d, 4H, *J* = 13.5 Hz, Ar*CH$_2$*Ar), 2.89 (br-t, 4H, -CONHCH$_2$*CH$_2$*-NH-), 2.44 (s, 3H, -*CH$_3$*). ESMS (*m/z*): found 790.58 (100%) calcd for [**L^2** + H$^+$] 790.89. Anal calcd for $C_{48}H_{47}N_5O_6$: calcd C, 72.98; H, 5.99; N, 8.86. Found: C, 72.16; H, 6.09; N, 8.96.

Synthesis of the intermediate compound I

In a solution of (**H**) (0.68 g, 1.0 mmol) in freshly distilled 1:1 ethanol–toluene (70 mL), diethylenetriamine (0.34 g, 2.2 mmol) was added and the reaction mixture was heated at reflux for 36 h under inert atmosphere. The solution was then allowed to cool to room temperature and evaporated to dryness by rotary evaporation. The resulting solid was dissolved in $CHCl_3$ (150 mL), and the organic layer was washed three times with water (100 mL each time), dried over $MgSO_4$, and evaporated in vacuum. The crude product was purified by column chromatography on activated alumina using 1:4 (v/v) chloroform/hexane as eluent. Yield: 0.46 g, (67 %). IR, ν_{max}(KBr pellet)/cm^{-1} 2919 (NH), 1671 (C=O). ^{1}H NMR (500 MHz, $CDCl_3$): δ 7.06 (d, 4H, *J* = 7 Hz, Ar-*H$_m$*), 6.93 (d, 4H, *J* = 7 Hz, Ar-*H$_m$*), 6.79 (t, 2H, , *J* = 7

Hz, Ar-H_p), 6.65-6.60 (m, 4H, 2H of Ar-H_p & 2H of -CON-*H*), 4.26 (s, 4H, -OCH_2CO), 3.69-3.64 (m, 12H, 4H of ArCH_2Ar, 4H of –O$CH_2$$CH_2$$CH_3$ & 4H of -CONH$CH_2$$CH_2$-NH-), 3.5 (d, 4H, J = 14.5 Hz, ArCH_2Ar), 2.94 (br-t, 4H, -CONHCH$_2$$CH_2$-NH-), 1.82-1.77 (m, 4H, –OCH$_2$$CH_2CH_3$), 0.96 (t, 6H, J = 7.5 Hz, –OCH$_2$CH$_2$$CH_3$). ESMS (*m/z*): found 714.65 (100%) calcd for [**I** + Na^+] 714.82. Anal calcd for $C_{42}H_{49}O_6N_3$: calcd C, 72.91; H, 7.13; N, 6.07 Found: C, 72.55; H, 6.93; N, 5.98.

Synthesis of ligand L^3

In a solution of (**I**) (0.35 g, 0.5 mmol) in freshly distilled acetonitrile (90 mL), K_2CO_3 (0.69 g, 5 mmol) and a catalytic amount of KI were added and the reaction mixture was stirred at room temperature for half an hour under nitrogen atmosphere. Then 0.53 g (2 mmol) of 4-(bromomethyl)-4'-methyl-2,2'-bipyridine dissolved in dry acetonitrile (50 mL) was added dropwise over a period of 1 h at room temperature under nitrogen atmosphere. After complete addition, the temperature of the reaction mixture was increased and the solution was heated at reflux for 36 h. The reaction mixture was then allowed to cool to room temperature and the solvent was removed by rotary evaporation. The residue was then dissolved in $CHCl_3$ (150 mL), and the organic layer was washed three times with brine solution (75 mL each time) and two times with water (50 mL each time), dried over $MgSO_4$ and evaporated in vacuum. The crude product was purified by column chromatography on activated alumina using 1:1 (v/v) chloroform/hexane as eluent. Yield: 0.231 g, (53 %). IR, ν_{max}(KBr pellet)/cm^{-1} 3061 (NH), 1672 (C=O). ^{1}H NMR (500 MHz, $CDCl_3$): δ 8.72 (d, 2H, J = 5 Hz, bipy-*H*), 8.59 (d, 2H, J = 5 Hz, bipy-*H*), 8.41 (s,1H, bipy-*H*), 8.31 (s,1H, bipy-*H*), 7.08 (d, 4H, J = 7.5 Hz, Ar-H_m), 7.02 (d, 4H, J = 7.5 Hz, Ar-H_m), 6.89-6.84 (m, 4H, Ar-H_p), 6.03 (br-s, 2H, -CON-*H*), 4.22 (s, 4H, -OCH_2CO), 3.97 (s, 2H, -N-CH_2-bipy), 3.81 (d, 4H, J = 15.5 Hz, ArCH_2Ar), 3.71 (d, 4H, J = 15.5 Hz, ArCH_2Ar), 3.5 (t, 8H, J = 7.25 Hz, -CONH$CH_2$$CH_2$-NH-), 2.76 (br-s, 4H, –OCH_2CH$_2$CH$_3$), 2.49 (s, 3H, -CH_3), 1.48-1.37 (m, 4H, –OCH$_2$$CH_2CH_3$), 0.81 (t, 6H, J = 7.5, –OCH$_2$CH$_2$$CH_3$). ESMS (*m/z*): found 874.76 (30%) calcd for [$\mathbf{L^3}$+H^+] 874.04, found 896.75 (40%) calcd for [$\mathbf{L^3}$+Na^+] 897.02. Anal calcd for $C_{54}H_{59}O_6N_5$: calcd C, 74.20 ; H, 6.80; N, 8.00 Found: C, 73.88; H, 6.54; N, 7.84.

3.2.3. Synthesis of complexes

General procedure for the synthesis of $[Ru(bpy)_2(L^1)][PF_6]_2$ (1), $[Ru(bpy)_2(L^2)][PF_6]_2$ (2) and $[Ru(bpy)_2(L^3)][PF_6]_2$ (3).

A mixture of *cis*-$[Ru(bpy)_2Cl_2]\cdot 2H_2O$ (0.52 g, 1.0 mmol) and the appropriate ligand ($\mathbf{L^1}/\mathbf{L^2}/\mathbf{L^3}$, 1.1 mmol) in ethanol-water (2:1, 80 mL) was refluxed for 10 h. The reaction mixture was then allowed to cool to room temperature; volume was reduced to *ca*. 20 mL by rotary evaporation, filtered and to the filtrate was added solid NH_4PF_6 (1.63 g, 10 mmol). The precipitate was filtered off and washed with water and diethyl ether. The complexes were purified by column chromatography using a column packed with deactivated (15% water) alumina Gr-III and acetonitrile-toluene (1:1) as eluent. The small first fraction was discarded; the large orange-red colored second fraction gave the desired complex. After removal of the solvent, the residue was redissolved in acetonitrile and was precipitated by vapor diffusion method using diethyl ether. In every case microcrystalline compounds was isolated.Yields; 55 % for **1,** 60% for **2** and 51 % for **3.**

Characterization data for 1

IR, ν_{max}(KBr pellet)/cm^{-1} 3417 (OH), 3215 (NH), 1676 (CO), 842 (PF_6). ^{1}H NMR (500 MHz, CD_3CN): δ 8.76 (s, 1H, ligand bipy-*H*), 8.73 (t, 2H, *J* = 5 Hz, -CON-*H*), 8.58 (s, 1H, ligand bipy-*H*), 8.48 (dd, 3H, J_1 = 7.5 Hz, J_2 = 4 Hz, ligand bipy-*H*), 8.43 (dd, 1H, J_1 = 7.5 Hz, J_2 = 3 Hz, ligand bipy-*H*), 8.05-8.0 (m, 4H, bipy-*H*), 7.95 (s, 2H, Ar-*OH*), 7.76 (t, 1H, *J* = 6 Hz, bipy-*H*), 7.75-7.70 (m, 4H, bipy-*H*), 7.62 (d, 1H, *J* = 5.5 Hz, bipy-*H*), 7.53 (d, 1H, *J* = 5.5 Hz, bipy-*H*), 7.47 (d, 1H, *J* = 5 Hz, bipy-*H*), 7.40-7.34 (m, 4H, bipy-*H*), 7.26-7.23 (m, 8H, Ar-H_m), 4.55-4.42 (m, 4H, -OCH_2CO), 4.18 (dd, 4H, J_1 = 13.0 Hz, J_2 = 7.5 Hz, ArCH_2Ar), 3.84 (s, 2H, -N-CH_2-bipy), 3.59-3.39 (m, 8H, 4H of ArCH_2Ar & 4H of -CONH$CH_2$$CH_2$-NH-), 2.86 (br-t, 4H, -CONHCH$_2$$CH_2$-NH-), 2.52 (s, 3H, -$CH_3$), 1.24 (s, 18H, -C($CH_3$)$_3$), 1.15 (s, 18H, -C($CH_3$)$_3$). ESMS (*m/z*): found 1427.05 (15%) calcd for [**1**-2PF_6^--H^+]$^+$ 1427.79, found 1570.74 (50%) calcd for [**1**-PF_6^-]$^+$ 1570.73. Anal calcd for $C_{84}H_{95}RuN_9O_6P_2F_{12}$: calcd C, 58.77; H, 5.58; N, 7.34 Found: C, 58.28; H, 5.30; N, 7.22. UV/Vis (CH_3CN): λ, nm (ε, $dm^3mol^{-1}cm^{-1}$), 457 (13.94 x 10^3), 427 (11.51 x 10^3), 287 (72.39 x 10^3).

Characterization data for 2

IR, ν_{max}(KBr pellet)/cm^{-1} 3401 (OH), 3078 (NH), 1675 (CO), 842 (PF_6). ^{1}H NMR (500 MHz, CD_3CN): δ 8.70 (s, 1H, ligand bipy-*H*), 8.55 (br-s, 2H, -CON-*H*), 8.47 (d, 2H, *J* = 9 Hz, ligand bipy-*H*), 8.44 (d, 1H, *J* = 5.5 Hz, ligand bipy-*H*), 8.42 (s, 1H, ligand bipy-*H*), 8.06-7.99 (m, 5H, 1H of ligand bipy-*H* & 4H of bipy-*H*), 7.92 (s, 2H, Ar-*OH*), 7.77-7.72 (m, 4H, bipy-*H*), 7.69 (d, 1H, *J* = 5.5 Hz, bipy-*H*), 7.61 (d, 1H, *J* = 5.5 Hz, bipy-*H*), 7.53 (d, 1H, *J* = 6 Hz, bipy-*H*), 7.46 (d, 1H, *J* = 5.5 Hz, bipy-*H*), 7.41-7.35 (m, 4H, bipy-*H*), 7.20 (d, 4H, *J* = 7.5 Hz, bipy-*H*), 7.04 (d, 4H, *J* = 7.5 Hz, Ar-H_m), 6.88 (t, 2H, *J* = 7.5 Hz, Ar-H_p), 6.77 (t, 2H, *J* = 7.5 Hz, Ar-H_p), 4.56-4.45 (m, 4H, -OCH_2CO), 4.20 (dd, 4H, J_1 = 13.5 Hz, J_2 = 4 Hz, ArCH_2Ar), 3.82 (s, 2H, -N-CH_2-bipy), 3.59-3.41 (m, 8H, 4H of ArCH_2Ar & 4H of -CONH$CH_2$$CH_2$-NH-), 2.86 (br-t, 4H, -CONHCH$_2$$CH_2$-NH-), 2.53 (s, 3H, -$CH_3$). ESMS (*m/z*): found 1347.74 (60%) calcd for [**2**- PF_6^-]$^+$ 1347.31. Anal calcd for $C_{68}H_{63}RuN_9O_6P_2F_{12}$: calcd C, 54.96; H, 4.25; N, 8.44 Found: C, 54.35; H, 4.01; N, 8.24. UV/Vis (CH_3CN): λ, nm (ε, dm^{3}mol^{-1}cm^{-1}), 456 (13.99 x 10^3), 427 (11.76 x 10^3), 287 (72.50 x 10^3).

Characterization data for 3.

IR, ν_{max}(KBr pellet)/cm^{-1} 3107 (NH), 1670 (CO), 842 (PF_6). ^{1}H NMR (500 MHz, CD_3CN): δ 8.56-8.46 (m, 4H, ligand bipy-*H*), 8.06-8.01 (m, 4H, 2H of ligand bipy-*H* and 2H of bipy-*H*), 7.75 (d, 2H, *J* = 5.5 Hz, bipy-*H*), 7.74 (d, 2H, *J* = 5.5 Hz, bipy-*H*), 7.72 (d, 2H, *J* = 5.5 Hz, bipy-*H*), 7.62 (s, 2H, bipy-*H*), 7.55 (d, 2H, *J* = 6 Hz, bipy-*H*), 7.46-7.37 (m, 6H, 4H of Ar-H_m & 2H of bipy-*H*), 7.25 (d, 2H, *J* = 6 Hz, bipy-*H*), 7.12 (d, 4H, *J* = 7.5 Hz, Ar-H_m), 6.97 (t, 2H, *J* = 7 Hz, Ar-H_p), 6.87 (t, 2H, *J* = 7 Hz, Ar-H_p), 6.72 (br-s, 2H, -CON*H*), 4.12-4.04 (m, 4H, -OCH_2CO), 3.96 (br-s, 2H, -NCH_2-bipy), 3.81 (d, 4H, *J* = 15 Hz, ArCH_2Ar), 3.71 (d, 4H, *J* = 15 Hz, ArCH_2Ar), 3.51 (t, 4H, , *J* = 7.5 Hz, -CONH$CH_2$$CH_2$-NH-), 3.81-3.32 (m, 4H, -CONHCH$_2$$CH_2$-NH-), 2.68 (br-t, 4H, -OCH_2CH$_2$CH3), 2.57 (s, 3H, -CH_3), 1.49-1.42 (m, 4H, -OCH$_2$$CH_2$CH3), 0.82 (t, 6H, -OCH$_2CH_2$*CH3*). ESMS (*m/z*): found 1433.49 (40%) calcd for [**3**-PF_6^-]$^+$ 1433.48. Anal calcd for $C_{74}H_{75}RuN_9O_6P_2F_{12}$: calcd C, 56.34; H, 4.79; N, 7.99 Found: C, 55.75; H,

4.61; N, 8.05. UV/Vis (CH_3CN): λ, nm (ε, $dm^3mol^{-1}cm^{-1}$), 456 (12.14 x 10^3), 423 (9.8 x 10^3), 287 (62.37 x 10^3).

Synthesis of [Re(L^2)$(CO)_5$ Cl] (4).

A mixture of [$Re(CO)_5Cl$] (0.121 g, 0.33 mmol) and the ligand $\mathbf{L^2}$ (0.27 g, 0.33 mmol) was refluxed in dry THF (50 mL) under nitrogen for 15 h. The solution was then cooled to room temperature and the solvent removed on a rotary evaporator. The residue thus obtained was dissolved in dichloromethane (10 mL) and added dropwise to n-hexane (50 mL) with stirring. The precipitate thus obtained was isolated by filtration. The complexes were purified by column chromatography using a column packed with deactivated (15% water) alumina and acetonitrile-toluene (1:4) as eluent. The small first fraction was discarded; the large yellow colored second fraction gave the desired complex. Yield; 0.190 g; (51 %). IR, ν_{max}(KBr pellet)/cm^{-1} 3357 (OH), 3069 (NH), 2018 (axial C=O), 1818(equatorial C=O), 1677(C=O). ^{1}H NMR (500 MHz, $CDCl_3$): δ 8.90 (d, 1H, *J* = 5.5 Hz, bipy-*H*), 8.86 (d, 1H, *J* = 5.5 Hz, bipy-*H*), 8.83 (t, 2H, *J* = 5.0 Hz, -CON-*H*), 8.72 (s, 1H, bipy-*H*), 8.55 (s, 1H, bipy-*H*), 7.75 (s, 2H, Ar-*OH*), 7.48 (d, 1H, *J* = 5.5 Hz, bipy-*H*), 7.30 (d, 1H, *J* = 5.5 Hz, bipy-*H*), 7.13 (d, 4H, *J* = 7.25 Hz, Ar-H_m), 6.96 (t, 4H, *J* = 6.5 Hz, Ar-H_m), 6.85 (t, 2H, *J* = 7.5 Hz**,** Ar-H_p**)** 6.78 (t, 2H, *J* = 7.5 Hz**,** Ar-H_p**),** 4.70-4.53 (m, 4H, -OCH_2CO), 4.18 (dd, 4H, J_1 = 13.5 Hz, J_2 = 10 Hz, ArCH_2Ar), 3.85-3.67 (m, 4H, -CONHCH_2CH_2-NH-), 3.53 (t, 6H, 4H of ArCH_2Ar & 2H of -N-CH_2-bipy), 2.97 (br-t, 4H, -CONHCH$_2CH_2$-NH-), 2.55 (s, 3H, -CH_3). ESMS (*m/z*): found 1059.58 (25%) calcd for [**3**-Cl^-] 1059.13. Anal calcd for $C_{51}H_{47}ReN_5O_9Cl$: calcd C, 55.91; H, 4.32; N, 6.39. Found: C, 56.14; H, 4.19; N, 6.26. UV/Vis (CH_3CN): λ, nm (ε, $dm^3mol^{-1}cm^{-1}$), 368 (3.22 x 10^3), 318 (6.87 x 10^3), 283 (16.35 x 10^3).

3.2.4. Absorption and Luminescence Study

Stock solutions of the complexes **1-4** (2 x 10^{-5} M) and that of perchlorate salts (2 x 10^{-3} M) of various metal ions (Li^+**,** Na^+, K^+, Rb^+**,** Cs^+**,** Ag^+**,** Mg^{2+}, Ca^{2+}, Sr^{2+}, Ba^{2+}, Zn^{2+}, Cd^{2+}, Hg^{2+}**,** Ni^{2+} and Pb^{2+}) were prepared in freshly distilled acetonitrile. Then 2 mL stock solution of the complex and 2 mL stock solution of each metal salts were taken in a 5 mL volumetric flask, so that the effective concentration of the complex became 1 x 10^{-5} M

and that of the metal ions were 1 x 10^{-3} M (100 fold). The UV/Vis spectra of all the solutions containing metal ions (100 equiv) were recorded and the same were compared to that of the original solutions to examine the changes in the UV/Vis spectrum.

After that the luminescence spectra of all the solutions and that of their original complex (1 x 10^{-5} M) were recorded with excitation at the absorption maxima (λ_{max}) of the MLCT band, which is 457, 456, 456, 368 nm for **1-4**, respectively. The spectra of the cation added solutions were compared with that of the original solution to ascertain the interactions of the metal ions with the ionophore. For the emission titration study, the same complex stock solutions were used and the metal perchlorate solutions of desired concentration were prepared by diluting the concentrated standard solution (2 x 10^{-3} M). Then, 2 mL of each solution was mixed in a 5-mL volumetric flask and the luminescence spectra of the resulting solutions were recorded. The binding constants were calculated following the literature procedure.

Similar experiments were also carried out with tetrabutyl ammonium salts (2 x 10^{-3} M) of various anions (F^-, Cl^-, Br^-, I^-, $H_2PO_4^-$, ClO_4^- , NO_3^-, BF_4^-, CH_3COO^-, and HSO_4^-) to investigate the interaction of the anions with the ionophore.

3.2.4. NMR study

To investigate the interaction of anions with fluoroionophore, ^{1}H NMR spectroscopic study was carried out. These complexes, except **4,** are highly soluble in acetonitrile, however after addition of anions, all the new products formed are not highly soluble in acetonitrile, particularly in the case of $H_2PO_4^-$. Because of this solubility problem, the NMR experiment with large excess of anions could not be done. ^{1}H NMR spectra of the solutions containing 2 mg of complex, dissolved in 0.5 mL of CD_3CN, were recorded. The solutions of anions were then added with increasing concentration to make it 1.5 molar equivalent of the concentration of complex for $H_2PO_4^-$ and 5 molar equivalent of the concentration of complex for F^-. The spectra of the anion added solutions were compared to that of the original compounds to ascertain the interaction of the anion with the ionophore. No NMR titration experiments were carried out as the binding constants were determined from fluorescence titration data.

3.2.5. Electrochemical study

The electrochemical measurements were carried out using a CHI 660A electrochemical workstation equipment. Cyclic voltammetry and DPV studies were carried in a three-electrode cell consisting of a platinum working electrode, a platinum-wire auxiliary electrode and an SCE reference electrode. Solutions of the complexes in purified acetonitrile containing 0.1M tetrabutylammonium tetrafluoroborate as supporting electrolyte were deaerated by bubbling argon for 5 min prior to each experiment. The cyclic voltammogram of $[Ru(bpy)_3]^{2+}$ was recorded first for calibration of the instrument. Cyclic voltammograms (CV) and differential pulse voltammetry (DPV) of complexes **1-3** were recorded. As the solubility of the complex **4** was not sufficient in acetonitrile, therefore the cyclic voltammogram and differential pulse voltammogram of complex **4** could not be recorded in acetonitrile.

3.3. Results and Discussion

3.3.1. Synthesis of the ligands (L^1-L^3)

The routes followed for the synthesis of $\mathbf{L^1}$–$\mathbf{L^3}$ are shown in Schemes 3.1 and 3.2, respectively and details of the experimental procedures are given in the Experimental Section. It may be noted that the intermediate compound **I** is insoluble in THF, therefore the ligand $\mathbf{L^3}$ was synthesized in acetonitrile using K_2CO_3 as base. Elemental analysis (C, H and N), IR, ESMS and ^{1}H NMR spectral data for all the intermediate compounds and for ligands $\mathbf{L^1}$-$\mathbf{L^3}$ are given in the Experimental Section. The elemental analysis and mass data are in excellent agreement with the calculated values. It may be noted that the *m/z* values of all these compounds correspond to the $Na^+/K^+/H^+$ adduct, which is a well known phenomenon when LC-MS is used for the measurement of mass. The IR spectra of $\mathbf{L^1}$ and $\mathbf{L^2}$ exhibited bands of moderate intensity at 3366 and 3364 cm^{-1}, respectively, which are due to ν(OH). The bands at 3187, 3065 and 3061 cm^{-1} for $\mathbf{L^1}$, $\mathbf{L^2}$ and $\mathbf{L^3}$, respectively are assigned to ν(N-H) of the amide moiety. The strong bands, which appeared at 1682, 1678 and 1672 cm^{-1} for $\mathbf{L^1}$, $\mathbf{L^2}$ and $\mathbf{L^3}$, respectively are due to ν(C=O). In the ^{1}H NMR spectrum of $\mathbf{L^1}$, the *meta*- protons (with respect to the OH substituent) of

the calixarene moiety appear as two distinct singlets in the range δ 7.14-6.78. But in the ^{1}H NMR spectra of $\mathbf{L^2}$ and $\mathbf{L^3}$, the *meta*- and *para*-protons of the calixarene moiety appear as two doublets and a multiplate (overlapped triplet), respectively. In fact, two sets of signals appear for these protons in the aromatic region δ 7.15-6.8 due to substituents at the two opposite OH of the four phenolic OH groups. In all the ligands the bipyridyl moiety is expected to give six signals. However, due to overlap of some of the signals, four distinct signals have been identified in the region δ 8.72-7.49. In ligand $\mathbf{L^1}$ and $\mathbf{L^2}$, the protons of –*CONH* group exhibited a broad signal in the region δ 8.49-8.48. But in the ligand $\mathbf{L^3}$, the protons of –*CONH* group appeared as a broad signal in at δ 6.03. This difference may be due to intramolecular H-bonding interactions. The protons of –*CONH* group of the ligands $\mathbf{L^1}$ and $\mathbf{L^2}$ are involved in H-bonding interaction with the oxygen atoms of the adjacent -OH of the calixarene moiety, which resulted in deshielding of these protons. As there is no -OH group in the calixarene moiety of $\mathbf{L^3}$, therefore, no intramolecular H-bonding leading to deshielding of NH protons took place. In all three ligands, the protons of ArO-CH_2-CO- appeared as a singlet in the region δ 4.57-4.22. In the ^{1}H NMR spectra of $\mathbf{L^1}$ and $\mathbf{L^2}$, the Ar-CH_2-Ar protons of the calixarene moiety appear as two well separated doublets in the region δ 4.22-3.4, which suggest that calixarene moiety in these two ligands exist in cone conformation.[15] The ArCH_2Ar protons of $\mathbf{L^3}$ appeared as two closely spaced doublets in the region δ 3.81-3.71, which is similar to that observed for 1,3-alternate conformation with substituents at the two of the four OH groups in the calix moiety.[13] The CH_2, which connects the bipyridine unit with the aza-crown moiety, and the CH_3 attached to the bipyridine unit appear as a singlet in the range δ 3.97-3.78 and at δ 2.49-2.42, respectively.

3.3.2. Synthesis of the complexes (1-4)

The Ru(II) complexes **1**, **2** and **3** were synthesized by the reaction of *cis*-$[Ru(bpy)_2Cl_2].2H_2O$ and $\mathbf{L^1}$/$\mathbf{L^2}$/$\mathbf{L^3}$ in refluxing ethanol-water, isolated with PF_6^- counter anion and purified by column chromatography. All of these complexes gave satisfactory C, H and N analysis. Mass spectrometry data are in excellent agreement with the calculated values. The IR spectra of **1** and **2** exhibited bands of moderate intensity at 3417 and 3402 cm^{-1}, respectively, which are due to ν(O-H). The bands

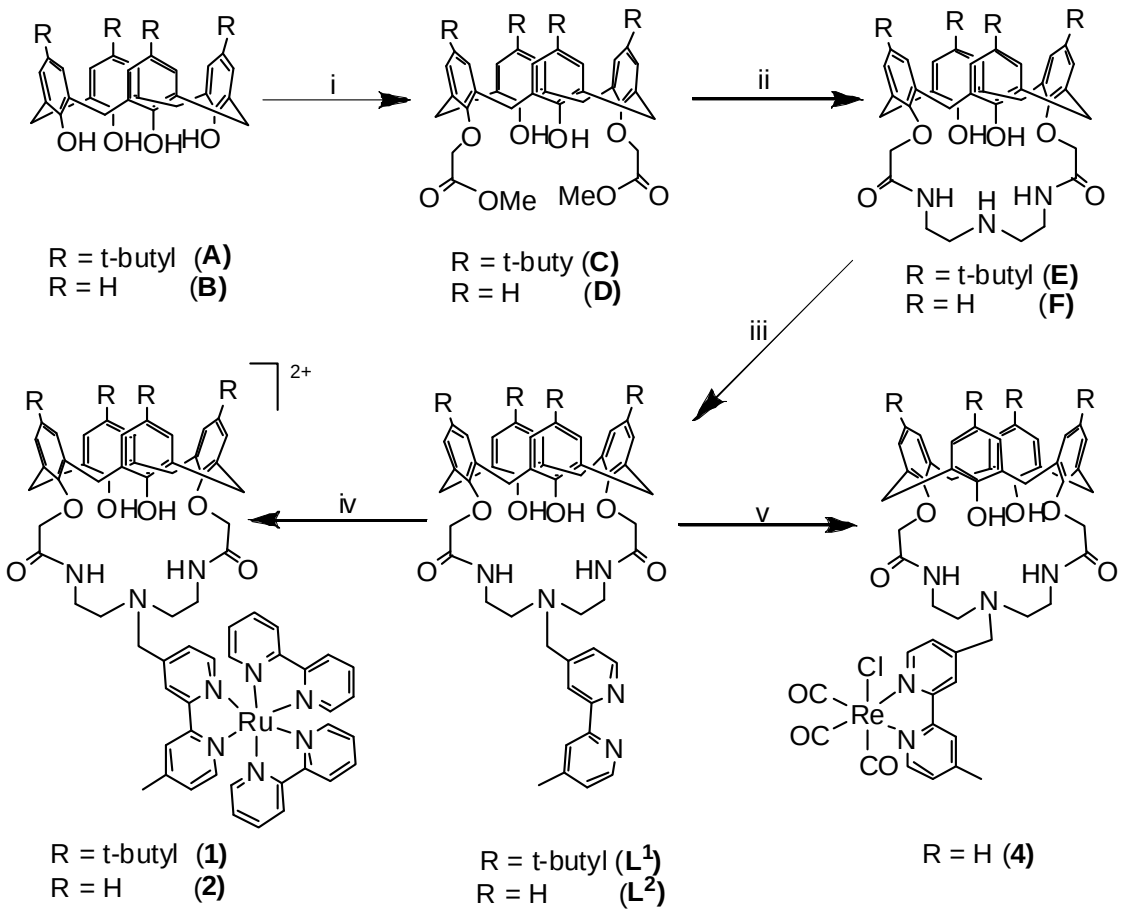

Reagents and conditions: (i) $BrCH_2CO_2CH_3$, K_2CO_3/Acetone, reflux (ii) Diethyl triamine, 1:1 MeOH-Toluene, reflux (iii) 4-bromomethyl-4'methyl-2,2'-bipyridine, Et_3N/THF, reflux (iv) $Ru(bpy)_2Cl_2.2H_2O$, EtOH and H_2O, reflux (v) $Re(CO)_5Cl$, THF, reflux.

Scheme 3.1. Synthetic routes for the ligands $\mathbf{L^1}$ and $\mathbf{L^2}$ and the complexes **1, 2** and **4.**

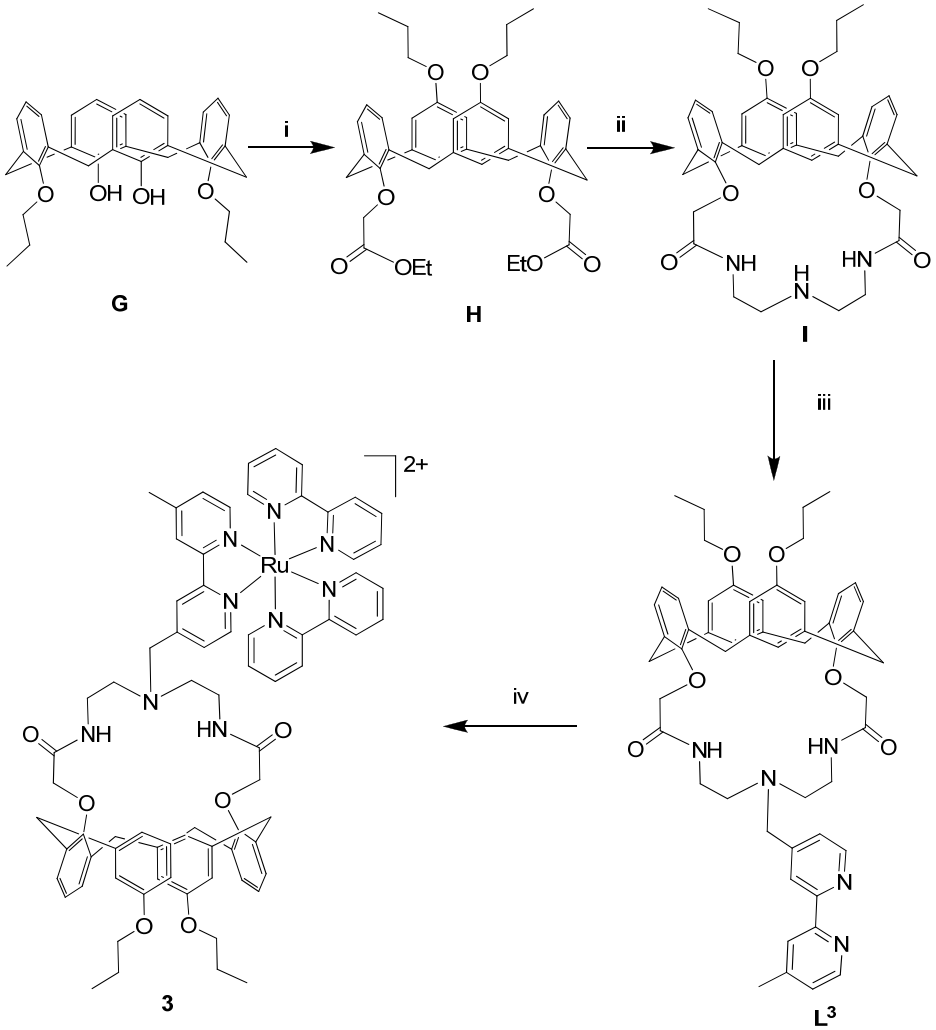

Reagents and conditions: (i) $BrCH_2CO_2Et$, Cs_2CO_3/ACN, reflux (ii) Diethyl triamine, 1:1 EtOH-Toluene, reflux (iii) 4-bromomethyl-4'methyl-2,2'-bipyridine, K_2CO_3/ACN, reflux (iv) $Ru(bpy)_2Cl_2.2H_2O$, EtOH and H_2O, reflux.

Scheme 3.2. Synthetic routes for the ligand $\mathbf{L^3}$ and the complex **3.**

at 3215, 3078, and 3107 cm^{-1} for **1**, **2** and **3**, respectively are assigned to ν(N-H) of the amide moiety. The bands, which appeared at 1676, 1675 and 1670 cm^{-1} for **1**, **2** and **3**, respectively are due to ν(C=O). All the three complexes (**1-3**) showed strong band at 842, 841, and 843 cm^{-1} respectively for PF_6^-. The ^1H NMR spectra of complexes **1-3** were

recorded in CD_3CN and the data with assignment of peaks are given in the experimental section. Mass and ^1H NMR spectra for the complexes **1**–**3** are shown in Figures.3.1-3.4. For complexes **1–3**, the signals due to protons of the two bipyridine units attached to Ru(II) centre appeared in the aromatic region along with the signals due to bpy attached to the ligands (**L^1**–**L^3**). In complex **1** and **2,** the protons of –CON*H* group appeared as broad singlet at *δ* 8.73 and 8.55 respectively and for **3**, the same protons appeared at δ 5.81. The protons of Ar-*OH* group of complex-**1** and **2,** appeared as singlet at δ 7.95 and 7.92 respectively. In case of complex **1**, the two singlets for the *meta*-hydrogen atoms of the calix moiety are overlapped and appeared as a multiplate in the region *δ* 7.26-7.23. In case of **2,** the *meta*-protons of the calixarene moiety appear as two doublets in the region *δ* 7.20-7.04 and *para*-protons appeared as two triplets in the region *δ* 6.88-6.77. For **3** the signals for *meta* and *para*-protons appeared as doublets and triplets, respectively in the region *δ* 7.12-6.87. In all three complexes (**1-3**), the protons of ArO-*CH_2*CO- group is expected to give a singlet for methylene protons. However, in the complexes this signal has splitted and apparently looks like a multiplet. This is probably due to the involvement of one of the CH_2 protons in intra- or intermolecular interaction, which makes them chemically non-equivalent leading to splitting of the signal. The Ar*CH_2*Ar protons of **1** and **2** appeared as two doublets, one in the region *δ* 4.20-4.17 and the other one is merged with the multiplet observed in the region *δ* 3.58-3.39. The appearance of two doublets (AB type) suggests that the calix moiety in these complexes exist in cone conformation. In the ^1H NMR spectra of complexes-**3,** Ar*CH_2*Ar protons exhibited two closely spaced doublets in the region *δ* 3.81-3.71, similar to the ligand, which suggested 1,3-alternate conformation of the calixarene moiety.

The Re(I) complex (**4)** was synthesized by the reaction of $[Re(CO)_5Cl]$ with **L^1** in refluxing THF. The crude product was purified by column chromatography. The microanalytical (C, H and N) and mass spectrometric data are consistent with the proposed composition of the complexes. The IR spectra of complex **4** exhibited a band of moderate intensity at 3356 for ν(O-H) and a sharp band at 2925 for ν(N-H). The IR spectra of this complex also exhibit three strong bands at 2018, 1889 and 1677 cm–1 for ν(axial C=O), ν(equatorial C=O) and ν(C=O) respectively. As this complex is not sufficient soluble in CD_3CN, the ^1H NMR spectra of this complex is recorded in $CDCl_3$.

In the ^{1}H NMR spectra of this complex, the bipyridyl unit attached to the ligand exhibited four doublets and two singlets in the aromatic region. The protons of the –CON*H* group appeared as broad signal at δ 8.83. The protons of Ar-*OH* group of the calixarene moiety appeared as a singlet at δ 7.75. In this complex the signals for *meta* and *para*-protons appeared as a doublets and triplets in the region δ 7.13-6.78. Like other three complexes, the protons of ArO-CH_2CO- of this complex exhibited a multiplate in the region δ 4.70-4.53. The NMR signal of the ArCH_2Ar protons of this complex suggests cone conformation for the calixarene moiety. The proposed structures of all the complexes are shown in scheme 3.1 and 3.2.

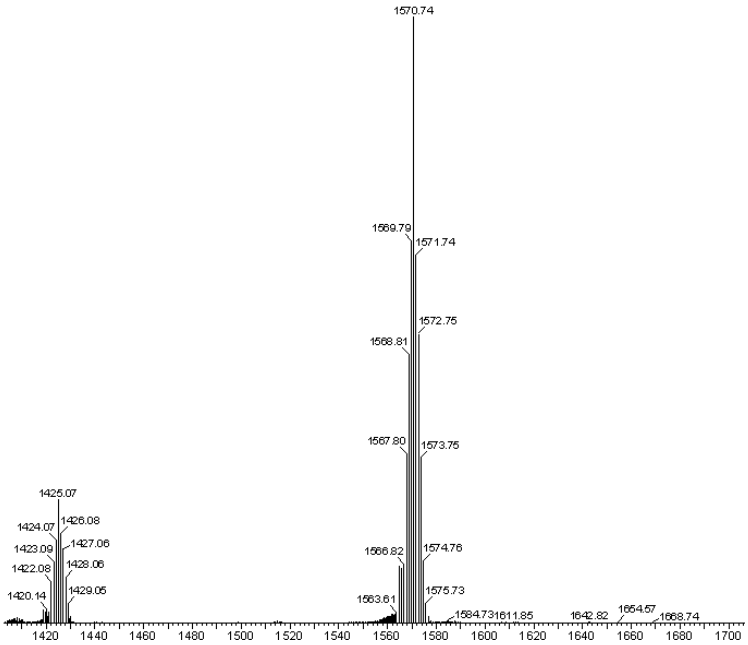

Figure. 3.1. Mass spectra of $[Ru(L^1)_3](PF_6)_2$ **(1)**.

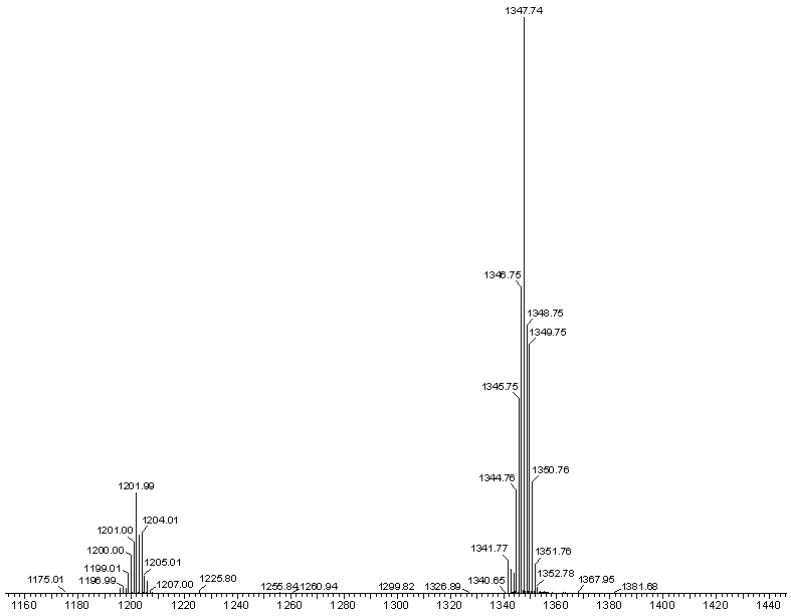

Figure. 3.2. Mass spectra of $[Ru(L^2)_3](PF_6)_2$ **(2)**.

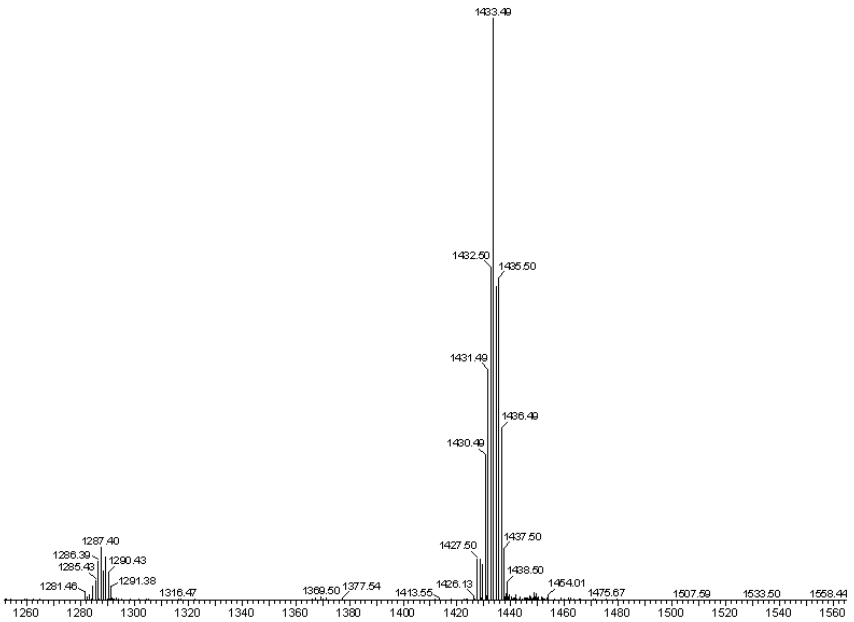

Figure. 3.3. Mass spectra of $[Ru(L^3)_3](PF_6)_2$ **(3)**.

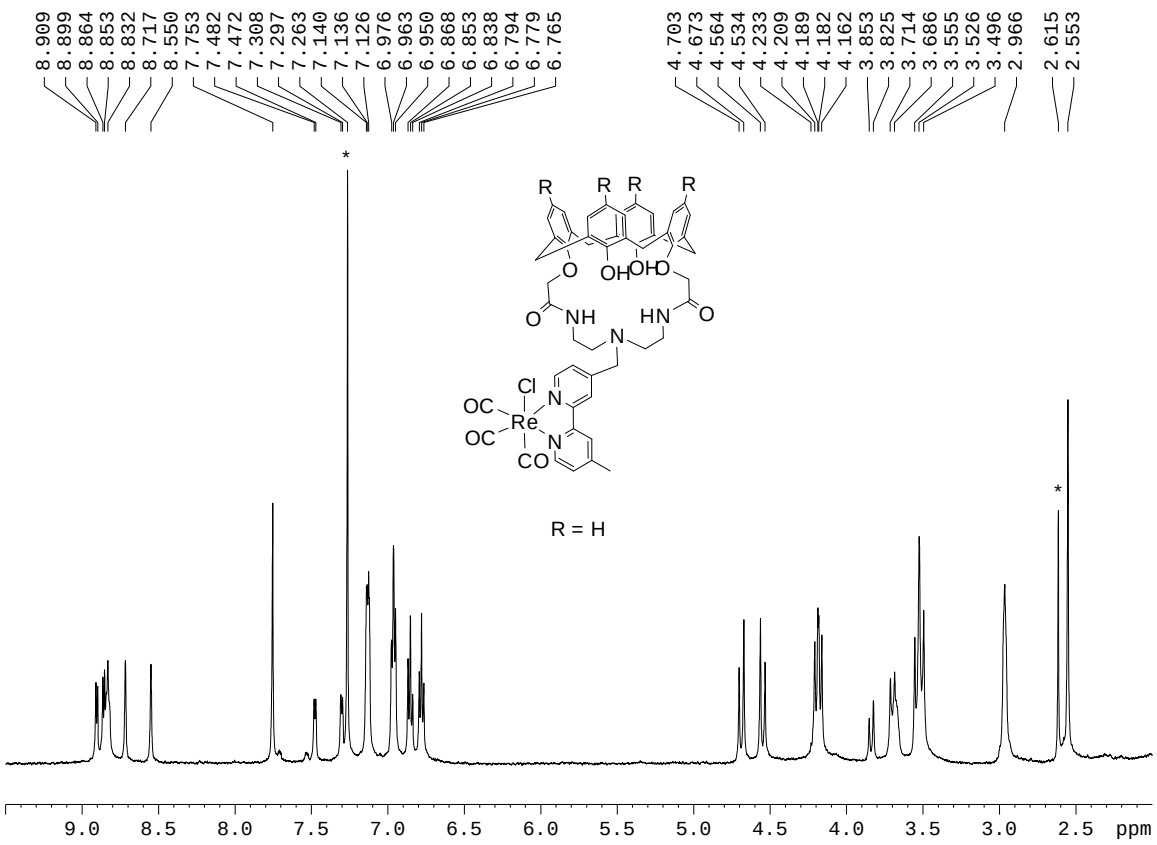

Figure. 3.4. NMR spectra of $[Re(L^2)(CO)_5 Cl]$ **(4).**

3.3.3. Absorption and Luminescence studies

The absorption and luminescence spectra of all complexes were recorded in acetonitrile, data for absorption spectra is given in the Experimental Section and luminescence data is given in the Table 3.1. In the absorption spectra, the low-energy bands in the region 423-457 nm for Ru(II) and at 368 and 318 nm for Re(I) are due to metal-to-ligand (bpy) charge-transfer (MLCT) transitions ($d\pi \rightarrow \pi^*$).[16] The high-energy bands, which appear at around 287 and 283 nm, are ligand-centred charge transfer (CT) bands due to $\pi \rightarrow \pi^*$ transitions.[17] The steady state emission spectra and quantum yield (φ) of all complexes were recorded in acetonitrile at room temperature, the Ru(II) complexes (**1**-**3**) exhibit a

strong ^{3}MLCT emission band (λ_{em}) around 615 nm, whereas the Re(I) complex (**4**) shows weak emission at 593 nm (Table 3.1). The luminescence quantum yields for **1–3** are 0.053, 0.055 and 0.052, which is close to the value for $[Ru(bpy)_3]^{2+}$ (f =0.062) in acetonitrile.

Table 3.1. Emission maxima, quantum yield, binding constant (K_s) with guest ions for the Ru(II)/ Re(I) receptors.

Complex	λ_{em}	Quantum yield (ϕ)	In presence of guest ions		
			Guest ion	λ_{em}[a]	Binding constant (K_s) M^{-1}
1	614	0.053	Hg^{2+}	630	47.67×10^3
			Pb^{2+}	628	14.49×10^3
			$H_2PO_4^-$	626	17.93×10^3
			F^-	620	11.98×10^2
2	614	0.055	Hg^{2+}	630	43.04×10^3
			Pb^{2+}	629	5.82×10^3
			F^-	619	35.04×10^2
3	614	0.052	Hg^{2+}	630	38.62×10^3
			Pb^{2+}	630	3.11×10^3
			$H_2PO_4^-$	626	22.99×10^3
4	594	0.015	Hg^{2+}	554	50.19×10^3

[a] Emission maxima (λ_{em}) of the spectra recorded in presence of maximum concentration of guest ion.

3.3.4. Electrochemistry

The Cyclic voltammograms (CV) and differential pulse voltammetry (DPV) of all Ru-complexes (**1-3**) were recorded in acetonitrile, and the data are presented in Table 3.2. The cyclic voltammograms of **1** and **3** are illustrated in Figure. 3.5. In each case, the voltammograms displayed a quasireversible oxidation wave, which is ascribed to Ru(II) → Ru(III) oxidation, and three ligand based reduction couples. The metal based oxidation for **1-3** is observed in the potential range 1.23-1.30 V, which is close to the oxidation potential of Ru(II) of $[Ru(bpy)_3]^{2+}$ complex (1.27V).[18] The ligand based redox couples are observed in the potential range -1.42 to -1.89 V (Table 3.2), which are assigned to sequential one-electron reduction of the three bipyridine ligands (bpy → bpy^-) coordinated to the metal ion.

Table 3.2. Electrochemical data for complexes **1-3** in acetonitrile solution[a]

Complex	$E_{1/2}^{ox}$/V (ΔEp/mV)[b]		$E_{1/2}^{red}$/V (ΔEp/mV)	
1	+1.30 (208)	-1.36 (66)	-1.58 (92)	-1.89 (169)
2	+1.24 (169)	-1.42 (45)	-1.63 (85)	-1.89 (91)
3	+1.23 (110)	-1.39 (79)	-1.57 (71)	-1.82 (85)

[a] V *vs* SCE. [b] $E_{1/2}$ = (*E*pa + *E*pc)/2; ΔEp = *E*pa - *E*pc.

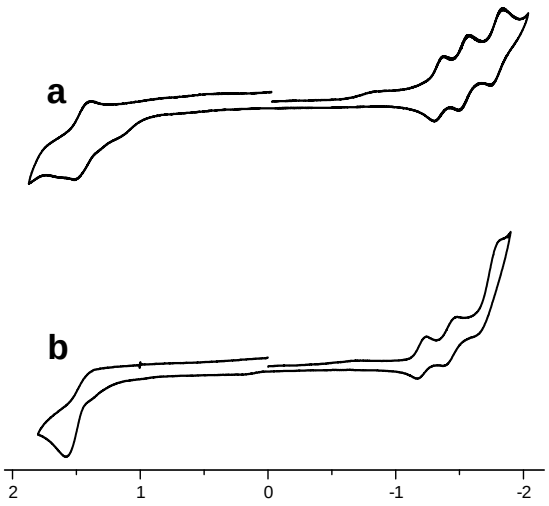

Figure. 3.5. Cyclic voltammograms of **1** (b) and **3** (a) recorded in acetonitrile solution

3.3.5. Ion-binding study

The ion-binding ability of the fluoroionophores **1-4** have been investigated with a large number of cations such as Li^+**,** Na^+, K^+, Rb^+**,** Cs^+**,** Ag^+**,** Mg^{2+}, Ca^{2+}, Sr^{2+}, Ba^{2+}, Zn^{2+}, Cd^{2+}, Hg^{2+}**,** Ni^{2+} and Pb^{2+} and anions F^-, Cl^-, Br^-, I^-, $H_2PO_4^-$, ClO_4^-, NO_3^-, BF_4^-, CH_3COO^-, and HSO_4^-. The ion recognition process was monitored mainly by luminescence spectral change. For certain anions ^1H NMR spectral change with addition of increasing amount of ions was also carried out to investigate the mode of interaction with donor atoms.

The luminescence spectra of all these fluoroionophores were recorded in acetonitrile in presence of the above-mentioned ions. For cations, the complexes **1-3** showed significant enhancement in emission intensity with ~ 15 nm red shift in presence of Hg^{2+} and Pb^{2+}, whereas complex **4** showed large enhancement in emission intensity with 40 nm blue shift in presence of Hg^{2+}. The other metal ions used in this study did not induce any significant change in the emission spectra for all the four ionophores. The change in emission intensity for complex **4** in presence of various metal ions is shown in

Figure.3.6. Substantial enhancement in emission intensity in presence of Hg^{2+} and Pb^{2+} indicate complexation of these metal ions with the ionophore. The enhancement in emission intensity is attributed to the fact that complexation of metal ion with the amide bridged aza-crown moiety resulted in decrease of the intramolecular reductive electron transfer quenching involving lone pair of the aza-N atom. Probably conformation of the ionophore in solution, nature of donor atoms, ionic size and charge play crucial role for selective interactions.

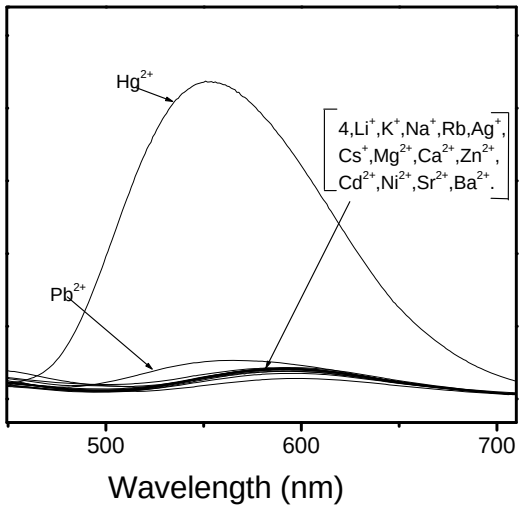

Figure. 3.6. Emission spectral changes of **4** (1 x 10^{-5} M) in presence of various cations. Excitation wavelength: 366 nm.

For anions, strong quenching in emission intensity is noted with F^- and $H_2PO_4^-$ for **1** and **2**, and only with $H_2PO_4^-$ for **3**. For **4**, no significant change in emission intensity with any of the anions studied is observed. The observation, therefore, suggest that complex **1** and **2** form strong complexes with F^- and $H_2PO_4^-$, and **3** forms complex only with $H_2PO_4^-$. The hydrogen atoms of the OH and NH in the cavity of the ionophore make interaction with the anions to form complex as evident from NMR study, which showed substantial change in chemical shifts of the OH and NH protons when spectra were recorded in presence of excess anions. The other factor is the electrostatic interaction between doubly charged metal ion and anions. In case of **4**, it is a neutral

compound, which did not attract anions to come close to the metal ion to encapsulate in the cavity of the ionophore. For **3**, no OH is available and the calixarene unit is in 1,3-alternate conformation and interaction with two NH protons probably not sufficient for F^- to form strong complex. The cavity size of complexes **1** and **2** are probably fitting nicely with F^- to make interaction with all the four hydrogen atoms to form stable complex. The geometry of $H_2PO_4^-$ is tetrahedral, which allowed it to interact with hydrogen atoms from out of the plane of the cavity. The interaction of **2** with $H_2PO_4^-$ is not straight forward; there is substantial change in emission intensity upon addition of anion but the pattern of changes are not consistent and linear with the concentration of anions. Probably with increasing the concentration of anions, change in conformation of the calixarene and/or host-guest ratio in the complex is changing. Further study on this system was not carried out. The proposed structures of the complexes formed by **1** with Pb^{2+}, **2** with F^-, **3** with $H_2PO_4^-$ and **4** with Hg^{2+} are shown in Figures. 3.7-10.

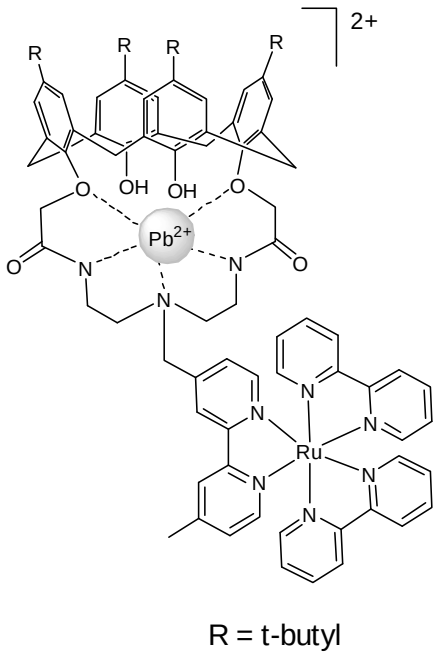

Figure.3.7. The proposed structures of the complex formed by **1** with **Pb^{2+}**.

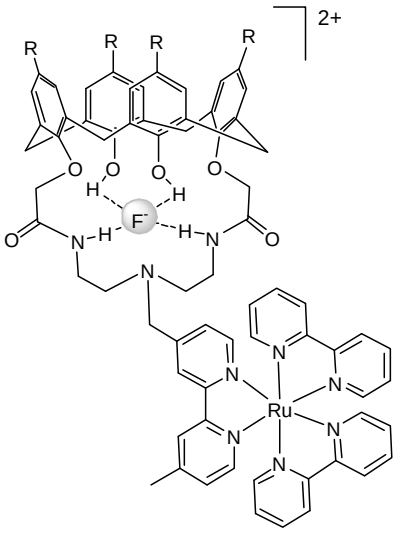

Figure.3.8. The proposed structures of the complex formed by **2** with $\mathbf{F^-}$.

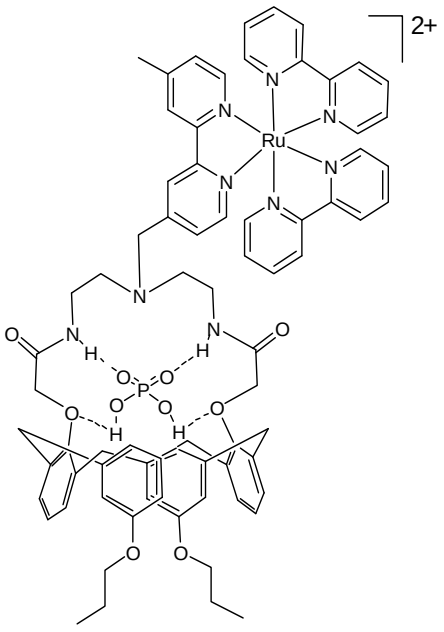

Figure.3.9. The proposed structures of the complex formed by **3** with $\mathbf{H_2PO_4^-}$.

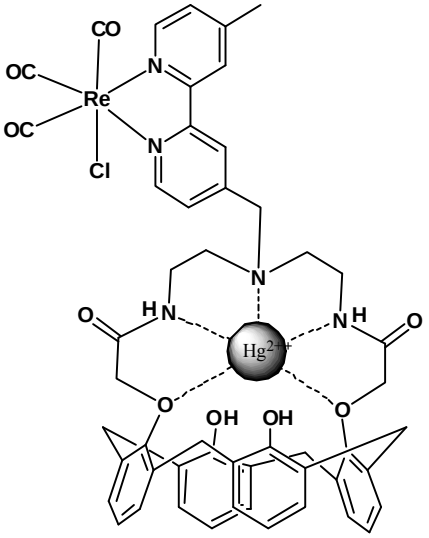

Figure.3.10. The proposed structures of the complex formed by **4** with $\mathbf{Hg^{2+}}$

Binding constants for **1-4** with the strongly interacting ions, which changed emission intensity significantly**,** were calculated using emission titration data following literature procedure.[19] The changes in emission spectra upon addition of increasing concentration of various ions are shown in Figures. 3.11-3.21. According to this procedure, the fluorescence intensity (F) scales with the metal ion concentration ([M]) according to the formula $(F_0 - F)/(F - F_\infty) = ([M]/K_{diss})^n$. The binding constant ($K_s$) is obtained by plotting $\log[(F_0 - F)/(F - F_\infty)]$ vs. log[M], where F_0 and F_∞ are the relative fluorescence intensities of the complex without addition of guest metal ion and with maximum concentration of metal ion (when no further change in emission intensity takes place), respectively. The value of log[M] at $\log[(F_0 - F)/(F - F_\infty)] = 0$ gives the value of $\log(K_{diss})$, the reciprocal of which is the binding constant (K_s). The plots $\log[(F_0 - F)/(F - F_\infty)]$ vs. log[M] are shown as insets in Figures. 3.11-21. The titration data showed very good linear fit (R = 0.99) with the above equation. The binding constants of all complexes are summarized in Table 3.1.

The binding constant values (Table -3.1) suggest that Hg^{2+} binds strongly (almost 10 times) compared to Pb^{2+} for all complexes. These two metal ions have similar ionic

radius, therefore the affinity towards the donor atoms in the cavity probably makes the difference in binding constant. Binding constants for a particular ion is comparable for complexes **1** and **2** but less for complex **3**. For anions, binding constant for $H_2PO_4^-$ is significantly higher compared to that of F^-, which is ascribed to bidentate chelating nature of the former. The two oxygen atoms with delocalized negative charge makes strong interaction with the hydrogen atoms of the NH group.

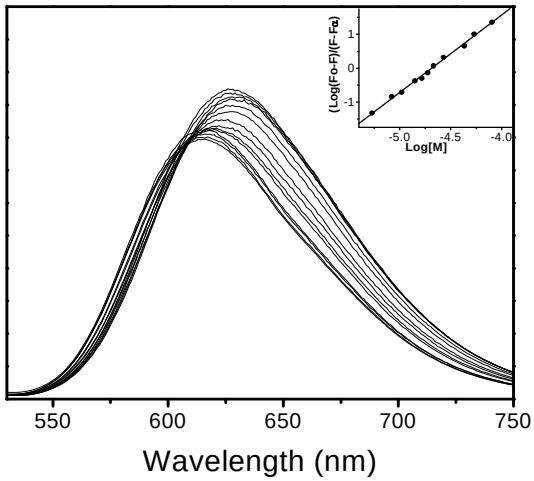

Figure. 3.11. Emission spectral changes of **1** (1 x 10^{-5} M) upon addition of increasing concentration of $Hg(ClO_4)_2$. Excitation wavelength: 455 nm. Inset: linear regression fit (double-logarithmic plot) of the titration data as a function of concentration of metal ion.

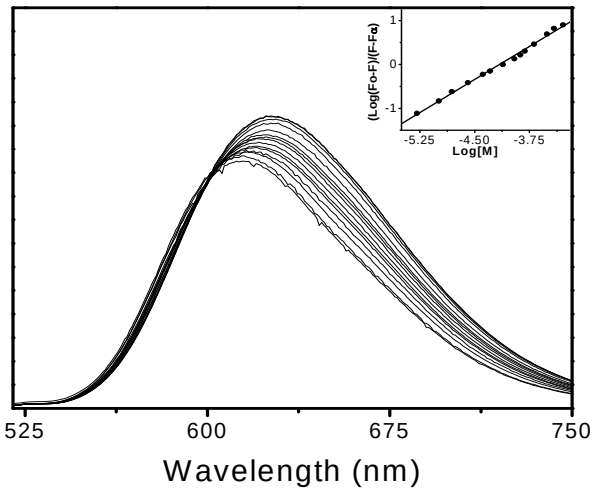

Figure. 3.12. Emission spectral changes of **1** (1 x 10^{-5} M) upon addition of increasing concentration of $Pb(ClO_4)_2$. Excitation wavelength: 455 nm. Inset: linear regression fit (double-logarithmic plot) of the titration data as a function of concentration of metal ion.

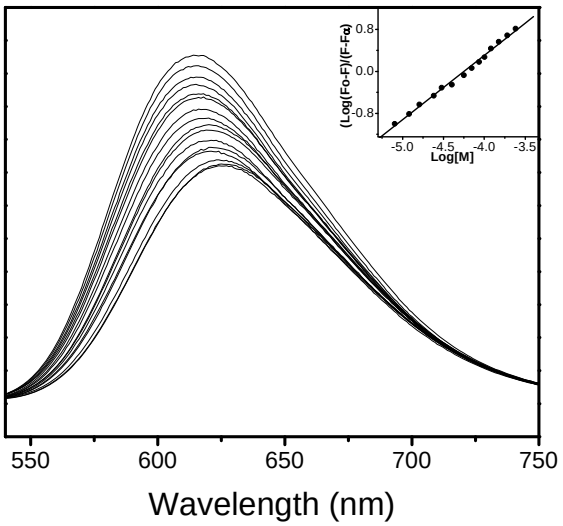

Figure. 3.13. Emission spectral changes of **1** (1 x 10^{-5} M) upon addition of increasing concentration of $H_2PO_4^-$. Excitation wavelength: 455 nm. Inset: linear regression fit (double-logarithmic plot) of the titration data as a function of concentration of metal ion.

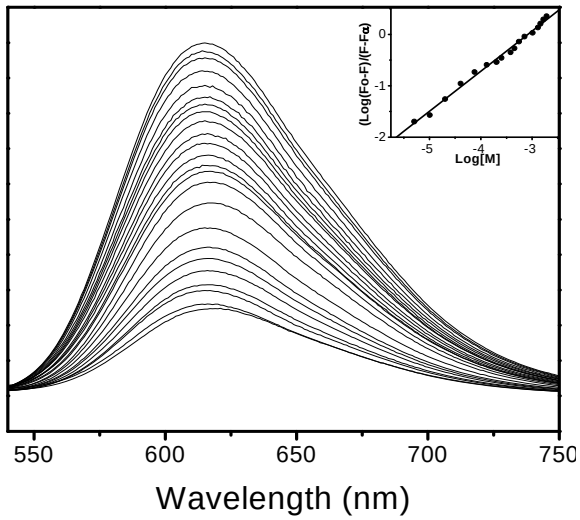

Figure. 3.14. Emission spectral changes of **1** (1 x 10^{-5} M) upon addition of increasing concentration of F^-. Excitation wavelength: 455 nm. Inset: linear regression fit (double-logarithmic plot) of the titration data as a function of concentration of metal ion.

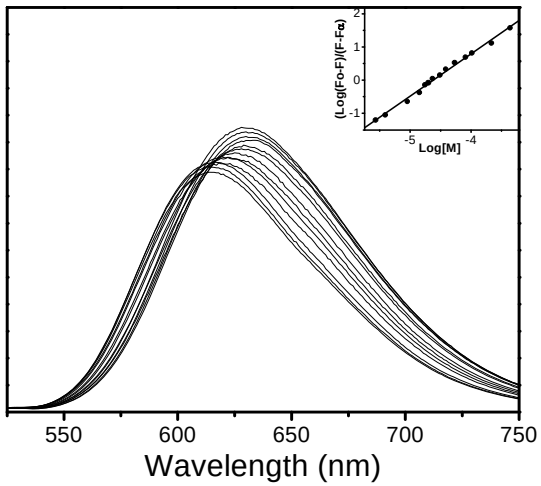

Figure. 3.15. Emission spectral changes of **2** (1 x 10^{-5} M) upon addition of increasing concentration of $Hg(ClO_4)_2$. Excitation wavelength: 455 nm. Inset: linear regression fit (double-logarithmic plot) of the titration data as a function of concentration of metal ion.

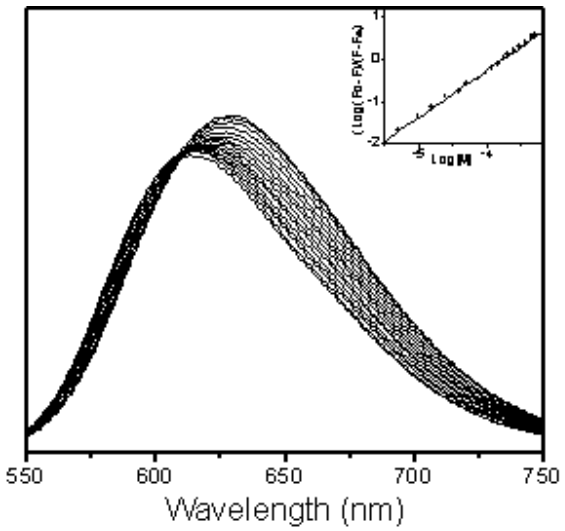

Figure. 3.16. Emission spectral changes of **2** (1 x 10^{-5} M) upon addition of increasing concentration of $Pb(ClO_4)_2$. Excitation wavelength: 455 nm. Inset: linear regression fit (double-logarithmic plot) of the titration data as a function of concentration of metal ion.

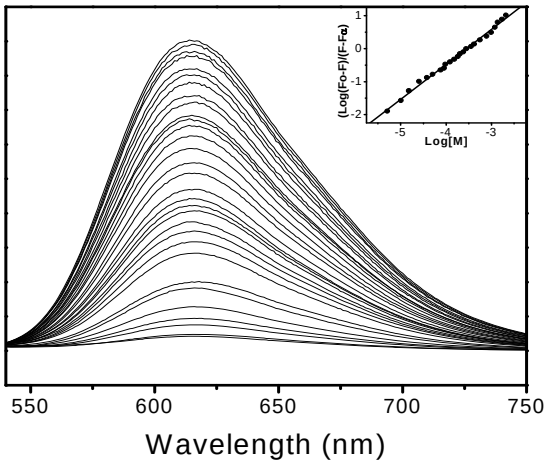

Figure. 3.17. Emission spectral changes of **2** (1 x 10^{-5} M) upon addition of increasing concentration of F^-. Excitation wavelength: 455 nm. Inset: linear regression fit (double-logarithmic plot) of the titration data as a function of concentration of metal ion.

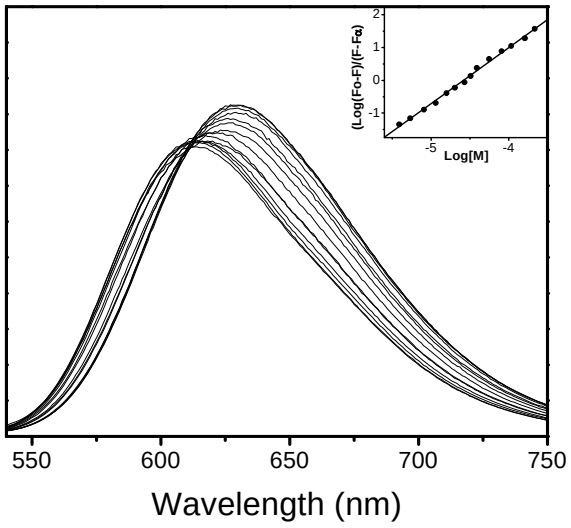

Figure. 3.18. Emission spectral changes of **3** (1 x 10^{-5} M) upon addition of increasing concentration of $Hg(ClO_4)_2$. Excitation wavelength: 455 nm. Inset: linear regression fit (double-logarithmic plot) of the titration data as a function of concentration of metal ion.

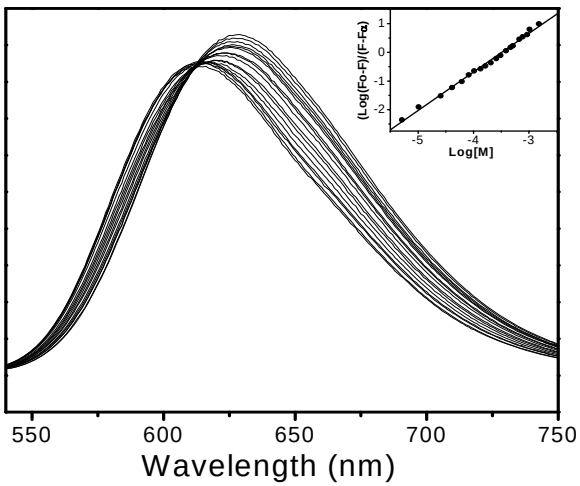

Figure. 3.19. Emission spectral changes of **3** (1 x 10^{-5} M) upon addition of increasing concentration of $Pb(ClO_4)_2$. Excitation wavelength: 455 nm. Inset: linear regression fit (double-logarithmic plot) of the titration data as a function of concentration of metal ion.

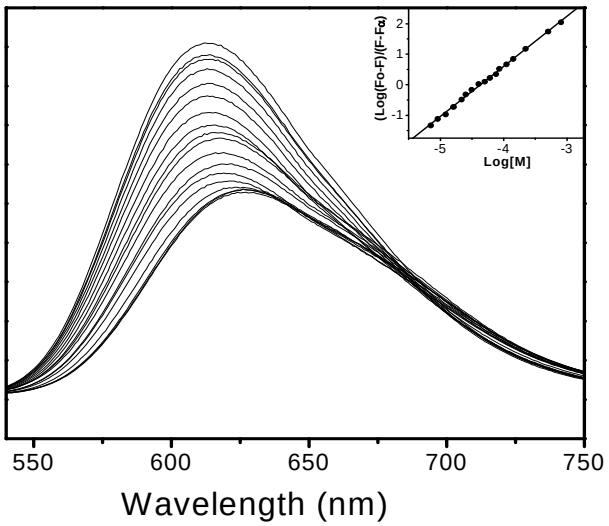

Figure. 3.20. Emission spectral changes of **3** (1 x 10^{-5} M) upon addition of increasing concentration of $H_2PO_4^-$. Excitation wavelength: 455 nm. Inset: linear regression fit (double-logarithmic plot) of the titration data as a function of concentration of metal ion.

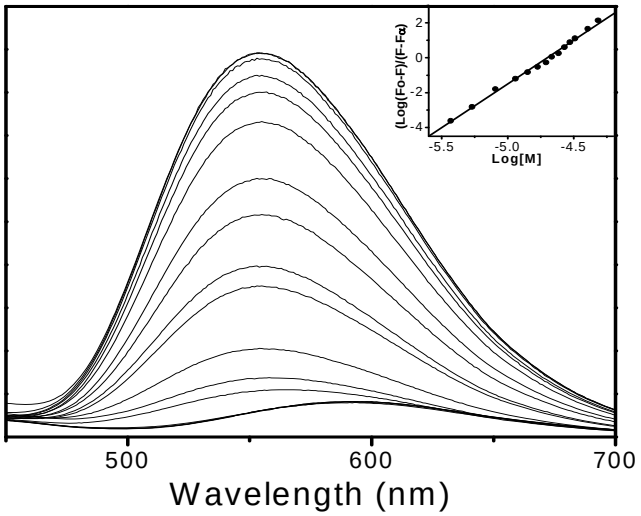

Figure. 3.21. Emission spectral changes of **4** (1 x 10^{-5} M) upon addition of increasing concentration of $Hg(ClO_4)_2$. Excitation wavelength: 366 nm. Inset: linear regression fit (double-logarithmic plot) of the titration data as a function of concentration of metal ion.

3.4. Conclusion

A series of fluoroionophores using ruthenium(II)/rhenium(I) bipyridine moiety as fluorophore and diamide bridged calix[4]arene aza-crown moiety as ionophore have been synthesized, characterized and their electrochemical, photophysical and ion-binding property were studied. The ion-binding ability of these fluoroionophores has been investigated with a large number of cations and anions. The luminescence study shows strong complexing ability of all the three Ru(II) fluoroionophores with Hg^{2+} and Pb^{2+} and the Re(I) complex exhibits strong complexation with Hg^{2+}. The fluorescence study also shows strong complexing ability of the Ru(II) complexes with $H_2PO_4^-$ and F^- (for two complexes). Binding constants for all of the strongly interacting ions have been calculated using luminescence titration data and they exhibit moderate to strong binding of ions. The Ru(II) ionophores exhibit strong interaction with $H_2PO_4^-$ and F^-, which is due to strong electrostatic interaction between metal centre and anions and the electropositive (δ^+) nature of the OH and CONH protons, which can make strong interaction with anions. The Re(I) ionophore, being a neutral complex, does not interact with anions. The affinity of the metal ions towards the coordinating atoms plays crucial role in selectivity of the metal ion.

3.5. References

1. Charbonni`ere, L. J.; Ziessel, R. E.; Sams, C. A.; Harriman, A. *Inorg. Chem.* **2003**, *42*, 3466.
2. Lazarides, T.; Miller, T. A.; Jeffery, J. C.; Ronson, T. K.; Adams, H.; Ward, M. D. *Dalton Trans.* **2005,** 528.
3. Schmittel, M.; Lin, H.-W. *Angew. Chem.* **2007,** *119,* 911.
4. Li, M.-J.; Chen, Z.; Zhu, N.; Yam, V. W.-W.; Zu, Y. *Inorg. Chem.*, **2008**, *47*, 1218.
5. Hissler, M.; Harriman, A.; Jost, P.; Wipff, G.; Ziessel, R. *Angew. Chem., Int. Ed.*, **1998,** *37,* 3249.
6. Beer, P.D.; Timoshenko, V.; Maestri, M.; Passaniti, P.; Balzani, V. *Chem. Commun.* **1999,** 1755.
7. Cooper, J. B.; Drew, M. G. B.; Beer, P. D. *J. Chem. Soc., Dalton Trans.* **2001**, 392.
8. Beer, P. D.; Szemes, F.; Passaniti, P.; Maestri, M. *Inorg. Chem.*, **2004,** *43,* 3965.
9. Lin, T-P.; chen, C-Y.; Wen, Y-S.; Sun, S-S. *Inorg. Chem*. **2007**, *46*, 9201.
10. Gholamkhass, B.; Mametsuka, H.; Koike, K.; Tanabe, T.; Furue, M.; Ishitani, O. *Inorg. Chem*. **2005**, *44*, 2326.
11. Sun, S-S.; Lees, A. J.; Zavalij, Y. *Inorg. Chem*. **2003**, *42*, 3445.
12. Unob, F.; Asfari, Z.; Vicens, J. *Tetrahedron Lett.* **1998,** *39*, 2951.
13. Kim, S. K.; Lee, S. H.; Lee, J. Y.; Lee, J. Y.; Bartsch, R. A.; Kim, J. S. *J. Am. Chem. Soc.* **2004,** *126*, 16499.
14. Banthia, S.; Samanta, A. *Org. Biomol. Chem.* **2005,** *3*, 1428.
15. Agnihotri, P.; Suresh, E.; Paul, P.; Ghosh, P. K. *Eur. J. Inorg.Chem.*, **2006,** 3369.

16. Boricha, V. P.; Patra, S.; Chouhan, Y. S.; Sanavada, P.; Suresh, E.; Paul, P. *Eur. J. Inorg. Chem.* **2009,** 1256.

17. Patra, S.; Paul, P. *Dalton Trans*., **2009**, 8683.

18. Cookson, J.; Vickers, M. S.; Paul, R. L.; Cowley, A. R.; Beer, P. D. *Inorg. Chim. Acta.* **2008**, 361, 1689.

19. Tedesco, A. C.; Oliveria, D. M.; Lacava, Z. J. M.; Azevedo, R. B.; Lima, E. C. D.; Morais, P. C. *J. Magn. Magn. Mater.*, **2004**, *272-276*, 2404.

Chapter-IV

Calix[4]arene-based Fluorescent Molecular Sensors with Coumarin as Fluorophore: High Selectivity Towards Fe^{3+} and Cu^{2+}

4.1. Introduction

The development of molecular sensors for efficient detection of specific metal ion is an emerging area in supramolecular chemistry.[1-5] Among various cations, iron is one of the most important metal ion as it plays crucial role in a variety of cell functions including oxygen carrying capacity of heme and electron transfer processes in DNA and RNA syntheses.[6,7] Deficiency and excess of iron in human body can induce a variety of diseases, therefore its detection is very important.[7] Copper(II) is another metal ion, which plays important role in various biological and environmental processes.[8] It is also toxic to human body at higher concentration and can causes a number of liver and kidney related diseases.[9,10] Therefore, detection of this metal ion is also important.

Various analytical techniques that are available for the detection of these metal ions in low concentration includes atomic absorption spectrometry, spectrophotometry, inductive coupled plasma spectrometry, ion chromatography, voltammetry etc.; however many of these methods are complicated and not suitable for quick and online analysis. In recent years, fluorescent molecular sensors have attracted much attention because of the advantages of ease of detection, high sensitivity and instantaneous response.[1-5,11-13] This method have been widely used for detection of various metal ions, however the examples of Fe(III) selective fluorescent sensors are scarce,[14-19] though similar examples for Cu(II) are relatively high. Therefore, designing of fluorescent sensors for Fe(III) is still a challenge.

To develop fluorescent molecular sensors for ions, calixarenes are found to be very attractive because modifications of calixarenes give rise to a great variety of derivatives with various functional groups and these modified calixarenes provide a highly preorganized architecture for the assembling of converging binding sites.[5,20-23] For example, calix[4]arene derivatives with crown ethers, azacrown ethers, esters and amides have been shown to form complexes with metal ions with high selectivity.[24-29] To the best of our knowledge, so far no calixarene based fluorescent sensors for Fe(III) has been reported, except one.[14] On the basis of the fact that Fe(III) prefers to bind with oxygen atoms and form octahedral geometry, the calix[4]arene has been modified incorporating ethylene glycol moieties as interacting sites and coumarin unit

as fluorophore. These compounds have been designed with variation in number of substituents, length of ethylene glycol moieties and conformations of the calixarene unit; and also *tert*-butylcalix[4]arene is used in one case to impose controlled amount of steric crowding, and a secondary crown ether unit is incorporated in another compound to introduce a secondary ionophore. The substituents of all these compounds are non-macrocyclic and flexible so that they can orient themselves in space to make effective interactions with metal ions. This chapter describes the synthesis and ion-binding property of this series of compounds.

4.2. Experimental Section

4.2.1. Materials

The compound 7-hydroxy 4-methyl umbelliferone was purchased from Sigma Aldrich Company. All metal perchlorate salts were purchased from Alfa Aesar (Johnson Matthey Company). Analytical thin-layer chromatographic plates (SiO_2, Merck 60 F_{254}) and all other reagents and solvents used in this study were obtained from S.D. Fine Chemicals. All organic solvents were analytical grade and were used as received for all synthetic work and were purified by standard procedures for spectroscopic work. The starting compound was synthesized following the published procedures.[30,31] The reagents 2-(2-chloroethoxy) ethyl-4–methylbenzenesulfonate, 2-(2-(2-chloriethoxy)ethoxy)ethyl-4-methylbenzenesul-fonate and tetraethylene glycol ditosylate were prepared following the literature procedures (references are given earlier).

4.2.2. Physical Measurements

All measurements have done using the same instruments as described in *Chapter – II*

Safety Note. ***Caution!*** Metal perchlorate salts are potentially explosive. So they should be handled with great care.

4.2.3. Synthesis of compounds

Synthesis of intermediate compounds

The intermediate compounds **B - I** were synthesized following the published procedures reported by us and others.[29,32-34] All of these compounds were

characterized on the basis of elemental analysis (C,H and N), mass and ^{1}H NMR data. Synthesis of the intermediate compound **A** is described below.

Synthesis of the intermediate compound A

In a solution of calix[4]arene (1 g, 2.36 mmol) in CH_3CN (90 mL), 2-(2-chloroethoxy)ethyl4-methylbenzenesulfonate (0.836 g, 3 mmol) and K_2CO_3 (0.415 g, 3 mmol) were added and the reaction mixture was heated at reflux for 24h under inert atmosphere. The solution was then allowed to cool to room temperature and evaporated to dryness by rotary evaporation. The residue was dissolved in $CHCl_3$ (150 mL) and treated with 5% aqueous HCl (100 mL), the non-aqueous layer was then separated and washed twice with water. The organic layer was dried over anhydrous sodium sulfate and evaporated. The compound was purified by column chromatography on silica gel (100-200 mesh) using 1:9 (v/v) ethyl acetate/hexane as eluent . Yield: 0.876 g, (70 %). ^{1}H NMR (500 MHz, $CDCl_3$): δ 9.86 (s, 1H, Ar-*OH*), 9.23 (s, *2H*, Ar-*OH*), 7.09 (d, 2H, *J* = 7.5 Hz, Ar-H_m), 7.04 (d, 2H, *J* = 7.5 Hz, Ar-H_m), 7.0 (d, 4H, *J* = 7.5 Hz, Ar-H_m , 6.80 (t, 1H, *J* = 7.5 Hz, Ar-H_p), 6.70 - 6.65 (m, 3H, Ar-H_p), 4.46 (d, 2H, *J* = 13.0 Hz, Ar-CH_2-Ar*)*, 4.33 (br-s, 2H, Ar-O-CH_2-CH_2-), 4.27 (d, 2H, *J* = 13.0 Hz, Ar-CH_2-Ar), 4.14 (br-s, 2H, Ar-O-CH_2-CH_2), 3.99 (t, 2H, *J = 5.0* Hz, -O-CH_2-CH_2-*Cl*), 3.79 (t, 2H, *J = 5.0* Hz, -O-CH_2-CH_2-*Cl*), 3.46 (d, 2H, *J = 13.0* Hz, Ar-CH_2-Ar), 3.45 (d, 2H, *J = 13.0* Hz, Ar-CH_2-Ar. ESMS (*m/z*): found 569.21(40%) calcd for [**A** + K^+] 570.14, found 553.23 (50%) calcd for [**A** + Na^+] 554.03, found 531.24 (100%) calcd for [**4** + H^+] 532.04. Anal calcd for $C_{32}H_{31}ClO_5$: C, 72.37; H, 5.88. Found: C, 73.07; H, 5.65.

Synthesis of the compound 1

In a solution of the intermediate compound **A** (0.265 g, 0.5 mmol) in acetone (70 mL), 7-hydroxy-4-methyl coumarin (0.140 g, 0.8 mmol), K_2CO_3 (0.276 g, 2 mmol) and catalytic amount of potassium iodide (5 mg) were added and the reaction mixture was heated at reflux for 2 days under nitrogen. The solution was then allowed to cool to room temperature and evaporated to dryness by rotary evaporation. The residue was extracted 3 times with water-$CHCl_3$ mixture. The organic layer was dried over anhydrous sodium sulfate and evaporated. The compound was purified by column chromatography on silica gel (100-200 mesh) using 1:1(v/v) ethyl acetate/hexane as

eluent . Yield: 0.178 g, (53 %). ^{1}H NMR (500 MHz, CDCl3): δ 9.84 (s, 1H, Ar-*OH*), 9.21 (s, *2H*, Ar-*OH*), 7.36 (d, 1H, *J* = 9.5 Hz, coumarin-*H*), 7.07 (d, 2H, *J* = 7.5 Hz, Ar-H_m), 7.01-6.96 (m, 6H, Ar-H_m), 6.86 (t, 1H, *J* = 7.5 Hz, Ar-H_p), 6.82 (s, 1H, coumarin-*H*), 6.82-6.80 (overlapped signal, 1H, coumarin-*H)*, 6.67 (t, 1H, *J* = 7.0 Hz, Ar-H_p), 6.63 (t, 2H, *J* = 7.0 Hz, Ar-H_p), 6.11 (s, 1H, coumarin-*H*), 4.45 (d, 2H, *J* = *13.0* Hz, ArCH_2Ar), 4.39-4.35 (m, 4H, -CH_2CH_2O-coumarin (2H) and Ar-O-CH_2-CH_2- (2H)), 4.20-4.18 (m, 4H, ArCH_2Ar (2H) and Ar-O-CH_2-CH_2- (2H)), 4.12 (t, 2H, *J = 4.0* Hz, -O-CH_2-CH_2.O-coumarin,), 3.41 (d, 4H, *J = 13.0* Hz, ArCH_2Ar), 2.35 (s, 3H, coumarin-CH_3), ESMS (m/z): found 671.96 (40%) calcd for [**1**+H^+] 671.75. Anal calcd for $C_{42}H_{38}O_8$: C, 75.20; H, 5.71. Found: C, 75.37; H, 5.60.

Synthesis of compound 2

The compound **2** was synthesized from the intermediate **B** following the similar method as described for **1**, except the ratio of reactants, refluxing time and purification procedure. In this case, 0.352 g (2 mmol) of 7-hydroxy-4-methyl coumarin and K_2CO_3 (0.553 g, 4 mmol) were added, the reaction mixture was refluxed for 3 days and the crude product was purified by column chromatography on silica gel (100-200 mesh) using 3:2 (v/v) ethyl acetate/hexane as eluent . Yield: 0.23 g (50%). ^{1}H NMR (500 MHz, CDCl3): δ 7.69 (s, 2H, Ar-*OH)*, 7.33 (d, 2H, *J = 8.5* Hz, coumarin-*H*), 7.12 (d, 4H, *J = 7.5* Hz, Ar-H_m), 7.07 (d, 4H, *J* = 7.5 Hz, Ar-H_m), 6.99 (s, 2H, coumarin-*H*), 6.86 (d, 2H, *J = 7.5* Hz, coumarin-*H*), 6.73-6.61 (m, 4H, Ar-H_p), 6.11 (s, 2H, coumarin-*H*), 4.40 (d, 4H, *J = 13.0* Hz, ArCH_2Ar), 4.26 (t, 4H, *J* = 4.5 Hz, Ar-O-CH_2-CH_2), 4.1 (t, 4H, *J = 4.5* Hz, -CH_2 -CH_2-O-coumarin), 3.63-3.59(m, 8H, CH_2-CH_2-O -CH_2 - CH_2-), 3.44 (d, 4H, *J = 13.0* Hz, ArCH_2Ar), 2.35 (s, 6H, coumarin-CH_3) ESMS (m/z): found 956.74, calcd for [**2** + K^+] 956.10, found 939.74 (100%) calcd for [**2** + Na^+] 939.99. Anal calcd for $C_{56}H_{52}O_{12}$: C, 73.35; H, 5.71. Found: C, 72.64; H, 5.35.

Synthesis of compounds 3-5

The compounds **3** - **5** were synthesized from the intermediates **E**, **F** and **G**, respectively following the method described for **2**, except solvents used for purification. The crude products were purified by column chromatography using ethyl

acetate/hexane as eluent in the ratios 1:1 for **3**, 7:3 for **4** and 2:3 for **5.** Yields; 50 % for **3,** 34% for **4** and 28 % for **5**.

Characterization data for 3

^{1}H NMR (500 MHz, CDCl3): δ 7.47 (d, 2H, *J = 8.5* Hz, coumarin-*H*), 7.08 (d, 4H, *J* = 7.5 Hz, Ar-H_m), 7.01 (d, 4H, *J = 7.5* Hz, Ar-H_m), 6.89 (d, 2H, *J = 8.5* Hz, coumarin-*H*), 6.82 (s, 2H, coumarin-*H*), 6.70 (t, 2H, *J* = 7.5 Hz Ar-H_p), 6.65 (t, 2H, *J* = 7.5 Hz, Ar-H_p), 6.12 (s, 2H, coumarin-*H*), 4.20 (t, 4H, *J = 4.5* Hz, - CH_2-CH_2-O-coumarin), 3.85 (t, 4H, *J = 4.5* Hz, -CH_2-CH_2-O-coumarin), 3.81 (t, 4H, *J = 4.5* Hz, -CH_2-O-CH_2-), 3.68-3.59 (m, 12H, ArCH_2Ar (8H) and Ar–O-CH_2-CH_2- (4H)), 3.54 (t, 4H, *J = 7.0* Hz,- O-CH_2- C_2H_5), 2.38 (s, 6H, coumarin-CH_3), 1.62 (m, 4H, -O-CH_2-CH_2-CH_3), 0.91 (t, 6H, *J* = 7.0, -O-CH_2-CH_2-CH_3). ESMS (m/z): found 1001.53 (100%), calcd for [**3** + H^+] 1002.16]. Anal calcd for $C_{62}H_{64}O_{12}$: C, 74.37; H, 6.44. Found: C, 73.65; H, 6.32.

Characterization data for 4

^{1}H NMR (500 MHz, CDCl3): δ 7.46 (d, 2H, *J = 8.5* Hz, coumarin-*H*), 7.06 (d, 4H, *J = 7.5* Hz, Ar-H_m), 6.99 (d, 4H, *J* = 7.5 Hz, Ar-H_m), 6.86 (d, 2H, *J* = 8.5 Hz, coumarin-*H*), 6.79 (s, 2H, coumarin-*H*), 6.66 (t, 2H, *J* = 7.0 Hz, Ar-H_p), 6.63 (t, 2H, *J* = 7.0 Hz, Ar-H_p), 6.13 (s, 2H, coumarin-*H*), 4.18 (t, 4H, *J* = 4.5 Hz, - CH_2-CH_2-O coumarin), 3.92 (t, 4H, *J* = 4.5 Hz, Ar-O-CH_2-CH_2), 3.81 (t, 4H, *J* = 4.0 Hz, O-CH_2-CH_2-O-coumarin), 3.80 (t, 4H, *J* = 4.0 Hz, -CH_2-O-CH_2-), 3.72 (t, 4H, *J = 4.0* Hz, Ar-O-CH_2-CH_2-), 3.63-3.55 (m, 16H, ArCH_2Ar (8H), -CH_2-O-CH_2- (4H), O-CH_2-C_2H_5 (4H)), 2.38 (s, 6H, coumarin-CH_3), 1.69 (m, 4H, -O-CH_2-CH_2-CH_3), 0.94 (t, 6H, *J* = 7.2 Hz, -O-CH_2-CH_2-CH_3). ESMS (m/z): found 1112.69 (40 %), calcd for [**4** + Na^+] 1112.25, found 1089.70 (100%) calcd for [**4** + H^+] 1089.26. Anal calcd for $C_{66}H_{72}O_{14}$: C, 72.77; H, 6.66 found: C, 71.83; H, 6.83.

Characterization data for 5

^{1}H NMR (500 MHz, CDCl3): δ 7.48 (d, 2H, *J = 8.5* Hz, coumarin-*H*), 7.04 (s, 4H, Ar-H_m), 6.96 (s, 4H, Ar-H_m), 6.84 (d, 2H, *J = 8.5* Hz, coumarin-*H*), 6.78 (s, 2H, coumarin-*H*), 6.13 (s, 2H, coumarin-*H*), 4.09 (t, 4H, *J = 4.5* Hz,- CH_2-CH_2-O-coumarin), 3.85-3.76 (m, 8H, ArCH_2Ar), 3.71 (t, 4H, *J = 4.5* Hz, Ar -O-CH_2-CH_2-),

3.53 (t, 4H, *J = 6.5* Hz, Ar-O-CH_2-*CH_2*-), 3.34 (t, 4H, *J = 7.5* Hz, -O-*CH_2*-CH_2-CH_3), 3.17 (t, 4H, *J = 6.5* Hz, -*CH_2*-CH_2-O-coumarin), 2.40 (s, 6H, coumarin-*CH_3*), 1.61 (m, 4H, -O-CH_2-*CH_2*-CH_3), 1.30 (s, 18H, -C(*CH_3*)*$_3$*), 1.25 (s, 18H, -C(*CH_3*)*$_3$*), 0.97 - 0.96 (t, 6H, *J = 7.0* Hz, -O-CH_2-CH_2-*CH_3*). ESMS (m/z): found 1248.88 (40%), calcd for [**5** + Na^+] 1248.57. Anal calcd for $C_{78}H_{96}O_{12}$: C, 76.43; H, 7.89. Found: C, 76.83; H,7.73.

Synthesis of compound 6

This compound was synthesized following the method described for **2**, except, solvents used for purification. The crude product was purified by column chromatography using ethyl acetate with 1 % methanol. Yield; 43%. ^{1}H NMR (500 MHz, CDCl3): δ 7.48 (d, 2H, *J = 8.5* Hz, coumarin-*H*), 7.11 (d, 4H, *J = 7.0* Hz, Ar-*H_m*), δ 7.10 (d, 4H, *J = 7.0* Hz, Ar-*H_m*), 6.91-6.88 (m, 4H, coumarin-*H* (2H) and Ar-*H_p* (2H)), 6.84 (t, 2H, *J = 7.2* Hz, Ar-*H_p*), 6.77(s, 2H, coumarin-*H*), 6.11 (s, 2H, coumarin-*H*), 4.05 (t, 4H, *J = 4.5* Hz, - CH_2-*CH_2*-O-coumarin), 3.91-3.83 (m, 8H, Ar*CH_2*Ar), 3.65-3.58 (m, 16H, crown-CH_2 and ether-CH_2), 3.43 (t, 4H, *J = 4.5* Hz, Ar-O-*CH_2*-CH_2-), 3.26 (t, 4H, *J =5.0* Hz, -O-*CH_2*-CH_2-O-coumarin), 3.15 (t, 4H, *J = 5.0* Hz, Ar-O-CH_2-*CH_2*-), 2.38 (s, 6H, coumarin-*CH_3*). ESMS (m/z): found 1097.64 (100%) calcd for [**6** + Na^+] 1098.17 Anal calcd for $C_{64}H_{66}O_{15}$: C, 71.50; H 6.14. Found: C, 70.78, H 5.97.

4.2.4. Ion-binding study

Luminescence study

Stock solutions of the complexes **1**-**6** (5 x 10^{-5} M) and that of perchlorate salts (5 x 10^{-3} M) of various metal ions (Li^+, Na^+, K^+, Cs^+, Sr^{2+}, Ca^{2+}, Mg^{2+}, Zn^{2+}, Cd^{2+}, Hg^{2+}, Pb^{2+}, Ni^{2+}, Cu^{2+}, Fe^{3+}, Ag+, and Ba^{2+}) were prepared in freshly purified acetonitrile. Then 2 mL stock solution of the complex and 2 mL stock solution of each metal salts were taken in a 5 mL volumetric flask, so that the effective concentration of the complex is 2.5 x 10^{-5} M and that of the metal ions are 2.5 x 10^{-3} M (100 fold). The luminescence spectra of the resulting solutions and that of the original complex (2.5 x 10^{-5} M) were recorded with excitation at the absorption maxima (λ_{max}) 317 nm for **1**-**6,** respectively. The spectra of the resulting solutions were compared with that of the original solution to ascertain the interactions of the metal ions with the ionophore.

For emission titration, the metal perchlorate solutions of desired concentration ($5.0 \times 10^{-5} - 5 \times 10^{-3}$ M) were prepared by proper dilution of the stock solution. Then 2 mL of metal perchlorate solutions of each concentration were mixed with the 2 mL solutions of the compound (5.0×10^{-5} M) in a 5 mL volumetric flask to prepare reaction mixtures with desired concentrations of the metal ion, 1 to 100 molar equivalent with respect to the concentration of compounds and the luminescence spectra of the resulting solutions were recorded. From titration data, binding constants were calculated following the literature procedure.[35]

4.3. Results and Discussion

4.3.1. Synthesis of the compounds 1 - 6

The route followed for the synthesis of compounds **1** – **6** is shown in Scheme 4.1. The intermediate compounds **B** – **I** were synthesised following the published procedures reported by us and others. Elemental analysis (C, H and N), ^{1}H NMR and mass spectral data of all these compounds are similar to those of reported values. The intermediate compound **A** was synthesised by the reaction of calix[4]arene with 2-(2-chloroethoxy)ethyl4-methylbenzenesulfonate in refluxed CH_3CN under inert atmosphere, the product was isolated by two-phase extraction and purified by column chromatography on silica gel using ethyl acetate/hexane as eluent. Compounds **1** – **6** were obtained from their preceding intermediates, **A**, **B**, **E**, **F**, **G** and **H**, (Scheme 4.1) respectively, by the reaction with 7-hydroxy-4-methyl coumarin in acetone under reflux for 3 days in inert atmosphere in presence of K_2CO_3 and catalytic amount of KI. All of these compounds were purified by column chromatography as described in the Experimental Section. These compounds were characterized on the basis of elemental analysis (C, H and N), ESMS and ^{1}H NMR spectral data. Details of the characterization data are given in the Experimental Section. ^{1}H NMR spectra of **3** and **6**, and mass spectra of **2** and **3** are shown in the Figures. 4.1 – 4.4, respectively.

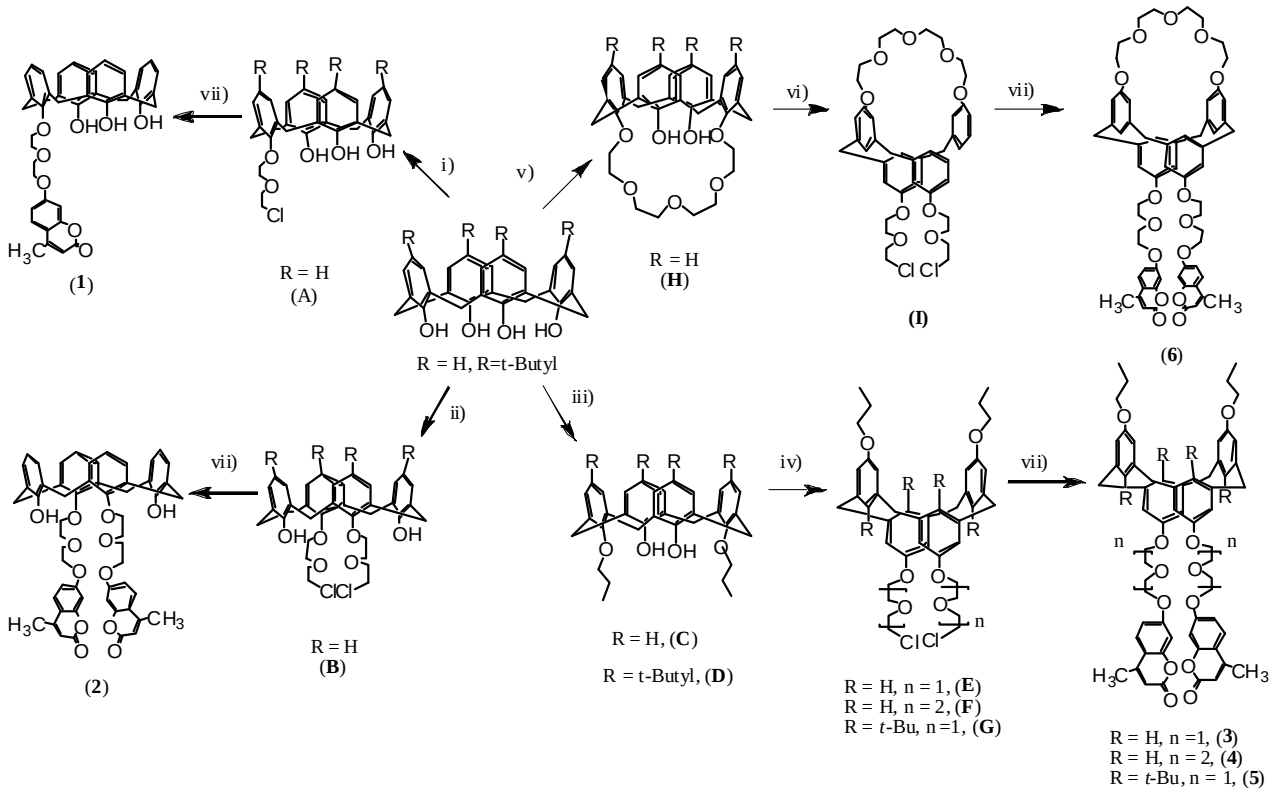

Scheme 4.1. Synthetic route followed for the synthesis of compounds **1** – **6**

Reagents and conditions: i) $ClCH_2CH_2OCH_2CH_2OTs$, K_2CO_3, acetonitrile, reflux; ii) $ClCH_2CH_2OCH_2CH_2$-OTs, K_2CO_3, acetonitrile, reflux; iii) *n*-Pr-I, K_2CO_3, acetonitrile, reflux; iv) $ClCH_2(CH_2OCH_2)_nCH_2OTs$ (n = 1,2), Cs_2CO_3, acetonitrile, reflux; v) Tetra ethyleneglycolditosylate, K_2CO_3, acetonitrile, reflux; vi) $ClCH_2CH_2OCH_2CH_2OTs$, Cs_2CO_3, acetonitrile, reflux; vii) 7-hydroxy-4-methyl coumarin, K_2CO_3, KI, acetone, reflux.

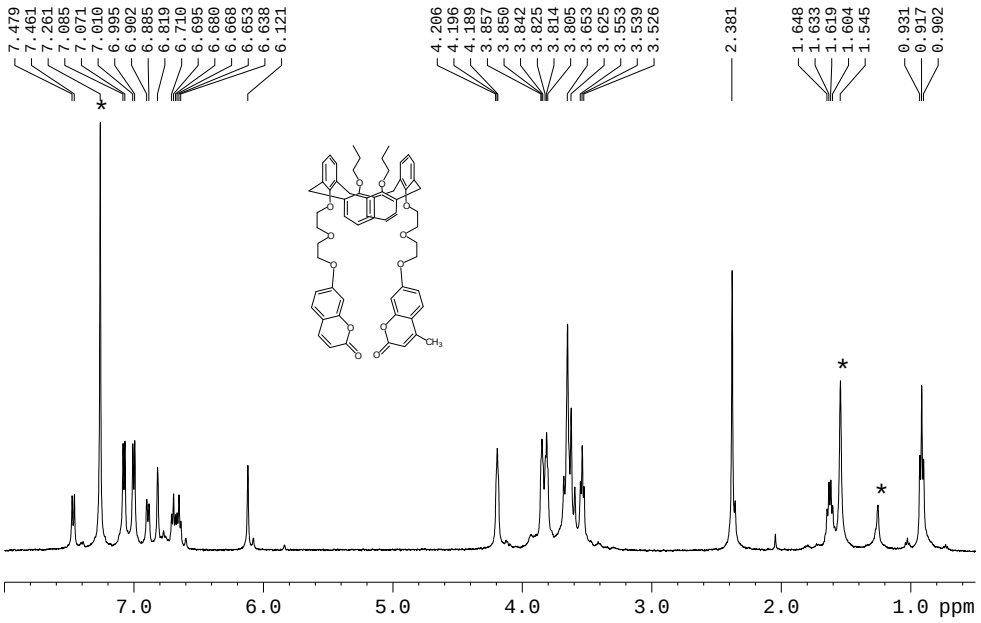

Figure. 4.1. ^{1}H NMR spectrum of the compound **3** recorded in $CDCl_3$, signals with * mark are from solvent.

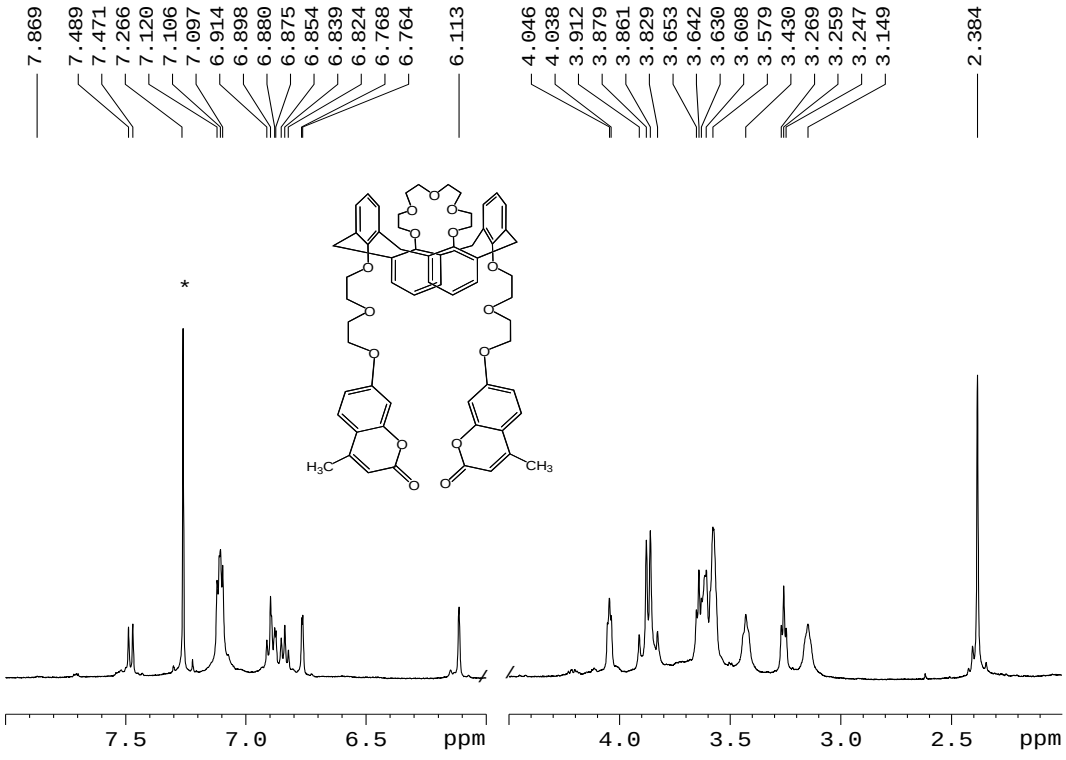

Figure. 4.2. ^{1}H NMR spectrum of the compound **6** recorded in $CDCl_3$, signal with * mark is from solvent.

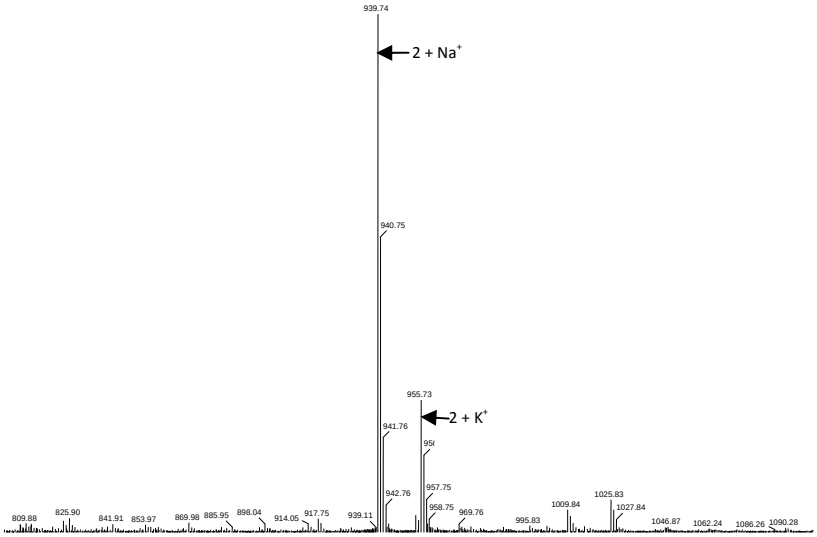

Figure. 4.3. Relevant portion of the mass spectrum of the compound **2.**

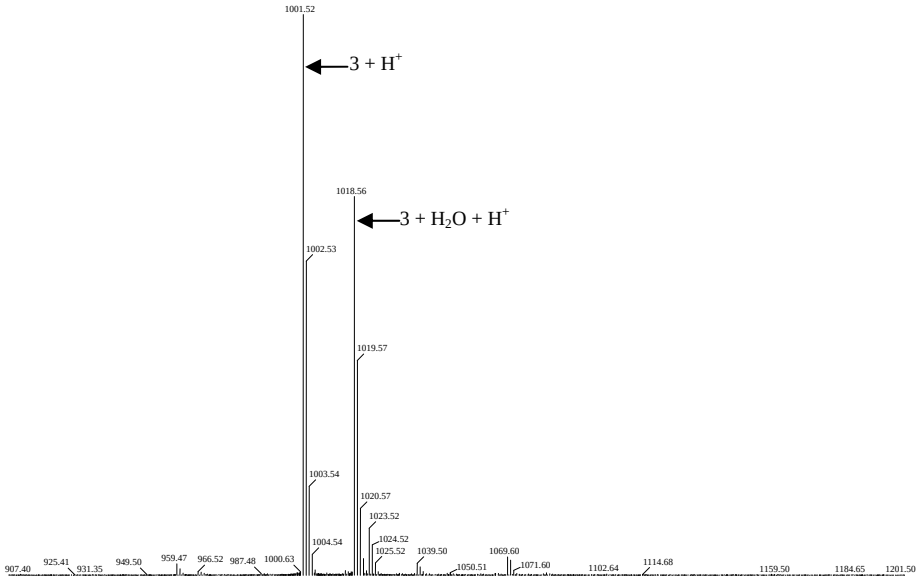

Figure. 4.4. Relevant portion of the mass spectrum of the compound **3.**

Satisfactory elemental analyses of these compounds were obtained; mass data are in excellent agreement with the calculated molecular mass and the ^{1}H NMR spectral data are in agreement with the proposed conformation of the compounds. Compound **2** exhibits two doublets (δ 4.40 and 3.44) for bridged CH_2 protons of the calix[4]arene moiety, indicating cone conformation of this unit.[26] For **1**, two doublets (δ 4.45 and 4.19) correspond to 2H each and another doublet (δ 3.41) corresponds to 4H for bridged CH_2 protons are due to the mono substituted cone conformation of the

calixarene unit. For **3** – **6**, no such doublets for bridged CH_2 protons were observed, however a strong singlet like signal in the region δ 3.5 – 3.9 overlapped with some other CH_2 signals is noted. Comparing these data and that of intermediates with the reported chemical shifts of these protons, 1,3-alternate conformation is assigned for the calixarene unit of these compounds.[25,29,36]

4.3.2. Absorption and luminescence spectra

The UV-vis spectra of all these compounds exhibit an absorption band at 317 nm in 9: 1 CH_3CN-$CHCl_3$ (ε, ~1.0 x 10^4 mol^{-1} cm^{-1}), this band is due to coumarine moiety.[19,37] On excitation of this band at 317 nm, all of these compounds showed strong emission band at 390 nm, which is used to monitor the interaction of metal ions with the receptors.

4.3.3. Cation-binding study by luminescence

To evaluate the metal-ion binding property, percholorate salts (100 equiv) of Li^+, Na^+, K^+, Cs^+, Sr^{2+}, Ca^{2+}, Mg^{2+}, Zn^{2+}, Cd^{2+}, Hg^{2+}, Pb^{2+}, Ni^{2+}, Cu^{2+}, Fe^{3+}, Ag+, and Ba^{2+} were added into the solution (CH_3CN-$CHCl_3$, 9:1) of the compounds and the fluorescence spectra of the resulting solution was recorded under similar conditions. Out of these 16 metal ions, Fe^{3+} exhibited strong quenching of fluorescence intensity (70-85%) for all the six compounds, Cu^{2+} showed moderate to strong quenching (60–75%) for **1**, **2**, **4** and **5** and Ca^{2+} exhibited 30-40% enhancement in fluorescence intensity for **3** and **5**. All other metal ions do not show any significant change in fluorescence intensity. With change in fluorescence intensity, Fe^{3+} exhibited red-shift of emission maxima by 22-25 nm for the compounds **2**-**6** and 8 nm for **1**, however Cu^{2+} did not show any significant change in emission maxima, except **2**, which exhibited 12 nm blue shift. Typical spectral change for **1**, **2**, **3** and **5** with all the metal ions are shown in Figures. 4.5 – 4.8. The results indicate that all the six compounds bind Fe^{3+} strongly, four compounds (**1**, **2**, **4** and **5)** also form complex with Cu^{2+} and only two compounds (**3** and **5**) interact with Ca^{2+}. The quenching of emission intensity with a red-shift is ascribed to the metal-induced intramolecular charge transfer, it is observed when transition metal ions bind the host molecule strongly.[1,19]

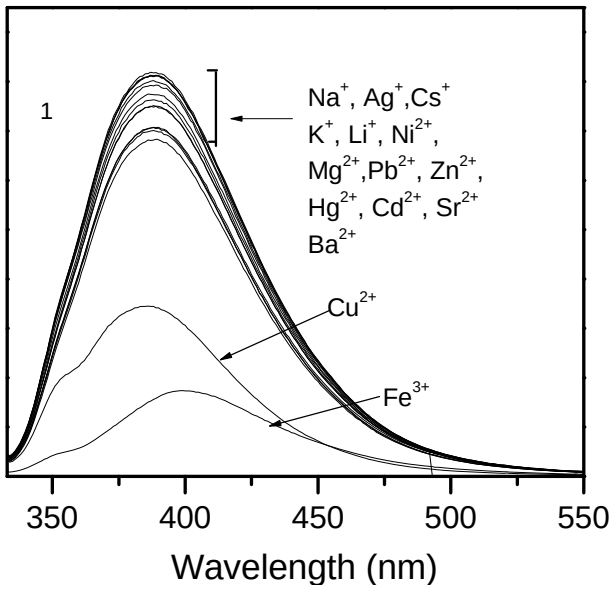

Figure. 4.5. Luminescence spectral change for **1** in presence of various cations (100 equiv).

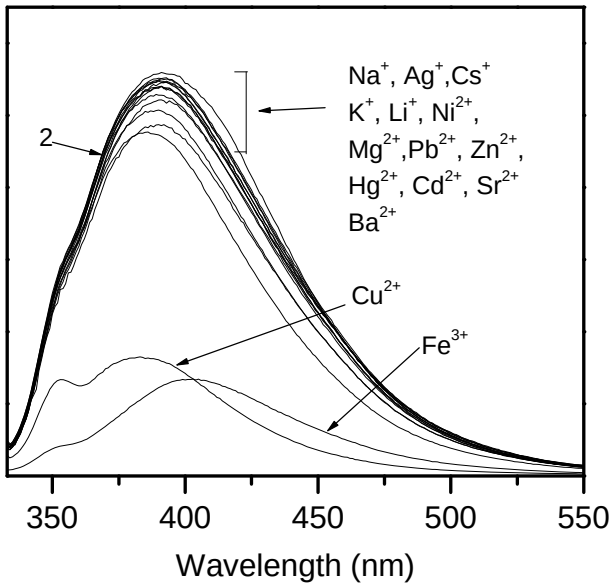

Figure. 4.6. Luminescence spectral change for **2** in presence of various cations (100equiv).

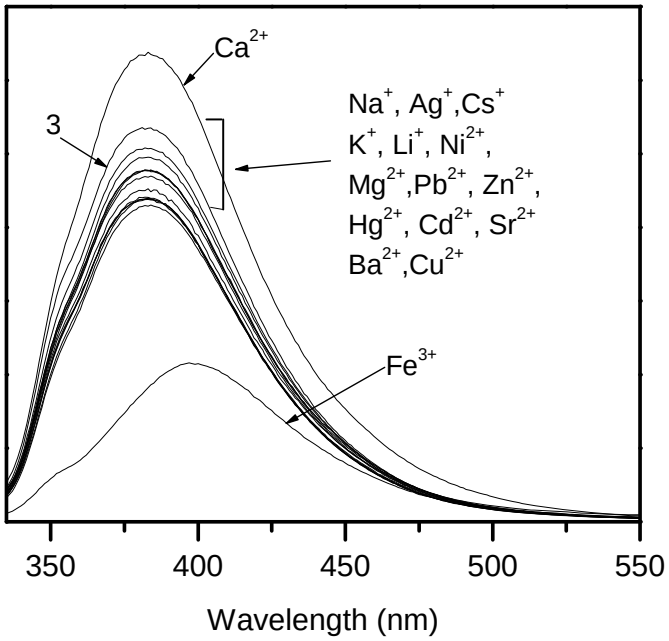

Figure. 4.7. Luminescence spectral change for **3** in presence of various cations (100 equiv).

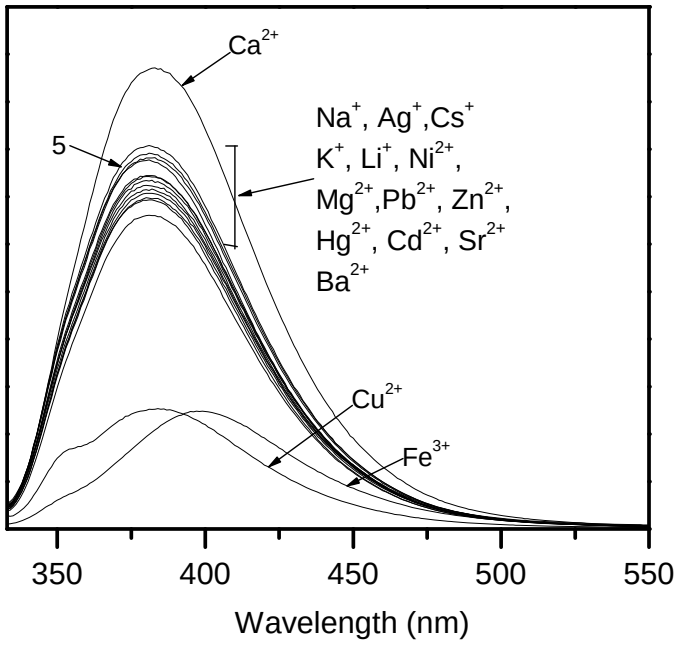

Figure. 4.8. Luminescence spectral change for **5** in presence of various cations (100 equiv).

Binding constants of the metal ions with all compounds were calculated using emission titration data following literature procedure.[29,35,38] The titration experiments were carried out following the method described in the Experimental Section. The changes observed in emission intensities upon addition of increasing concentration of metal ions for **1** with Fe^{3+}, **2** with Fe^{3+} and Cu^{2+}, **3** with Fe^{3+}, **4** with Fe^{3+}, **5** with Cu^{2+} and Ca^{2+} and **6** with Fe^{3+} are shown in Figures. 4.9 – 4.16, respectively. According to this procedure, the fluorescence intensity (F) scales with the metal ion concentration ([M]) through $(F_0 - F)/(F - F_\infty) = ([M]/K_{diss})^n$. The binding constant ($K_s$) is obtained by plotting $\log[(F_0 - F)/(F - F_\infty)]$ versus log[M] (notations are same as described earlier). The value of log[M] at $\log[(F_0 - F)/(F - F_\infty)] = 0$ gives the value of $\log(K_{diss})$, the reciprocal of which is the binding constant (K_s). The plots $\log[(F_0 - F)/(F - F_\infty)]$ versus log[M] are shown as insets of the Figures. 4.9 – 4.16. The binding constants are summarized in Table 4.1.

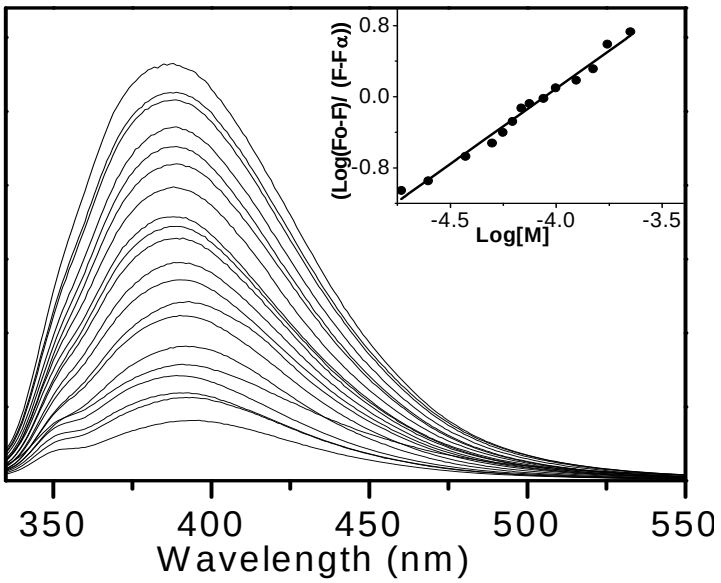

Figure. 4.9. Emission spectral changes for **1** upon addition of increasing concentration of Fe^{3+}.

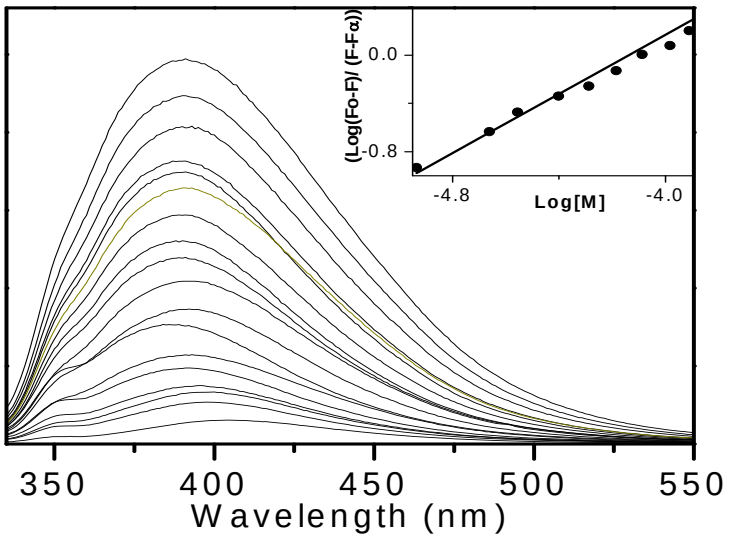

Figure. 4.10. Emission spectral changes for **2** upon addition of increasing concentration of Fe^{3+}.

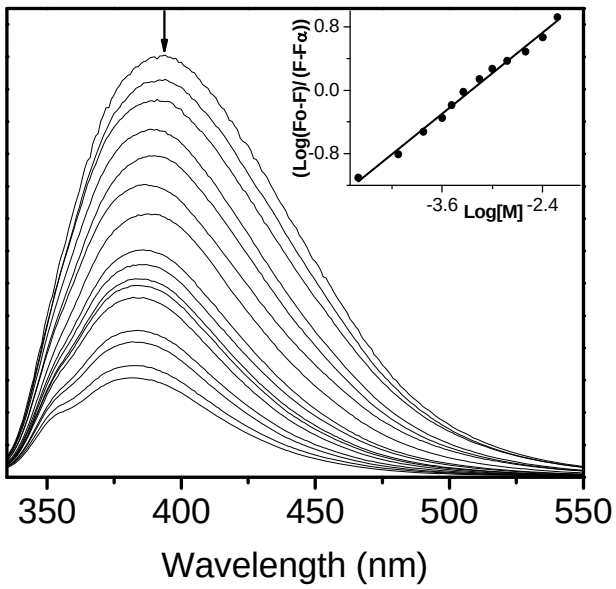

Figure. 4.11. Emission spectral changes for **2** upon addition of increasing concentration of Cu^{2+}.

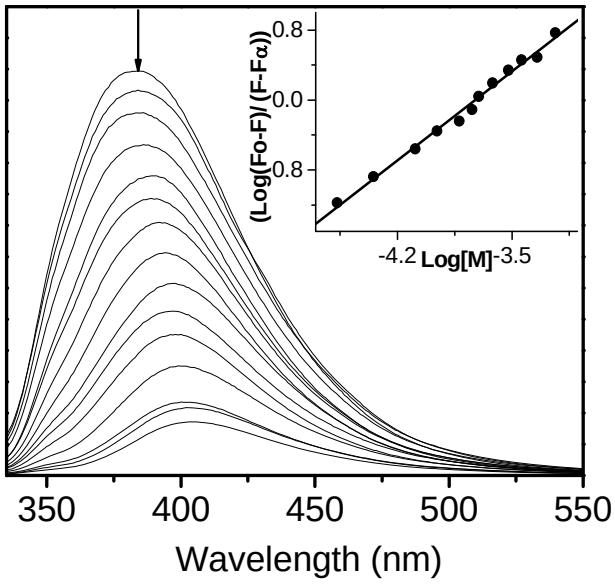

Figure. 4.12. Emission spectral changes for **3** upon addition of increasing Concentration of Fe^{3+}

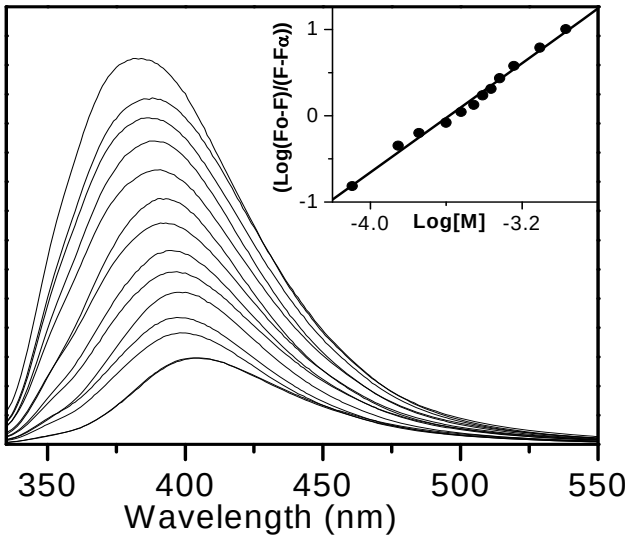

Figure. 4.13. Emission spectral changes for **4** upon addition of increasing Concentration of Fe^{3+}.

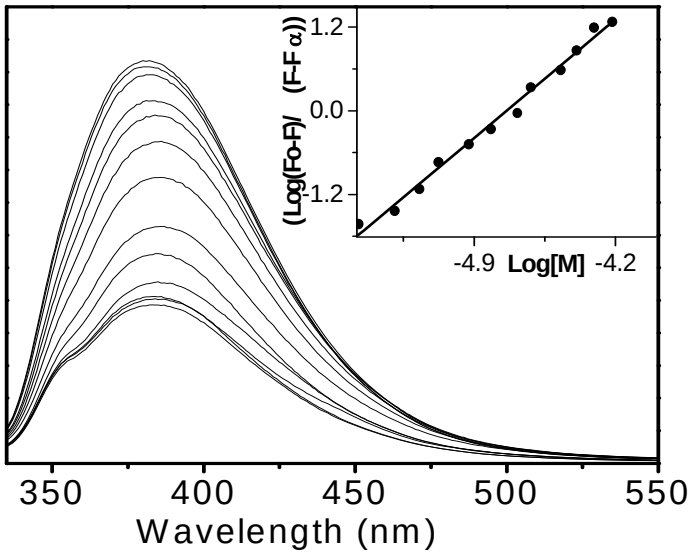

Figure. 4.14. Emission spectral changes for **5** upon addition of increasing concentration of Cu^{2+}.

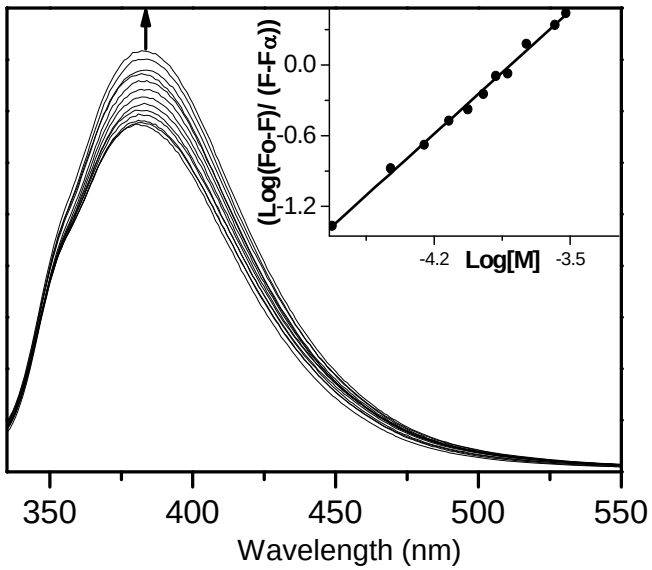

Figure. 4.15. Emission spectral changes for **5** upon addition of increasing Concentration of Ca^{2+}.

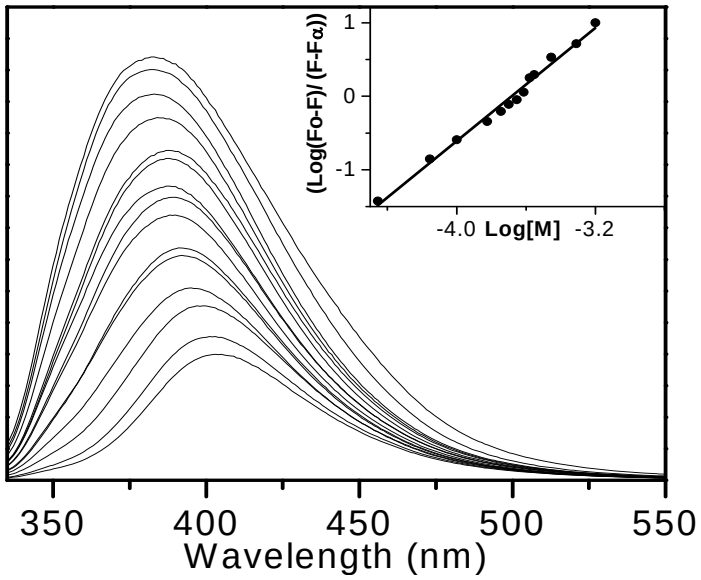

Figure. 4.16. Emission spectral changes for **6** upon addition of increasing concentration of Fe^{3+}.

Table 1 Binding constants for the compounds **1-6**

Compound	Binding constant (K_s) M^{-1}		
	Fe^{3+}	Cu^{2+}	Ca^{2+}
1	1.12×10^4	9.77×10^2	
2	1.40×10^4	1.58×10^3	
3	5.34×10^3		4.79×10^3
4	3.85×10^3	5.62×10^4	
5	7.31×10^3	5.54×10^4	6.41×10^3
6	4.27×10^3		

The binding constant values indicate moderate to strong complexation of iron with all the receptor molecules. Examples of fluorescent chemosensor for Fe^{3+} are not many, and most of the reported cases only the oxygen atoms made interaction with the metal ion to form octahedral geometry.[14-16,18,19] In compounds **1**-**6**, oxygen atoms for coordination with metal ion are available from both the calix and ethylene glycol moieties, and can form octahedral complex as shown in Figure. 4.17 for compound **2**. For **3**-**5**, where two of the oxygen atoms of the calix unit are not available for coordination because of the 1,3-alternate conformation of the calixarene, probably all the six oxygen atoms from ethylene glycol units in the lower rim of the calixarene are involved in coordination as shown in Figure. 4.18 for compound **3**. The coordinating units are open chain and flexible, which is an advantage in this case because it can orient and adjust in space to make interaction with metal ion. The Cu^{2+} ion did not form complex with **3** and **6** and showed weak interaction with **1**, which probably related to the affinity of Cu^{2+} towards ethylene glycol moiety and favourable positions of the coordinating atoms. The proposed molecular structure of the Cu^{2+} with **5** is shown in Figure. 4.19. Ca^{2+} showed interaction with **3** and **5**, interestingly in both the cases calix unit exist in 1,3-alternate conformation. It gives an indication that there is a possibility that Ca^{2+} ion is encapsulated in the cavity at the upper rim of the calix making interaction with the two oxygen atoms of the O-Pr groups and electron rich centroyed of the benzene ring (Figure. 4.20). The other possibility for Ca^{2+} is to interact with the oxygen atoms of the two coumarine units and thus blocking the quenching process for coumarine, leading to the enhancement in fluorescence intensity.

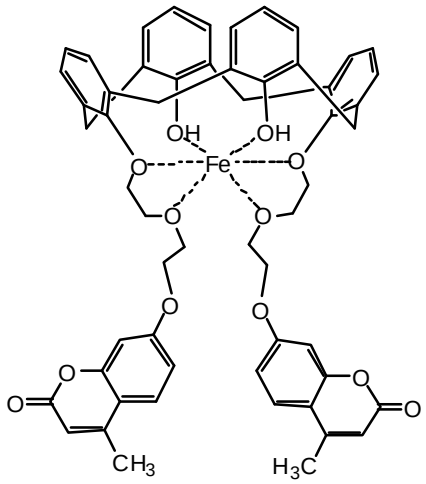

Figure. 4.17. Molecular structure of the proposed Fe^{3+} complex for compound **2**.

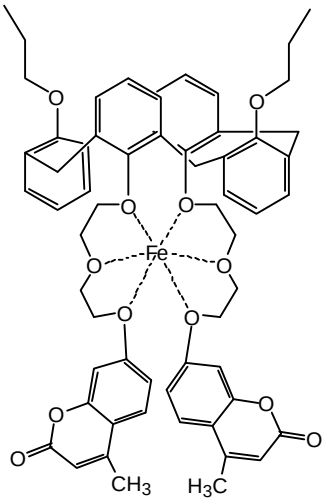

Figure. 4.18. Molecular structure of the proposed Fe^{3+} complex for compound **3**.

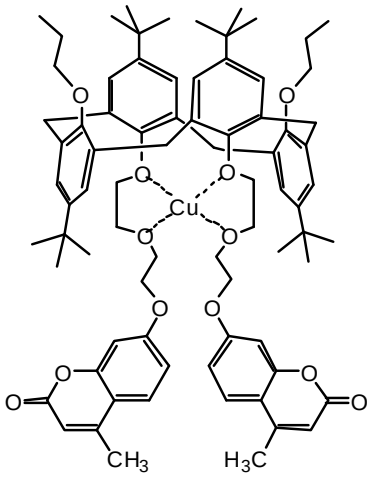

Figure. 4.19. Molecular structure of the proposed Cu^{2+} complex for compound **5**.

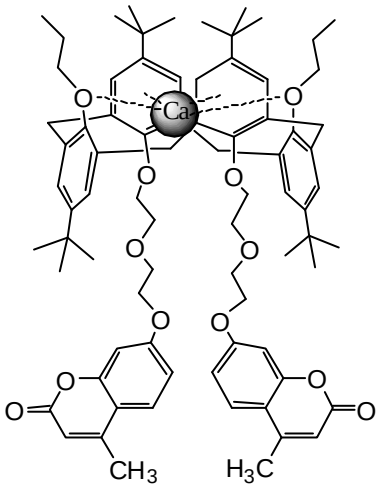

Figure. 4.20. Molecular structure of the proposed Ca^{2+} complex for compound **5**

4.4. Conclusions

In conclusion, a series of modified calix[4]arene as fluoroionophore have been synthesised in cone and 1,3-alternate conformation, incorporating ethylene glycol moieties as coordinating sites and coumarine as fluorophore. The ion-binding property of these receptors has been tested with a large number of metal ions and the ion recognition event was monitored by fluorescence spectral changes. This study suggests that this series of receptors are highly selective towards Fe^{3+} and a few also show complexation with Cu^{2+} and Ca^{2+}. The flexibility of the open chain coordinating units with oxygen donors is the crucial part of these molecules, which promoted high selectivity towards Fe^{3+}.

4.5. References

1. de Silva, A. P.; Gunaratne, H. Q. N.; Gunnlaugsson, T.; Huxley, J. M.; Mchoy, C. P.; Rademacher, J. T.; Rice, T. E. *Chem. Rev*. **1997**, *97*, 1515.
2. Beer, P. D.; Gale, P. A. *Angew. Chem. Int. Ed.* **2001**, *40*, 486.
3. Beer, P. D.; Hayes, E. J. *Coord. Chem. Rev*. **2003**, *240*, 167.
4. Yoon, J.; Kim, S. K.; Sing, N. J.; Kim, K. S. *Chem. Soc. Rev*. **2006.** *35*, 355.
5. Kim, J. S.; Quang, D. T. *Chem. Rev*. **2007,** *107*, 3780.
6. Lynch, S. R. *Nutr. Rev*. **1997**, *55*, 102.
7. Touati, D. *Arch. Biochem. Biophys*. **2000,** *373*, 1.
8. Fabbrizi, L.; Pooggi, A. *Chem. Soc. Rev.* **1995**, *24*, 197.
9. Linder, M. C.; Hazegh-Azam, M. *Am. J. Clin. Nutr*. **1996,** *63*, 797S-811S.
10. Uauy, R.; Olivares, M.; GonZalez, M. *Am. J. Clin. Nutr*. **1998,** *67*, 952S-959S.
11. Rurack, K.; Resch-Genger, U. *Chem. Soc. Rev.* **2002.** *31*, 116.
12. Xu, Z.; Kim, S.; Kim, H. N.; Han, S. J.; Lee, C.; Kim, J. S.; Qian, X.; Yoon, J. *Tetrahedron Lett.* **2007**, *48*, 9151.
13. Joseph, R.; Ramanuja, B.; Acharya, A.; Rao, C. P. *Tetrahedron Lett*. **2009**, *50*, 2735.
14. Liu, J.-M.; Zheng, Q.-Y.; Yang, J.-L.; Chen, C.-F.; Huang, Z.-T. *Tetrahedron Lett*. **2002,** *43*, 9209.
15. Hua, J.; Wang, Y.-J. *Chem. Letters* **2005**, *34*, 98.
16. Bae, S.; Tae, J. *Tetrahedron Lett*. **2007**, *48*, 5389.
17. Zhang, M.; Gao, Y.; Li, M.; Yu, M.; Li, F.; Li, L.; Zhu, M.; Zhang, J.; Yi, T.; Huang, C. *Tetrahedron Lett.* **2007**, *48*, 3709.
18. Singh, N.; Kaur, N.; Mackay, J. D. M; Callan, J. F. *Tetrahedron Lett*. **2009,** 50, 953.

19. Yao, J.; Dou, W.; Quin, W.; Liu, W. *Inorg. Chem. Commun*. **2009,** *12*, 116.

20. Jr, J. R. *Chem Commun*. **2000**, 637.

21. Webber, P. R. A.; Cowley, A.; Drew, M. G. B. *Chem Eur. J.* **2003**, *9*, 2439.

22. Li, G.-K.; Xu, Z.-X.; Chen, C.-F.; Huang, Z.-T. *Chem Commun*. **2008,** 1774.

23. Dhir, A.; Bhalla, V.; Kumar, M. *Org. Lett.* **2008,** *10*, 4891.

24. Guillon, J.; Leger, J.-M.; Sonnet, p.; Jarry, C.; Robba, M. *J.Org. Chem.* **2000,** *65,* 8283.

25. Zhou, H.; Surowiec, K.; Purkiss, D. W.; Bartsch, R. A. *Org. Biomol. Chem.* **2005,** *3*, 1676.

26. Agnihotri, P.; Suresh, E.; Paul, P.; Ghosh, P. K. *Eur. J. Inorg. Chem*. **2006,** 3369.

27. Lee, Y. J.; Kwon, J.; park, C. S.; Lee, J.-E.; Sim, W.; Kim, J. S.; Yoon, J. S. II.; Jung, J. H.; Lee, S. S. *Org. Lett*. **2007**, *9*, 493.

28. Yuan, M.; Zhou, W.; Liu, X.; Zhu, M.; Li, J.; Yin, X.; Zheung, H.; Zuo, Z.; Ouyang, C.; Liu, H.; Li, Y.; Zhu, D. *J.Org. Chem.* **2008,** *73, 5008.*

29. Patra, S.; Paul, P. *Dalton Trans.* **2009,** 8683.

30. Gutsche, C. D.; Iqbal, M. *Organic Syntheses*. **1990,** *68*, 234.

31. Gutsche, C. D.; Levine, J. A.; Sujeeth, P. K. *J. Org. Chem.* **1985,** 50, 5802.

32. Kim, J. S.; Lee, W. K.; No, K.; Asfari, Z.; Vicens, J. Tetrahedron Lett. **2000**, *41*, 3345.

33. Casnati, A.; Pochini, A.; Ungaro, R.; Ugozzoli, F.; Arnaud, F.; Fanni, S.; Schwing, M-J.; Egberink, R. J. M.; Jong, F. de.; Reinhoudt, D. N. *J. Am. Chem. Soc.* **1995**, *117,* 2767.

34. Kim, J. S.; Lee, W. K.; Sim, W.; Ko, J. W.; Cho, M. H.; Ra, D.Y.; Kim, J. W. *J. Inclusion Phenom. Macrocyclic Chem.*, **2000**, *37*, 359.

35. Tedesco, A. C. Oliveria, D. M.; Lacava, Z. J. M.; Azevedo, R. B.; Lima, E. C. D.; Morais, P. C. *J. Magn. Mater.* **2004,** *272-276*, 2404.

36. Jaiyu, A.; Rojanathanes, R.; Sukwattanasinitt, M. *Tetrahedron Lett.* **2007**, 48, 1817.

37. Lee, S. H.; Kim, H. J.; Lee, Y. O.; Vicens, J.; Kim, J. S. *Tetrahedron lett*. **2006,** *47*, 4373.

38. Boricha, V. P.; Patra, S.; Chouhan, Y. S.; Sanavada, P.; suresh, E.; Paul, P. *Eur. J. Inorg. Chem*. **2009,** 1256.

Chapter-V

Calix[4]arene-based Fluorescent Molecular Sensors with Quinoline as Fluorophore: Synthesis, Structures and Ion-Selectivity Study

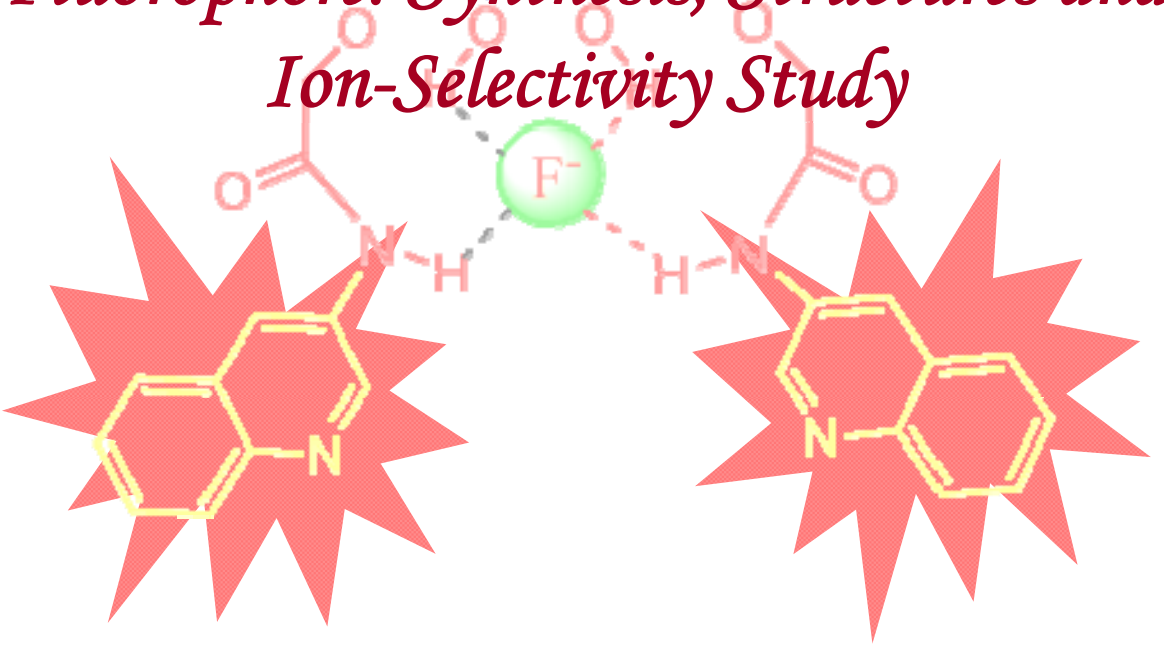

5.1. Introduction

In the *Chapter - IV*, ion-binding property of calix[4]arene based molecular sensors with ethylene glycol moieties as interacting sites and coumarin unit as fluorophore have been described. These molecules were basically designed for Fe^{3+} and they worked for it in addition to the recognition of Cu^{2+} for some of the compounds. It was then planned to replace the ethylene glycol moieties as interacting sites by amide moiety. The aim of this change of coordinating sites is to design sensors for both cations and anions because amide is known to interact with anions, particularly with fluoride through H-bonding.

The other aspect of designing of this series of ionophores is the addition of quinoline moiety as fluorophore. One of the recent approaches of designing the fluorescent signaling systems relies on guest-induced folding of flexible receptors, which brings the fluorophores close enough as to function as an excimer. This excimer emission formation is sometimes used to 'read out' the molecular recognition process more conveniently.[1,2] Kim *et al* have reported calixarene-containing pyrenes as fluorogenic units, which form intramolecular excimer due to strong π-π interaction between two pyrene units.[3-6] In these cases the intermolecular excimer emission perturb in presence of guest ions. They have also reported indium(III)-induced excimer formation in pyrene containing calix[4]arene based fluoroionophore.[7] It is known that highly π-delocalized planar systems such as pyrene and anthracene show greater tendency to form excimers. In calixarene systems, pyrene based excimers have been used but to the best of our knowledge no quinoline based excimers has been reported so far. In some other systems, however, quinoline as fluorophore have been reported, in which intamolecular excimer emission in presence of guest ions is observed.[1,2]

In this Chapter, calix[4]arene based chemosensors containing quinoline as fluorophore is reported. They have been designed with variation in substituents at the upper and lower rims and also in the conformation of the calix moiety. All of these molecules have been characterized on the basis of analytical and spectroscopic data and molecular structures have been established by single-crystal X-ray study. Their ion-selectivity property has been tested with a large number of cations and anions. They exhibit strong selectivity towards Hg^{2+}, Pb^{2+}, Fe^{3+} and Cu^{2+}, and a few with F^-.

Recognition event was monitored by fluorescence and NMR spectroscopy and binding constants with strongly interacting ions are determined by fluorescence titration data.

5.2 Experimental Section

5.2.1. Materials

The compounds 3-aminoquinoline, methylbromo acetate and ethylbromo acetate were purchased from Sigma Aldrich Company. All other materials were received from various Company as mentioned earlier Chapters. The starting compounds *p-tert*-butylcalix[4]arene, calix[4]arene and 25,27-dipropyloxy calix[4]arene were synthesized according to the literature procedures.[8-10]

5.2.2. Physical Measurements

Physical measurements were carried out using the instruments described in the earlier Chapters. Single crystal X-ray structures were determined using Bruker SMART 1000 (CCD) diffractometers.

Safety Note. ***Caution!*** Metal perchlorate salts are potentially explosive. So they should be handled with great care.

5.2.3. Synthesis of compounds

The starting compounds **A**, **B** and **C** were prepared following the literature procedure. [8-10]

Synthesis of the intermediate compound D

In a solution of *p-tert*-butylcalix[4]arene (**A**) (1.296 g, 2 mmol) in freshly distilled acetone (80 mL), methylbromo acetate (0.764 g, 5 mmol) and K_2CO_3 (0.345 g, 2.5 mmol) were added and the reaction mixture was heated at reflux for 20h under inert atmosphere. The solution was then allowed to cool to room temperature and evaporated to dryness by rotary evaporation. The residue was then trituated three times with methanol (25 mL each time) and filtered off the white solid. The desired white solid was kept in high vacuum over night. Yield: 1.124 g, (71 %). IR, ν_{max}(KBr pellet)/cm^{-1} 3435 (OH), 1759 (C=O); ^{1}H

NMR (200 MHz, $CDCl_3$): δ 7.03 (s, 4H, Ar-H_m), 6.98 (s, 2H, Ar-*OH*), 6.81 (s, 4H, Ar-H_m), 4.73 (s, 4H, -OCH_2CO), 4.43 (d, 4H, *J* = 13.2 Hz, ArCH_2Ar), 3.85 (s, 6H, -CH_3), 3.32 (d, 4H, *J* = 13.2 Hz, ArCH_2Ar), 1.27 (s, 18H, -C(CH_3)$_3$), 0.97 (s, 18H, -C(CH_3)$_3$). ESMS (*m/z*): found 831.31(100%) calcd for [**D** + K^+] 832.13. Anal calcd for $C_{50}H_{64}O_8$: calcd C, 75.72; H, 8.13. Found: C, 74.89; H, 7.95.

Synthesis of the intermediate compound E

A solution of **D** (0.794 g, 1 mmol) and NaOH (0.6 g, 15 mmol) in a mixture of solvents THF (10 mL), methanol (20 ml) and water (10 ml) was heated at reflux for 15h. The solution was then allowed to cool to room temperature and evaporated to dryness by rotary evaporation. The residue was dissolved in EtOAc (150 ml), and the solution was washed thrice with 20% HCl (60 ml each time). After that this solution was washed thrice by water (100 ml each time). The organic layer was separated, dried over $MgSO_4$ and evaporated in vacuo to give **E** as white solid. Yield: 0.762 g, (90 %). IR, ν_{max}(KBr pellet)/cm^{-1} 3434 (OH), 1742 (C=O); ^{1}H NMR (500 MHz, $CDCl_3$): δ 7.06 (s, 4H, Ar-H_m), 6.95 (s, 4H, Ar-H_m), 4.68 (s, 4H, -OCH_2CO), 4.15 (d, 4H, *J* = 13.5 Hz, ArCH_2Ar), 3.44 (d, 4H, *J* = 13.5 Hz, ArCH_2Ar), 1.25 (s, 18H, -C(CH_3)$_3$), 1.07 (s, 18H, -C(CH_3)$_3$). ESMS (*m/z*): found 787.989 (100%) calcd for [**E** + Na^+] 787.93. Anal calcd for $C_{48}H_{60}O_8$: calcd C, 75.36; H, 7.90. Found: C, 74.83; H, 7.67.

Synthesis of the intermediate compound G

The compound **G** was synthesized from the intermediate **B** following the modified literature method[11], similar to that described for synthesis of **D.** Yield: (76 %). IR, ν_{max}(KBr pellet)/cm^{-1} 3402 (OH), 1760 (C=O); ^{1}H NMR (200 MHz, $CDCl_3$): δ 7.55 (s, 2H, Ar-*OH*), 7.04 (d, 4H, *J* = 7.4 Hz, Ar-H_m), 6.9 (d, 4H, *J* = 7.4 Hz, Ar-H_m), 6.77-6.61 (m, 4H, Ar-H_p), 4.74 (s, 4H, -OCH_2CO-), 4.46 (d, 4H, *J* = 13.2 Hz, ArCH_2Ar), 3.87 (s, 6H, -CH_3), 3.39 (d, 4H, *J* = 13.2 Hz, ArCH_2Ar). ESMS (*m/z*): found 591.54 (95%) calcd for [**G** + Na^+] 591.60, found 607.51 (100%) calcd for [**G** + K^+] 607.71. Anal calcd for $C_{34}H_{32}O_8$: calcd C, 71.81; H, 5.67. Found: C, 71.67; H, 5.43.

Synthesis of the intermediate compound H

Compound **H** was prepared from the intermediate **G** following the similar procedure as described for **E.** Yield: (87 %). IR, ν_{max}(KBr pellet)/cm^{-1} 3369 (OH), 1736 (C=O); ^{1}H NMR (500 MHz, DMSO-d_6): δ 7.87 (s, 2H, Ar-*OH*), 7.04(d, 4H, *J* = 8 Hz, Ar-H_m), 7.00 (d, 4H, *J* = 8 Hz, Ar-H_m), 6.81 (t, 2H, *J* = 7.5 Hz, Ar-H_p), 6.60 (t, 2H, *J* = 7.5 Hz, Ar-H_p), 4.70 (s, 4H, -OCH_2CO), 4.47 (d, 4H, *J* = 13.0 Hz, ArCH_2Ar), 3.40 (d, 4H, *J* = 13.0 Hz, ArCH_2Ar). ESMS (*m/z*): found 563.29 (100%) calcd for [**H** + Na^+] 563.55, found 579.49 (30%) calcd for [**H** + K^+] 579.56. Anal calcd for $C_{32}H_{28}O_8$: calcd C, 71.10; H, 5.22. Found: C, 70.93; H, 5.08.

Synthesis of the intermediate compound J

The synthesis of the compound **J** has been reported in the literature,[12] however, in our laboratory it has been synthesized by a different procedure. A mixture of **C** (3 gm, 5.90 mmol), ethylbromo acetate (2.5 ml, 22.4 mmol) and Cs_2CO_3 (6 gm, 18.41 mmol) in 90 ml of dry acetonitrile was refluxed with stirring for 2 days in inert atmosphere. The solution was then allowed to cool to room temperature and evaporated to dryness by rotary evaporation. The resulting solid was dissolved in $CHCl_3$ (150 ml), and the organic layer was washed three times with water (100 ml each time), dried over $MgSO_4$, and evaporated in vacuo. The crude product was purified by column chromatography on silica gel (100-200 mesh) using 3:17 (v/v) ethyl acetate/hexane as eluent . Yield: 1.72 g, (41 %). IR, ν_{max}(KBr pellet)/cm^{-1} 1756 (C=O). ^{1}H NMR (500 MHz, $CDCl_3$): δ 7.11 (d, 4H, *J* = 7.5 Hz, Ar-H_m), 7.03 (d, 4H, *J* = 7.5 Hz, Ar-H_m), 6.76-6.72 (m, 4H, Ar-H_p), 4.14 (q, 4H, *J* = 7.0 Hz, -O$CH_2$$CH_3$), 3.92 (d, 4H, *J* = 15.0 Hz, ArCH_2Ar), 3.70 (d, 4H, *J* = 15.0 Hz, ArCH_2Ar), 3.58 (s, 4H, -OCH_2CO-), 3.54 (t, 4H, *J* = 7.5 Hz, -O$CH_2$$CH_2$$CH_3$), 1.51-1.43 (m, 4H, -OCH$_2$$CH_2$$CH_3$), 1.26 (t, 6H, *J* = 7.25 Hz, -OCH$_2$$CH_3$), 0.86 (t, 6H, *J* = 7.25 Hz, -OCH$_2$CH$_2$$CH_3$). ESMS (*m/z*): found 703.46 (100%) calcd for [**J** + Na^+] 703.81, found 719.34 (95%) calcd for [**J** + K^+] 719.92. Anal calcd for $C_{42}H_{48}O_8$: calcd C, 74.09; H, 7.10. Found: C, 73.57; H, 7.14.

Synthesis of the intermediate compound K

The compound **K** was synthesized from the intermediate **J** following the similar procedure as described for **E**. Yield: (89 %). IR, ν_{max}(KBr pellet)/cm^{-1} 3377 (OH), 1699 (C=O); ^{1}H NMR (500 MHz, 2:1 $CDCl_3$-CD_3SOCD_3): δ 7.07 (d, 4H, *J* = 7.5 Hz, Ar-H_m), 7.04 (d, 4H, *J* = 7.5 Hz, Ar-H_m), 6.85 (t, 2H, *J* = 6.5 Hz, Ar-H_p), 6.78 (t, 2H, *J* = 6.5, Ar-H_p), 3.95-3.91 (m, 4H, ArOCH_2CO), 3.85-3.81 (m, 8H, ArCH_2Ar), 3.46 (t, 2H, *J* = 6.5, -O$CH_2CH_2CH_3$), 1.30-1.25 (m, 4H, -$OCH_2CH_2CH_3$), 0.703 (t, 6H, *J* = 6.5, -$OCH_2CH_2CH_3$). ESMS (*m/z*): found 647.65 (100%) calcd for [**K** + Na^+] 647.71, found 663.63 (25%) calcd for [**K** + K^+] 663.72. Anal calcd for $C_{38}H_{40}O_8$: calcd C, 73.05; H, 6.45. Found: C, 72.62; H, 6.23.

Synthesis of the intermediate compound F and compound 1

A mixture of **E** (0.765 g, 1 mmol) and thionyl chloride (10 mL) in 30 ml dry toluene was stirred and refluxed under nitrogen for 6 h. The excess $SOCl_2$ and toluene was then removed by rotary evaporation. The resulting yellowish solid mass (**F**) was used directly in the next step for the synthesis of **1**.

In the next step, 3-aminoquinoline (0.363 g, 2.5 mmol) was dissolved in dry THF (50 mL) and triethylamine (3 mL) was added to this solution. Then the THF solution (30 mL) of the acid chloride obtained in the previous step was added dropwise to the reaction mixture over a period of 1.0 h and the solution was then stirred at room temperature for another 2 h. Finally the reaction mixture was refluxed for 24 h under nitrogen atmosphere. The solution was then allowed to cool to room temperature and evaporated to dryness by rotary evaporation. The residue was dissolved in $CHCl_3$ (100 ml), and the organic layer was washed three times with water (70 ml each time), dried over $MgSO_4$ and evaporated in vacuo. The crude product was purified by column chromatography on activated neutral alumina by using 3:7 (v/v) chloroform/hexane as eluent. Yield: 0.64 g, (63 %). IR, ν_{max}(KBr pellet)/cm^{-1} 3417 (OH), 3316 (NH), 1703 (C=O). ^{1}H NMR (500 MHz, $CDCl_3$): δ = 10.62 (s, 2 H, quinoline-*H*), 8.87 (br-s, 2H, -CON-*H*), 8.29 (s, 2H, quinoline-*H*), 8.06 (d, 2H, *J* = 8.5 Hz, quinoline-*H*), 7.96 (br-s, 2H, quinoline-*H*), 7.64 (t, 2H, *J* = 7.5 Hz, quinoline-*H*), 7.42 (t, 2H, *J* = 7.5 Hz, quinoline-*H*), 7.16 (s, 4H, Ar-H_m), 7.05 (s, 4H, Ar-H_m), 4.76 (s, 4H, -OCH_2CO-), 4.30 (d, 4H, *J* = 13.5 Hz, ArCH_2Ar), 3.56 (d, 4H, *J* = 13.5 Hz, ArCH_2Ar), 1.29 (s, 18H, -C(CH_3)$_3$), 1.11 ((s, 18H, -C(CH_3)$_3$). ESMS (*m/z*): found

1017.00 (20%) calcd for [**1**] 1017.27, found 1038.94 (100%) calcd for [**1** + Na^+ - $2H^+$] 1038.25. Anal calcd for $C_{66}H_{72}N_4O_6.2DMF.H_2O$: calcd C, 74.12; H, 7.61; N, 7.20. Found: C, 74.56; H, 7.47; N, 7.15. UV/Vis (CH_3CN): λ, nm (ε, $dm^3mol^{-1}cm^{-1}$), 333 (7.2 x 10^3), 318 (7.5 x 10^3), 277 (1.7 x 10^4).

Synthesis of the intermediate compound I and compound 2

The intermediate compound **I** and the ionophore **2** were synthesized from the intermediates **H** following the same method as described for **F** and **1**, except the solvents used for purification. The crude product of **2** was purified by column chromatography using chloroform/hexane as eluent in the ratios 2:3 for **2.** Yield; 60 %. for **2,** 65% for **3.** IR, ν_{max}(KBr pellet)/cm^{-1} 3366 (OH), 3287 (NH), 1695 (C=O). ^{1}H NMR (500 MHz, $CDCl_3$): δ = 10.54 (s, 2 H, quinoline-*H*), 8.85 (br-s, 2H, -CON-*H*), 8.43 (s, 2H, quinoline-*H*), 8.06 (d, 2H, *J* = 6 Hz, quinoline-*H*), 7.95 (br-s, 2H, quinoline-*H*), 7.66 (t, 2H, *J* = 7.5 Hz, quinoline-*H*), 7.44 (t, 2H, *J* = 7.5 Hz, quinoline-*H*), 7.18 (d, 4H, *J* = 7.75 Hz, Ar-H_m), 7.07 (d, 4H, *J* = 7.75 Hz, Ar-H_m), 6.93 (t, 2H, *J* = 7.5 Hz, *Ar*-H_p), 6.82 (t, 2H, *J* = 7.5 Hz, *Ar*-H_p), 4.78 (s, 4H, -OCH_2CO-), 4.32 (d, 4H, *J* = 13.5 Hz, ArCH_2Ar), 3.64 (d, 4H, *J* = 13.5 Hz, ArCH_2Ar). ESMS (*m/z*): found 793.03 (100%) calcd for [**2**+H^+] 792.85. Anal calcd for $C_{50}H_{40}N_4O_6$: calcd C, 75.74; H, 5.08; N, 7.06 Found: C, 75.41; H, 4.97; N, 6.93. UV/Vis (CH_3CN): λ, nm (ε, $dm^3mol^{-1}cm^{-1}$), 333 (7.2 x 10^3), 318 (7.5 x 10^3), 277 (1.7 x 10^4).

Synthesis of the intermediate compound L and compound 3

The intermediate compound **L** and the ionophore **3** were synthesized from the intermediate **K** following the similar procedure as described for **F** and **1**, except the solvents used for purification. The crude product of **3** was purified by column chromatography using chloroform/hexane as eluent in the ratios 3:7**.** Yield; 65%. IR, ν_{max}(KBr pellet)/cm^{-1} 3362 (NH), 1674 (C=O). ^{1}H NMR (500 MHz, $CDCl_3$): δ = 9.46 (s, 2 H, quinoline-*H*), 9.09 (br-s, 2H, -CON-*H*), 8.5 (s, 2H, quinoline-*H*), 8.06 (d, 2H, *J* = 8 Hz, quinoline-*H*), 7.90 (d, 2H, *J* = 8 Hz, quinoline-*H*), 7.67 (t, 2H, *J* = 8 Hz, quinoline-*H*), 7.59 (t, 2H, *J* = 8 Hz, quinoline-*H*), 7.13 (d, 4H, *J* = 7.5 Hz, Ar-H_m), 6.92 (t, 2H, *J* = 7.5 Hz, Ar-H_p), 6.88 (d, 4H, *J* = 7.5 Hz, *Ar*-H_m), 6.23 (t, 2H, *J* = 7.5 Hz, *Ar*-H_p), 4.37 (s, 4H,

-O*CH*$_2$CO-), 3.84-3.76 (m, 8H, Ar*CH*$_2$Ar), 3.39 (t, 4H, *J* = 7.5 Hz, -O*CH*$_2$CH$_2$CH$_3$), 1.54-1.47 (m, 4H, -OCH$_2$*CH*$_2$CH$_3$), 0.80 (t, 6H, *J* = 7.5 Hz, -OCH$_2$CH$_2$*CH*$_3$). ESMS (*m/z*): found 877.09 (10%) calcd for [**3**+H$^+$] 877.01, found 899.03 (100%) calcd for [**2**+ Na$^+$] 900.00. Anal calcd for $C_{56}H_{52}N_4O_6$: calcd C, 76.69; H, 5.98; N, 6.38 Found: C, 75.84; H, 5.83; N, 6.26. UV/Vis (CH_3CN): λ, nm (ε, $dm^3mol^{-1}cm^{-1}$), 335 (1.2 x 10^4), 321 (1.2 x 10^4), 278 (1.8 x 10^4).

5.2.4. X-ray crystallography for compounds 1-3

Crystal of suitable size was selected from the mother liquor and immersed in partone oil, then mounted on the tip of a glass fiber and cemented using epoxy resin. Intensity data for all three crystals were collected at 100 K using MoK_α (λ = 0.71073Å) radiation on a Bruker SMART APEX diffractometer equipped with CCD area detector. The data integration and reduction were processed with SAINT software.[13] An empirical absorption correction was applied to the collected reflections with SADABS.[14] The structures were solved by direct methods using SHELXTL[15] and were refined on F^2 by the full-matrix least-squares technique using the SHELXL-97[16] program package. Graphics are generated using PLATON[17] and MERCURY 1.3.[18] In all the compounds non-hydrogen atoms were refined anisotropically till convergence is reached and the hydrogen atoms attached to the ligand moieties are sterochemically fixed. The crystallographic data and details of data collection for all the three compounds are given in Table 5.1.

5.2.5. Ion-binding study

Luminescence study

Stock solutions of the complexes **1-3** (5 x 10^{-6} M) and that of perchlorate salts (5 x 10^{-4} M) of various metal ions (Li^+, Na^+, K^+, Rb^+, Cs^+, Mg^{2+}, Ca^{2+}, Sr^{2+}, Ba^{2+}, Zn^{2+}, Cd^{2+}, Hg^{2+}, Cu^{2+}, Ni^{2+}, Ag^+, Cr^{3+}, Fe^{3+} and Pb^{2+}) were prepared in freshly purified acetonitrile. Then 2 mL stock solution of the complex and 2 mL stock solution of each metal salts were taken in a 5 mL volumetric flask, so that the effective concentration of the complex is 2.5 x 10^{-6} M and that of the metal ions are 2.5 x 10^{-4} M (100 fold). The luminescence spectra of the resulting solutions and that of the original complex (2.5 x 10^{-6} M) were recorded with

excitation at the absorption maxima (λ_{max}) of the MLCT band, which is 318, 318, 321, nm for **1-3,** respectively. The spectra of the cation added solutions were compared with that of the original solution to ascertain the interactions of the metal ions with the ionophore.

For emission titration study, the same stock solutions of the complexes were used and the metal perchlorate solutions of desired concentration (1.0 – 100.0 equivalents) were prepared by proper dilution of the stock solution and titration were carried out as described in *Chapter – II*.

NMR study

Interactions with anions were also investigated by ^{1}H NMR spectroscopy. ^{1}H NMR spectra of the compounds **1-3** were recorded with 2 mg of the sample dissolved in 0.5 mL of CD_3CN. Tetrabutylammonium salts of F^-/HSO_4^- of desired concentration were added into the solution to make concentration of metal ions 1, 3, 5 and 10 molar equivalent of the ionophores and the spectra of the resulting reaction mixture were recorded. The spectra of the anion added solutions were compared to that of the original compounds to ascertain the interaction of the metal ion with the ionophore. No NMR titration experiments were carried out as the binding constants were determined from fluorescence titration data. The aim of this experiment was to investigate the sites, where anions binds.

5.3. Results and discussion

5.3.1. Synthesis and characterization of the compounds

The route followed for the synthesis of **1-3** is shown in Scheme 5.1 and the details of experimental procedures are given in Experimental Section. Elemental analysis (C, H and N), IR, ESMS and ^{1}H NMR spectral data for all the intermediate compounds and for **1-3** are given in the Experimental Section. The elemental analysis and mass data are in well agreement with the calculated values. It may be noted that the *m/z* values of all these compounds correspond to the $Na^+/K^+/H^+$ adduct, which is a well known phenomenon when LC-MS is used for the measurement of mass. The IR spectra of **1** and **2** exhibited bands of moderate intensity at 3417 and 3366 cm^{-1}, respectively, which are due to ν(O-H). The sharp bands at 3316, 3287 and 3362 cm^{-1} for **1**, **2** and **3**, respectively are assigned to

ν(N-H) of the amide moiety. The strong bands, which appeared at 1703, 1695 and 1674 cm^{-1} for **1**, **2** and **3**, respectively are due to ν(C=O), respectively. The ^{1}H NMR spectra of the compounds **1-3** are given in the Figures. 5.1–5.3, respectively. The ^{1}H NMR data are in consistent with the structures shown in Scheme 5.1. In the ^{1}H NMR spectrum of **1**, the *meta*- protons (with respect to the OH substituent) of the calixarene moiety appear as two distinct singlets in the range *δ* 7.15-7.04. But in the ^{1}H NMR spectra of **2** and **3,** the *meta*- and *para*-protons of the calixarene moiety appear as doublets and triplets, respectively. In fact, two sets of signals appear for these protons in the aromatic region *δ* 7.18- 6.23 due to substituents at the two opposite OH of the four phenolic OH groups. The aminoquinoline moieties exhibit two singlets in the ranges δ 9.46-10.62 and 8.29-8.50, two doublets at δ 8.06 and 7.90-7.96, and two triplets in the ranges δ 7.64-7.67 and 7.42-7.59, as expected from two chemically equivalent quinoline moieties in solution. In all the three compounds, the protons of –CONH group exhibited a singlet in the range δ 8.85-9.09. In the aliphatic region, the OCH_2 protons for all three compounds appear as singlet in the range δ 4.37-4.78. The Ar*CH*$_2$Ar protons of the calix moiety for **1** and **2** appear as two well separated doublets in the regions δ 4.30-4.32 and δ 3.56-3.64, respectively. The appearance of two doublets for the methylene protons (AB type) suggest that the calix moiety in these compounds exist in cone conformation.[19,20] The Ar*CH*$_2$Ar protons for **3** appear as multiplate in the region δ 3.84-3.76, which is similar to that observed for 1,3-alternate conformation with substituents at the two of the four OH groups in the calix moiety.[21,22] The proposed structures of **1-3** are shown in Scheme 5.1. The molecular structures of these compounds were also confirmed from single crystal X-ray data.

5.3.2. Crystal structures of 1-3

Compound **1** crystallizes in orthorhombic space group Pccn with two DMF and a water molecule in the crystal lattice as solvent of crystallization along with the modified *tert*-butyl calix moiety. The calix moiety adopted a cone conformation and the quinolene moiety is appended to the opposite rings (alternate positions) at the lower rim of the calix moiety. The ORTEP view of 1 is shown in the Figure. 5.4. It is interesting to note that one

Table 5.1. Summary of crystallographic data for compounds **1** – **3**

Compound	**1**	**2**	**3**
Emperical formula	$C_{72}H_{88}N_6O_9$	$C_{52}H_{41}N_4O_6$	$C_{56}H_{52}N_4O_6$
Formula mass	1181.48	1030.59	877.08
Crystal Colour	Colourless	Colourless	Colourless
Crystal Size (mm^3)	0.53 x 0.46 x 0.12	0.73x0.34x 0.13	0.54x0.32x 0.12
Temperature (K)	100	100	100
Crystal System	Orthorhombic	Triclinc	Orthorhombic
Space Group	Pccn	P-1	Pbca
a(Å)	33.741(6)	10.1151(18)	28.539(4)
b(Å)	17.823(3)	12.632(2)	17.712(2)
c(Å)	21.667(4)	20.705(4)	36.055(4)
α(°)	90.0	106.850(3)	90.0
β(°)	90.0	90.681(3)	90.0
γ (°)	90.0	103.566(3)	90.0
Z	8	2	16
V($Å^3$)	13029(4)	2452.3(7)	18225(4)
Density (Mg/m^3)	1.205	1.396	1.279
Abs. Coefficient (mm^{-1})	0.079	0.405	0.083
F(000)	5072	1062	7424
Reflections Collected	54952	17449	87742
Independent Reflections	10218	8534	16038
R_{int}	0.0883	0.0282	0.1199
Number of Parameters	810	653	1205
S (GOF) on F^2	1.199	1.053	1.185
Final R1 , wR2 (I>2σ(I)	0. 0899/0. 2031	0.0883 / 0.2300	0.0966/0.1660
WR1, wR2 (all data)	0. 1104/ 0. 2157	0.1184 / 0.2505	0.1349/ 0.1795

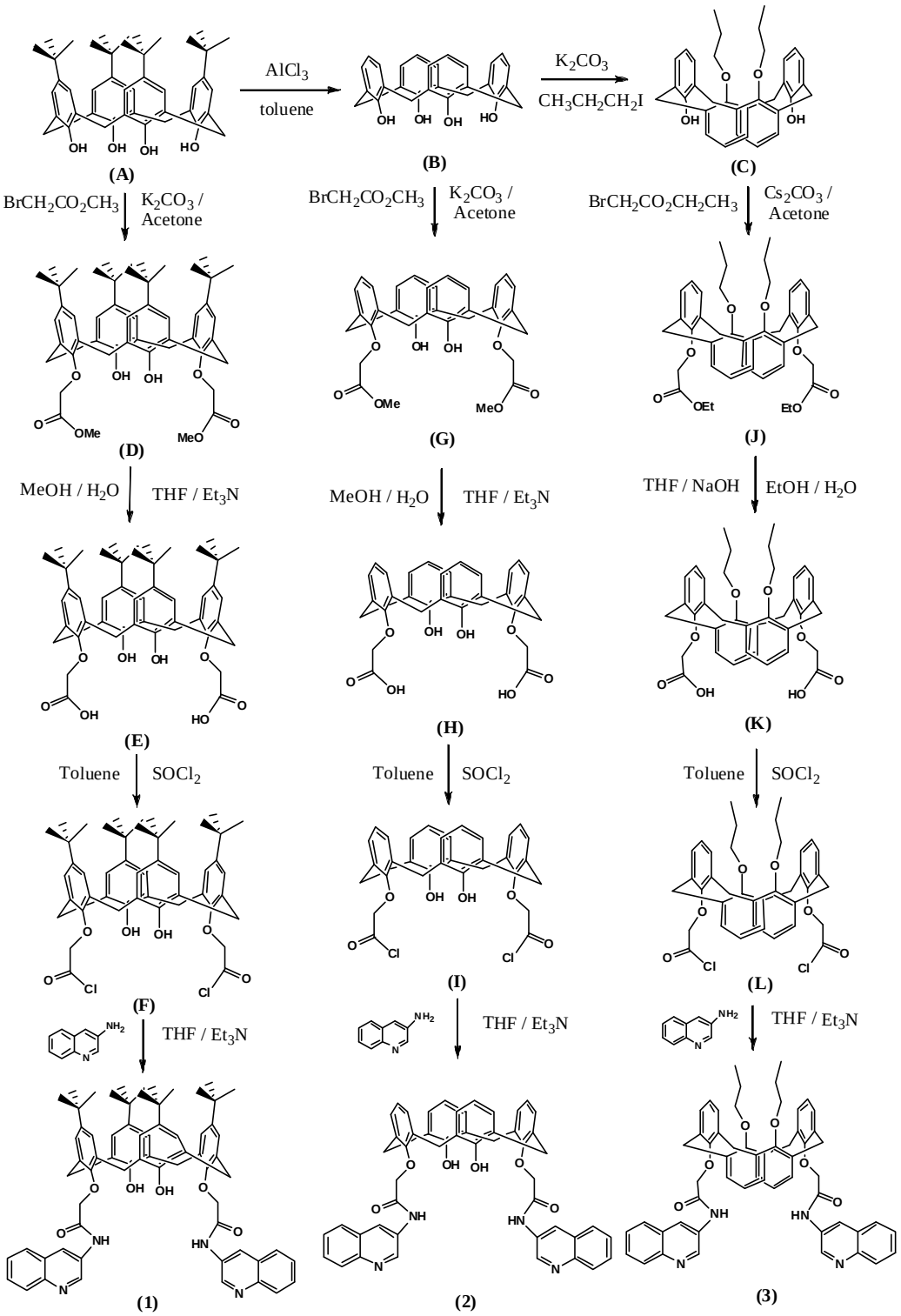

Scheme 5.1. Route for synthesis of compounds **1 – 3**.

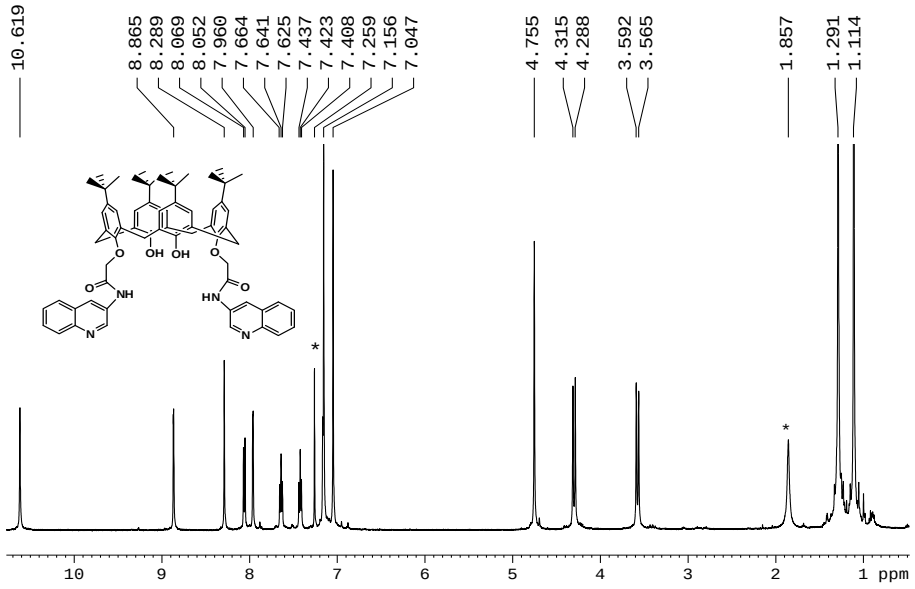

Figure. 5.1. ^{1}H NMR spectrum of the compound **1** recorded in $CDCl_3$, signals with * mark are from solvent.

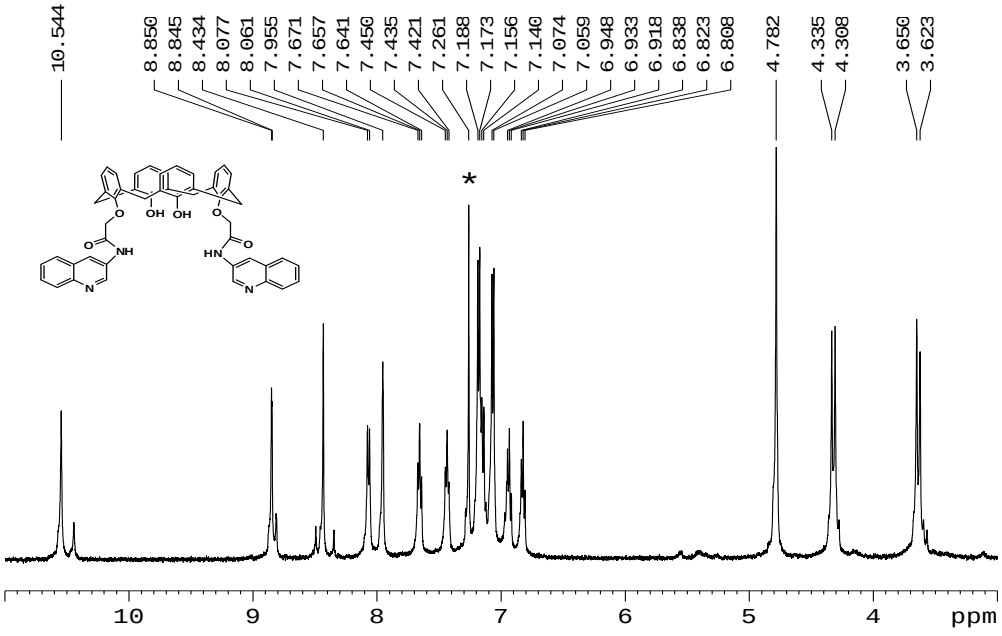

Figure. 5.2. ^{1}H NMR spectrum of the compound **2** recorded in $CDCl_3$, signal with * mark is from solvent.

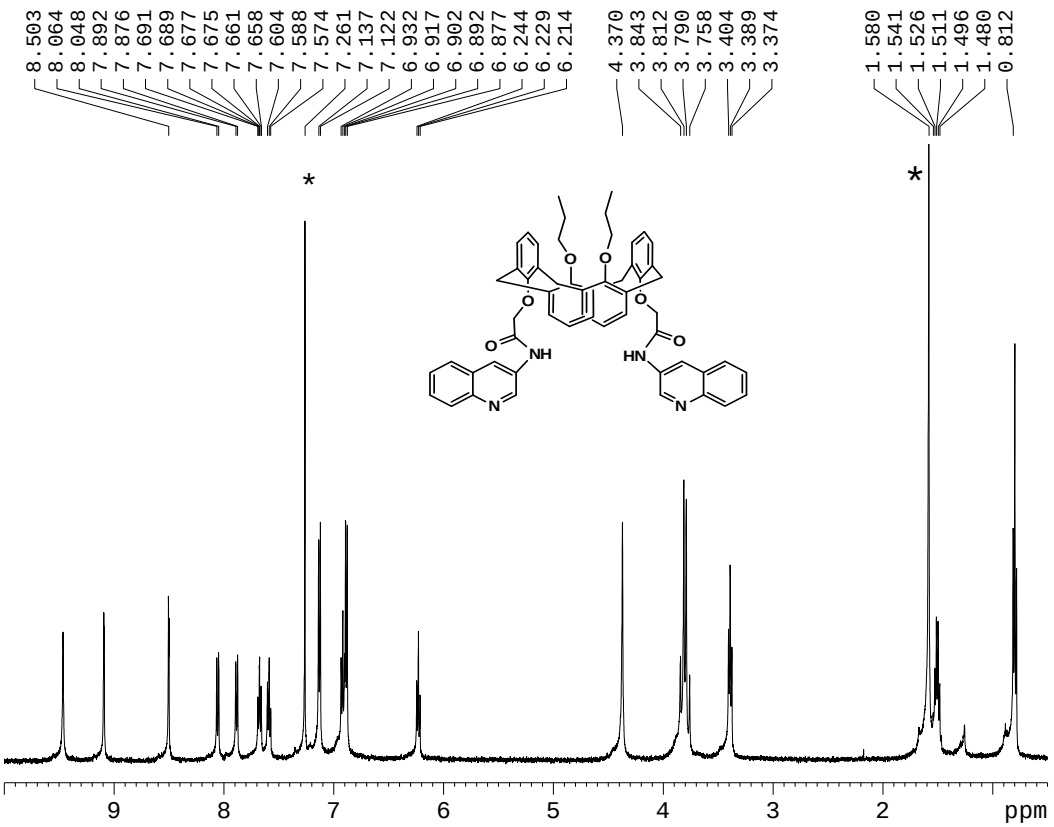

Figure. 5.3. ^{1}H NMR spectrum of the compound **3** recorded in $CDCl_3$, signals with * mark are from solvent.

of the DMF molecule is encapsulated inside the calix cone with strong C-H….π interaction, as depicted in Figure.5.5. The methyl hydrogens H68B and H68C of the DMF molecule is involved in C-H….π contact with H….Cg (centroied of the benzene ring), distance 2.84 and 2.87 Å respectively. The aldehide hydrogen H69 is also involved in H….Cg contact making a distance 2.82 Å with the centroid of different benzene ring of the conical *tert*-butyl calix moiety (C(68-H(68B)….. Cg(4) : H(68B)….. Cg(4) = 2.84; C(68….. Cg(4)= 3.445(5) ; <C(68-H(68B)….. Cg(4)= 122: symmetry code;x,y,z; C(68-H(68C)….. Cg(1) : H(68C)….. Cg(1) = 2.87; C(68….. Cg(1) = 3.536(5) ; <C(68- H(68C)

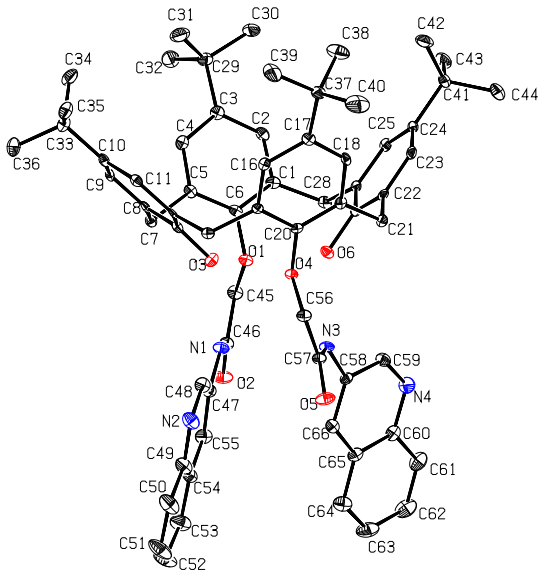

Figure. 5.4. ORTEP diagram of the compound **1** with atom numbering scheme (40% probability factor for the thermal ellipsoids, DMF, H_2O and H-atoms are omitted for clarity).

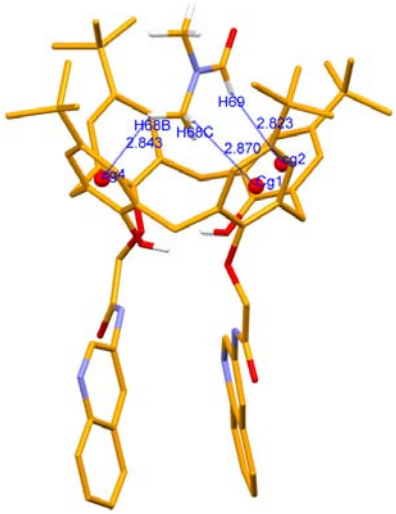

Figure. 5.5. Mercury diagram of **1** depicting the encapsulation of DMF molecule inside the calix cone making C-H…π interactions.

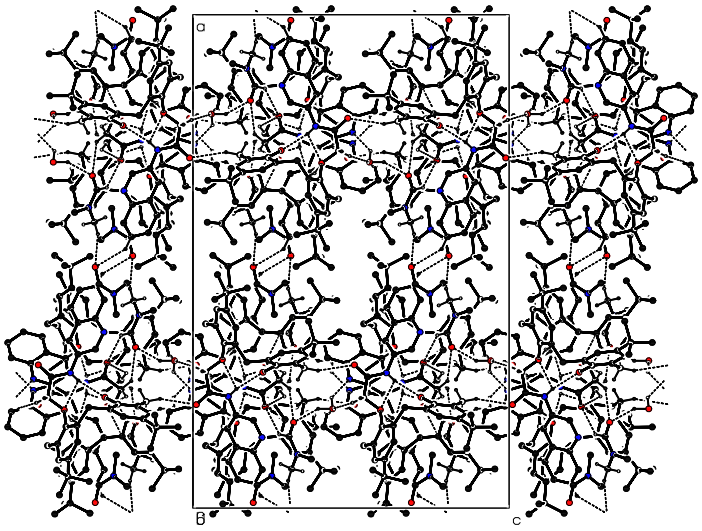

Figure.5.6. Packing diagram of compound **1** with hydrogen bonding interaction viewed down c-axis depicting the two dimensional H-bonding network along ab-plane.

….. Cg(1)= 127: symmetry code;x,y,z; C(69)-H(69)….. Cg(2) : H(69)….. Cg(2) = 2.82; C(69)….. Cg(2)= 3.725(5) ; <C(69)-H(69)….. Cg(2)= 164: symmetry code;x,y,z; where Cg(1), Cg(2) and Cg(4) are centroids of the phenyl rings C1-C6, C8-C13 andC22-C27 respectively.) Strong intramolecular O-H..O interaction between the phenolic hydrogen with the substituted phenolic oxygen is responsible for the cone conformation of the calixarine moiety (Table 5.2). It is interesting to note that the mean plane involving quinolene rings of the substituted OH groups is 35.2 degree and the twist can be attributed to the additional N-H…O interaction involving the amide hydrogen H1C, H3C with the phenolic oxygen O3 and O6, respectively in addition to intramolecular O-H…O interaction. The second lattice DMF molecule acts as an acceptor and involved in O-H…O interaction with the lattice water hydrogens H9D and H9C making O-H…N interaction with the pyridyl ring of the appended quinolene moiety. Oxygen atoms from the phenolic group, water, and DMF is further involved in C-H..O interaction (as acceptors) with the substituted calix moiety in the formation of a two dimensional hydrogen bonded network

Table 5.2. Hydrogen bonding parameters with symmetry code for **1**-**3**.

D-H...A	d(H...A) (Å)	d(D...A) (Å)	<D-H…A (°)
Compound 1			
N(1)-H(1C)...O(3) [1]	2.33	3.135(4)	164
O(3)-H(3)....O(4) [1]	1.89	2.677(4)	161
N(3)-H(3C)....O(6) [1]	2.15	2.908(4)	169
O(6)-H(6)....O(1)[1]	1.92	2.727(4)	169
O(9)-H(9D)....O(8) [1]	1.92(7)	2.844(6)	146(5)
O(9)-H(9C)....N(2) [2]	2.05(6)	2.913(5)	138(5)
C(28)-H(28B)….O(5) [3]	2.59	3.513(5)	159
C(45)-H(45A)....O(8)[4]	2.42	3.119(8)	129
C(45)-H(45B)....O(2)[1]	2.59	3.259(5)	126
C(55)-H(55)....O(2)[1]	2.28	2.864(5)	120
C(56)-H(56A) ….O(9)[5]	2.38	3.289(5)	157
C(62)-H(62) ..O(7)[6]	2.52	3.320(6)	145
C(71)-H(71B) ..O(7)[7]	2.49	3.408(7)	161
C(72)-H(72) ..O(2)[4]	2.42	3.165(7)	137
[1] x, y, z; [2] x, 3/2-y, 1/2+z; [3] 1/2-x, y, 1/2+z; [4] 1/2-x, 3/2-y, z; [5] x, 3/2-y, -1/2+z;[6]1/2+x, 2-y ,1/2-z; [7]-x, -1/2+y, 1/2-z			
Compound 2			
N(1)-H(1C)....O(2)[1]	2.28(4)	3.067(5)	167(4)
O(2)-H(2).…O(3)[1]	1.94	2.744(4)	166
N(3)-H(3C)....O(4)[1]	2.40(4)	3.152(5)	172(3)
O(4)-H(4)....O(1)[1]	1.92	2.726(4	168
C(51)-H(51)....O(6)[2]	2.10	3.019(7)	156
[1] x, y, z; [2] 1+x,y,z;			

Compound 3			
N(1)-H(1C)…..N(4)[1]	2.02	2.959	174
N(5) --H(5C)…..N(8)[1]	2.09	2.924	172
C(110)--H(10E)…..O(5)[2]	2.35	3.2246	150
C(11) --H(11) …..O(2)[3]	2.56	3.474	167
C(112)--H(12F)…..O(5)[2]	2.54	3.384	148
C(53) --H(53)…..O(1)[1]	2.47	3.359	160
C(88) --H(88)…..O(8)[1]	2.32	2.900	120
C(109)--H(109)…..O(7)[1]	2.43	3.214	142
[1] x, y, z;			

as depicted in Figure.5.6. Details of all these pertinet hydrogen bonding parameters with symmetry code are given in Table.5.2.

Compound **2** crystallizes in triclinic system with P-1 space group with two chloroform molecules as solvent of crystallization. As observed in compound **1,** strong intramolecular O-H…O interaction do exist between the phenolic hydrogen atoms with the oxygen atoms of the adjacent amide moiety and the amide N-H hydrogens are also involved in N-H…O interaction with the phenolic oxygen O2 and O4. The ORTEP view of the compound **2** is shown in Figure. 5.7. Packing diagram viewed down b-axis is shown in Figure.5.8. The calix moieties are oriented in zigzag fashion along c-axis and the chloroform molecules are occupied between the adjacent zigzag layers via C-H…O interaction between the chlorofom hydrogen and amide oxygenO6. Details of all the pertinet hydrogen bonding interaction with symmetry code is given in Table.5.2.

Compound **3** crystallizes in orthorhombic system in Pbca space group with two calix moieties in the asymmetric unit. Unlike compounds **1** and **2**, the two of the phenolic OH are attached to the propyl substituents and the calix moiety adopted 1,3 alternate conformation. The ORTEP diagram of **3** is shown in Figure. 5.9. It is interesting to note that due to the 1,3 alternate conformation of the calix cone, the amide hydrogens (NH) H1C and H5C of each calix moiety is involved in intramolecular N-H…N interaction

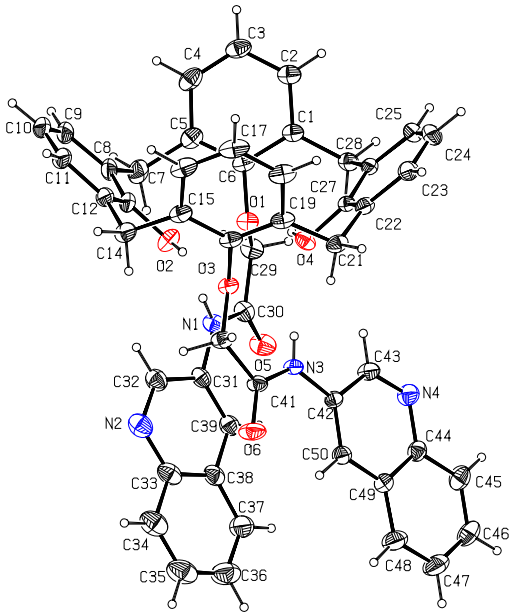

Figure. 5.7. ORTEP diagram of **2** with atom numbering scheme (30% probability factor for the thermal ellipsoids. Lattice chloroform molecules are omitted for clarity

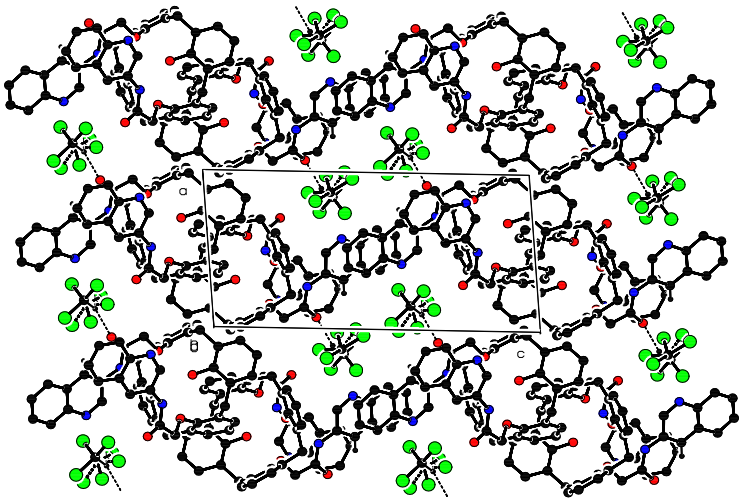

Figure. 5.8. Packing diagram of compound 2 viewed down b-axis depicting the Zigzag orientation of the calix moiety with the orientation of the chloroform molecule between the adjacent zigzag layers.

with the quinolene nitrogens N4 and N8 of the corresponding calixarene. In addtion to this intramolecular N-H…N contacts, intramolcular C-H…O contacts is also observed because of the different orientations of the moiety in 1,3 alternate conformation. A close up view of the intermolecular hydrogen bonds between the molecules present in the asymmetric unit is depicted in Figure. 5.10.

Both the molecules present in the asymmetric units are linked via intermolecular C-H…O interaction, in which the amide oxygen O5 acts as an bifurcated acceptor with the propyl hydrogens H12F and H10E while O2 is making C-H…O H-bonding with the phenyl hydrogen H11. These intermolecular C-H..O H-bonding generates a two dimensional hydrogen bonded calix nets in ac-plane in which the adjacent layered zigzag nets are interconnected as depicted in packing diagram with H-bondings in Figure. 5.11. Details of all these pertinet hydrogen bonds with symmetry code are given in Table. 5.2.

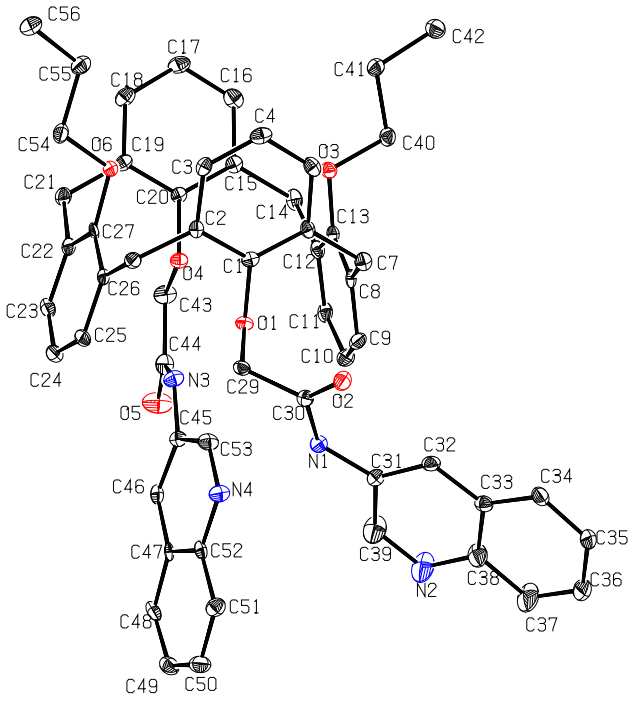

Figure. 5.9. ORTEP diagram of **3** depicting the calix moiety of one molecule present in the asymmetric unit with atom numbering scheme (hydrogen atoms are omitted for clarity)

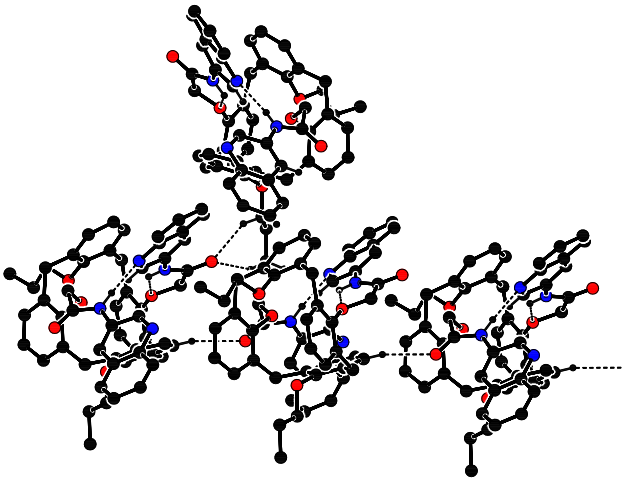

Figure. 5.10. Clsoe-up view depicting the C-H.…O hydrogen bonding interaction between both the molecules of **3** present in the asymmetric unit in the formation of zigzag layers.

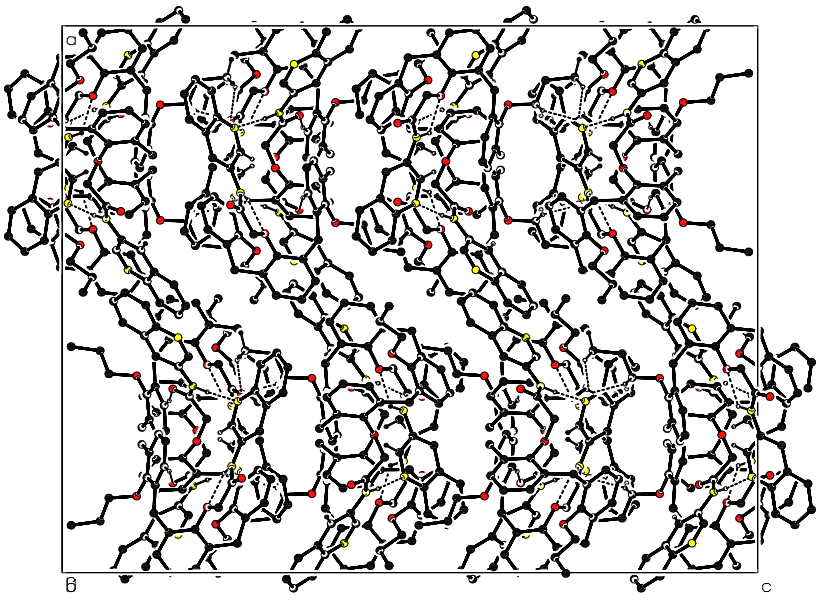

Figure. 5.11. Packing diagram with hydrogen bonding interaction for compound **3** viewed down b-axis showing the zigzag arrangement of the calix moiety in layers likned via hydrogen bonding and π stacking interactions.

5.3.3. Absorption and luminescence spectra

Absorption spectra of **1–3** were recorded in acetonitrile and the data are given in the Experimental Section. All these three compounds exhibit three absorption bands in the region 275–335 nm, among which the band around 318 nm is due to quinoline moiety.[23,24] The other band around 278 nm is for calix[4]arene moiety.[25,26] The luminescence spectra were also recorded in acetonitrile with excitation at the absorption maxima (λ_{max}) of the quinoline band, which is 318, 318 and 321 nm for **1–3**, respectively. The strong luminescence band observed at 355 nm.

5.3.4. Ion-binding study

The ion-binding property of the fluoroionophores **1–3** have been investigated with a large number of cations (Li^+, Na^+, K^+, Rb^+, Cs^+, Mg^{2+}, Ca^{2+}, Sr^{2+}, Ba^{2+}, Zn^{2+}, Cd^{2+}, Hg^{2+}, Cu^{2+}, Ni^{2+}, Ag^+, Cr^{3+}, Fe^{3+} and Pb^{2+}) as their perchlorate salts and anions (F^-, Cl^-, Br^-, I^-, HSO_4^-, ACO^-, $H_2PO_4^-$, ClO_4^-, NO_3^- and BF_4^-) as their tetrabutyl ammonium salts. The ion-recognition process is monitored by luminescence, UV-Vis and ^1H NMR spectral changes. In the first step, the fluorescence spectra of the compounds were recorded in acetonotrile and then it was recorded again in presence of various ions (100 fold excess) under similar experimental conditions and the fluorescence intensity of all these spectra were compared with that of the original solution. Out of these large number of cations, Hg^{2+}, Pb^{2+}, Fe^{3+} and Cu^{2+} exhibit substantial quenching in emission intensities (75-90%) whereas other metal ions do not induce any significant quenching, indicating stable complex formation of these metal ions with all the three compounds (**1-3**). While quenching in emission intensity with the addition of increasing concentration of metal ions, the position of the emission maxima ($\lambda_{max,em}$) around 355 nm did not show any significant shift but a broad new band centering around 410 nm with moderate intensity appeared, which is assigned to the excimer emission.[1,2] Formation of complex with metal ion brought the quinoline moieties closer, which resulted in hydrogen bond induced intramolecular excimer formation. In the case of anions, compound **1** and **2** exhibited substantial quenching in presence of F^- (50 and 70%), compound **2** exhibited substantial quenching in presence of HSO_4^-, whereas compound **3** did not show any significant change in presence of any

anions studied. This observation suggest that out of all anions studied, F^- binds strongly with **1** and **2**, and HSO_4^- binds only with **2** and compound **3** does not make strong interaction with any anions. Interactions with anions also studied by ^1H NMR spectroscopy.

Binding constants of the ions with the fluoroionophores **1-3** were calculated using emission titration data following literature procedure.[27-29] The titration experiments were carried out following the method described in the Experimental Section. The changes observed in emission intensities upon addition of increasing concentration of Hg^{2+}, Pb^{2+}, Fe^{3+} and Cu^{2+} for **1-3** are shown in Figures. 5.12 – 5.21, respectively. For anions, the change in emission intensities for **2** with F^- and HSO_4^- are shown in Figures 5.22 and 5.23. According to this procedure, the fluorescence intensity (F) scales with the metal ion concentration ([M]) through $(F_0 - F)/(F - F_\infty) = ([M]/K_{diss})^n$. The binding constant ($K_s$) is obtained by plotting $\log[(F_0 - F)/(F - F_\infty)]$ versus log[M] following the procedure as described earlier Chapters The plots $\log[(F_0 - F)/(F - F_\infty)]$ versus log[M] are shown as insets of the Figures. 5.12 – 5.21. The binding constants are summarized in Table 5.3.

Table 5.3. Binding constants with strongly interacting ions for **1-3**

Compound	Binding constant, (K_s/M^{-1})					
	Hg^{2+}	Pb^{2+}	Fe^{3+}	Cu^{2+}	F^-	HSO_4^-
1	3.70×10^5	6.02×10^4	1.23×10^6	3.93×10^4	4.48×10^3	
2	1.32×10^5	1.20×10^5	2.07×10^5	1.05×10^5	2.88×10^4	1.14×10^3
3	4.05×10^5	4.89×10^5	1.17×10^5	4.30×10^4		

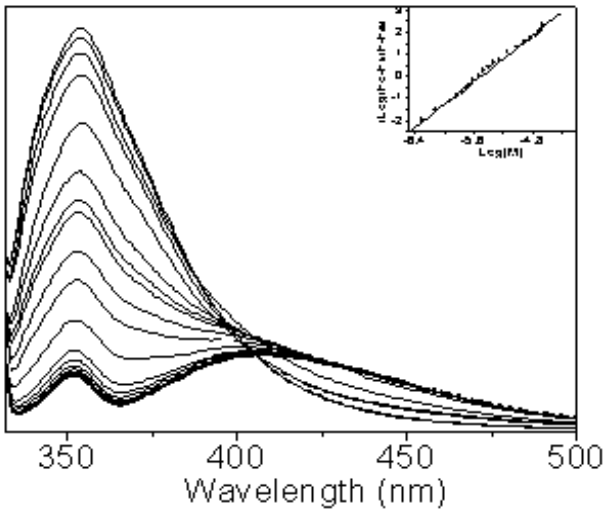

Figure. 5.12. Emission spectral changes for **1** (5 x 10^{-6} M) upon addition of increasing concentration of $Hg(ClO_4)_2$. Excitation wavelength: 318 nm. Inset: linear regression fit (double-logarithmic plot) of the titration data as a function of concentration of metal.

Figure. 5.13. Emission spectral changes for **1** (5 x 10^{-6} M) upon addition of increasing concentration of $Pb(ClO_4)_2$. Excitation wavelength: 318 nm. Inset: linear regression fit (double-logarithmic plot) of the titration data as a function of concentration of metal.

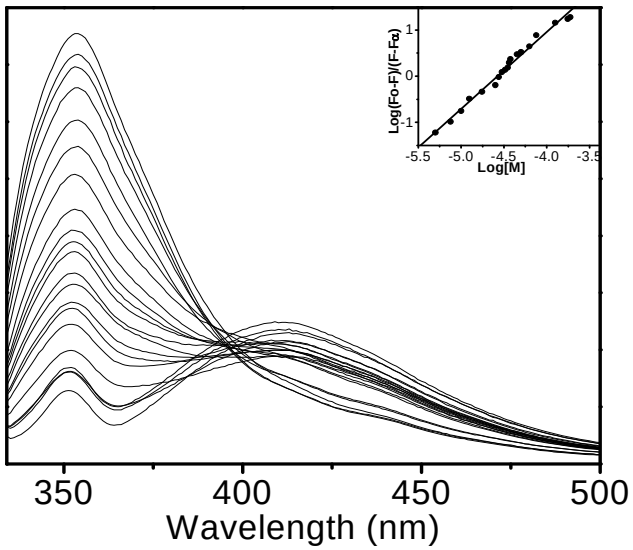

Figure. 5.14. Emission spectral changes for **1** (5 x 10^{-6} M) upon addition of increasing concentration of $Cu(ClO_4)_2$. Excitation wavelength: 318 nm. Inset: linear regression fit (double-logarithmic plot) of the titration data as a function of concentration of metal.

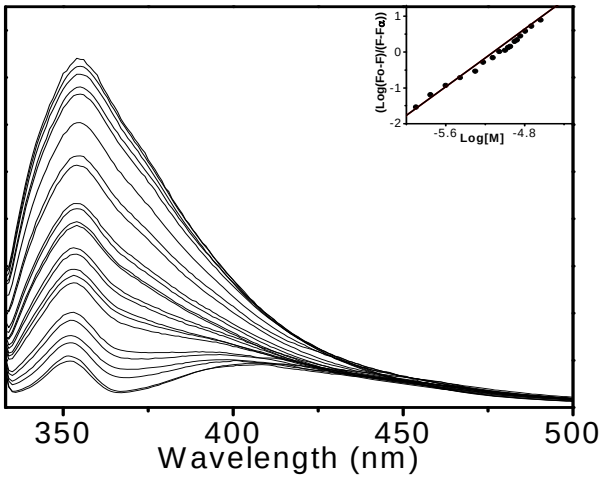

Figure. 5.15. Emission spectral changes for **2** (5 x 10^{-6} M) upon addition of increasing concentration of $Hg(ClO_4)_2$. Excitation wavelength: 318 nm. Inset: linear regression fit (double-logarithmic plot) of the titration data as a function of concentration of metal.

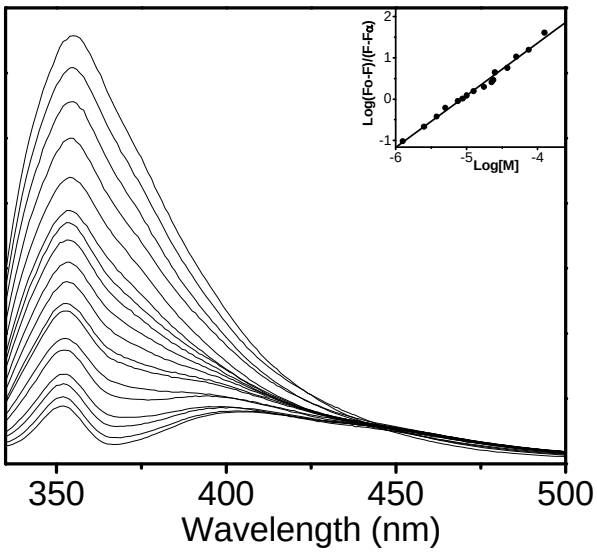

Figure. 5.16. Emission spectral changes for **2** (5 x 10^{-6} M) upon addition of increasing concentration of $Pb(ClO_4)_2$. Excitation wavelength: 318 nm. Inset: linear regression fit (double-logarithmic plot) of the titration data as a function of concentration of metal.

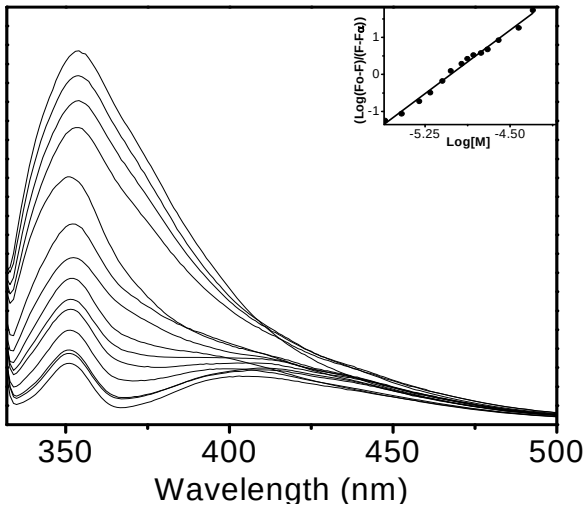

Figure. 5.17. Emission spectral changes for **2** (5 x 10^{-6} M) upon addition of increasing concentration of $Cu(ClO_4)_2$. Excitation wavelength: 318 nm. Inset: linear regression fit (double-logarithmic plot) of the titration data as a function of concentration of metal.

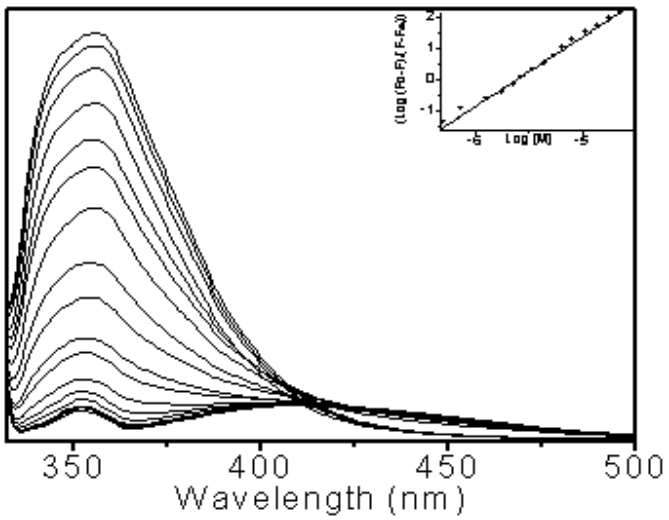

Figure. 5.18. Emission spectral changes for **3** (5 x 10^{-6} M) upon addition of increasing concentration of $Hg(ClO_4)_2$. Excitation wavelength: 321 nm. Inset: linear regression fit (double-logarithmic plot) of the titration data as a function of concentration of metal.

Figure. 5.19. Emission spectral changes for **3** (5 x 10^{-6} M) upon addition of increasing concentration of $Pb(ClO_4)_2$. Excitation wavelength: 321 nm. Inset: linear regression fit (double-logarithmic plot) of the titration data as a function of concentration of metal.

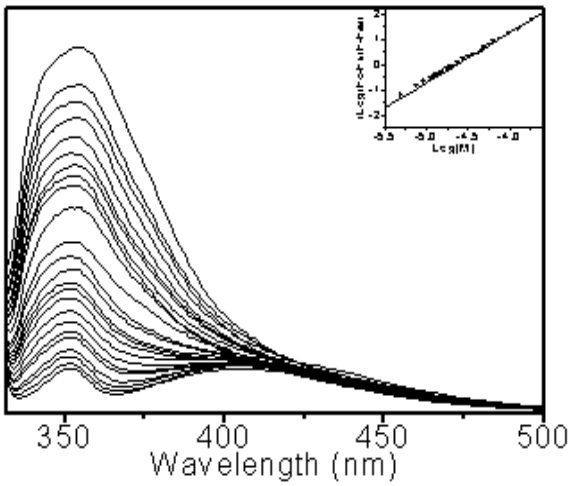

Figure. 5.20. Emission spectral changes for **3** (5 x 10^{-6} M) upon addition of increasing concentration of $Cu(ClO_4)_2$. Excitation wavelength: 321 nm. Inset: linear regression fit (double-logarithmic plot) of the titration data as a function of concentration of metal.

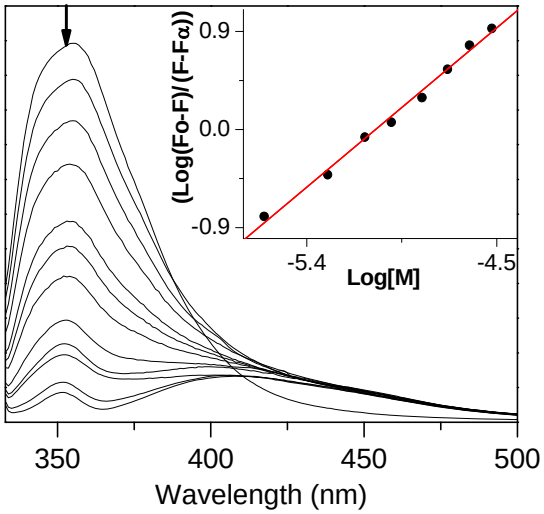

Figure. 5.21. Emission spectral changes for **3** (5 x 10^{-6} M) upon addition of increasing concentration of $Fe(ClO_4)_3$. Excitation wavelength: 321 nm. Inset: linear regression fit (double-logarithmic plot) of the titration data as a function of concentration of metal.

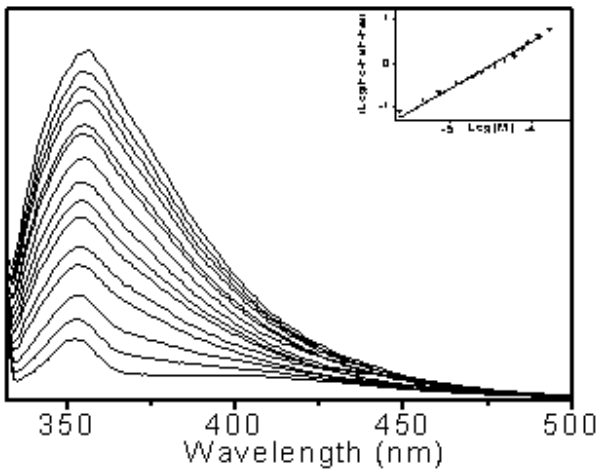

Figure. 5.22. Emission spectral changes for **2** (5 x 10^{-6} M) upon addition of increasing concentration of F^- (TBAF). Excitation wavelength: 318 nm. Inset: linear regression fit (double-logarithmic plot) of the titration data as a function of concentration of metal.

Figure. 5.23. Emission spectral changes for **2** (5 x 10^{-6} M) upon addition of increasing concentration of HSO_4^-. Excitation wavelength: 318 nm. Inset: linear regression fit (double-logarithmic plot) of the titration data as a function of concentration of metal

^{1}H NMR spectra of the compounds **1-3** were recorded upon addition of increasing concentration of F^- and HSO_4^-. The spectral change for the compounds **1** and **2** with the addition of F^- and for **2** and **3** with the addition of HSO_4^- are shown in Figures. 5.24-5.27. It may be noted that the signals for OH and NH protons at δ 10.47 and 8.86 for **1** and δ 10.25 and 8.78 for **2,** respectively are remarkably shifted to the higher field, 1.38 ppm for OH and 0.66 ppm for NH in compound **1**, and 0.99 ppm for OH and 0.51 ppm for NH in compound **2** (Figures 5.24 and 5.25). However for HSO_4^-, the shift of the OH proton is in the opposite direction and no significant change in the chemical shift for NH proton is noted. In this case the OH proton for **2** is shifted downfield by 0.49 ppm (Figure. 5.26). The observation suggests that for F^-, both OH and NH protons are involved in making interaction with the anion. Single crystal X-ray analysis has shown that both OH and NH protons are involved in intramolecular H-bonding; it is expected in solution also as evident from the appearance of these protons at significantly low field. Due to interaction with F^-, the intramolecular H-bonding interaction of these protons has lost, which resulted in upfield shift of these protons. The O/N-H….F^- interaction has also changed the chemical environment of these protons, which in turn has also contributed in changing the chemical shifts. It is difficult to assess how much contribution from each of these effects has come to make the final shift observed. But the substantial changes in chemical shifts of these protons confirmed their involvement in making interaction with the F^-. On the basis of this information the proposed structure of the F^- complex is shown in Figure. 28. It may be noted that considerable changes in chemical shifts of the other aromatic protons have also occurred, which may be due to conformational change of the whole molecule because of complex formation with anion. For compound **3**, due to 1,3-alternate conformation of the calix moiety, the OH protons are not available to make interaction with F^-, obviously no interaction is observed. In the case of HSO_4^-, change in chemical shift of the OH protons is observed (Figure.5.26), indicating their interactions with the anion. ^{1}H NMR spectral change for **3** upon addition of the increasing concentration of HSO_4^- is also shown for comparison (Figure. 5.27). It is clearly seen that there is absolutely no change in chemical shift upon addition of HSO_4^- suggesting that no complex formation took place in this case. Probably the oxygen atoms of the HSO_4^- anion interact with the hydrogen atoms of the OH groups for complex formation.

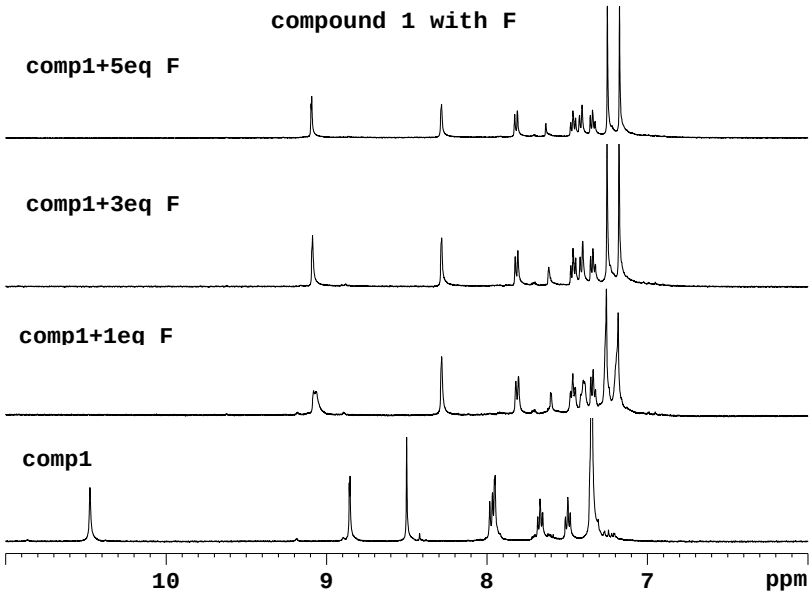

Figure. 5.24. Selected portion of the ^{1}H NMR spectral change for **1** upon addition of the increasing concentration of F^-

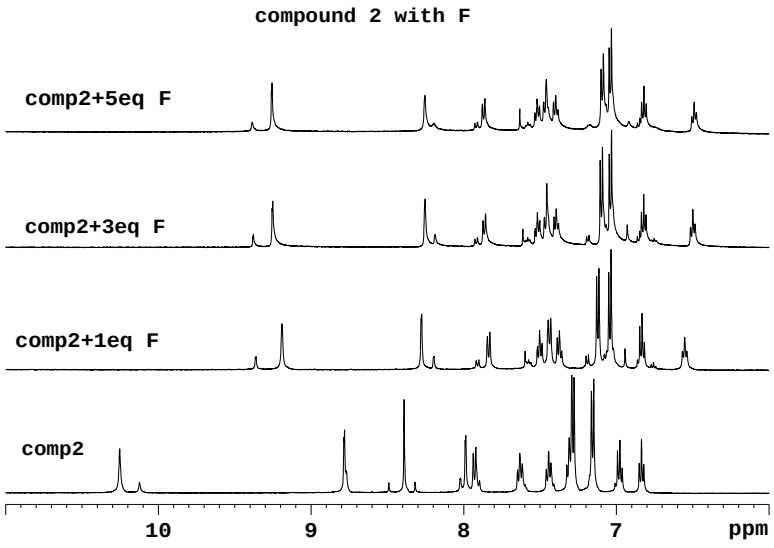

Figure. 5.25. Selected portion of the ^{1}H NMR spectral change for **2** upon addition of the increasing concentration of F^-

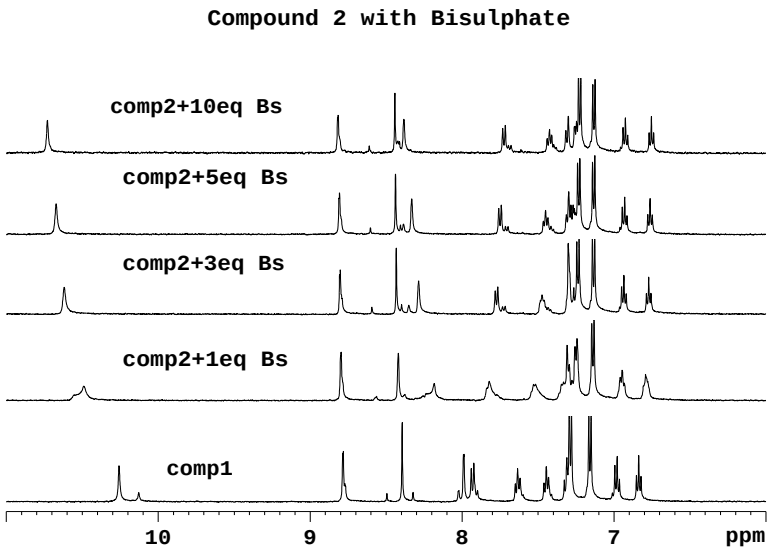

Figure. 5.26. Selected portion of the ^{1}H NMR spectral change for **2** upon addition of the increasing concentration of HSO_4^-.

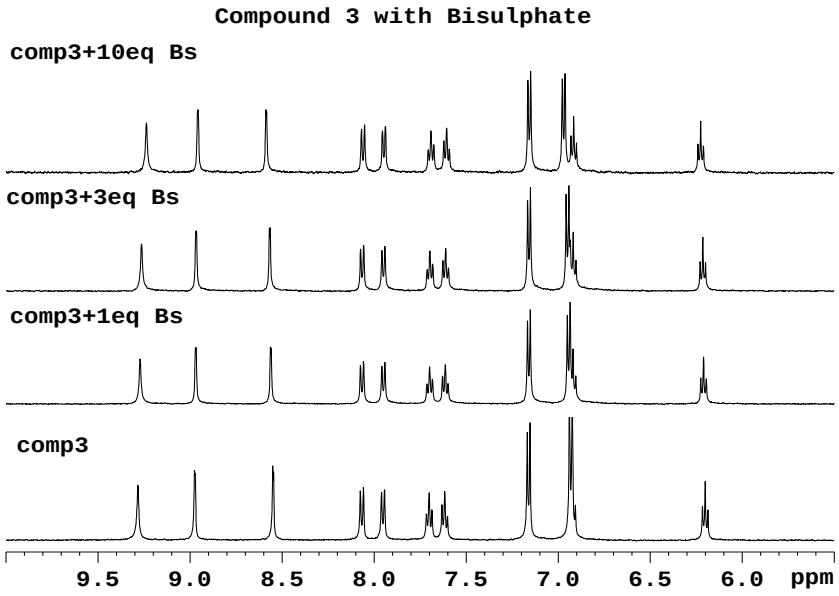

Figure. 5.27. Selected portion of the ^{1}H NMR spectral change for **3** upon addition of the increasing concentration of HSO_4^-.

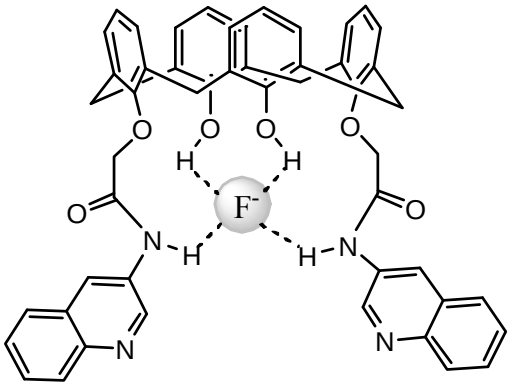

Figure. 5.28. Structural drawing of the F^- complex of compound **2.**

5.4. Conclusions

Three calix[4]arene based fluoroionophores containing quinoline as fluorophore and amide moiety as coordinating unit have been synthesized and characterized crystallographically. The calix moiety in these compounds exists in cone and also 1,3-alternate conformations. The ion-selectivity property of these compounds has been investigate with a large number of cations and anions, the ion recognition event is monitored by fluorescence and NMR (for anion) spectroscopy. They exhibit strong interactions with Hg^{2+}, Pb^{2+}, Fe^{3+} and Cu^{2+}, two of the compounds exhibit strong interaction with F^- and one compound shows interaction with HSO_4^-. Binding constants with strongly interacting ions were determined by fluorescence titration and possible molecular structure of the F^- complex is proposed on the basis of NMR data. The 1,3-alternate conformation of **3** apparently has no significant effect on complexation with metal ions but anions do not form complex with it because of non-availability of the OH protons in the cavity at the lower rim.

5.5. References

1. Ghosh, K.; Adhikari, S.; Chattopadhyay, A. P.; Chowdhury, P. R. *Beilstein Journal of Organic Chemistry* **2008**, *4*, No. 52. doi:10.3762/bjoc.4.52.
2. Ghosh, K.; Adhikari, S. *Tetrahedron Lett.* **2006,** *47*, 3577.
3. Kim, S. K.; Lee, S. H.; Lee, J. Y.; Lee, J. Y.; Bartsch, R. A.; Kim, J. S. *J. Am. Chem. Soc.* **2004,** *126*, 16499.
4. Kim, S. K.; Bok, J. N.; Bartsch, R. A.; Lee, J. Y.; Kim, J. S. *Org. Lett.* **2005**, *7*, 4839.
5. Kim, J. S.; Quang, D. T. *Chem. Rev*. **2007**, *107,* 3780.
6. Lee, S. H.; Kim, S. H.; Kim, S. K.; Jung, J. H.; Kim, J. S. *J. Org. Chem.* **2005,** *70,* 9288.
7. Kim, S. K.; Kim, S. H.; Kim, H. J.; Lee, S. H.; Lee, S. W.; Ko, J.; Bartsch, R. A.; Kim, J. S. *Inorg. Chem*. **2005**, *44*, 7866.
8. Gutsche, C. D.; Iqbal, M. *Organic Syntheses*. **1990**, *68*, 234.
9. Gutsche, C. D.; Levine, J. A.; Sujeeth, P. K. *J. Org. Chem*. **1985,** *50*, 5802.
10. Casnati, A.; Pochini, A.; Ungaro, R.; Ugozzoli, F.; Arnaud, F.; Fanni, S.; Schwing, R. M.-J.; Egberink, J. M.; de Jong, F.; Reinhoudt, D. N. *J. Am. Chem. Soc.* **1995,** *117*, 2767.
11. Unob, F.; Asfari, Z.; Vicens, J. *Tetrahedron Lett.* **1998,** *39*, 2951.
12. Kim, S. K.; Lee, S. H.; Lee, J. Y.; Lee, J. Y.; Bartsch, R. A.; Kim, J. S. *J. Am. Chem. Soc.* **2004,** *126*, 16499.
13. Sheldrick, G.M. SAINT 5.1 ed.; Siemens Industrial Automation Inc.: Madison, WI, (1995).

14. SADABS, Empirical Absorption Correction Program; University of Göttingen: Göttingen, Germany (1997).

15. Sheldrick, G.M. SHELXTL Reference Manual: Version 5.1; Bruker AXS: Madison, WI (1997).

16. Sheldrick, G.M. SHELXL-97: Program for Crystal Structure Refinement; University of Göttingen: Göttingen, Germany (1997).

17. Spek, A. L. PLATON-97, University of Utrecht: Utrecht, The Netherlands, (1997).

18. Mercury 1.3, Supplied with Cambridge Structural Database; CCDC: Cambridge, U.K., (2003).

19. E. Ghidini, F. Ugozzoli, R. Ungaro, S. Harkema, A. A. El-Fadl, D. N. Reinhoudt, *J. Am. Chem. Soc.* **1990**, *112,* 6979.

20. Agnihotri, P.; Suresh, E.; Paul, P.; Ghosh, P. K. *Eur. J. Inorg. Chem*. **2006,** 3369.

21. Zhou, H.; Surowiec, K.; Purkiss, D. W.; Bartsch, R. A. *Org. Biomol. Chem.* **2005,** *3,* 1676.

22. Jaiyu, A.; Rojanathanes, R.; Sukwattanasinitt, M. *Tetrahedron. Lett.* **2007,** *48,* 1817.

23. Farruggia, G.; Iotti, S.; Prodi, L.; Montalti, M.; Zaccheroni, N.; Savage, P. B.; Trapani, V.; Sale, P.; Wolf, F. J. Am. Chem. Soc. 2006, 128, 344.

24. Ghosh, K.; Sen, T.; Frohlich, R. *Tetrahedron. Lett.* **2007,** *48*, 2935.

25. Patra, S.; Paul, P. *Polyhedron.* **2007,** *26,* 4971.

26. Lee, M. N.; Quang, D. T.; Jung, H. S.; Yoon, J.; Lee, C. H.; Kim, J. S. *J. Org. Chem*. **1985,** *50*, 5802.

27. Tedesco, A. C. Oliveria, D. M.; Lacava, Z. J. M.; Azevedo, R. B.; Lima, E. C. D.; Morais, P. C. *J. Magn. Mater.* **2004,** *272-276*, 2404.

28. Boricha, V. P.; Patra, S.; Chouhan, Y. S.; Sanavada, P.; suresh, E.; Paul, P. *Eur. J. Inorg. Chem*. **2009,** 1256.

29. Patra, S.; Paul, P. *Dalton Trans.* **2009,** 8683.

Chapter-VI

Effect of steric crowding on ion selectivity for calix-crown hybrid ionophores: Experimental, molecular modeling and crystallographic studies

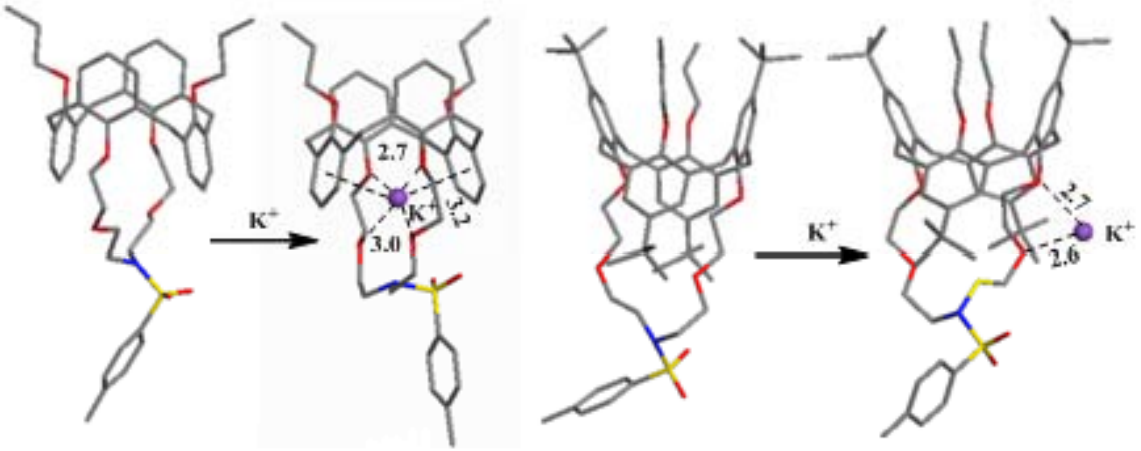

6.1. Introduction

In the calixarene family, calix[4]arenes are most popular because of their rigid structures, which make them ideal candidates for the complexation with various ions.[1-4] The modified calixarenes provide a highly preorganized architecture for the assembling of converging binding sites.[5-9] Among calixarene derivatives, calix[4]arene-crown hybrid molecules have attracted intense interest because of their remarkable selectivity towards alkali and alkaline earth metal ions.[10-17] The ion selectivity of this class of compounds is controlled mainly by the conformation of the calixarene platform, the size of the crown ring and the substituents at the upper and lower rims of the calixarene unit. Incorporation of the substituents at the OH groups of the lower rim suppresses hydrogen-bonding and increases steric hindrance, which results in the formation of conformational isomers such as cone, partial-cone, 1,3-alternate and 1,2-alternate.[10,18-20] In the cone conformation, the appended functional groups at the two sides of the crown ring and in the 1,3-alternate conformation the substituents attached to the crown moiety play important role to determine selectivity.[3,11,14,16,17] Among various size of crown rings, crown-5 and crown-6 containing calixarene derivatives are found more suitable for complexation with alkali-metal ions.[10,13,16,17]

Another class of calix-crown based receptors, in which nitrogen atom is incorporated in the crown ring (azacrown), has been developed. The advantage of it is that any desire substitutent can be attached with the nitrogen atom for specific study, the inclusion of photoactive substituents thus produce a new class of luminescent molecular sensor and it has been widely used to monitor ion recognition event.[11,17,21-23] Apart from luminescence output, the substituents also play important role in the determination of selectivity because of steric effect, which has not been studied much. Attachment of non-photoactive substituents is probably the best way to study the effect of steric crowding on the selectivity of the calix-crown hybrid ionophore.

With the aim to study the effect of bulky substituents on selectivity of the ionophore, four calix[4]arene-azacrown compounds have been synthesized with different substituents at the upper and lower rims and also with variation in ring size of the crown moiety. The substituent, *p*-toluene sulfonamide is attached with the nitrogen atom(s) of

the crown moiety and *tert*-butyl/hydrogen is incorporated in the upper rim. All of these compounds have been characterized on the basis of analytical and spectroscopic methods and molecular structures have been established by single crystal X-ray study. Molecular modeling study has been carried out to examine the ion selectivity of these ionophores. The experimental ion selectivity and binding constants with strongly interacting cations have been determined by ^{1}H NMR study. In this chapter, synthesis, characterization, structural features, molecular modeling and experimental study on ion-selectivity of the ionophores with a large number of cations have been reported. These studies have enabled to unravel the influence of bulky substituents on ion-binding property of these ionophores.

6.2. Experimental section

6.2.1. Materials

All the starting materials were purchased either from Sigma Aldrich Company or from S.D. Fine Chemicals. All the perchlorate salts of the cations were purchased from Alfa Aesar (Johnson Matthey Company). Analytical thin-layer chromatography was carried out on silica gel plates (SiO_2, Merck 60 F_{254}) obtained from E. Mark Chemical Co. All organic solvents were analytical grade and used as received for synthesis work; and purified by standard procedures for spectroscopic study.[24] The reagents 2-(2-chloroethoxy)-ethanol-*p*-toluenesulfonate,[25] 2-(2-(2-chloriethoxy) ethoxy)-ethanol *p*-toluenesulfonate,[26] N, N', N'-tritosyldiethylenetriamine,[27] ethanediol ditosyl,[27,28] and the starting compound dipropyloxydihydroxycalix[4]arene (**A** and **B**)[27,28] were prepared following the literature procedures.

6.2.2. Physical measurement

All measurements have done using the same instruments as described in *Chapter – II*.

Safety Note. ***Caution!*** Metal perchlorate salts are potentially explosive. So they should be handled with proper care.

6.2.3. Synthesis of the compounds C-F and 1-4

Synthesis of the intermediate compounds C and D

The compounds **C** and **D** were prepared following the modified literature procedures[11,17] and the characterization data (NMR and ES-MS) are similar to that reported earlier by us (*Chapter – II*).[17]

Synthesis of the intermediate compound E

To a solution of dipropoxydihydroxy-*p*-tert-butylcalix[4]arene **B** (1.47 g, 2 mmol), 2-(2-chloroethoxy)-ethanol-*p*-toluenesulfonate (1.11 g, 4 mmol) and Cs_2CO_3 (2.61 g, 8 mmol) in 80 mL of freshly distilled acetonitrile was heated at reflux for 40 h under nitrogen. The reaction mixture was allowed to cool to room temperature and evaporated to dryness by rotary evaporation. To this residue HCl (10%, 100 mL) and CH_2Cl_2 (100 mL) were added and the organic phase was separated and washed twice with water (100 mL each). The organic layer was dried over anhydrous sodium sulfate and evaporated to afford brownish oil. Column chromatography on silica gel (200-400 mess) with 98:2 (v/v) ethyl hexane/ethyl acetate as an eluent provided **E** as white solid. Yield: 1.30 g, (69 %). ^{1}H NMR (500 MHz, CDCl3): δ 7.02 (4H, s, calix-Ar-H), 6.96 (4H, s, calix-Ar-H), 3.83-3.75 (8H, m, Ar*CH*$_2$Ar), 3.58-3.55 (8H, m, -O*CH*$_2$*CH*$_2$O-), 3.50 (4H, t, *J*=6.75 Hz, -O*CH*$_2$CH$_2$Cl), 3.34 (4H, t, *J*=7.75 Hz, -O*CH*$_2$CH$_2$CH$_3$), 3.09 (4H, t, *J*=6.75 Hz, -OCH$_2$*CH*$_2$Cl), 1.30 (18H, s, -C(*CH*$_3$)$_3$), 1.26 (18H, s, -C(*CH*$_3$)$_3$), 1.12-1.08 (4H, m, -OCH$_2$*CH*$_2$CH$_3$), 0.67 (6H, t, *J*=7.75 Hz, -OCH$_2$CH$_2$*CH*$_3$). MS, *m/z*: found 968.54 (100%), Calcd for [**E** + Na^+] 968.50; found 984.53 (40%), Calcd for [**E** + K^+] 984.48. Anal. Calcd for $C_{58}H_{82}Cl_2O_6$: C, 73.61; H, 8.74. Found: C, 73.38; H, 8.52.

Synthesis of the intermediate compound F

This compound was prepared following the literature procedure[11] except purification. The compound was purified by column chromatography using silica gel (100-200 mesh) as column material and ethyl acetate/hexane (1:3) as eluent. The solvent of the desired fraction was evaporated and the mass was dissolved in chloroform (5 mL) and was added to *n*-hexane (40 mL) with stirring. The solid compound thus separated was isolated by

filtration and dried in vacuum. Yield: (35%). ^{1}H NMR (500 MHz, CDCl3): δ 7.83 (4H, d, *J*=8.0 Hz, Ar-H of Ts), 7.40 (4H, d, *J*=7.5 Hz, Ar-H of Ts), 6.98 (4H, d, *J*=7.0 Hz calix-Ar-H), 6.90 (4H, d, *J*=7.0 Hz, calix-Ar-H), 6.75 (2H, t, *J*=7.25 Hz calix-Ar-H), 6.54 (2H, t, *J*=7.0 Hz, calix-Ar-H), 3.81-3.42 (16H, m, 8H for Ar*CH*$_2$Ar, 8H for –O*CH*$_2$*CH*$_2$O-), 3.43 (4H *J*=7.0 Hz, -O*CH*$_2$CH$_2$CH$_3$), 2.48 (6H, s, -*CH*$_3$ of Ts), 1.41-1.37 (4H, m, -OCH$_2$*CH*$_2$CH$_3$), 0.75 (6H, t, *J*=6.75 Hz, -OCH$_2$CH$_2$*CH*$_3$); MS, *m/z*: found 927.61 (100%), Calcd for [**F** + Na$^+$] 927.20; found 943.50 (20%), Calcd for [**F** + K$^+$] 943.20. $C_{52}H_{56}O_{10}S_2$: C, 69.02, H, 6.19; found C, 68.97, H, 6.31.

Synthesis of the compounds 1 and 2

These two compounds were prepared following the modified literature procedures[11,17] and the ^{1}H NMR data with assignment of signals (which was not reported earlier) is given here. ^{1}H NMR (500 MHz, $CDCl_3$): for **1;** δ 7.73 (2H, d, *J*=8.0 Hz, Ar-H of Ts), 7.40 (2H, d, *J*=8.0 Hz, Ar-H of Ts), 7.04 (4H, d, *J*=7.5 Hz, calix-Ar-H), 7.02 (4H, d, *J*=7.5 Hz, calix-Ar-H), 6.78-6.72 (4H, m, calix-Ar-H), 3.80-3.72 (8H, m, Ar*CH*$_2$Ar), 3.48 (4H, t, *J*=4.75 Hz, -O*CH*$_2$CH$_2$O-), 3.41(4H, t, *J*=7.75 Hz, -O*CH*$_2$CH$_2$CH$_3$), 3.31-3.24 (12H, m, -O*CH*$_2$*CH*$_2$N(Ts) and -OCH$_2$*CH*$_2$O-), 2.45 (3H, s, -*CH*$_3$), 1.33-1.29 (4H, m, -OCH$_2$*CH*$_2$CH$_3$), 0.73 (6H, t, *J*=7.5 Hz, -OCH$_2$CH$_2$*CH3*). For **2**; δ 7.73 (2H, d, *J*=8.0 Hz, Ar-H of Ts), 7.38 (2H, d, *J*=8.0 Hz, Ar-H of Ts), 7.10 (4H, d, *J*=7.5 Hz, calix-Ar-H), 7.02 (4H, d, *J*=7.5 Hz, calix-Ar-H), 6.76-6.72 (4H, m, calix-Ar-H), 3.71 (8H, m, Ar*CH*$_2$Ar), 3.64 (4H, t, *J*=6.0 Hz, -O*CH*$_2$CH$_2$O-), 3.60 (4H, t, *J*=5.25 Hz, -OCH$_2$*CH*$_2$O-), 3.57-3.55 (4H, overlapped triplet, -O*CH*$_2$CH$_2$O-), 3.53-3.51(4H, overlapped triplet, -OCH$_2$*CH*$_2$O-), 3.47 (4H, t, *J*=7.75 Hz, -O*CH*$_2$CH$_2$CH$_3$), 3.42 (4H, t, *J*=6.0 Hz, -O*CH*$_2$CH$_2$N(Ts)), 3.38 (4H, t, *J*=5.25 Hz, OCH$_2$*CH*$_2$N(Ts)), 2.45 (3H, s, -*CH*$_3$), 1.5-1.46 (4H, m, -OCH$_2$*CH*$_2$CH$_3$), 0.81 (6H, t, *J*=7.5 Hz, -OCH$_2$CH$_2$*CH*$_3$).

Synthesis of the compound 3

A solution of **E** (1.89 g, 2 mmol), K_2CO_3 (1.38 g, 10 mmol) and *p*-toluene sulfonamide (0.38 g, 2.2 mmol) in 50 mL of freshly distilled DMF was heated at reflux for 30 h under nitrogen atmosphere. The reaction mixture was allowed to cool to room temperature and DMF was completely removed by rotary evaporation. To this residue 100 mL of 10%

aqueous $NaHCO_3$ solution and 150 mL of $CHCl_3$ were added and the organic phase was separated and washed with distilled water 3 times (100 mL each). Finally the organic layer was separated and dried over anhydrous sodium sulphate and evaporated to afford brownish oil. Column chromatography on silica gel (100-200 mess) with 9:1 (v/v) hexane/ethyl acetate as an eluent provided **3** as white solid, which on recrystallization from acetonitrile gave white crystalline compound **3.** Yield: 1.5 g, (72%). IR (KBr, cm^{-1}) *v* 1335 (SO_2), 1120 (SO_2). ^1H NMR (500 MHz, $CDCl_3$): δ 7.63 (2H, d, *J*=8.0 Hz, Ar-H), 7.30 (2H, d, *J*=8.0 Hz, Ar-H), 6.98 (4H, s, calix-Ar-H), 6.96 (4H, s, calix-Ar-H), 3.90-3.82 (8H, m, Ar*CH*$_2$Ar), 3.40 (4H, t, *J*=5.5 Hz, -O*CH*$_2$$CH_2CH_3$), 3.19-3.16 (8H, m, -$CH_2OCH_2$-), 3.14 (4H, t, *J*=6.5 Hz, -O*CH*$_2$$CH_2$N(Ts)), 2.92 (4H, t, *J*=6.5 Hz, -*CH*$_2$N(Ts)*CH*$_2$-), 2.45 (3H, s, -*CH*$_3$), 1.25 (18H, s, -C*(CH*$_3$*)*$_3$), 1.23 (18H, s, -C*(CH*$_3$*)*$_3$), 0.76-0.71 (4H, m, -OCH_2*CH*$_2$$CH_3$), 0.58 (6H, t, *J*=7.5 Hz, -OCH_2CH_2*CH*$_3$). MS *m/z*: found 1066.77 (100%), Calcd for [**3** + Na^+] 1066.61. Anal. Calcd for $C_{65}H_{89}NO_8S$: C, 74.74; H, 8.59; N, 1.34; S, 3.06. Found: C, 74.24; H, 8.30; N, 1.32; S, 3.13.

Synthesis of the compound 4

Under nitrogen atmosphere, a solution of **F** (0.45 g, 0.5 mmol), N, N', N''-tritosyldiethylenetriamine (0.40 g, 0.7 mmol) and Cs_2CO_3 (0.82 g, 2.5 mmol) in 80 mL of freshly distilled acetonitrile was heated at reflux for 60 h. The reaction mixture was allowed to cool to room temperature and evaporated to dryness by rotary evaporation. To this residue 100 mL of aqueous saturated $NaHCO_3$ solution and 150 mL of CH_2Cl_2 were added. The organic phase was separated and washed twice with distilled water (100 mL each). Finally the organic layer was dried over anhydrous sodium sulfate and evaporated to afford brownish oil. Column chromatography on silica gel (100-200 mess) with 7:3 (v/v) hexane/ethyl acetate as eluent provided **4** as white solid. Recrystallization of the crude product from 1:1 acetonitrile/chloroform mixture at room temperature gave white crystalline compound **4.** Yield: 0.24 g, (43%). IR (KBr, cm^{-1}) *v* 1348 (SO_2), 1159 (SO_2). ^1H NMR (500 MHz, $CDCl_3$): δ 7.75 (4H, d, *J*=8.0 Hz, Ar-H of Ts), 7.62 (2H, d, *J*=8.0 Hz, Ar-H of Ts), 7.35 (6H, d, *J*=8.0 Hz, Ar-H, of Ts), 7.0 (4H, d, *J*=7.5 Hz calix-Ar-H), 6.93 (4H, d, *J*=7.5 Hz, calix-Ar-H), 6.8-6.77 (4H, m, calix-Ar-H), 3.74-3.60 (12H, m, 8H from Ar*CH*$_2$Ar and 4H from –O*CH*$_2$$CH_2$N-), 3.39 (4H, t, *J*=7.75 Hz, -O*CH*$_2$$CH_2CH_3$),

3.12 (8H, m, -$OCH_2CH_2N(Ts)CH_2CH_2N$-), 2.93 (4H, t, *J*=7.5 Hz, –$NCH_2CH_2N(Ts)CH_2CH_2N$-), 2.49 (3H, s, -CH_3), 2.47 (6H, s, -CH_3), 1.31-1.26 (4H, m, -$OCH_2CH_2CH_3$), 0.74 (6H, t, *J*=7.5 Hz, -$OCH_2CH_2CH_3$). MS *m/z*: found 1148.84 (100%), Calcd for [**4** + Na^+] 1148.41; found 1163.78 (25%), Calcd for [**4** + K^+] 1163.39. Anal. Calcd for $C_{63}H_{71}N_3S_3O_{10}$: C, 67.17; H, 6.35; N, 3.73; S, 8.52. Found: C, 66.83; H, 6.56; N, 3.58; S, 8.35.

6.2.4. NMR study

^{1}H NMR spectra of the complexes were recorded with 2 mg of the sample dissolved in 0.5 mL of CD_3CN-$CDCl_3$ (3:1). Solid perchlorate salt of desired metal ions (20 equiv) was added into this solution and the spectra of the resulting mixture were recorded. The spectra of the cation added solutions were compared to those of the original complexes to ascertain the interaction of the metal ions with the ionophore. On the basis of the observation of this study (details is given in the results and discussion section), the interaction of Na^+ and K^+ for **1**, K^+, Rb^+ and Ba^{2+} for **2** and Na^+ for **3** were chosen to carry out NMR titration.

Stock solutions with desired concentration of metal (Na^+, K^+, Rb^+, and Ba^{2+}) perchlorate salts were prepared in CD_3CN-$CDCl_3$ (3:1) mixture. ^{1}H NMR spectra of the solutions containing 2 mg of the desired complex dissolved in 0.5 mL of the same solvent mixture were recorded. Into these solutions, required amount of stock solutions containing metal ions were added by micro syringe to make the concentrations of the cations 0.3 to 15 equivalent of the concentration of the complex and the spectra of the resulting solutions were recorded. In some cases, upon addition of increasing concentration of metal ion new peaks grew with gradual disappearing of the original signals whereas in other cases, gradual shift of certain signals were noted. In the later cases, binding constants were calculated using the literature procedure.[29] For the systems, where new peaks have grown, the binding constants were determined by direct method using peak intensity ratio as described in the Results and Discussion Section.[29,30]

6.2.5. Mass spectroscopic study

Formation of metal complex was also confirmed by mass spectrometry. The ionophores (1**,** **2** and **3,** 0.5 mmol) were dissolved in CH_3CN-$CHCl_3$ (3:1) mixture (30 mL) and desired solid metal perchlorate salts (2.5 mmol) were added into the solutions. The reaction mixtures were stirred at room temperature for 2 h, the solutions were then filtered off and the filtrates were analyzed by Q-TOF Micro^{TM} LC-MS instrument. The mass data obtained are: MS *m/z*: found 859.01 (100%), Calcd for [**1** + K^+] 859.01; found 843.57 (100%), Calcd for [**1**+ Na^+] 843.03; found 946.43 (100%), Calcd for [**2** + K^+] 946.39; found 992.20 (100%), Calcd for [**2** + Rb^+] 992.80; found 1044.87 (50%), calcd for [**2**+ Ba^{2+}] 1044.46; found 1065.79 (100%), Calcd for [**3** + Na^+] 1065.61.

6.2.6. X-ray experiments, structure determination and refinements

Crystal of suitable size was selected from the mother liquor and immersed in partone oil, then mounted on the tip of a glass fiber and cemented using epoxy resin. Intensity data for all four crystals were collected at 100 K using graphite monochromatised MoK_α (λ = 0.71073Å) radiation on a Bruker SMART APEX diffractometer equipped with CCD area detector. The data integration and reduction were processed with SAINT software.[31] An empirical absorption correction was applied to the collected reflections with SADABS.[32] The structures were solved by direct methods using SHELXTL[33] and were refined on F^2 by the full-matrix least-squares technique using the SHELXL-97[34] program package. Graphics are generated using PLATON[35] and MERCURY 1.3.[36] In all the compounds non-hydrogen atoms were refined anisotropically till convergence is reached and the hydrogen atoms attached to the ligand moieties are sterochemically fixed. Crystallographic data are given in Table 6.1.

Table 6.1. Summary of crystallographic data for compounds **1** to **4.**

Compound	**1**	**2**	**3**	**4**
Emperical formula	$C_{49}H_{57}N_1O_8S_1$	$C_{53}H_{65}N_1O_{10}S_1$	$C_{65}H_{89}N_1O_8S_1$	$C_{63}H_{71}N_3O_{10}S_3$
Formula mass	820.02	908.12	1044.43	1126.41
Crystal Colour	Colourless	Colourless	Yellow	
Crystal Size (mm^3)	0.48 x 0.34 x 0.22	0.56 x 0.38 x 0.25	0.40 x 0.20 x .12	
Temperature (K)	100	100	100	
Crystal System	Monoclinic	Triclinic	Monoclinic	Monoclinic
Space Group	$P2_1$	P-1	$P2_1/n$	$P2_1/c$
a(Å)	16.9671(12)	14.7394(11)	15.3737(15)	17.422(2)
b(Å)	10.0972(7)	17.0425(13)	14.3951(15)	16.931(2)
c(Å)	25.6043(19)	20.6798(16)	27.451(3)	20.781(3)
α(°)	90	74.8730(10)	90	90
β(°)	104.276(2)	82.0290(10)	105.396(2)	110.187(2)
γ (°)	90	75.0190(10)	90	90
Z	4	4	4	4
V($Å^3$)	4251.1(5)	4830.1(6)	5857.1(10)	5753.2(13)
Density (Mg/m^3)	1.281	1.249	1.184	1.300
Abs. Coeff. (mm^{-1})	0.133	0.126	0.110	0.191
F(000)	1752	1944	2264	2392
Reflections Collected	21383	41560	31126	28620
Independent Reflect.	7930	21770	11461	10100
R_{int}	0.0722	0.0232	0.0803	0.0821
Number of Parameters	1066	1171	691	717
S (GOF) on F^2	1.076	1.026	1.168	1.197
Final R1 , wR2 (I>2σ(I)	0.0648/ 0.1264	0.0649 / 0.1756	0.0953/ 0.1721	0.0998/0.1916
Weighted R1, wR2(all data)	0.0914/ 0.1368	0.0813 / 0.1910	0.1425/ 0.1895	0.1328/ 0.2051

6.2.7. Computation methodology

Conformational search was performed using the Monte Carlo algorithm for the random variation of all of the rotatable bonds combined with Merck force field (MMFF94).[37-39] The structural parameters for the receptors, Na^+ and K^+ ions were taken from the inbuilt MMFF94 parameters available in parameters file. For Ba^{2+} and Rb^+ ions, the parameters were taken from published literature reports.[40] For each calculation, 5000 Monte Carlo steps have been carried out. Lowest energy conformers in each case were taken for the energetic comparisons with density functional calculations. DFT calculations were performed with generalized gradient potential GGA/PW91/DNP level of density functional program Dmol3 in Material Studio (version 4.1) of Accelrys Inc.[41-45] The conductor-like screening model (CSOMO) has been employed at GGA/PW91/DNP level for solvent (Acetonitrile, dielectric = 37.5) calculations.[46,47] The binding energies were computed using the equation, $\Delta E = \Delta E_{complex} - (\Delta E_{lig} + \Delta E^{M+/2+})$.

6.3. Results and discussion

6.3.1. Synthesis and characterization of the ionophores 1-4

The method followed for the synthesis of **1-4** is shown in Scheme 6.1 and details of experimental procedures are given in the Experimental Section. Elemental analysis (C, H, N and S), ^{1}H NMR and mass spectrometric data of **1-4** and for some of the intermediates are given in the Experimental Section. The elemental analysis and mass data are in excellent agreement with the calculated values. It may be noted that *e/m* values of all these compounds correspond to the $Na^+/K^+/H^+$ adduct, which is a well known phenomena when LC-MS is used for the measurement of mass.[16,17, 20,48] The ^{1}H NMR spectral data are in consistent with the structures shown in Scheme 6.1. The appearance of ArCH_2Ar methylene protons as multiplet in the region δ 3.60 – 3.90 confirmed the 1,3-alternate conformation of these compounds in solution.[13,49] The methyl group of the tosyl moiety appears as singlet for **1-3** at δ 2.45, however for **4** it appears as two closely spaced singlet

at δ 2.47 (6H) and 2.49 (3H), indicating that two of the three methyl groups are chemically equivalent and the third one is slightly different.

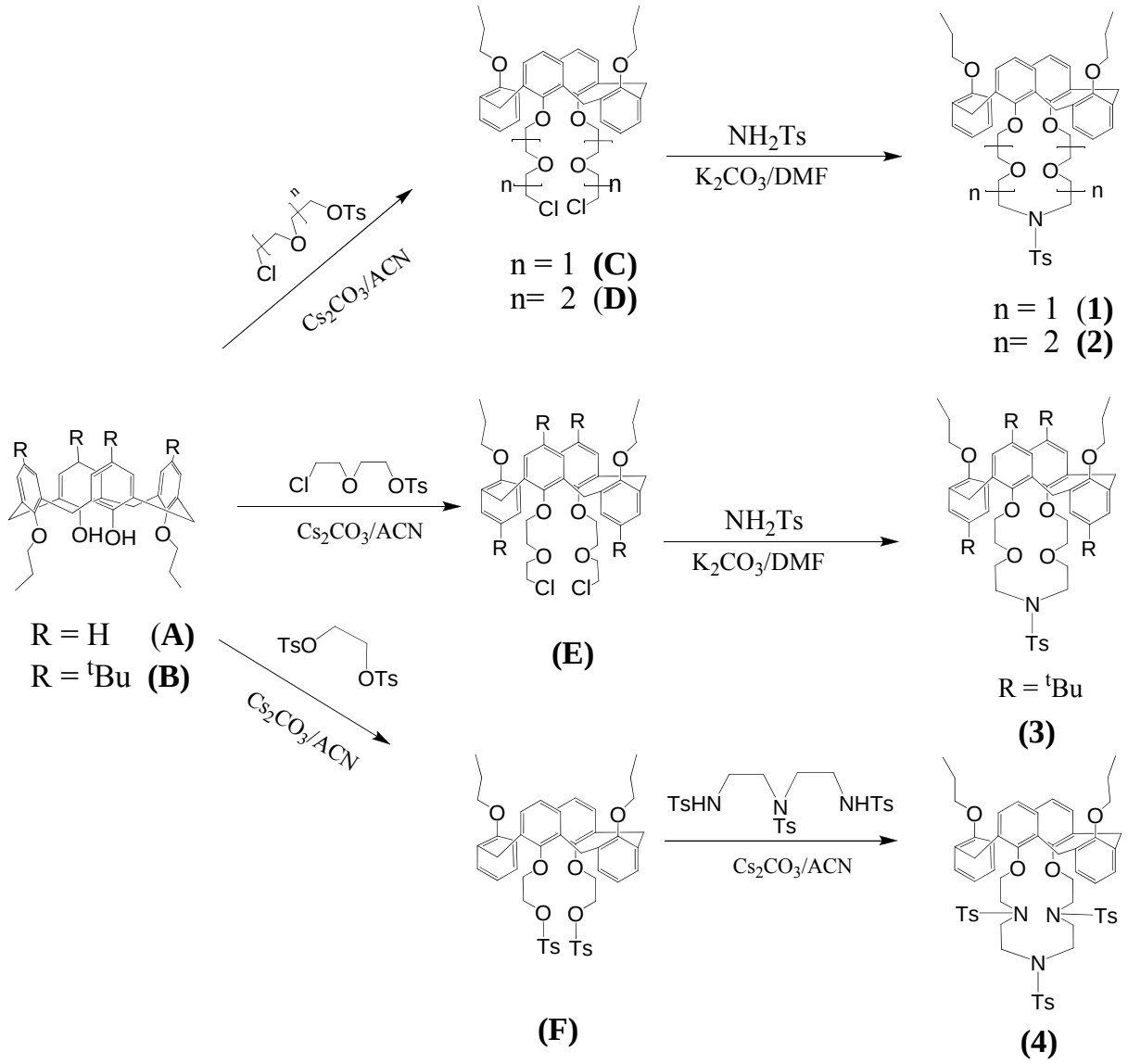

Scheme 6.1. Route followed for the synthesis of compounds **1** – **4**.

6.3.2. Crystal structures of 1-4

The ORTEP diagrams of **1-4** of one of the molecules present in the asymmetric unit with atom numbering scheme are shown in Figures. 6.1-6.4**.** A detail of experimental procedure is described in the Experimental Section and crystallographic data are presented in Table 6.1. For all of the four compounds, bond lengths and bond angles are in the usual ranges,[5,6,10,16,20] and the following discussion refers mainly to the conformation and shape of the calixarene skeleton. Crystal structures clearly show that all of these compounds have adopted 1,3-alternate conformation; however the precise shape of the molecule differs due to variation in substituents. Compounds containing *tert*-butyl

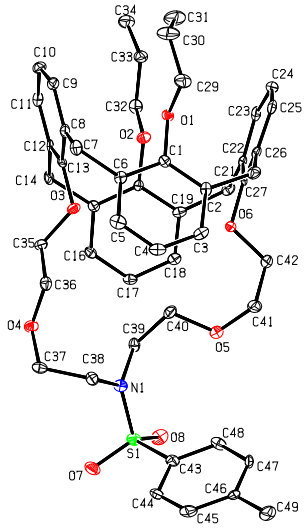

Figure. 6 1. ORTEP view of **1.**

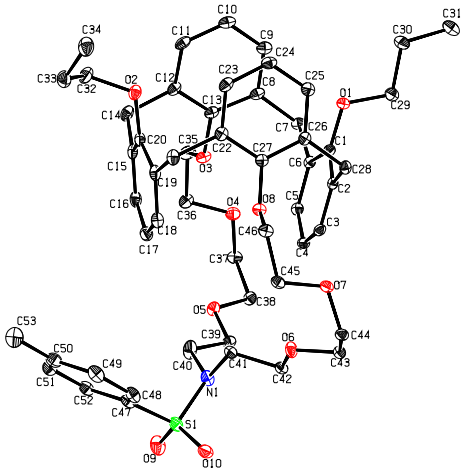

Figure. 6.2. ORTEP view of **2.**

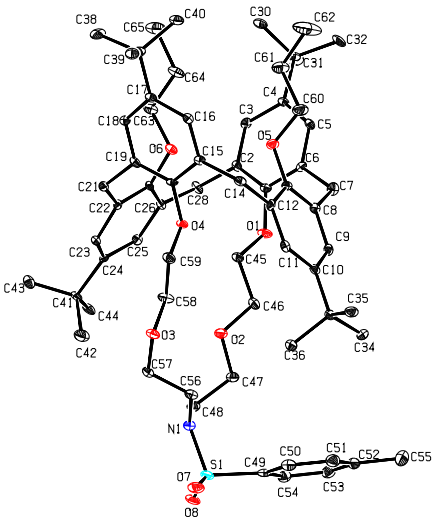

Figure. 6.3. ORTEP view of **3.**

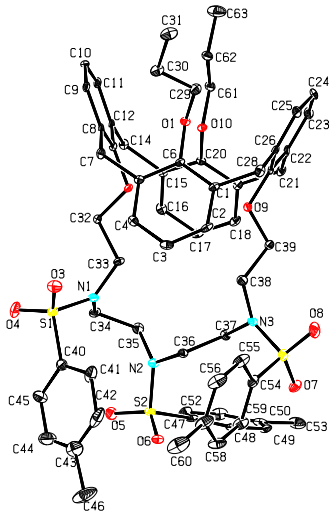

Figure. 6.4. ORTEP view of **4.**

group at the upper rim usually exists in cone conformation because of its difficulty to rotate due to steric hindrance. However, it is interesting to note that compound **3**, which contains bulky *tert*-butyl group at the upper rim, also exists in 1,3-alternate conformation. In 1,3 alternate arrangement, the dihedral angles between the four phenyl rings and the mean plane of the methylene groups varies significantly (51.97° - 81.51°) because of the presence of different substituents at the upper and lower rims.

To understand the arrangement of the molecules in the crystal lattice, the hydrogen bonding interaction and packing pattern have been analyzed in detail. All the four compounds exhibited a number of strong intermolecular H-bonding interactions, however the type of interactions are distinctly different from compound to compound. Brief description of these interactions is given below and the H-bonding parameters are summarized in the Table 6.2.

In compound **1**, the two molecules (molecules 1 and 2) present in the asymmetric unit, are associated themselves via strong C-H···O interactions generating two independent layers of helical hydrogen bonded network via 2_1 screw related adjacent molecules along

bc-plane as depicted in Figure. 6.5. The ether oxygen O4 of molecule **1** is involved in C-H···O interaction with phenyl hydrogen atom H45 of the adjacent molecule1 of the tosyl group; while in the case of molecule **2**, the sulphonate oxygen O16 of the tosyl group makes C-H···O interaction with the phenyl hydrogen H66 of the calix moiety forming a layered helical network. For compound **2**, the two molecules in the asymmetric unit are associated like compound **1** via C-H···O interactions; however the pattern of H-bonding is different. In the molecule 1, the sulphonate oxygen O9 and the phenyl hydrogen H25 of the calix moiety make strong interaction generating hydrogen bonded strand along a-axis. Molecule 2 present in the asymmetric unit is oriented along with the H-bonded strand of molecule1 in such a way that the sulphonate group of molecule 1 (O10) and 2 (O20) are sufficiently close to make effective C-H···O interaction with phenyl hydrogen atoms H101 and H45, respectively generating the hydrogen bonded layers as shown in Figure. 6.6. For **3**, the adjacent calix moieties are oriented in opposite direction as a layer along b-axis involving strong C-H···O interaction between the phenolic oxygen of the calix with the *tert*-butyl hydrogen H43 of the neighbouring molecule. These layers are further cross-linked via C-H···O interaction between the sulphonate oxygen O7 of the tosyl group from either side of the oppositely oriented H-bonded calix layers with phenyl hydrogen H11 and forms two dimensional sheets (Figure. 6.7). For the compound **4**, the adjacent molecules are oriented in opposite direction and associated via strong C-H···O interaction between the sulphonate oxygen O8 and phenyl hydrogen H25 of the calix moiety in dimeric association. These hydrogen bonded dimers are oriented almost diagonal to ac plane (Figure. 6.8). It is also interesting to note that the phenyl hydrogen H18 of the calix moiety is involved in intermolecular C-H···π interaction with the phenyl ring C8-C13 [C(18)-H(18)…. Cg(2): H(18)…Cg(2) = 2.75Å, C18….Cg(2) = 3.672(6)Å, <C(18)-H(18)….Cg(2) = 78°, symmetry code: 1-x,-1/2+y,1/2-z, where Cg(2) is the center of gravity of the phenyl ring (C8-C13)].

Table 6.2. Hydrogen bonding parameters in compounds **1** to **4**

D-H...A	d(H...A) (Å)	d(D...A) (Å)	<DHA (°)
Compound 1			
C(39)-H(39A)...O(4)[1]	2.42	3.119(8)	129
C(40)-H(40A)...O(6)[1]	2.36	2.957(13)	120
C(45)-H(45)....O(4)[2]	2.45	3.349(7)	162
C(66)-H(66)...O(16)[3]	2.60	3.513(9)	169
Symmetry code : [1] x, y, z; [2] 2-x,1/2+y,-z; [3]1-x,1/2+y,2-z.			
Compound 2			
C(45)-H(45B).…O(6) [1]	2.45	3.048(2)	120
C(98)-H(98A)...O(16) [1]	2.50	3.088(2)	119
C(25)-H(25)....O(9)[2]	2.58	3.399(3)	147
C(48)-H(48).. ..O(20)[3]	2.50	3.366(2)	155
C(101)-H(101)...O(10)[4]	2.53	3.393(2)	155
Symmetry code : [1] x, y, z; [2] 1+x,y,z; [3]x,-1+y,z; [4]x,1+y,z; .			
Compound 3			
C(56)-H(56B)...O(2) [1]	2.57	3.211(5)	123
C(58)-H(58A)....O(2) [1]	2.56	3.325(5)	136
C(11)-H(11)....O(7) [2]	2.54	3.433(4)	174
C(43)-H(43C)....O(1)[3]	2.49	3.425(5)	164
Symmetry code : [1] x, y, z; [2] 1+x,y,z; [3]x,-1+y,z; [4]x,1+y,z; .			
Compound 4			
C(25)-H(25)…..O(8)	2.40	3.248(7)	151
Symmetry code : 1.x, y, z;			

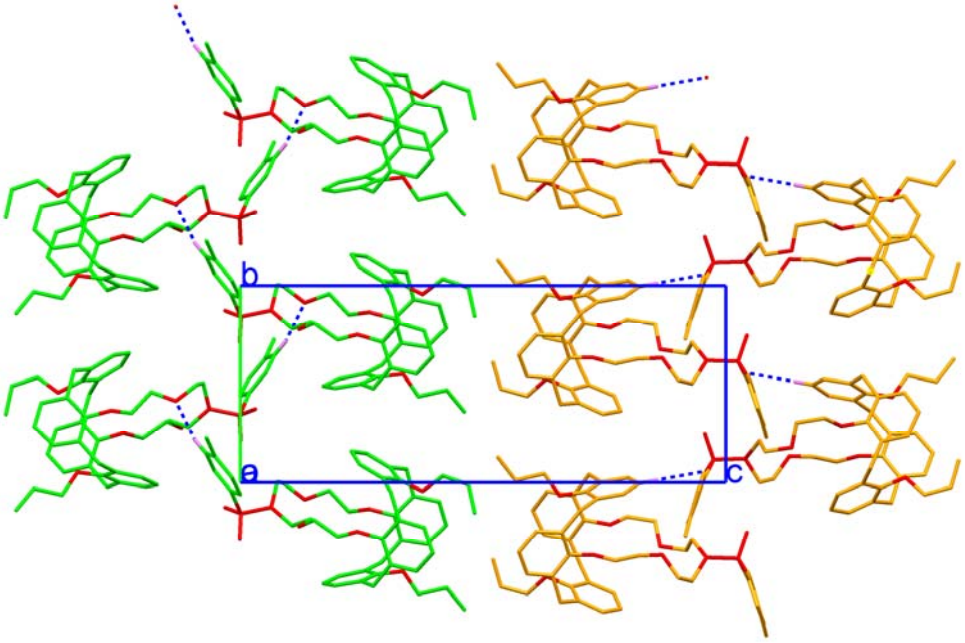

Figure. 6.5. Packing diagram viewed down a-axis showing the hydrogen bonded layered helical network between the screw related molecule **1** (in green colour) and molecule **2** (orange colour) in bc-plane

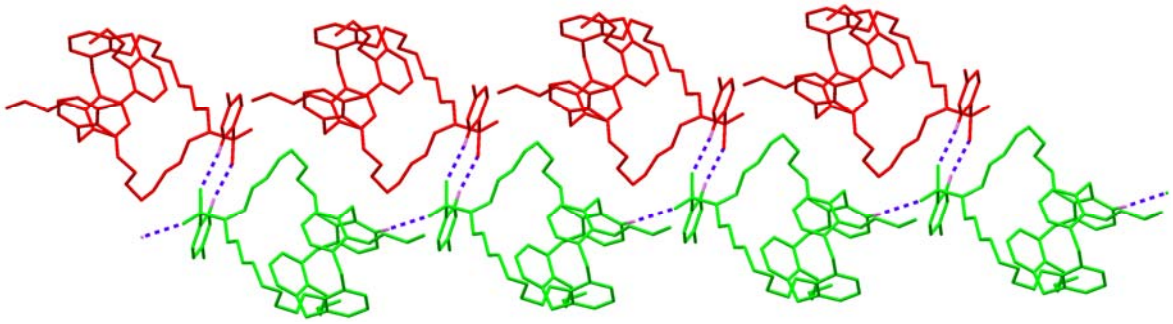

Figure. 6.6. Packing diagram depicting the close-up view of the hydrogen bonding interaction (dotted blue line) between the two molecules of cailx moieties (green and red) present in the asymmetric unit.

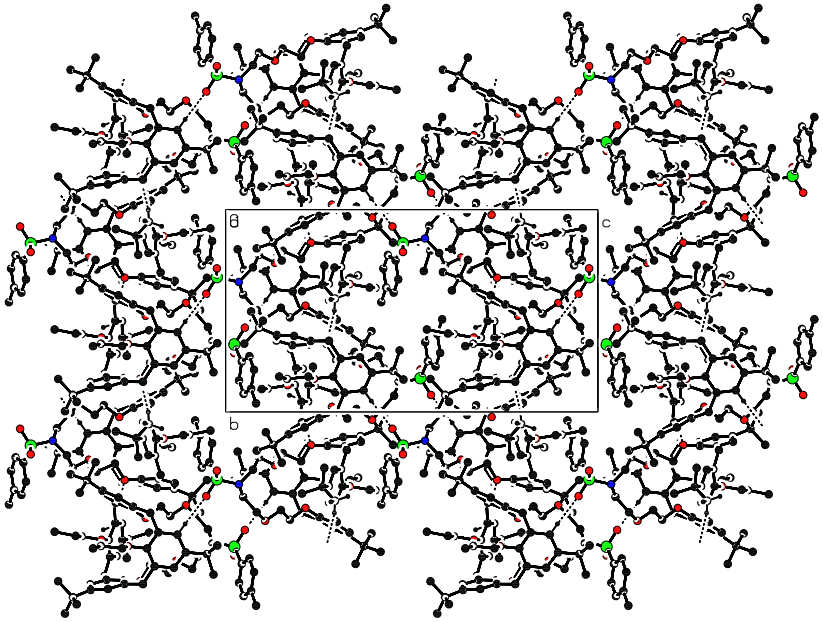

Figure. 6.7. Packing diagram with hydrogen bonding interactions viewed down a-axis showing the two dimensional hydrogen networks in bc-plane for compound **3.**

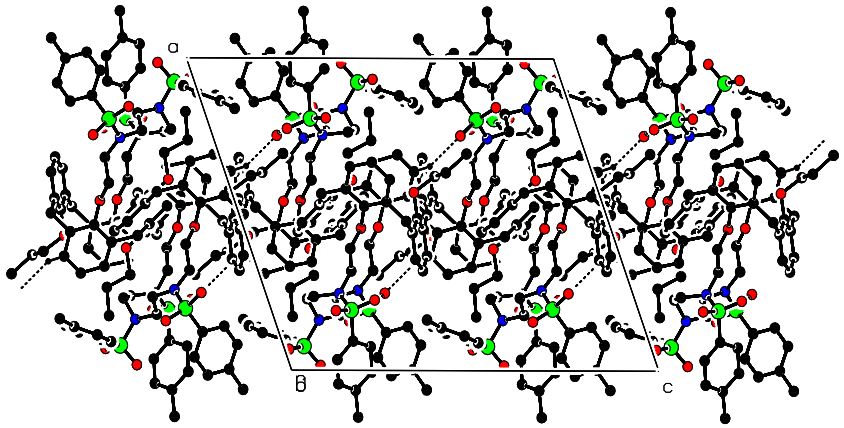

Figure. 6.8. Packing diagram with hydrogen bonding interactions viewed down b-axis showing the orientation of the hydrogen bonded dimmer diagonal to ac-plane in compound **4.**

4.3.3. Ion binding study

Cation-binding ability of the ionophores **1-4** have been studied by ^{1}H NMR using a number of metal ions Li^+**,** Na^+**,** K^+, Rb^+, Cs^+, Mg^{2+}, $Ca^{2+,}$ Sr^{2+}, Ba^{2+}, Zn^{2+}, Cd^{2+}, Hg^{2+} and Pb^{2+}. The ^{1}H NMR spectra of all of the four complexes were recorded in presence of 100 fold excess of the above-mentioned metal ions and these spectra were compared with those recorded in absence of metal ion to ascertain the complexation behaviour of the ionophores. For compounds **1**-**3**, significant changes in ^{1}H NMR spectra were noted in presence of certain metal ions, whereas compound **4** did not show any change with all of these metal ions. The spectral changes observed with Na^+ and K^+ for **1,** with Na^+, K^+, Rb^+ and Ba^{2+} for **2,** and with only Na^+ for **3**, indicating complexation of these metal ions with the respective ionophores.

Complexation with various metal ions was also confirmed by mass spectrometry. The ionophore and the desired metal ion was mixed in appropriate solvent and stirred at room temperature as described in the experimental section and the mass spectrum of the resultant solution was recorded. The mass data, given in the Experimental Section, are in excellent agreement with the 1:1 complex formation.

For the determination of binding constants, NMR titrations were carried out with the above-mentioned metal ions. Interestingly, in the case of K^+ for **1**, and Na^+ for **3,** upon addition of increasing concentration of metal ions new peaks grew with a gradual disappearing of the original signals as shown in Figure. 6.9. In all other cases, gradual shift of certain signals were noted with the addition of metal ions. The changes were observed in aliphatic region for the signals due to crown moiety because of its involvement in coordination with the metal ion. However, changes in chemical shifts of some other signals were also noted due to conformational change induced by metal coordination. Upon addition of metal ion growing of new signals with disappearing of original one indicates formation of stable complex, *i.e.* the rate of decomplexation is too slow in NMR time scale. This is due to the fact that 1,3-alternate calix[4]arenes are conformationally rigid and if the size of the cavity containing π-electron clouds in the distal phenyl units is close to the size of the

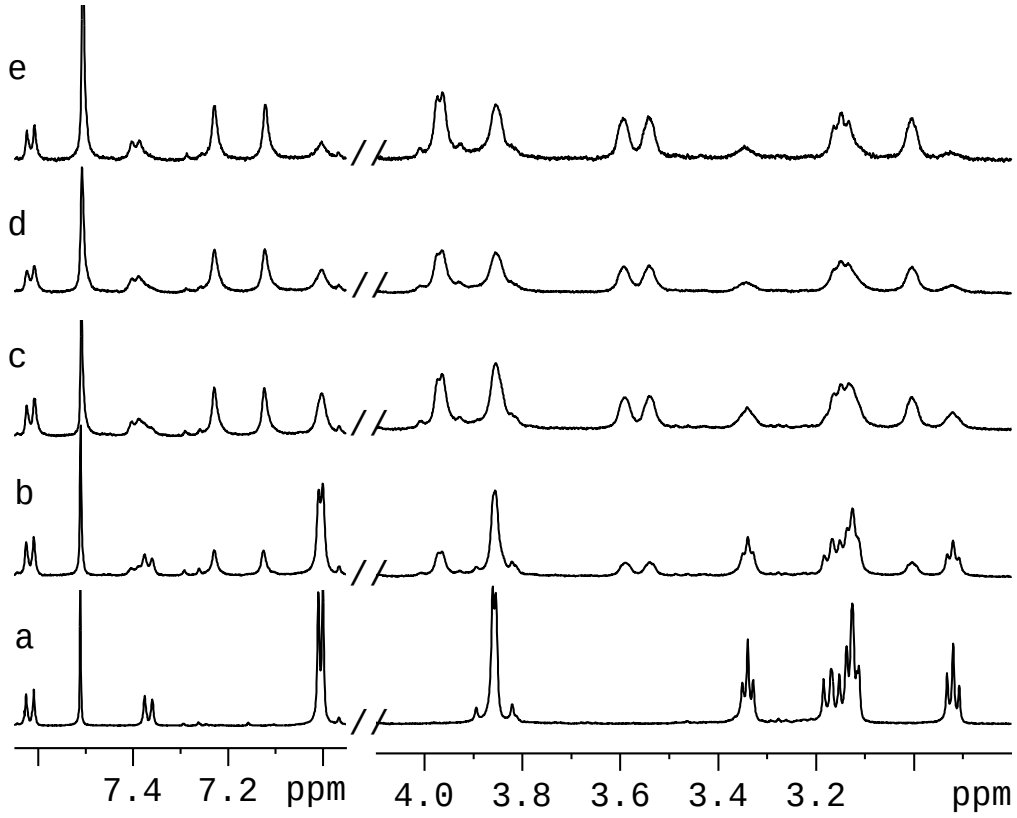

Figure.6.9. Selected portion of the ^{1}H NMR spectral change for **3** upon addition of the increasing concentration of $NaClO_4$, new peaks are growing with disappearance of the peaks of original complex.

ionic diameter then strong binding of metal ion takes place.[50,51] However, if the size of metal ions are not large enough compared to the cavity size to enjoy cation-π interaction with the π-electron clouds, then weak complexation takes place. In this case, the rate of decomplexation is fast enough in NMR time scale for an average of chemical shifts due to complexed and uncomplexed species and a shift in the NMR signal to be observed. In the case of **2,** which has large cavity size, the metal ions (Na^+, K^+, Rb^+ and Ba^{2+}) are not big enough to make conformationally rigid strong complexes using π-electron clouds in the distal phenyl units. The cavity size of the crown moiety of **1** and **3** should be appropriate for K^+, however the latter did not show complexation with K^+. Probably the

steric effect due to bulky *tert*-butyl groups from both sides in 1,3-alternate conformation prevents K^+ to enter in the cavity for complexation. In the case of shifting of the signals, the extent of shift with respect to the limiting value corresponds to the concentration of the complex formed. Figure. 6.10 shows the changes in chemical shifts of certain signals for complex **2** upon addition of Ba^{2+}. The changes observed in the region δ 3.35 – 3.65 is due to the coordination of Ba^{2+} with the crown moiety, whereas the changes in chemical shifts for some other signals of the calix unit is due to the metal induced conformational change of the molecule as a whole.

Binding constants for the systems, where chemical shifts gradually changed upon addition of increasing concentration of metal ion (Na^+ for **1**, and Na^+, K^+, Rb^+ and Ba^{2+} for **2**), were calculated using the program developed by Hirose[29] and the data are given in Table 6.3. The non-linear least square fit for **2** with Ba^{2+} is shown in Figure. 6.11. For the systems, where new peaks have grown, the binding constants were determined by direct method using peak intensity ratio.[17,19,30] Summation of the intensities of both the peaks

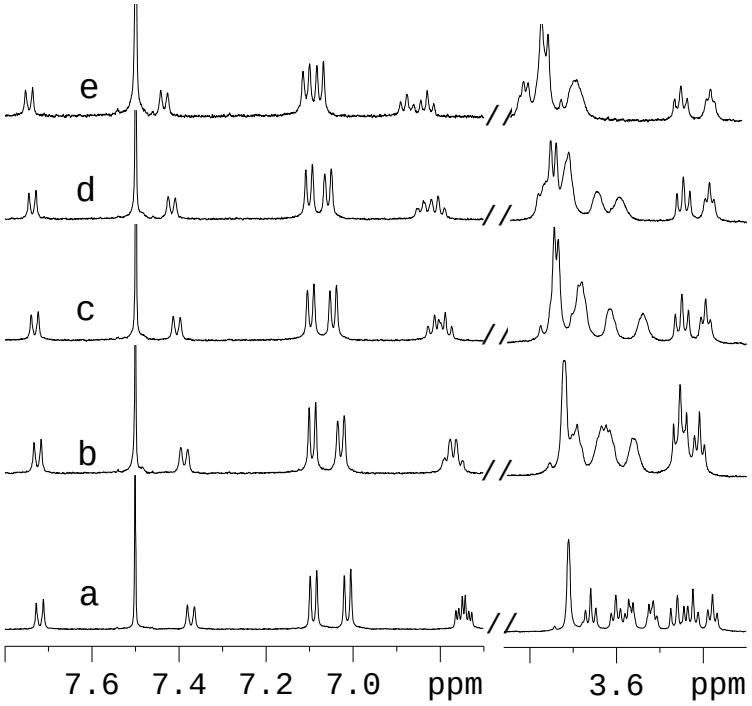

Figure.6.10. Selected portion of the ^1H NMR spectral change for **2** upon addition of the increasing concentration of $Ba(ClO_4)_2$, chemical shifts of certain signals change with increasing concentration of metal ion.

Table 6.3. Binding constants (K_s) for the ionophores **1-3**

Ionophore	Metal ion	Binding constant (K_s/M^{-1})
1	Na^+	3.10×10^3
	K^{+1}	4.17×10^3
2	Na^+	6.00×10
	K^+	4.19×10^3
	Rb^+	4.55×10^4
	Ba^{2+}	3.35×10^2
3	Na^{+1}	2.05×10^3

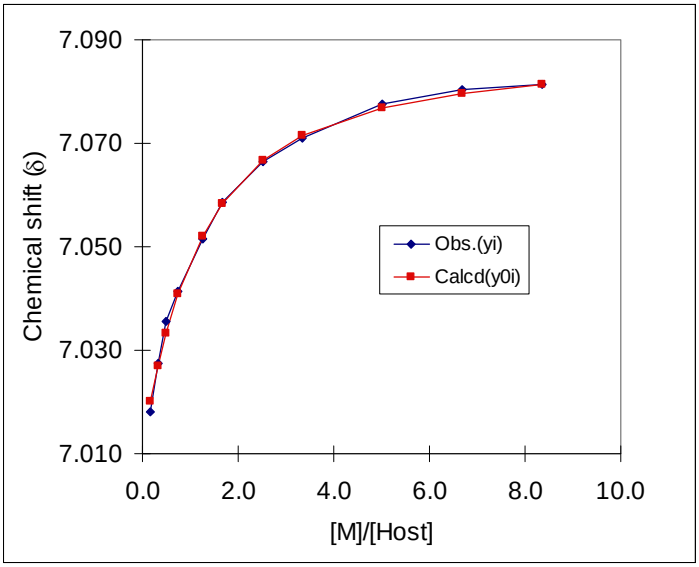

Figure.6.11. The non-linear least square fit from ^{1}H NMR titration data for the binding of **2** with Ba^{2+} in CD_3CN-$CDCl_3$ (3:1).

corresponds to the initial (total) concentration of the complex, the intensity ratio of the growing peak corresponds to the concentration of the cation-bound complex and the intensity ratio of the disappearing peak corresponds to the concentration of the remaining complex (without cation-binding). Binding constant (K_s) was then calculated using the

equation $K_s = [C]/([H_t] - [C])([G_t] - [C])$, where [C] is the concentration of the cation-bound complex, $[H_t]$ is the total concentration of the host (complex) and $[G_t]$ is the total concentration of the guest metal ion.[29] Measurements were carried out with four different concentrations of complex and also K_s values with 20% to 80% complexation ratio were considered to minimize error in measurement.[29] The K_s values from NMR measurement are summarized in Table 6.3 and the data suggest moderate to strong complexation of the ionophores with the metal ions. For compound **2**, the binding constants are in the order $60 < 6.14 \times 10^2 < 4.19 \times 10^3 < 4.54 \times 10^4$ for Na^+, Ba^{2+}, K^+ and Rb^+, respectively, the highest value is for the metal ion (Rb^+) having largest ionic diameter (2.94 Å) among the cations studied (K^+ = 2.66 Å, Ba^{2+} = 2.68 Å). For **1**, binding constant of K^+ is slightly higher than that of Na^+. It may be noted that the size of the ionophores (aza-crown ring) and substituent at the azacrown ring for **1** and **3** are same but they exhibit remarkably different ion selectivity due to steric crowding imposed by the *tert*-butyl group attached with **3**. The ring size of **4** is similar to that of **1,** but the former has three tosyl substituents at the aza-crown ring and did not form complex with any metal ion studied here. The results, therefore, indicates that steric crowding plays an important role in determining ion selectivity in these systems.

6.4. Modeling studies

The remarkable difference in the selectivity of alkali metal ions with the calix receptors **1** and **3** of similar size prompted us to examine the complexing ability of these systems. Molecular modeling studies were performed for **1** and **3** with sodium and potassium ions. The crystal structure analyses showed that the parent receptors **1**-**4** are arranged in 1,3 alternate conformations. Having such information in hands, we have modeled the complexations of receptors **1** and **3** with Na^+ and K^+ ions computationally. Solid state structures have been considered as initial guesses in this study.[52] Molecular mechanics (MMFF94) force field has been employed using Monte Carlo search method to examine the complexations of Na^+ and K^+ ions with **1** and **3** calix receptor molecules. The details of the calculations are mentioned in the computational methodology section. The lowest energy complexed geometries were taken for higher level density functional calculations in the solvent (acetonitrile). The conformational search was performed with the parent

crystal structures placing the metal ions near the nitrogen atom connected to the tosyl group, however, pointing away from the calix-crown rings in each case. In general, the *ab initio* and molecular mechanics calculations have been performed with placing the metal ions in centroid of crowns and calix rings.[53,54] However, we intended to see that during the Monte-Carlo searches using MMFF94 force field, metal ions reaches inside the cavity of receptors or moves away from the confined calix-crown ring. The effect of counter ion is not present in these calculations. Sodium and potassium ions moved inside the cavity of receptor **1**, whereas, only sodium ion complexed inside the cavity of receptor **3** (Figure. 6.12). The *tert*-butyl attached to phenyl rings present in the receptor **3** presumably did not allow the bigger potassium ion to move inside the ring. The binding energies calculated for the complexations of Na^+ and K^+ ions with receptor **1** at (DFT) GGA/PW91/DNP level in acetonitrile suggests that the potassium ion should bind preferentially than that of sodium ion. Experimental complexations were carried out with mixed solvent acetonitrile and chloroform, however, in the computational studies.

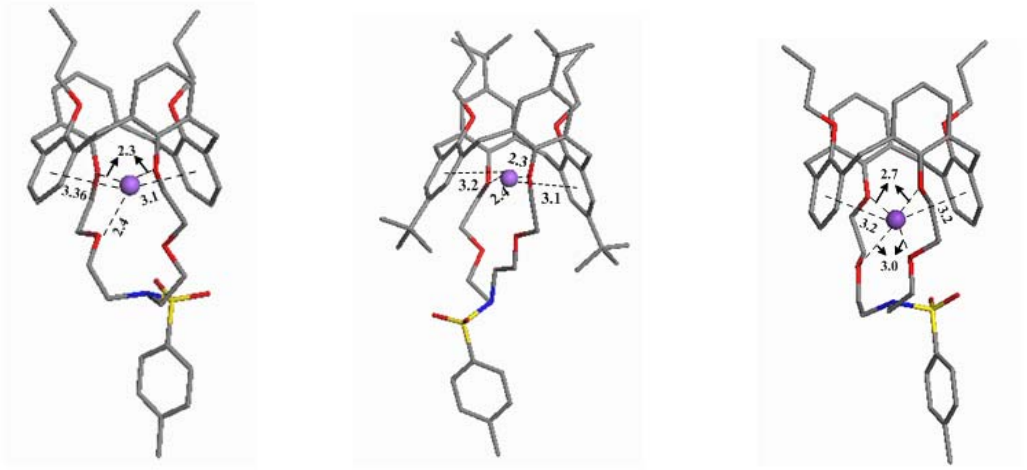

1:Na^+ **1**:K^+ **3**:Na^+

ΔE (-36.0) (-44.4) ΔE (-30.5)

Figure. 6.12. Lowest energy conformations for the receptor **1** with Na^+ and K^+; and for **3** with Na^+, binding energies (ΔE) are in kcal/mol and the distances are in Å (black: carbon, red: oxygen, blue: nitrogen, yellow: sulfur).

polar solvent acetonitrile was used. Sodium ion being smaller in size moves slightly upper side of the azacrown and coordinates with three oxygen atoms. On the other hand, potassium ions bind with 4 oxygen atoms of azacrown rings and the additional stability in **1**:K^+ complex compared to **1**:Na^+ seems to come from the cation-π interactions. The calculated distance between the aryl plane and the potassium ion is 3.2 Å suggests that cation-π interactions is possible in this case.[55,56] These calculated results corroborate the experimentally observed selectivity pattern.

Calix[4]arene-aza-crown-6 receptor **2** is bigger compared to **1** and **3** (Figure. 6.13). It has been reported that the Calix[4]arene-crown-6 can bind larger ions compared to Calix[4]arene-crown-4 host molecules.[57] Receptor **2** forms complexes with sodium and potassium ions and in addition binds with rubidium and barium ions also. We have examined the complexation ability of these ions with **2** employing the similar approach with MMFF94 force field and DFT calculations. The structure of receptor **2** and complexation geometries of **2** with Na^+, K^+, Rb^+, and Ba^{2+} are given in Figure.6.13. These metal ions complexes inside the cavity of receptor **2** where crown oxygen atoms and the lower rim phenyl rings participate in binding with these metal ions. The calculated binding energies at GGA/PW91/DNP qualitatively corroborate the weaker binding of Na^+ ion with receptor **2**. However, the lower selectivity of barium ion compared to Rb^+ and K^+ ions was not borne out from these calculated results and such a discrepancy may be ascribed to the fact that effect of counter-anion is not taken into account. Calix[4]arene crown-6 receptors are known to bind Cs^+ ion,[53,57] however, the receptor **2** of similar size does not seem to complex with cesium ion, as we have not observed any significant change in ^{1}H NMR analysis. Our calculations, however, showed the complexation of Cs^+ ion with receptor **2** (Figure. 6.13). The complexation structures show that larger deviations in the lower rim of **2** are seen while complexing with Na^+, K^+, Rb^+ and Ba^{2+} ions compared to the parent conformation elliptical shape of azacrown (Figure. 6.13). Elliptical shape of azacrown in the Cs^+ ion complexation with **2** is less perturbed and presumably not noticeable in NMR spectra.[11] The smallest Calix[4]aza-crown-**5** having three tosyl substituents did not show complexation with any metal ions studied here. Our modeling studies performed with Na^+ and K^+ ions showed that the metal ions sit at the top of the upper rim of receptor **4**, and not much perturbation was

seen in the lower part of **4** with respect to parent conformation (Figure. 6.14). The complexation energies for Na^+ and K^+ ions were found to be lower with **4** compared to the other receptors**.** Examining the $–CH_2$- groups attached with phenyl rings on the upper side of azacrown are not deviated largely while complexing with these metal ions and presumably does not show any notable change in the NMR studies.

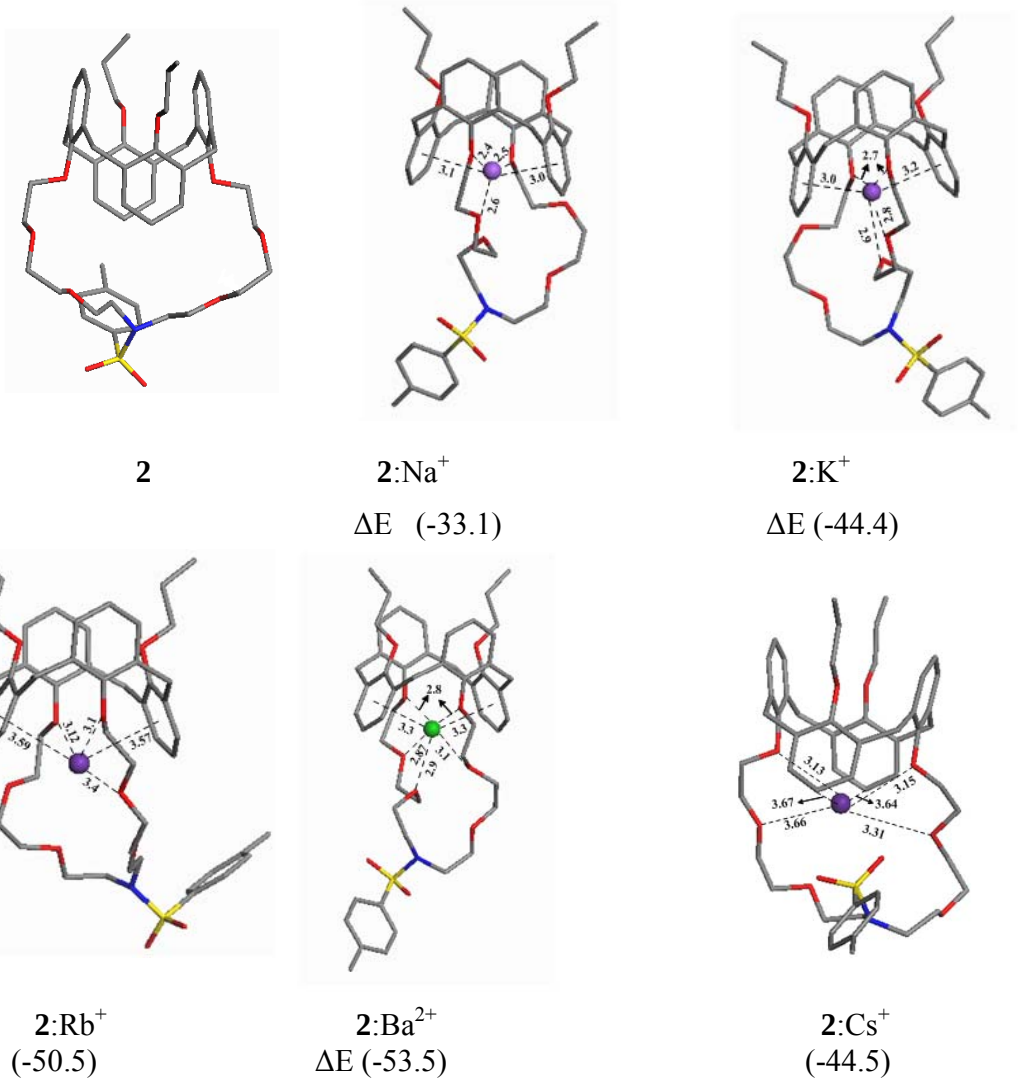

Figure. 6.13. Receptor **2** parent structure and its lowest energy conformations with Na^+, K^+, Rb^+, Ba^{2+} and Cs^+, binding energies (ΔE) are in kcal/mol and the distances are in Å (black: carbon, red: oxygen, blue: nitrogen, yellow: sulfur).

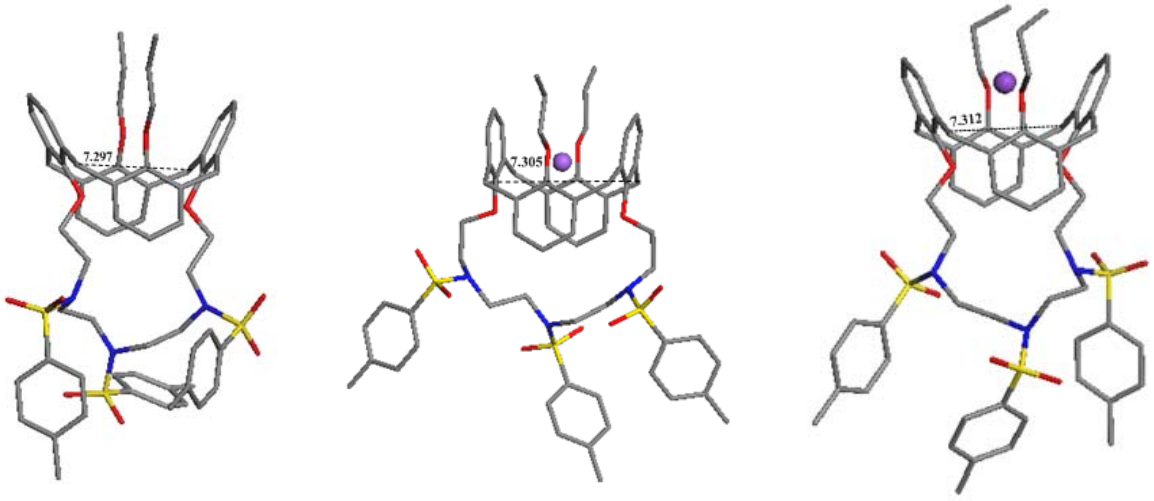

4 **4**: Na^+ **4**: K^+

ΔE (-28.16) ΔE (-31.2)

Figure. 6.14. Receptor **4** and its lowest energy conformer with Na^+ and K^+ ions and binding energy (ΔE) is given in kcal/mol. The distances between the –CH_2- groups attached with phenyl rings on the upper side of azacrown are given in Å (black: carbon, red: oxygen, blue: nitrogen, yellow: sulfur).

6.5. Conclusions

A number of calix[4]arene-azacrown receptor molecules with and without *tert*-butyl group at the upper rim and substituents at the nitrogen atom of the azacrown ring have been synthesized to investigate the effect of steric crowding on ion selectivity. Variation in the crown ring size has also been made by incorporating azacrown-5 and azacrown-6 as ionophores. ^{1}H NMR and crystallographic studies have revealed that all of these ionophores exist in 1,3-alternate conformation in solution and also in solid state. Cation-binding property of these ionophores with a large number of metal ions has been investigated by ^{1}H NMR study, which shows complexing ability of **1** with Na^+ and K^+, **2** with Na^+, K^+, Rb^+ and Ba^{2+}, **3** with Na^+ and no complexation for **4.** Binding constants for all these metal ions have been determined by ^{1}H NMR titration and the K_s values suggest that steric crowding and size-matching factors have profound influence on ion-selectivity.

The difference in the selectivity with cations for **1** and **3** was predicted by molecular modeling studies employing (MMFF94) force field and DFT calculations. The calculated results also showed that the receptor **2** can bind with Cs^+ and the smaller receptor **4** can bind with Na^+ and K^+ ions on the upper rim, however, such interactions do not perturb the complexation geometries to a larger extent, and presumably such changes are not observable in NMR studies.

6.6. References

1. Kim, S. K.; Lee, S. H.; Lee, J. Y.; Lee, J. Y.; Bartsch, R. A.; Kim, J. S. *J. Am. Chem. Soc.* **2004**, *126,* 16499.
2. Diamond, D.; Nolan, K. *Anal. Chem*. **2001,** *23A*
3. Lo, P. K.; Wong, M. S. *Sensors*. **2008,** *8*, 5313.
4. Creaven, B. S.; Donlon, D. F.; Mcginley, J. *Coordination Chemistry Reviews.* **2009**, *253*, 893.
5. Matthews, S. E.; Schmitt, P.; Felix, V.; Drew, M. G. B.; Beer, P. D. *J. Am. Chem. Soc.* **2002**, *124,* 1341.
6. Webber, P. R. A.; Cowley, A.; Drew, M. G. B.; Beer, P. D. *Chem. Eur. J.* **2003,** *9*, 2439.
7. Creaven, B. S.; Gernon, T. L.; McGinley, J.; Moore, A.; Toftlund, H. *Tetrahedron,* **2006,** *62,* 9066.
8. Li, G.-K.; Xu, Z.-X.; Chen, C.-F.; Huang, Z.-T. *Chem. Commun.* **2008,** 1774.
9. Joseph, R.; Ramanujam, B.; Achariya, A.; Khutia, A.; Rao, C. P. *J. Org. Chem*. **2008,** *73,* 5745.
10. Ghidini, E.; Ugozzoli, F.; Ungaro, R.; Harkema, S.; El-Fadl, A. A.; . Reinhoudt, D. N. *J. Am. Chem. Soc.* **1990,** *112,* 6979.
11. Kim, J. S.; Shon, O. J.; Ko, J. W.; Cho, M. H.; Yu, I. Y.; Vicens, J. *J. Org. Chem*. **2000,** *65,* 2386.
12. Casnati, A.; Della, N. C.; Sansone, F.; Ugozzoli, F.; Ungaro, R. *Tetrahedron.* **2004***, 60,* 7869.
13. Zhou, H.; Surowiec, K.; Purkiss, D. W.; Bartsch, R. A. *Org. Biomol. Chem.* **2005,** *3,* 1676.

14. Yuan, M.; Zhou, W.; Liu, X.; Zhu, M.; Li, J.; Yin, X.; Zheng H.; Zuo, Z.; Ouyang, C.; Liu, H.; Li, Y.; Zhu, D. *J. Org. Chem.* **2008**. *73,* 5008.

15. Liu, X.; Surowiec, K.; Bartsch, R. A. *Tetrahedron*. **2009***, 65,* 5893.

16. Agnihotri, P.; Suresh, E.; Paul, P.; Ghosh, P. K. *Eur. J. Inorg. Chem*. **2006,** 3369.

17. Patra, S.; Paul, P. *Dalton Trans*. **2009,** 8683.

18. Iwamoto, K.; Araki, K.; Shinkai, S. *Tetrahedron.* **1991**, *47*, 4325.

19. Ikeda, A.; Shinkai, S. *J. Am. Chem. Soc.* **1994**, *116*, 3102.

20. Patra, S.; Suresh, E.; Paul, P. *Polyhedron*. **2007,** *26*, 4971.

21. Kim, j. S.; Shon, O. J.; Sim, W.; Kim, S. K.; Cho, M. H.; Kim, J-G.; Suh, II-H.; Kim, D. W. *J. Chem. Soc.' Perkin trans. 1*, **2001**, 31.

22. Kim, J. S.; Shon, O. J.; Rim, J. A.; Kim, S. K.; Yoon, J. *J. Org. Chem.* **2002***, 67*, 2348.

23. Kim, J. S.; Noh, K. H.; Lee, S. H.; Kim, S. K.; Kim, S. K.; Yoon, J. *J. Org. Chem.* **2003,** *68***,** 597.

24. Perrin, D. D.; Armarego, W. L. F.; Perrin, D. R. *Purification of Laboratory Chemicals,* 2nd Ed, Pergamon Press: Oxford, **1980.**

25. Ouchi, M.; Inoue, Y.; Kanzaki, T.; Hakushi, T. *J. Org. Chem*. **1984***, 49*, 1408.

26. Hay, R. W.; Norman, P. R. *J. Chem. Soc., Dalton Trans.* **1979**, 1441.

27. White, D. W.; Karcher, b. A.; Jabcoson, R. A.; Verkade, J. G. *J. Am. Chem. Soc*. **1979,** *101*, 4921;

28. Casnati, A.; Pochini, A.; Ungaro, R.; Ugozzoli, F.; Arnaud, F.; Fanni, S.; Schwing, M.-J.; Egberink, R. J. M.; Jong, F. De.; Reinhoudt, D. N. *J . Am. Chem. Soc*. **1995,** *117,* 2767.

29. Hirose, K. *J. Incl. Phenom.* **2001,** *39,* 193.

30. Koh, K. N.; Araki, K.; Shinkai, S.; Asfari, Z.; Vicens, J. *Tetrahedron Lett*. **1995,** *36,* 6095.

31. Sheldrick, G.M. SAINT 5.1 ed.; Siemens Industrial Automation Inc.: Madison, WI, **(1995).**

32. SADABS, Empirical Absorption Correction Program; University of Göttingen: Göttingen, Germany **(1997).**

33. Sheldrick, G.M. SHELXTL Reference Manual: Version 5.1; Bruker AXS: Madison, WI **(1997).**

34. Sheldrick, G.M. SHELXL-97: Program for Crystal Structure Refinement; University of Göttingen: Göttingen, Germany **(1997).**

35. Spek, A. L. PLATON-97, University of Utrecht: Utrecht, The Netherlands, **(1997).**

36. Mercury 1.3, Supplied with Cambridge Structural Database; CCDC: Cambridge, U.K., **(2003).**

37. Spartan'06, Wavefunction Inc.: Irvine, California.

38. Halgren, T. A. *J. Comput. Chem*. **1996**, *17,* 490.

39. Hehre, W. J. *A Guide to Molecular Mechanics and Quantum Chemical Calculations*, 2nd edition, Wavefuncton, Inc., Irvine, CA **2006**.

40. Coker, H. *J. Phys. Chem*. **1976,** *80*, 2078.

41. Delley, B. *J. Chem. Phys.* **2000**, *113*, 7756.

42. Perdew, J. P.; Wang, Y. *Phys. ReV. B* **1992**, *45*, 13244.

43. Wu, Z.; Cohen, R. E.; Singh, D. J. *Phys. Re*V. *B* **2004**, *70*, 104112.

44. Perdew, J. P.; Burke, K.; Wang, Y. *Phys. Re*V. *B* **1996**, *54*, 16533.

45. Materials Studio DMOL3 Version 4.1, Accelrys Inc., SanDiego, USA.

46. Klamt, A. COSMO and COSMO-RS, in *Encyclopedia of Computational Chemistry*, Schleyer, P. v. R. and Allinger, L. Eds.; Wiley: New York, **1998**, *Vol. 2,* pp. 604-615.

47. Klamt, A. *J. Phys. Chem*. **1995,** *99*, 2224.

48. Boricha, V. P.; Patra, S.; Chouhan, Y. S.; Sanavada, P.; Suresh, E.; Paul, P. *Eur. J. Inorg. Chem.* **2009**, 1256.

49. Jaiyu, A.; Rojanathanes, R.; Sukwattanasinitt, M. *Tetrahedron. Lett.* **2007,** *48,* 1817.

50. Grootenhuis, P. D. J.; Kollman, P. A.; Groenen, L. C.; Reinhoudt, D. N.; Hummel G. J. V.; Ugozzoli, F.; Andreeti, G. D. *J. Am. Chem. Soc*. **1990**, *112*, 4165.

51. Harda, T.; Ohseto, F.; Shinkai, S. *Tetrahedron*. **1994**, *50,* 13377.

52. Grootenhius, P. D. J.; Kollman, P. *J. Am. Chem*. Soc., **1989**, *111*, 2152.

53. Casnati, A.; Ca' D. N.; Sansone, F.; Ugozzoli, F.; Ungaro, R. *Tetrahedron*, **2004**, *60*, 7869.

54. Agnihotri, P.; Suresh, E. Ganguly, B.; Paul, P.; Ghosh, P. K. *Polyhedron,* **2005**, *24*, 1023.

55. Macias, A. T.; Joseph, E. N, and Evanseck, J. D. *J. Am. Chem. Soc.* **2003**, *125*, 2351.

56. Cioslowski, J. and Lint, Q. *J. Am. Chem.* Soc. **1995***,117,* 2553.

57. Casnati, A.; Pochini, A.; Ungaro, R.; Ugozzoli, F.; Arnaud, F.; Fanni, S.; Schwing, M.-J.; Egberink, R. J. M.; Jong, F. de; Reinhoudt, D. N. *J. Am. Chem.* Soc. ***1995****, 117,* 2767.

Chapter-VII

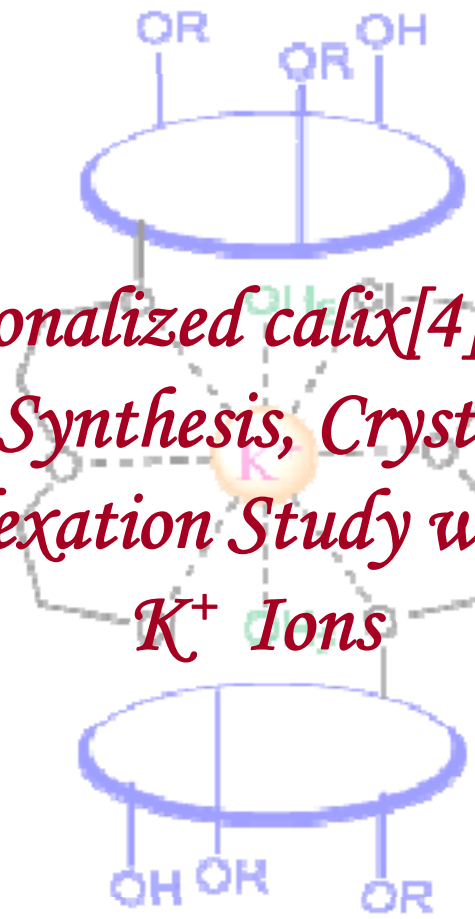

Functionalized calix[4]arene as Ionophore: Synthesis, Crystal Structures and Complexation Study with Na^+ and K^+ Ions

7.1. Introduction

Calixarenes are receiving increasing attention because of their application in diverse areas; selective interaction with metal ion is one of the most important applications.[1-8] Metal ions generally bind at the lower rim of the calixarene moiety involving phenolic oxygen atoms and the complexation is controlled mainly by the conformation of the calixarenes and substituents at the lower rim. Introduction of substituents into OH groups at the lower rim suppresses hydrogen-bonding and increases steric hindrance, which results in the formation of conformational isomers such as cone, partial-cone, 1,3-alternate and 1,2-alternate.[1–4] Complexation of calix[4]arene with substituents at the two opposite OH or at all of the four OH groups are mostly studied and generally they exist in cone and 1,3-alternate cone conformations.[5,6,9,10] However, complexation study of calix[4]arene with three substituents at the lower rim are rarely studied.[11,12,13] One of the reasons could be synthetic difficulty, substitution at three out of four OH groups require control reaction conditions. The second reason may be conformational aspect, this class of compounds generally exists in partial cone conformation, which is not a favourable geometry to form complex utilizing all of the four oxygen atoms of the calixarene moiety.

It is interesting to study conformational and complexation behaviour of trisubstitued calix[4]arene with Na^+ and K^+ ions with an emphasis to achieve selectivity for K^+ over Na^+. With this aim, incorporating the propyl, 2-(2-chloroethoxy)-ethanol moiety and *p*-toluenesulfonyl moiety as the third substituent at the OH group of the disubstituted (bis-propyl) calix[4]arene derivatives, three new compounds have been synthesized and structurally characterized. In this Chapter, synthesis, characterization and ion-binding property with Na^+ and K^+ ions for these calix[4]arene derivatives having substituents at the three out of four OH groups is described. All of these three compounds exhibit partial cone conformation and one of them shows remarkable selectivity towards K^+ over Na^+. The K^+-complex has been isolated and characterized by analytical and spectroscopic methods, binding constant has also been evaluated.

7.2. Experimental Section

7.2.1. Materials

The compounds calix[4]arene[14] and 2-(2-chloroethoxy)-ethanol *p*-toluenesulfonate[15] were synthesized following the literature procedures. All the reagents used in this study were purchased from Aldrich and S. D. Fine Chemicals. All solvents were analytical grade and purified by standard procedure before use.[16]

7.2.2. Physical measurements

Physical measurements were carried out using the instruments described in earlier Chapters.

7.2.3. Synthesis of ligands

Synthesis of 25,27-bis(1-propyloxy)calix[4]arene (L^1)

This compound was synthesized following the literature procedure,[17] Yield 60%. ^{1}H NMR (200 MHz, $CDCl_3$) δ 8.30 (s, 2H, OH), 7.05, 6.90 (d, *J* = 7.4 Hz, 4H each, Ar), 6.72, 6.67 (t, *J* = 7.4 Hz, 2H each, Ar), 4.30 (d, *J* = 13.0 Hz, 4H, Ar*CH*$_2$Ar), 3.97 (t, *J* = 6.2 Hz, 4H, OCH_2), 3.37 (d, *J* = 13.0 Hz, 4H, Ar*CH*$_2$Ar), 2.05 (m, 4H, CH_2), 1.30 (t, *J* = 7.4 Hz, 6H, CH_3). LC-MS *m/z* 531.91 ($\mathbf{L^1}$ + Na^+).

Synthesis of 25,26,27-Tris(1-propyloxy)calix[4]arene (L^2)

To a suspension of calix[4]arene (0.848 g, 2 mmol) in acetonitrile (80 mL) were added iodopropane (2.04 g, 12 mmol) and K_2CO_3 (1.66 g,12 mmol) in excess and the reaction mixture was stirred under reflux for 34 h. The solvent was then removed under reduced pressure and the residue was treated with 10% HCl (50 mL) and extracted with CH_2Cl_2 (100 mL). The organic phase was separated, washed twice with distilled water (100 mL x 2) and dried over $MgSO_4$. The solvent was removed by rotary evaporation and the product was purified by column chromatography using silica gel as packing material and ethyl acetate/hexane (1:9) as eluent. The solvent was removed from the desired fraction

and the solid compound was dried under vacuo (yield 330mg, 30%). Single crystals suitable for X-ray crystallography were obtained by slow evaporation of the dilute solution of the compound dissolved in acetonitrile-hexane (1:1). IR (KBr pellet, cm^{-1}) 3408 (OH). UV/vis ($CHCl_3$, λ_{max} nm, ϵ $M^{-1}cm^{-1}$), 285sh (2.57×10^3), 277 (3.46×10^3), 243 (3.3×10^3). ^{1}H NMR (200 MHz, $CDCl_3$) δ 7.25 (s, 1H, OH), 7.06-6.81 (m, 9H, Ar), 6.73-6.62 (m, 3H, Ar), 4.08 (d, *J* = 13.2 Hz, 2H, Ar*CH*$_2$Ar), 3.95 (m, 2H, OCH_2), 3.84 (s, 2H, Ar*CH*$_2$Ar), 3.82 (s, 2H, Ar*CH*$_2$Ar), 3.59 (m, 2H, OCH_2), 3.24 (d, *J* = 13.0 Hz, 2H, Ar*CH*$_2$Ar), 3.14 (t, *J* = 7.6 Hz, 2H, OCH_2), 1.79 (m, 4H, CH_2), 1.33 (m, 2H, CH_2), 0.99 (t, *J* = 7.2 Hz, 6H, CH_3), 0.57 (t, *J* = 7.4 Hz, 3H, CH_3). LC-MS *m/z* 573.40 (**L**^{2} + Na^+). Anal. Calcd for $C_{38}H_{45}O_4N$: C, 79.15; H, 7.66, N, 2.36. Found: C, 78.45; H, 7.53; N, 2.21.

Synthesis of 25,27-bis(1-propyloxy)-26(5-chloro-3-oxapentyloxy)calix[4]arene (L^3)

A mixture of dipropyl calix[4]arene (0.740 g, 1.45 mmol), 2-(2-chloroethoxy)-ethanol *p*-toluenesulfonate (0.405 g, 1.45 mmol), and Cs_2CO_3 (0. 474 g, 1.45 mmol) in acetonitrile (50 mL) was heated at reflux for 24 h under nitrogen atmosphere. The reaction mixture was allowed to cool to room temperature, solvent was then removed under reduced pressure and the residue was treated with 10% HCl (50 mL) and 100 mL uof CH_2Cl_2. The organic phase was separated, dried over $MgSO_4$ and evaporation of the solvent under reduced pressure afforded brownish oil. The compound was purified by column chromatography using silica gel as packing material and ethyl acetate/hexane (1:11) as eluent. Yield 0.358 g, (40%). Single crystals suitable for X-ray study were grown by slow evaporation of the solution containing THF-hexane (1:5). IR (KBr pellet, cm^{-1}) 3268 (OH). UV/ vis ($CHCl_3$, λ_{max} nm, ϵ $M^{-1}cm^{-1}$) 285sh (3.46×10^3), 277 ($4.1x10^3$), 243 (3.75×10^3). ^{1}H NMR (200 MHz, $CDCl_3$) δ 7.32 (s, 1H, OH), 7.24 (d, *J* = 3.8 Hz, 2H, Ar), 7.07-6.89 (m, 7H, Ar), 6.80-6.63 (m, 3H, Ar), 4.10 (d, *J* = 13.0 Hz, 2H, Ar*CH*$_2$Ar), 3.95 (m, 2H, OCH_2), 3.89 (s, 2H, Ar*CH*$_2$Ar), 3.87 (s, 2H, Ar*CH*$_2$Ar), 3.65-3.55 (m, 4H, OCH_2), 3.33 (t, *J* = 5.2 Hz, 2H, OCH_2), 3.26 (d, *J* = 13.0 Hz, 2H, Ar*CH*$_2$Ar), 2.92 (t, *J* = 5.0 Hz, 2H, OCH_2), 2.64 (t, *J* = 5.0 Hz, 2H, CH_2Cl), 1.73 (m, 4H, CH_2), 0.98 (t, *J* = 7.4 Hz, 6H, CH_3). LC-MS *m/z* 638.30 (**L**^{3} + Na^+). Anal. Calcd for $C_{38}H_{43}O_5Cl$: C, 74.19; H, 7.04. Found: C, 73.94; H, 6.92.

Synthesis of 25(O-p-toluenesulfonate)26,28-bis(1-propyloxy)calix[4]arene (L^4)

A mixture containing dipropyl calix[4]arene (0.762 g, 1.5 mmol), *p*-toluenesulfonyl chloride (0.286 g, 1.5 mmol), and Cs_2CO_3 (0.489 g,1.5 mmol) in acetonitrile (50 mL) was heated at reflux for 20 h under nitrogen atmosphere. The reaction mixture was allowed to cool to room temperature and solvent was removed by rotary evaporation. The residue was treated with 10% HCl (50 mL) and CH_2Cl_2 (100 mL). The organic phase was separated and dried over $MgSO_4$ and evaporation of the solvent under reduced pressure afforded yellow oil. The compound was purified by column chromatography using silica gel as packing material and ethyl acetate/hexane (1:16) as eluent. The desired compound was obtained as white solid. Yield 0.397 g (40%). Single crystals suitable for X-ray study were grown by slow evaporation of the solution containing THF-hexane (1:5). IR (KBr pellet, cm^{-1}) 3452 (OH). UV/ vis ($CHCl_3$, λ_{max} nm, ϵ $M^{-1}cm^{-1}$) 284sh (3.46×10^3), 276 ($4.01x10^3$), 243 (4.55×10^3). ^{1}H NMR, (200 MHz, $CDCl_3$) δ 7.34 (d, *J* = 7.4 Hz, 2H, Ar), 7.20 (s, 1H, OH), 7.15 (d, *J* = 7.2 Hz, 2H, Ar), 7.07-7.01 (m, 4H, Ar), 6.75-6.68 (m, 6H, Ar), 6.38 (t, *J* = 7.6 Hz, 2H, Ar), 4.10 (d, *J* = 14.8 Hz, 2H, Ar*CH*$_2$Ar), 4.04 (d, *J* = 13.2 Hz, 2H, Ar*CH*$_2$Ar), 3.98-3.87 (m, 2H, OCH_2), 3.75 (d, *J* = 14.8 Hz, 2H, Ar*CH*$_2$Ar), 3.65-3.53 (m, 2H, OCH_2), 3.22 (d, *J* = 13.2 Hz, 2H, Ar*CH*$_2$Ar), 2.39 (s, 3H, Ts-CH_3), 1.84-1.53 (m, 4H, CH_2), 0.99 (t, *J* = 7.2 Hz, 6H, CH_3). LC-MS *m/z* 685.53 ($\mathbf{L^4}$ + Na^+). Anal. Calcd for $C_{41}H_{42}O_6S$: C, 74.29; H, 6.39, S, 4.84. Found: C, 73.87; H, 6.15; S, 4.58.

7.2.4. In-situ complexation study by NMR

^{1}H NMR spectra of ligands $\mathbf{L^2}$- $\mathbf{L^4}$ (0.01 mmol each) in $CDCl_3$-CD_3OH (0.5 mL, 4:1) were recorded. Then metal (Na^+/K^+) iodide (20 times of the molar equivalent) was added into the solution in NMR tube and the reaction mixture was shaken well to dissolve metal salt and the NMR spectra of the solutions were recorded at different time intervals. Compound $\mathbf{L^3}$ with KI showed significant changes in the NMR spectra within 6 h. Compounds $\mathbf{L^2}$, $\mathbf{L^3}$ and $\mathbf{L^4}$ with NaI and compounds $\mathbf{L^2}$ and $\mathbf{L^4}$ with KI did not show any significant change in the NMR spectra even after 4 days.

7.2.5. Synthesis of Na^+ and K^+ complexes

Each of the three ligands (15 mg) were dissolved in chloroform-methanol mixture (10 mL, 4:1) and required metal iodide (20 molar equivalent) was added into the solution and the reaction mixture was stirred at room temperature for 4 days. The reaction mixture was filtered using sintered crucible to remove undissolved metal iodide. The solvent was then removed at reduced pressure, the solid mass was dissolved in $CDCl_3$-CD_3OH (4:1), and filtered and ^1H NMR spectra of the solutions were recorded. The observations are consistent to that found in in-situ NMR experiment. Data for the K^+-complex of $\mathbf{L^3}$: IR (KBr pellet, cm^{-1}) 3459, 1624 and 801 cm^{-1} (H_2O), 3269 (OH). ^1H NMR (200 MHz, $CDCl_3$) δ 7.45 (s, 1H, OH), 7.32 (d, *J* = 7.4 Hz, 2H, Ar), 7.17-6.96 (m, 7H, Ar), 6.89 (d, *J* = 7.4 Hz, 2H, Ar), 6.83-6.72 (m, 1H, Ar), 4.26 (s, 4H, $2H_2O$), 4.10 (d, *J* = 13.4 Hz, 2H, Ar*CH*$_2$Ar), 4.03-3.99 (m, 2H, OCH_2), 3.95 (s, 2H, Ar*CH*$_2$Ar), 3.92 (s, 2H, Ar*CH*$_2$Ar), 3.86-3.81 (m, 2H, OCH_2), 3.67-3.50 (m, 4H, OCH_2), 3.34 (d, *J* = 13.2 Hz, 2H, Ar*CH*$_2$Ar), 3.20-3.15 (m, 2H, OCH_2), 3.05-3.00 (m, 2H, CH_2Cl), 1.84-1.71 (m, 4H, CH_2), 1.00 (t, *J* = 7.4 Hz, 6H, CH_3). LC-MS *m/z* = 1305.0 ($2\mathbf{L^3}$ + K^++ $2H_2O$), 1287.23 ($2\mathbf{L^3}$ + K^++ H_2O).

7.2.6. Determination of association constant (K_a) by NMR titration

A stock solution of the host compound ($\mathbf{L^3}$, 5.176 x 10^{-3} M) was prepared in 4:1 $CDCl_3$: MeOH. A portion of this solution (0.5 mL) was taken in a NMR tube and used as host, in the remaining solution KI was dissolved (16.64 x 10^{-3} M) and it was used as guest so that the host concentration remained constant throughout the titration. Successive aliquots (0.1mL each time) of the guest solution were added to the host in the NMR tube and after 30 min of each addition the ^1H NMR spectra were recorded. The changes in chemical shift of the CH_2 protons of the 2-(2-chloroethoxy)-ethanol moiety of the host was measured as a function of guest concentration and the binding constant (K_a) is calculated following the procedure described in the literature for 2:1 host:guest complex.[18] The value of K determined is 1.4 x 10^5 M^{-1}.

7.2.7. X-ray crystallography for L^2- L^4

The crystallographic data and details of data collection for all the three compounds are given in Table 7.1. Crystal of suitable size was selected from the mother liquor and immersed in partone oil, then mounted on the tip of a glass fiber and cemented using epoxy resin. Intensity data for all three crystals were collected at 100 K using MoK_α (λ = 0.71073Å) radiation on a Bruker SMART APEX diffractometer equipped with CCD area detector. The data integration and reduction were processed with SAINT[19] software. An empirical absorption correction was applied to the collected reflections with SADABS.[20] The structures were solved by direct methods using SHELXTL[21] and were refined on F^2 by the full-matrix least-squares technique using the SHELXL-97[22] program package. Graphics are generated using PLATON[23] and MERCURY 1.3[24] In all the compounds non-hydrogen atoms were refined anisotropically till convergence is reached and the hydrogen atoms attached to the ligand moieties are sterochemically fixed.

7.3. Results and discussion

7.3.1. Synthesis of ligands L^1- L^4

Compounds **L^1- L^4** are shown in Figure. 7.1. For the synthesis of these trisubstituted derivatives, reaction conditions and the molar proportions of the reactants are crucial to control the reaction to achieve maximum yield of the desired product. All these reactions were carried out in acetonitrile under reflux condition using Cs_2CO_3 as base. In case of **L^2,** double of the required amount of iodopropane was used whereas for **L^3** and **L^4**, molar proportions of the reactants have been used to achieve maximum yield. These compounds were obtained with low to moderate yield after purification by extensive column chromatography.

All of these compounds gave satisfactory C, H and N analysis. Mass spectra of all these compounds were recorded on LC-MS and the observed *e/m* values show excellent agreement with the calculated values. It may be noted that *e/m* values (100%) of all

Table 7.1. Summary of crystallographic data for **L^2, L^3** and **L^4**

Compound	**L^2**	**L^3**	**L^4**
Emperical formula	$C_{39}H_{45}NO_4$	$C_{38}H_{43}Cl_1O_5$	$C_{41}H_{42}O_6\ S_1$
Formula mass	591.76	615.17	662.81
Crystal Colour	Colourless	Colourless	Yellow
Crystal Size (mm^3)	0.29 x 0.19 x 0.10	0.22 x 0.14 x 0.09	0.45 x 0.28 x 0.22
Temperature (K)	100	100	100
Crystal System	Monoclinic	Monoclinic	Monoclinic
Space Group	$P2_1/n$	$P2_1/c$	$P2_1$
a(Å)	11.1795(12)	11.5711(8)	9.3129(9)
b(Å)	20.227(2)	13.9153(9)	35.339(3)
c(Å)	15.2139(16)	20.6531(14)	11.0407(10)
α(°)	90	90	90
β(°)	94.964(2)	105.7560(10)	106.340(2)
γ (°)	90	90	90
Z	4	4	4
V($Å^3$)	3427.4(6)	3200.5(4)	3486.8(6)
Density (Mg/m^3)	1.147	1.277	1.263
Absorption Coefficient (mm^{-1})	0.073	0.163	0.140
F(000)	1272	1312	1408
Reflections Collected	16789	18628	17170
Independent Reflections	6011 [R(int) = 0.0359]	7382 [R(int) = 0.0256]	6218 [R(int) = 0.0685]
Number of Parameters	402	400	873
S (Goodness of Fit) on F^2	1.054	1.029	1.072
Final R1 , wR2 (I>2σ(I)	0.0679 / 0.1949	0.0430 / 0.1063	0.0627/ 0.1322
Weighted R1, wR2(all data)	0.1128 / 0.2278	0.0548 / 0.1152	0.0830/ 0.1442
Largest diff. peak and hole(e.$Å^{-3}$)	0.511 / -0.228	0.361 / -0.258	0.318 / -0.331

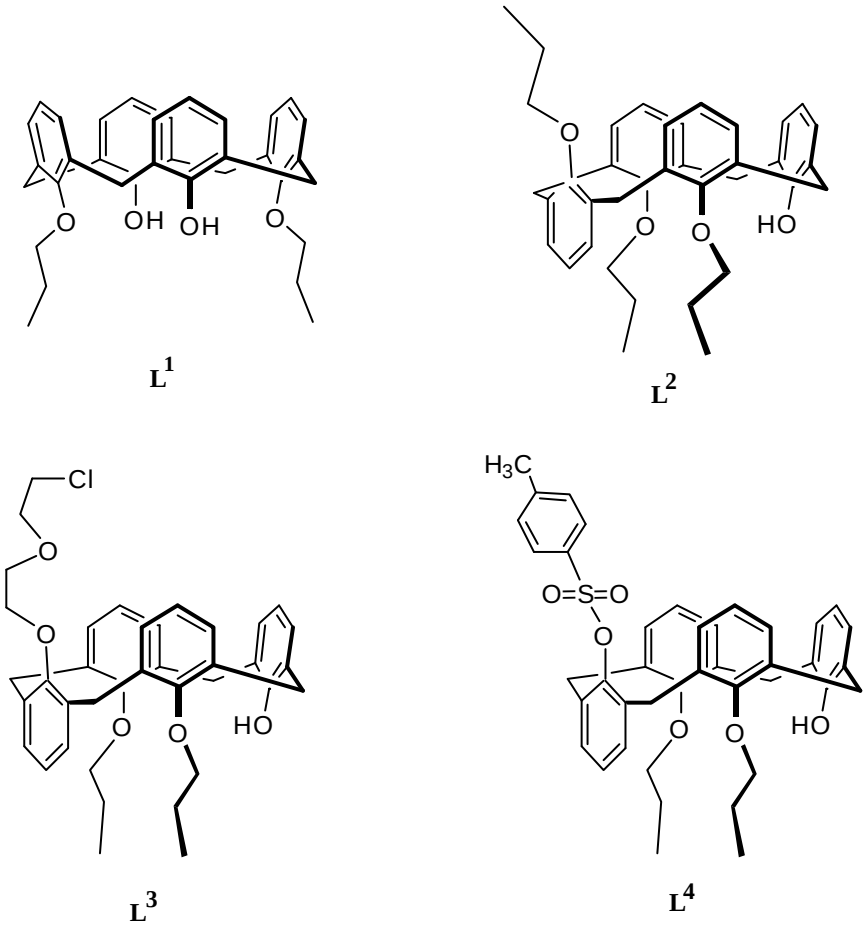

Figure. 7.1. Structures of the compounds $\mathbf{L^1}$- $\mathbf{L^4}$

compounds correspond to the Na^+ adduct (ligand + Na^+), which is a well-known phenomenon when LC-MS is used for the measurement of mass.[9,10] In the IR spectra, the strong bands at 3408, 3268 and 3452 cm^{-1} for $\mathbf{L^2}$, $\mathbf{L^3}$ and $\mathbf{L^4}$, respectively suggest the presence of OH group. The difference in band positions is due to various degree of O-H.….O interactions with the adjacent oxygen atom of the calixarene moiety, as evident from the crystal structures. Conformational analysis of the molecules was done by NMR and single crystal X-ray study.

7.3.2. Conformational study of ligands by NMR

^{1}H NMR spectra of all compounds were recorded in $CDCl_3$ and the data with assignment of signals are presented in the experimental section. However, signals for the bridged methylene groups (Ar*C*H_2Ar) are noteworthy, particularly in the context of conformational analysis. They exhibit four signals, two doublets and two closely spaced singlets for **L^2** and **L^3**, whereas **L^4** exhibits four doublets. The appearance of doublets for bridged methylene protons is the indication of a typical AB pattern with non-equivalent axial and equatorial hydrogen atoms. The doublets around δ 4.10 (2H) and around δ 3.25 (2H) for **L^2** and **L^3** suggest that two of the four methylene groups are equivalent. The other two methylene groups exhibit closely spaced two singlets indicating that the two protons (axial and equatorial) of each methylene group are equivalent but the two methylene groups are nonequivalent. In case of **L^4**, the *J*-values indicate that the doublets at δ 4.10 (*J* = 14.8 Hz, 2H) and at δ 3.75 (*J* = 14.8 Hz, 2H) correspond to two equivalent methylene groups with nonequivalent axial and equatorial protons. Similarly, the doublets at δ 4.04 (*J* = 13.2 Hz, 2H) and at δ 3.22 (*J* = 13.2 Hz, 2H) correspond to two equivalent methylene groups with AB type protons. This kind of splitting pattern for the bridged methylene groups suggest partial cone conformation for these molecules.[11-13,25,26] For **L^2- L^4**, two substituents are common, the third substituent in **L^2** and **L^3** are similar but for **L^4,** it is significantly different. This third substituent has affected precise geometry of the calix unit and because of this effect the splitting patterns of the bridged methylene groups for **L^2** and **L^3** are similar but different from **L^4**.

7.3.3. Molecular structures of the ligands

The ORTEP diagrams of the compounds **L^2- L^4** are shown in Figures. 7.2-7.4. For all the three compounds, bond lengths and bond angles are in the usual ranges,[9,27,28] and the following discussion refers mainly to the conformation and shape of the calixarene skeleton. Crystal structures clearly show that all the three compounds have adopted partial cone conformation, however the precise shape of the molecule differs due to variation in substituent. The conformation of the calixarene can also be described by a typical sequence of the signs of torsion angles around aromatic units and the σ-bonds

connecting the methylene bridges.[29] These sequences for all the three compounds (Table 7.2) are (+,-)(+,+)(-,-)(+,-), which corresponds to the partial cone (paco) conformation.

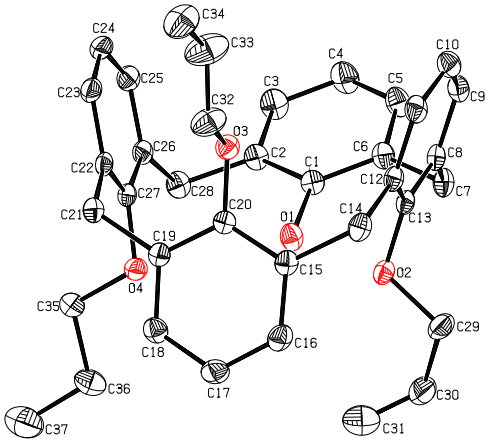

Figure. 7.2. ORTEP diagram with atom numbering scheme depicting the conformation of the calixarene moiety for compounds $\mathbf{L^2}$ (hydrogen atoms are omitted for clarityty).

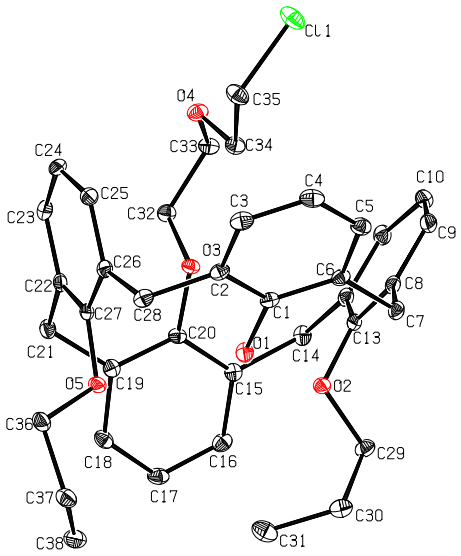

Figure. 7.3. ORTEP diagram with atom numbering scheme depicting the conformation of the calixarene moiety for compounds $\mathbf{L^3}$ (hydrogen atoms are omitted for clarity).

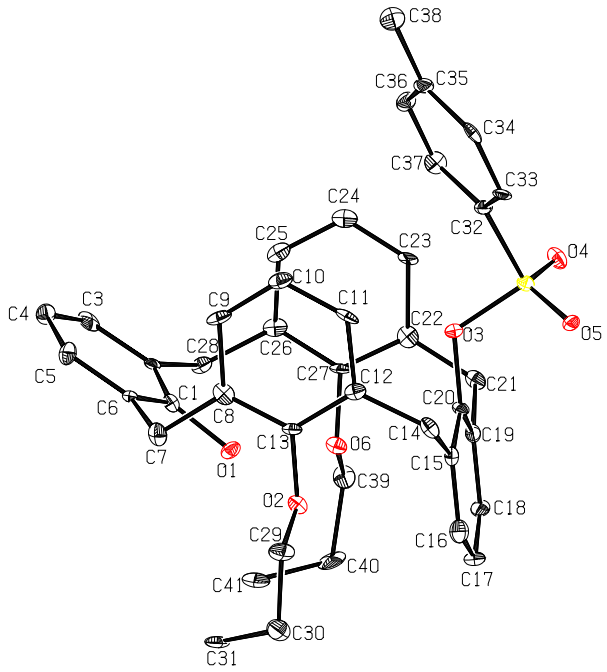

Figure. 7.4. ORTEP diagram with atom numbering scheme depicting the conformation of the calixarene moiety for compounds **L**^{4} (hydrogen atoms are omitted for clarity).

Compound **L**^{2} encapsulates an acetonitrile molecule inside the calix cone with strong C-H…π interaction between the hydrogen atoms of the acetonitrile with the centroid of the calix phenyl rings as depicted in Figure. 7.5. Details of this C-H…π interaction is given in Table 7.3. Similar mode of guest encapsulation has also been reported with different substituted calixarene molecules.[30] It may be noted that the phenolic hydrogen H1 makes strong intramolecular H-bonding with O2 of the neighboring O-propyl group (Table 7.4) as depicted in Figure. 7.5. The propyl groups attached to third and fourth phenyl ring is in extended conformation whereas that attached to the second phenyl ring is in folded conformation as indicated by the torsion angles (O3-C32-C33-C34 = 175.30°, O4-C35-C36-C37 = 176.94° and O2-C29-C30-C31 = 48.69°). The folded conformation of the propyl group is attributed to the involvement of O2 in intramolecular H-bonding interactions with the adjascent phenolic oxygen O1.

Table 7.2. Selected crystallographic data for compounds **L^2-L^4:** (I) torsion angles around the Ar–CH2 bonds; (II) distances within the reference plane (the best plane through the carbon atoms of the methylene bridges); and (III) inclination δ of the aromatic units with respect to the reference plane.

I. Torsion angles (°)				
	L^2	**L^3**	**L^4**(I^{st} mol.)	**L^4** (2^{nd} mol.)
C1-C6-C7-C8	-72.29	77.08	72.00	72.99
C6-C7-C8-C13	98.45	-93.77	-120.34	-105.49
C12-C12-C14-C15	-53.18	38.13	58.53	60.70
C12-C14-C15-C20	-59.64	56.14	62.54	57.82
C20-C19-C21-C22	62.76	-47.72	-60.07	-60.567
C19-C21-C22-C27	56.50	-59.53	-61.34	-57.32
C27-C26-C28-C2	-110.54	108.59	105.89	119.18
C26-C28-C2-C1	73.75	-73.63	-65.86	-75.93
II. Reference planes C7-C14-C21-C28 and C48-C55-C62-C69 (for 2^{nd} molecule of L^4)				
Rsmd (Å)	0.088, -0.087, -0.087, 0.087	0.028,-0.028, 0.028, -0.028	0.102, -.100, 0.100, -.102	0.103, -0.101, 0.101, -0.103
Distance C7-C14/ C48-C55	5.094	5.117	5.056	5.115
Distance C7-C28/C48-C69	5.061	5.067	5.030	5.030
Distance C14-C21/C55-C62	5.093	5.124	5.097	5.118
Distance C21-C28/C62-C69	5.055	5.067	5.062	5.099
Distance C7-C21/C48-C62	7.180	7.192	7.024	7.228
Distance C14-C28/C55-C69	7.167	7.214	7.278	7.097
III. Inclination of the aromatic units (δ) in (°)				
C1-C6/ C42-C47	37.33	37.49	35.64	40.42
C8-C13/ C49/54	70.79	59.14	87.53	79.72
C15-C20/C56-C61	81.98	66.54	85.69	82.97
C22-C27/ C63-C68	55.09	77.91	84.04	85.63

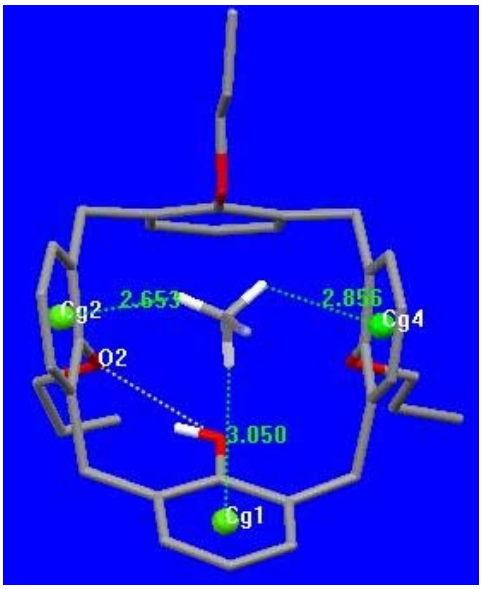

Figure. 7.5. MERCURY diagram depicting encapsulated acetonitrile molecule inside the calixarene cone in $\mathbf{L^2}$, and also shown the intramolecular O-H…O interaction

Table 7.3. C-H….π interactions for $\mathbf{L^2}$, $\mathbf{L^3}$ and $\mathbf{L^4}$ (Å and °)

C-H…..Cg	*d*(H...Cg)	*d*(C...Cg)	∠ C-H…Cg
Compound $\mathbf{L^2}$			
C39-H39B….Cg1	3.05	3.987(4)	166
C39-H39A….Cg2	2.65	3.452(5)	141
C39-H39C....Cg4	2.86	3.505(5)	126
Compund $\mathbf{L^3}$			
C34-H34A…..Cg2	2.86	3.731(6)	150
C34-H34B…..Cg4	2.89	3.689(6)	142
Compound $\mathbf{L^4}$			
C70-H70…..Cg1[1]	2.98	3.640(7)	126
C79-H79A….Cg2	2.85	3.574(7)	133

[1] 1-x, ½+y, -z ; Cg1, Cg2 and Cg4 are the centroid of the phenyl rings C1 to C6 , C8 to C13 and C22 to C27, respectively for all compounds.

Table 7.4. Hydrogen bond distances for $\mathbf{L^2}$, $\mathbf{L^3}$ and $\mathbf{L^4}$ (Å and °)

D-H...A	*d*(H...A)	*d*(D...A)	∠ D-H…A
Compound $\mathbf{L^2}$			
O1-H1....O2	1.96	2.733(3)	156
Compound $\mathbf{L^3}$			
O1-H1….O2	1.85	2.653(3)	166
Compound $\mathbf{L^4}$			
O1-H1....O6	2.04	2.840(5)	167
O7-H7…O12	2.42	3.209(5)	161
C21-H21A....O4	2.43	3.216(7)	138
C55-H55A... O10	2.44	3.193(7)	134
C7-H7A....O4[1]	2.59	3.506(7)	158
C38-H38A... O5[2]	2.41	3.322(8)	158
C69-H69A... O10[3]	2.52	3.458(7)	163
C79-H79C... O11[4]	2.38	3.284(7)	156

[1]x, y, -1+z ; [2]1+x,y, z ; [3]x, y, 1+z; [4]-1+x, y, z

Packing diagram of $\mathbf{L^2}$ viewed down a-axis is shown in Figure. 7.6 with offset π stacked array of calix moiety along b-axis. Calixarene molecules are oriented with C1g and Cg3 phenyl centroids of adjascent molecules making offset π…π stacking interactions from either side extending the array along b-axis, Cg1…Cg3 = 4.86 Å with Cg…Cg perpendicular distance 3.52 Å where Cg1 and Cg3 are centroid of C1-C6 and C15-C20 phenyl ring. Thus the stabilization of the compound in the crystal lattice can be mainly attributed to intermolecular phenyl offset π…π stacking interactions and intramolecular O-H…O and the C-H….π interactions.

In the case of $\mathbf{L^3}$**,** both the methylene hydrogen atoms of the 2-(2-chloroethoxy)-ethanol is involved in strong intramolecular C-H….π interaction with the opposite phenyl rings of the calix moiety (Figure. 7.7) brining this group inward the calix cone preventing the entry of any solvent molecule for encapsulation in the cavity. The phenolic hydrogen H1 is involved in strong intramolecular O-H…O hydrogen bonding with the

neighboring oxygen atom attached to the benzene ring. Details of the C-H….π and O-H…O interactions are given in Tables 7.3 and 7.4, respectively. The distances and angles of these interactions are well within the values reported by Meyer et. al. in their review article.[31] The propyl groups attached to the second and fourth phenyl rings are in folded conformation (torsion angles O2-C29-C30-C31 = 62.99 °, O5-C36-C37-C38 = -65.48°) and projected outward from the calix cone. Torsion angle of the attached 2-(2-chloroethoxy)-ethanol moiety (O3-C32-C33-O4 = 66.02°, C32-C33-O4-C34 = 78.66°, C33-O4-C34-C35 = 163°, O4-C34-C35-Cl1 = -68.22°) clearly shows that except the middle portion of the string all other parts are in folded conformation to attain the right orientation for the effective C-H….π interaction of the methylene hydrogens with the phenyl rings as mentioned above.

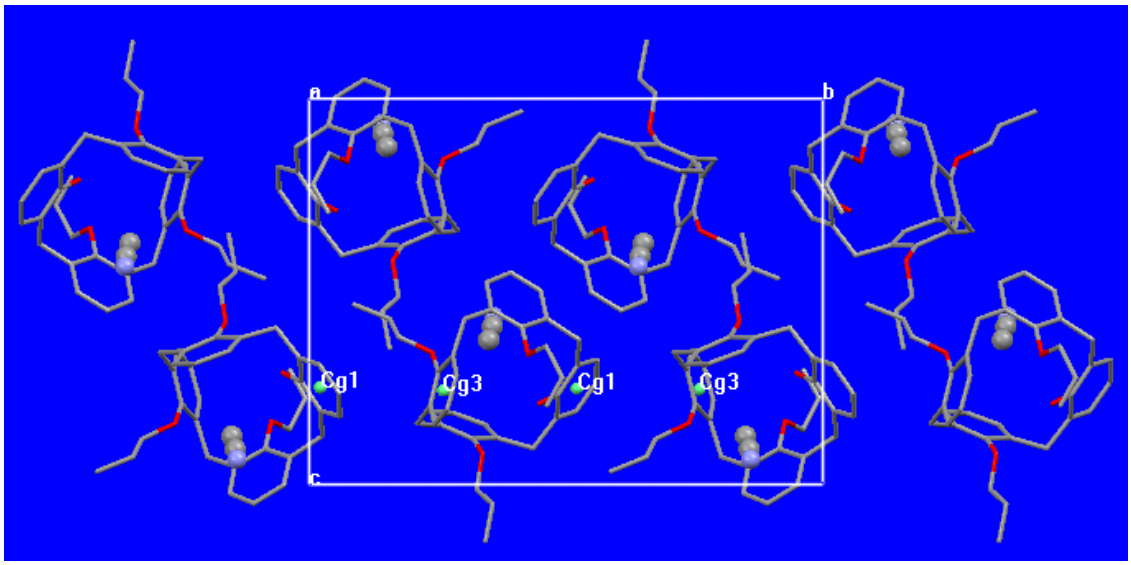

Figure. 7.6. Packing diagram of $\mathbf{L^2}$ viewed down a-axis showing the orientation of the calixarene moiety with encapsulated acetonitrile molecule; calixarene molecules are oriented with C1g and Cg3 phenyl centroids of adjascent molecules making offset π…π stacking interactions from either side extending the array along b-axis.

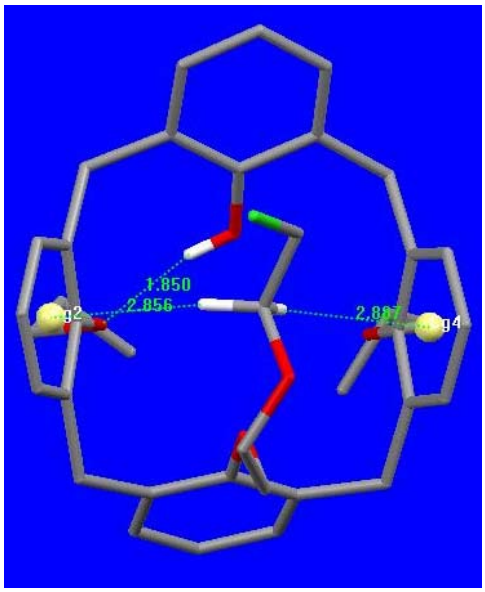

Figure. 7.7. MERCURY diagram of $\mathbf{L^3}$ depicting the intramolecular O-H…O interaction and C-H….π interaction between the aromatic rings of the calixarene unit with the methylene hydrogen atoms of the attached 2-(2-chloroethoxy)-ethanol moiety.

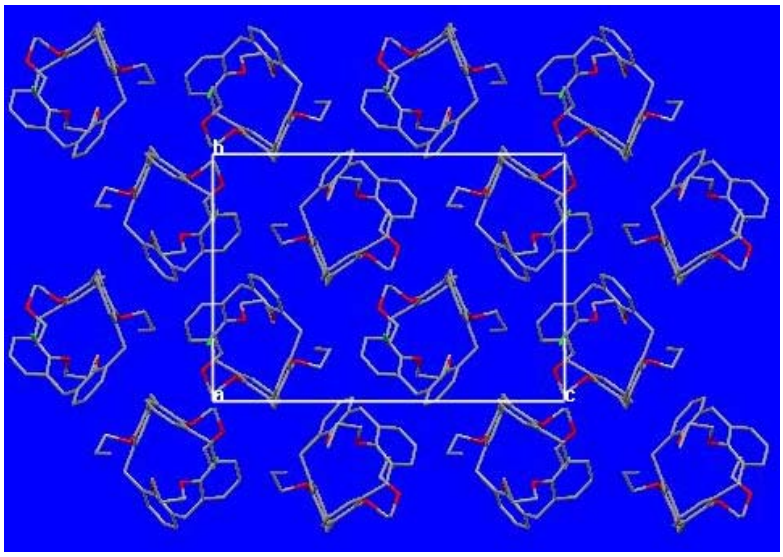

Figure. 7.8. MERCURY packing diagram of compound $\mathbf{L^3}$ viewed down a-axis showing the leaner arrangement of the calix ligands along c-axis.

Packing arrangement of $\mathbf{L^3}$ is similar to that of $\mathbf{L^2}$, however no significant intermolecular C-H….π interaction is observed between the adjacent calix moieties as in the case of $\mathbf{L^2}$ (Figure. 7.8). Intramolecular C-H….π interaction dominates in governing the conformation of the calix moiety and effective crystal packing in $\mathbf{L^3}$.

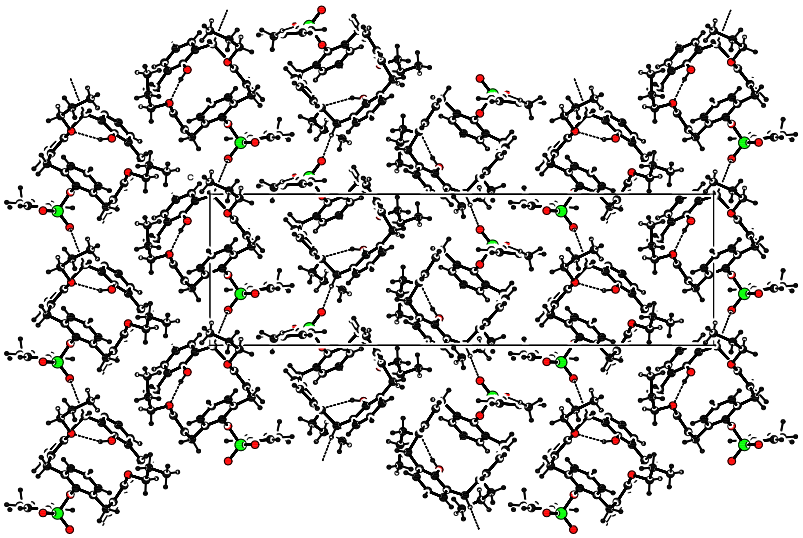

Figure. 7.9. PLATON packing diagram of $\mathbf{L^4}$ viewed down a-axis depicting the C-H….O hydrogen bonding interaction between the sulfonate oxygen with methyl carbons forming a layered array along c-axis.

Packing diagram of $\mathbf{L^4}$ shows that the calix molecules are arranged as hydrogen bonded offset layers along c-axis and can be viewed as a corrugated layer along b-axis (Figure. 7.9). The screw related calix moieties of the asymmetric units are associated via C-H….π interaction to form a corrugated arragement along b-axis (Figure. 7.10). Details of these C-H….π interaction between the calix ring C1-C6 with methyl hydrogen H79A of the *p*-toluenesulfonate and C8-C13 with methylene hydrogen of the propyl moiety is given in Table 3. The offset layers of the ligands oriented along c-axis are formed by strong C-H…O interactions of the sulfonate oxygen atoms from both the molecules in the asymmetric unit. Thus sulfonate oxygens O4 and O5 of the first molecule is involved in intermolecular C-H…O interaction with the rim methylene hydrogen H7A along c-axis and with H38A along a-axis, respectively. It is interesting to note that O4 is further

involved in an intramolecular C-H…O interaction with the rim methylene hydrogen H21A. Sulfonate oxygen atoms O10 and O11 of the second calix molecule are also involved in C-H…O interactions in similar fashion to that of O4 and O5. Details of all these H-bonding interactions with and their pertinent symmetry code are summarized in Table 4. Thus concomitant C-H…O interactions along a- and b-axis with C-H….π interactions create a supramolecular three dimensional network.

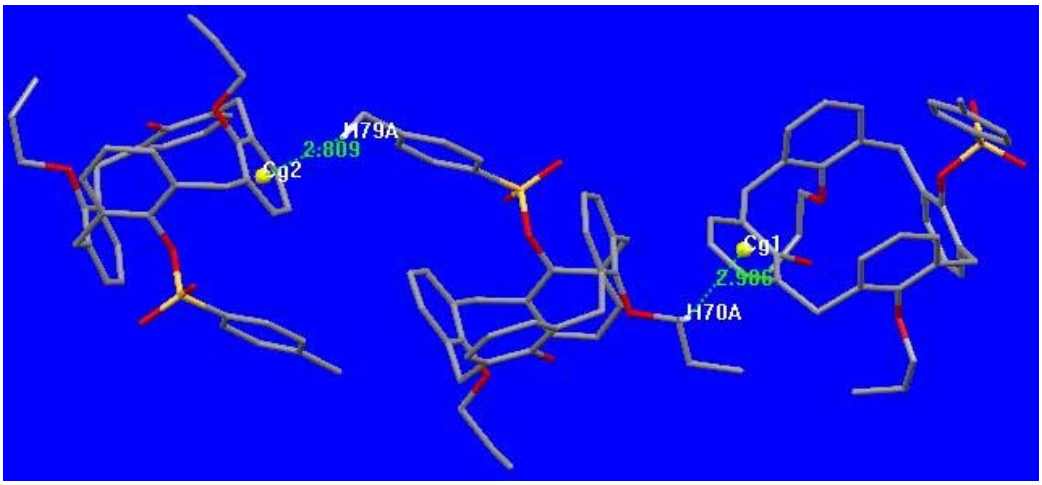

Figure. 7.10. C-H….π interactions between the aromatic rings of the calixarene moiety and methylene hydrogen (H70A) and methyl hydrogen (H79A) atoms of the propyl and *p*-toluenesulfonate groups, respectively in **L**^{4}.

7.3.4. Complexation study with Na^+ and K^+ ions

In-situ NMR study

Complexation study of **L**^{2}- **L**^{4} with Na^+ and K^+ by NMR experiment was carried out following the method as described in the experimental section. ^{1}H NMR spectra of the ligands and that with excess metal (Na^+/K^+) iodide were recorded at different time intervals in $CDCl_3$-CD_3OH (4:1) at room temperature. The ligand **L**^{3} with K^+ ion exhibits significant down field shift of all the signals due to the protons of the 2-(2-chloroethoxy)-ethanol moiety (-$OCH_2CH_2OCH_2CH_2Cl$) and also some changes in the aromatic region

compared to that of parent compound ($\mathbf{L^3}$), however in all other cases no significant change in NMR spectra was observed. This observation suggests that complex formation takes place only between $\mathbf{L^3}$ and K^+ and not any other cases under the experimental condition. The relevant portion of the NMR spectra of $\mathbf{L^3}$, ($\mathbf{L^3}$+NaI) and ($\mathbf{L^3}$+KI) are shown in Figure. 7.11. It may be noted that in the spectra of ($\mathbf{L^3}$+KI), the chemical shifts of all the CH_2 protons of the -$OCH_2CH_2OCH_2CH_2Cl$ moiety have moved down field by 0.23, 0.30, 0.33 and 0.52 ppm, respectively, while chemical shifts due to all other aliphatic protons remain almost at the same positions as observed for $\mathbf{L^3}$. This data suggests that only the -$OCH_2CH_2OCH_2CH_2Cl$ moiety is involved in complex formation with K^+. For further confirmation, attempt has been made to synthesize and isolate solid complexes of Na^+ and K^+ of these ligands.

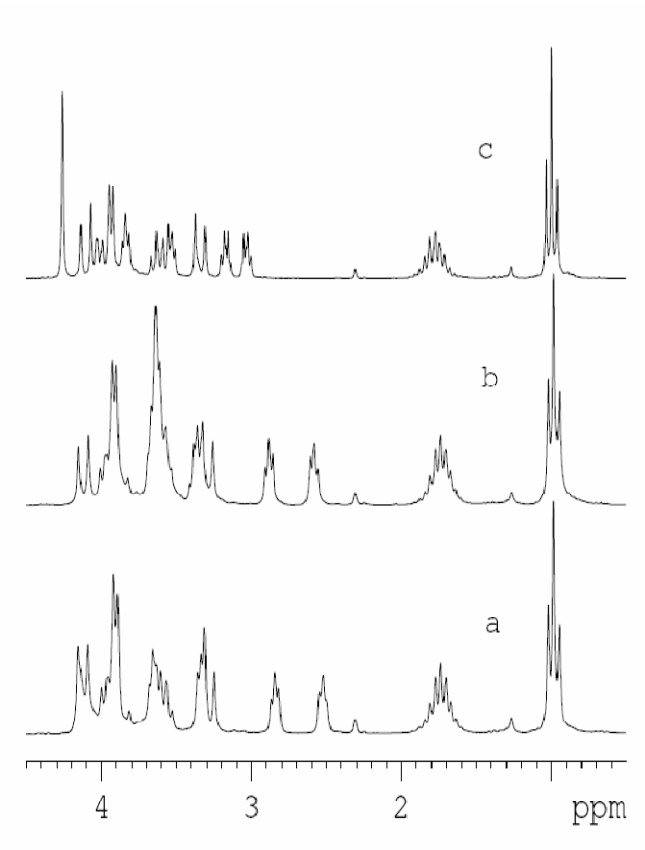

Figure. 7.11. Selected portion of the ^{1}H NMR spectra of (a) $\mathbf{L^3}$, (b) [$\mathbf{L^3}$+NaI], and (c) [$\mathbf{L^3}$+KI)]; recorded in $CDCl_3$-CD_3OH (4:1) at room temperature.

Association constant (K_a) of $\mathbf{L^3}$ with K^+ was determined by NMR titration following the method described in the experimental section. For calixarene, determination of K_a by NMR titration is not very common because of the fact that it is difficult to find a clean separate peak of the host, which shifts with increasing metal ion (guest) concentrations. The value of K_a obtained (1.4 x 10^5 M^{-1}) is comparable to that found by Beer et al by NMR titration for K^+ with calix[4]semitubes, where two calix[4]arene units are bridged by two ethylene chains and the K^+ ion is encapsulated in the cavity formed by calix units and ethylene bridge.[32]

Synthesis of solid complexes

Attempt has been made to synthesis Na^+ and K^+ complexes of these ligands following the method described in the experimental section. The solid mass was isolated and ^{1}H NMR spectra of all samples were recorded in $CDCl_3$-CD_3OH. The observations are consistent to that found in in-situ NMR experiment; the spectra of the K^+ complex of $\mathbf{L^3}$ is similar to that obtained from in-situ NMR experiment, whereas for all other cases minor or no change was observed.

The mass spectra of the K^+- complex of $\mathbf{L^3}$ exhibits a peak with low intensity at *m/z* = 1305.0 and a peak with moderate intensity at *m/z* = 1287.23. The first peak corresponds to the composition [2$\mathbf{L^3}$ + K^++ $2H_2O$] and the second peak corresponds to [2$\mathbf{L^3}$ + K^++ H_2O], the observed *m/z* values are in excellent agreement with the calculated values, 1305.52 and 1287.51, respectively. The data suggest that complex formation takes place with two molecules of ligand, K^+ ion and two molecules of water. The proposed structure of the complex is shown in Figure. 7.12. Similar observation was also noted by Beer at al, for calix tubes consists of two calix units (M), where the proposed composition is (M+ K^++$2H_2O$).[33] In the K^+- complex, the involvement of water molecules in coordination is also indicated by IR and NMR spectra. The IR spectra of $\mathbf{L^3}$ and its K^+- complex is shown in the Figure. 7.13. The three new strong peaks (compared to $\mathbf{L^3}$), which appeared at 3459, 1624 and 801 cm^{-1} are due to υ_s (O-H), bending mode of H-O-H and wagging mode of coordinated water molecule.[34] In the ^{1}H NMR spectra, the new singlet at δ 4.3

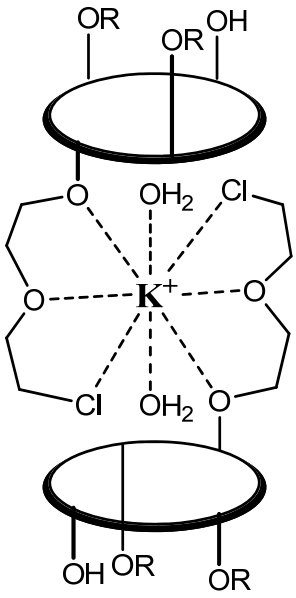

R= -$CH_2CH_2CH_3$

Figure. 7.12. Proposed structure for the K^+ complex of $\mathbf{L^3}$.

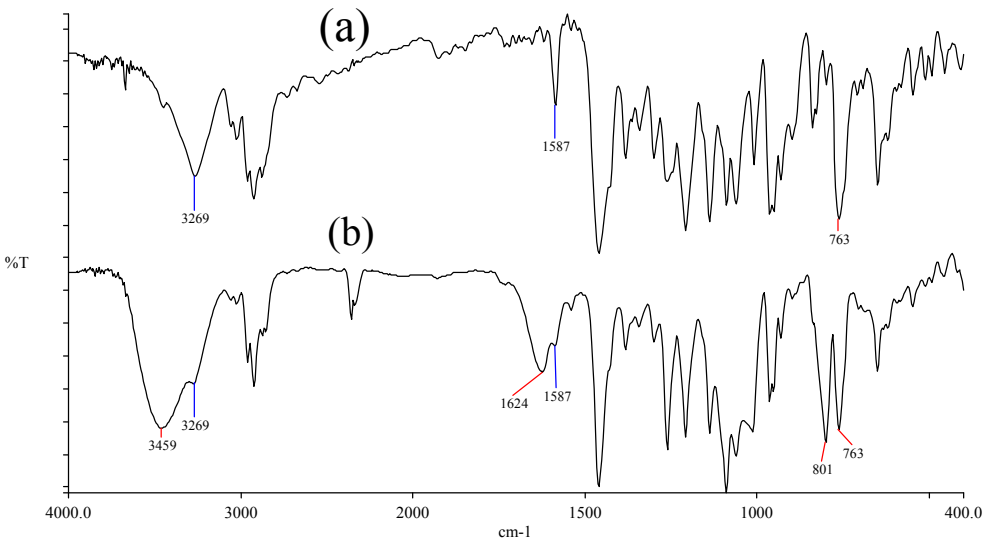

Figure. 7.13. IR spectra of compound $\mathbf{L^3}$ (a) and its K^+-complex (b).

(Figure. 7.11c), which corresponds to 4H, is assigned to the coordinated water molecules. Free water molecule used to appear at δ 4.8, the signal due to coordinated water molecule is expected to move towards down field, however in this case it has moved towards up field by ~ 0.5 ppm. From the possible structure of the complex it appears that the protons of the coordinated water molecules are inside or close to the cavity of the calixarene, which is a highly π-electron rich zone due to the presence of four aromatic rings. Because of this high π-electron density in the vicinity, the protons of the water molecules moved towards the up field region. Coordination of alkali metal ion with chlorine in presence of crown ether has also been demonstrated crystallographically.[35,36] The selective complexation with K^+ is probably because of hole-size matching, the size of the cavity formed by the two 2-(2-chloroethoxy)-ethanol moieties fits well with the ionic size of the K^+, the size of the Na^+ is probably too small to make strong interactions with all the coordination sites to form a stable complex.

7.4. Conclusions

A family of calix[4]arene with three substituents at the lower rim have been synthesized and structurally characterized. Out of three substituents, one is different and the effect of this variable substituent on metal binding ability and structural arrangement has been investigated. The calixarene moiety of all these three compounds adopted partial cone conformation, however, all the three compounds exhibit different type of intra- and intermolecular C-H….π interactions, which provide them different unique structural arrangements. The compound **L^2** encapsulated an acetonitrile molecule in the cavity of the calix moiety, whereas in the **L^3** the third substituent itself moved inwards the cavity to make strong C-H….π interaction with the phenyl rings, which prevented the entry of solvent molecule in the calix cone. The compound **L^4**, which contains *p*-toluenesulfonate groups as third substituent, behaves differently; no encapsulation in the cavity is observed but the CH_2 of the propyl group and the CH_3 of the *p*-toluenesulfonate group make strong intermolecular C-H….π interactions with the centroid of the phenyl groups of the adjacent molecules. Packing diagram of **L^2** shows strong π…π stacking interactions making an array along b-axis, whereas **L^4** exhibits intermolecular C-H….O interactions

to form layered three dimensional architecture. Complexation study of all these compounds with Na^+ and K^+ ions reveal that the conformation of $\mathbf{L^3}$ is such that it forms complex selectively with K^+, association constant also indicates strong complex formation, and therefore, it may be used as K^+ selective ionophore in presence of Na^+.

7.5. References

1. Gutsche, C. D. *Calixarenes,* Royal Society of Chemistry, Cambridge, UK, **(1989).**
2. Vicens, J.; Boehmer, V. (Eds), *Calixarenes, A Versatile Class of Macrocyclic Compounds.* Kluwer, Dordrecht, Netherlands**, (1991).**
3. Ikeda, A.; Shinkai, S. *Chem. Rev.* **1997**, *97*, 1713.
4. Gutsche, C. D. *Calixarene Revisited, Royal Society of Chemistry,* Cambridge, UK, (1998).
5. Casnati, A.; Pochini, A.; Ungaro, R.; Ugozzoli, F.; Arnaud, F.; Fanni, S.; Schwing, M.-J.; Egberink, R. J. M.; Jong, De. F.; Reinhoudt, D. N. *J. Am. Chem. Soc.* **1995**, *117*, 2767.
6. Kim, J. S.; Shon, O. J.; Ko, J. W.; Cho, M. H.; Yu, I. Y.; Vicens, J. *J. Org. Chem.* **2000**, 65, 2386.
7. Kim, S. K.; Bok, J. H.; Bartsch, R. A.; Lee, J. Y.; Kim, J. S. *Org. Lett.* **2005**, *7,* 4839.
8. Kim, S. K.; Kim, S. H.; Kim, H. J.; Lee, S. H.; Lee, S. W.; Ko, J.; Bartsch, R. A.; Kim, J. S. *Inorg. Chem.* **2005,** *44,* 7866.
9. Agnihotri, P.; Suresh, E.; Paul, P.; Ghosh, P. K.; *Eur. J. Inorg. Chem.* **2006**, 3369.
10. Csokai, V.; Grün, A.; Balàzs, B.; Simon, A.; Tóth, G.; Bitter, I. *Tetrahedran.* **2006**, *62*, 10215.
11. Iwamoto, K.; Shinkai, S.; *J. Org. Chem.***1992**, *57,* 7066.
12. Luo, J.; Zheng, Qi-Yu.; Chen, C.-F.; Huang, Z.-T. *Chem. Eur. J.* **2005**, *11*, 5917.
13. Zeng, X.; Weng, L.; Chen, L.; Xu, F.; Li, Q.; Leng, X.; He, X.; Zhang, Z.-Z. *Tetrahedron.* **2002,** *58,* 2647.
14. Gutsche, C. D.; Iqwal, M. *Org. Syntheses*. **1990**, *68*, 234.

15. Ouchi, M.; Inoue, Y.; Kanzaki, T.; Hakushi, T. *J. Org. Chem*. **1984,** *49*, 1408.

16. Perin, D. D.; Amarego, W. L. F.; Perrin, D. R. *Purification of Laboratory Chemicals 2nd Ed,* **1980.**

17. Casnati, A.; Pochini, A.; Ungaro, R.; Ugozzoli, F.; Arnaud, F.; Fanni, S.; Schwing, M.-J.; Egberink, R. J. M.; Jong, De. F.; Reinhoudt, D. N. *J. Am. Chem. Soc.* **1995**, *117*, 2767.

18. Hao, Ya-Q.; Wu, Y.; Liu, J.; Luo, G.; Yang, G. *J. Inclus. Phenom. & Macro. Chem.* **2006,** *54***,** 171.

19. Sheldrick, G. M. SAINT and XPREP, 5.1 Ed., Siemens Industrial Automation Inc., Madison, WI, **(1995).**

20. SADABS, empirical absorption Correction Program; University of Göttingen: Göttingen, Germany **(1997).**

21. Sheldrick, G. M. SHELXTL Reference Manual: Version 5.1; Bruker AXS: Madison, WI, **(1997).**

22. Sheldrick, G. M. SHELXL-97: Program for Crystal Structure Refinement, University of Göttingen, Göttingen, Germany, **(1997).**

23. Spek, A. L. PLATON-97, University of Utrecht: Utrecht, The Netherlands, **(1997).**

24. Mercury 1.3, Supplied with Cambridge Structural Database; CCDC: Cambridge, U.K., **(2003).**

25. Verboom, W.; Datta, S.; Asfari, Z.; Harkema, S.; Reinhoudt, D. N. *J. Org. Chem.* **1992,** *57*, 5394.

26. Guillon, J.; Leger, J.-M.; P. Sonnet, P.; Jarry, C.; Robba, M. *J. Org. Chem.* **2000,** *65*, 2386.

27. Shivanyuk, A.; Saadioui, M.; Broda, F.; Thondorf, I.; Vysotsky, M. O.; Rissanen, K.; Kolehmainen, E.; Boehmer, V. *Chem. Eur. J.* **2000,** 2138.

28. Dubes, A.; Udachin, K. A.; Shahgaldian, P.; Lazar, A. N.; Coleman, A. W.; Ripmeester, J. A. *New J. Chem.***2000,** *29*, 1141.

29. Danila, C.; Bolte, M.; Böhmer, V. *Org. Biomol. Chem*. **2005,** *3*, 172.

30. Arduini, A.; Nachtigall, F.; Pochini, A.; Secchi, A.; Ugozzoli, F. *Supramol. Chem.* **2000**, *12*, 273.

31. Meyer, E. A.; Castellano, R. K.; Diederich, F. *Angew. Chem. Int. Ed.* **2003**, *42*, 1210.

32. Webber, P. R. A.; Cowley, A.; Drew, M. G. B.; Beer, P. D. *Chem. Eur. J.* **2003**, *9*, 2439.

33. Matthews,S. E.; Schmitt, P.; Felix, V.; Drew, M. G. B.; Beer, P. D. *J. Am. Chem. Soc*. **2002,** *124*, 1341.

34. Nakamoto, K. Infrared Spectra of Inorganic and Coordination Compounds, John Wiley and Sons, New York, **(1963**) 155.

35. Hu, J.; Barbour, L. J.; G. W. Gokel. *Chem. Commun.* **2002,** 188.

36. Wang, D.-Q.; Dou, J.-M.; Niu, M.-J.; Li, D.-C.Liu, Y. *Acta Chim. Sinica***. 2002**, *60*, 2145.

Publications / Symposia / Conferences / Awards

A. Paper Published / Communicated

1. Selective Precipation of Alkaline Earth Metal Cations With Dipicrylamine Anion: structure-Selective Correlation. P. Agnihotri, **Subrata Patra**, E. Suresh, P. Paul and P. K. Ghosh, ***Eur. J. Inorg. Chem***. 2006, 4938.

2. Functionalized calix[4]arene as an ionophore: Synthesis, crystal structures and complexation study with Na^+ and K^+ ions. **Subrata Patra**, E. Suresh and P. Paul, ***Polyhedron,*** 2007, *26,* 4971

3. Synthesis, Characterization, Electrochemistry and Ion-Binding Studies of Ruthenium(II) and Rhenium(I) Bipyridine/Crown Ether Receptor Molecules. V. P. Boricha, **Subrata Patra**, Y. S. Chouhan, P. Sanavada, E. Suresh and P. Paul**.** ***Eur. J. Inorg. Chem.*** 2009, 1256.

4. Synthesis, characterization, electrochemistry and ion-binding studies of ruthenium(II) bipyridine receptor molecules containing calix[4]arene-azacrown as ionophore. **Subrata Patra** and P. Paul**.** ***Dalton Trans.*** 2009, 8683.

5. Luminescent metalloreceptors with pendant macrocyclic ionophore: Synthesis, characterization, electrochemistry and ion-binding study. **Subrata Patra**, V. P. Boricha, Srinidhi K. R., E. Suresh and P. Paul**.** ***Inorg. Chim. Acta***. 2010. *(article in Press).*

6. Effect of steric crowding on ion selectivity for calix-crown hybrid ionophores: experimental, molecular modeling and crystallographic studies. **Subrata Patra,** D. Maity, A. Sen, E. Suresh, B. Ganguly and P. Paul. ***New. J. Chem.*** (*Communicated*)**.**

7. Calix[4]arene-based fluorescent molecular sensors for Fe^{3+}, Cu^{2+} and Ca^{2+}: Synthesis, characterization and ion-binding study. **Subrata Patra,** A. Chakraborty and P. Paul. ***Tetrahedron. Lett.*** (*communicated*).

8. Diamide bridged calix[4]arene azacrown-based Rhenium(I) complex as a fluorescent sensors for Hg^{2+} ion. Synthesis, characterizatrion and ion binding study. **Subrata Patra**, E. Suresh and P. Paul. (*manuscript in preparation*)

9. Synthesis, Characterization, Electrochemistry and Ion-Binding Property of Ruthenium(II) Containing Receptors Having appended Modified Calix[4]arene as Ionophore. **Subrata Patra** and P. Paul. (*manuscript in preparation*)

10. Calix[4]arene-based fluoroionophores containing open chain chelating moiety with nitrogen and oxygen donor atoms: synthesis, crystal structures and ion binding study. **Subrata Patra**, R. Gunupuru, E. Suresh and P. Paul. (*manuscript in preparation*)

B. Patent

1. A novel integrated process for the recovery of sulphate of potash (SOP) from sulphate rich bittern using dipicrylamine; P. Paul, P. K. Ghosh, K. J. Langalia, P. S. Subramanian, S. Eringthodi, **Subrata Patra**, P. Agnihotri. Patent No. **05850953.0 – 1218,** *PCT/In2005000441* and also submitted for *US patent* through Patent Division, New Dehli (2008)

C . Paper presented in Conferences/ Symposia

1. X-Ray Crystallographic Studies of Self-Assemblies of Alkali and Alkaline Earth Metal Ions With Dipicrylamine Anion: Structure-Selectivity Correlation. Pragati Agnihotri, **Subrata Patra**, Suresh E., Parimal Paul and Pushpito K. Ghosh. **7th CRSI National Symposium in Chemistry,** IACS, Kolkata, (February, 2005).

2. Fluorescent Molecular Sensors: Synthesis and Ion Recognition Study; **Subrata Patra** and Parimal Paul, **National Seminar on Emerging Trends in Supramolecular Research,** Gujarat University, Ahmadabad (March, 2007)

   (Selected for Best Poster Award)

3. Luminescent Metalloreceptors of Ru(II) and Re(I): Synthesis, Electrochemical Behaviour and Optical Sensing Towards Cations and Anions. **Subrata Patra,** Sreenidhi. K. R., Vinod P. Boricha, E. Suresh and Parimal Paul. **MTIC-XII Symposium**, Indian Institute of Technology, Chennai, India, (December, 2007).

4. Luminescent Metalloreceptors of Ru(II): Synthesis, Characterization and their optical Sensing Towards Anions. **Subrata Patra,** Sreenidhi. K. R., Vinod P. Boricha, E. Suresh and Parimal Paul. **All Gujarat Research Scholar Meet**, M. S. University, Baroda (February, 2008) ***(****Oral Presentation****)***

5. Luminescent Metalloreceptors of Ru(II) Based Macrocyclic Compounds: Synthesis, Characterization and their Ion Recognition Property. **Subrata Patra,** V. P**.** Boricha, E. Suresh and Parimal Paul, **XXII Gujarat Science Congress 2008.** Bhavnagar University, Gujarat (March, 2008) *(Oral Presentation)*

6. Calix[4]arene-based Fluorescent Molecular Sensors: Synthesis and Ion recognition study. **Subrata Patra** and Parimal Paul. **MTIC-XIII symposium**, Indian Institute of Science, Bangalore (December, 2009)